EXPERIMENTAL CELL RESEARCH

Published under the auspices of

THE INTERNATIONAL SOCIETY FOR CELL BIOLOGY

EDITORS:

H. BAUER · T. CASPERSSON · A. ENGSTRÖM · E. FAURÉ-FREMIET

H. B. FELL · G. MONTALENTI · J. T. RANDALL · J. RUNNSTRÖM

F. O. SCHMITT · P. WEISS · R. W. G. WYCKOFF

VOLUME 11 · AUGUST 1956 · NUMBER 1

ACADEMIC PRESS INC., PUBLISHERS, NEW YORK, N. Y.

EXPERIMENTAL CELL RESEARCH

EDITORS:

H. Bauer, Max Planck Institut f. Meeresbiologie, Wilhelmshaven 23, Germany
T. Caspersson, Department of Cell Research, Karolinska Inst., Stockholm 60, Sweden
A. Engström, Department of Physical Cell Research, Karolinska Inst., Stockholm 60, Sweden
E. Fauré-Fremiet, Collège de France, Paris V:e, France
Honor B. Fell, Strangeways Laboratory, Cambridge, England
G. Montalenti, Istituto di Genetica dell'Università di Napoli, Naples, Italy
J. T. Randall, Wheatstone Physics Laboratory, King's College, London W. C. 2, England
J. Runnström, Wenner-Gren Institute for Experimental Biology, Stockholm Va., Sweden
F. O. Schmitt, Massachusetts Institute of Technology, Cambridge 39, Mass., U.S.A.
P. Weiss, Rockefeller Institute for Medical Research, New York 21, N.Y., U.S.A.
R. W. G. Wyckoff, Laboratory of Physical Biology, National Institute of Health, Bethesda, Md., U.S.A.

Editorial Secretaries: L. Ernster and Vera Reio, Norrtullsgatan 16, Stockholm Va., Sweden
Papers should be submitted to one of the editors or to the Editorial Office, Norrtullsgatan 16, Stockholm Va., Sweden.

ADVISORY BOARD:

W. Bloom (Chicago), J. Brachet (Bruxelles), F. Buchthal (Copenhagen), W. S. Bullough (London), A. Buzzati-Traverso (La Jolla, Calif.), R. Chambers (New York), E. Chargaff (New York), M. Chèvremont (Liège), J. F. Danielli (London), C. D. Darlington (London), J. N. Davidson (Glasgow), M. Demerec (Cold Spring Harbor, N.Y.), J. Engelbreth-Holm (Copenhagen), A. Fischer (Copenhagen), A. Forssberg (Stockholm), A. Frey-Wyssling (Zürich), N. Fries (Uppsala), S. Gard (Stockholm), R. J. Gautheret (Paris), L. Geitler (Wien), G. Gomori (Chicago), T. Gustafson (Stockholm), A. Haddow (London), E. Hammarsten (Stockholm), B. Hanström (Lund), E. Newton Harvey (Princeton, N. J.), L. V. Heilbrunn (Philadelphia, Pa), G. C. Heringa (Amsterdam), A. Hollaender (Oak Ridge, Tenn.), H. Holter (Copenhagen), J. Holtfreter (Rochester, N.Y.), T. Hultin (Stockholm), G. Klein (Stockholm), P. Koller (London), F. Lehmann (Bern), P. L'Héritier (Paris), G. Levi (Torino), P. E. Lindahl (Uppsala), O. Lindberg (Stockholm), G. Lindeberg (Ås, Norway), C. C. Lindegren (Carbondale, Ill.), R. J. Ludford (London), S. E. Luria (Urbana, Ill.), A. Lwoff (Paris), A. Mirsky (New York), H. Okkels (Copenhagen), O. Olivo (Bologna), A. W. Pollister (New York) S. Ranzi (Milano), W. J. Schmidt (Giessen), F. Schrader (New York), F. Sjöstrand (Stockholm), T. M. Sonneborn (Bloomington, Ind.), J. M. Sosa (Montevideo), J. Spek (Rostock), W. M. Stanley (Berkeley, Calif.), E. Suomalainen (Helsingfors), E. L. Tatum (Stanford University, Calif.), T. Teorell (Uppsala), A Tyler (Pasadena, Calif.), W. Wilbrandt (Bern), E. Zeuthen (Copenhagen).

Subscriptions

EXPERIMENTAL CELL RESEARCH

will be published in two volumes annually at $ 13:— per volume. Please send your subscription orders to Academic Press Inc., 125 East 23 St., New York 10, N.Y.

FORMATION OF HEMOGLOBIN AND THE CYTOCHROMES BY YEAST IN THE PRESENCE OF ANTIMYCIN "A"

M. YČAS

Pioneering Research Division, Quartermaster Research and Development Center, Natick, Mass., U.S.A.

Received November 9, 1955

Mutations producing cytochrome deficiencies in yeast and *Neurospora crassa* differ from most other "biochemical" mutations by producing pleiotropic effects. All mutants, irrespective of what other cytochromes may be affected, lack cytochrome *a*. Table I lists the mutants so far described. In addition to a deficiency of cytochrome *a*, cytochrome mutants of yeast are characterized by the presence of a weak band in the yellow at about 583 mμ, formerly referred to a "cytochrome a_1". Keilin [5] has shown that this band is actually due to intracellular hemoglobin. Of the numerous samples of baker's yeast originally studied by Keilin, only two were found to show the hemoglobin band. Later, however, hemoglobin was found to be regularly present in "petite colonie" mutants, lacking cytochromes *a* and *b* [6]. It is also found in *Neurospora crassa*, being again more abundant in certain cytochrome-deficient strains [7]. A similar band in the yellow, presumably also due to hemoglobin, is present in the spectrum of normal yeast grown in the absence of oxygen and therefore lacking cytochromes *a*, *b*, and *c* [4].

These observations suggest that the pleiotropic effects of mutations effecting the cytochrome system may be due to the physiological effects of an inability

Table I

Organism	Strain designation	Cytochromes *a*	*b*	*c*	Inheritance	Reference
S. cerevisiae	petite vegetative	−	−	+	cytoplasmic	11
,,	petite segregante	−	−	+	mendelian	2
,,	W-1	−	−	+	mendelian	10, 12
N. crassa	poky	−	−	+	cytoplasmic	8
,,	mi-3	−	+	+	cytoplasmic	8
,,	C-115	−	+	+	mendelian	8
,,	C-17	−	+	−	mendelian	8

to respire. Were this correct, it should be possible to produce effects similar to those produced by various mutations on the formation of the cytochrome system by the action of respiratory inhibitors. The effects of one such inhibitor, antimycin "A", are described here.

Antimycin "A" is believed to inhibit a factor, probably identical with that described by Slater, mediating the reduction of cytochrome *c* by diaphorase and succinic dehydrogenase [1, 9]. So far as is known, this is its only site of action. The effect of antimycin "A" on the respiration and fermentation of yeast has been described [1]. As would be expected from its postulated site of action, the action of antimycin "A" is readily observable spectroscopically. In its presence, aerated yeast cells show cytochromes *a* and *c* in the oxidized and cytochrome *b* in the reduced state, making it possible to determine by visual inspection whether the inhibitor is active.

METHODS

The yeast used was a strain of *Saccharomyces cerevisiae*, strains 59R and 59RA, from the laboratory of Dr. Boris Ephrussi in Paris. Strain 59R is normal with respect to the cytochrome components, while 59RA is a "petite colonie", lacking cytochromes *a* and *b*. Since Antimycin "A" inhibits the growth of yeast more strongly in synthetic media [1], a culture medium of 2 per cent glucose, 1 per cent Bactopeptone and 1 per cent yeast extract in tap water was used. Yeast was harvested and washed by centrifugation. For experiments on resting cultures, washed cells were suspended in a solution of 2 per cent glucose and $M/10$ KH_2PO_4 in distilled water. Aerobic cultures were grown on a shaker in 1 l Erlenmeyer flasks containing 200 cc of medium. Anaerobic cultures were grown without shaking in 2 l flasks containing 1 l of medium, with suitable arrangements for flushing with nitrogen and with an exit capped by a Bunsen valve for the escape of gas. All incubations were at 30°C. Growth was measured as turbidity, using a Lumetron colorimeter with a red filter.

For examination of the cytochrome spectrum, a 50 per cent suspension of washed cells were placed in a cuvette with a 1 cm optical path. Hydrosulfite or other reagents, as needed, were added to the cell suspension. The spectrum was examined visually, using a low dispersion hand spectroscope and a microscope lamp for illumination.

Antimycin "A" was a gift from Dr. F. M. Strong of the University of Wisconsin. It was dissolved in 50 per cent ethanol and added aseptically to autoclaved media. Control cultures received ethanol only.

RESULTS

To check whether antimycin "A" has any effect other than that on respiration, the growth of strains 59R and 59RA in medium containing the inhibitor was examined. The growth of 59RA, genetically deficient in cytochromes *a*

and *b* and thus unable to respire, is entirely unaffected by the inhibitor in the concentration used. On the other hand, the wild type 59R is strongly inhibited and reaches a maximal growth level identical with that of the cytochrome-deficient mutant (Fig. 1). It therefore appears that antimycin "A", so far as it is possible to tell from the growth curves, acts only on the respiratory metabolism of yeast.

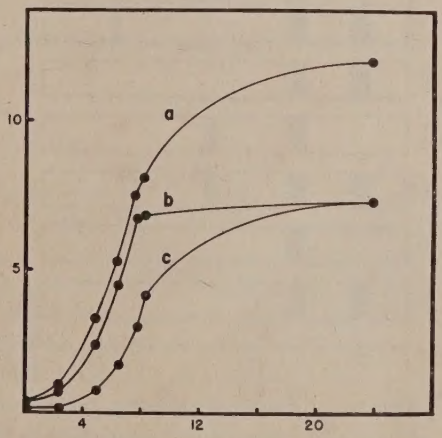

Fig. 1. Effect of antimycin "A" on growth of yeast. Abscissa—time in hours. Ordinate—optical density × 10. *a*, Strain 59R without inhibitor. *b*, 59R with inhibitor. *c*, 59RA with and without inhibitor. Natural medium, inhibitor concentration 0.64 μg/ml.

The effect of antimycin "A" on cytochrome synthesis was examined under two different conditions: (a) on anaerobically grown cells suspended in aerated glucose-phosphate solution ("adaptive" cytochrome formation) [4], and (b) on cells growing aerobically in complete medium. The effect of the inhibitor was found to be quite different under these two conditions.

Antimycin "A" has no noticeable effect on "adaptive" cytochrome formation.

Strain 59R was grown for 24 hours anaerobically, the cells harvested and washed, and resuspended in glucose buffer with and without 2.5 μg/cc antimycin "A". Spectroscopic examination showed absence of cytochromes *a*, *b*, and *c*, and the presence of a diffuse band at about 555 mμ (b_1). After being shaken in air for 16 hours, the spectrum of the cells was re-examined. The b_1 band was no longer present. On addition of hydrosulfite, the reduced bands of cytochromes *a*, *b*, and *c* were of equal intensity in both cultures. Aerating the cells without hydrosulfite showed cytochromes *a* and *c* to be oxidized, while cytochrome *b* remained reduced. Thus, sufficient inhibitor was present to prevent oxidation of cytochrome *b*, but this did not noticeably prevent the formation of all aerobic cytochrome components.

If the experiment is repeated as above, but antimycin "A" is added also to the initial anaerobic growth medium, the results are qualitatively the same. All three cytochrome components are formed on aeration in glucose buffer-containing inhibitor, but the intensity of the bands is considerably reduced relative to the controls.

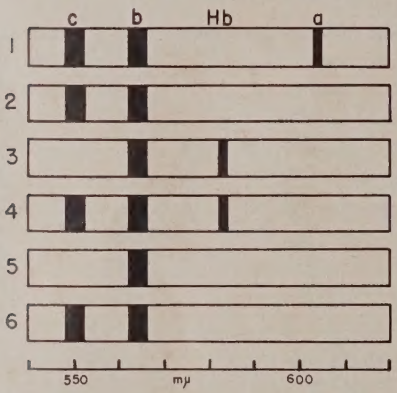

Fig. 2. Cytochrome spectrum of yeast 59R. *1*, Normal; *2* to *6*, grown with antimycin "A". *2*, After standing; *3*, after shaking in air; *4*, KCN added; *5*, CO added; *6*, reduced with hydrosulfite.

There is, however, a striking effect of antimycin "A" if the culture is grown aerobically from a small inoculum in the presence of inhibitor. At concentrations of inhibitor of 0.37 to 2.5 μg/cc, the formation of cytochrome *a* is suppressed and a relatively strong band appears at about 580 mμ. The bands of cytochromes *b* and *c* are not affected (Fig. 2). Although cytochrome *a* cannot be detected spectroscopically, some cytochrome oxidase is probably present, since in an aerated suspension the reduced band of cytochrome *c* is not visible, but becomes visible on addition of cyanide. Presumably the suppression of cytochrome *a* formation is incomplete.

The effect of various experimental conditions on the 580 mμ band is shown in Fig. 2. It is visible on aeration, but fades on standing, concomitantly with the appearance of the band of reduced cytochrome *c*. The 580 mμ band is visible again after addition of cyanide to an aerated suspension. Addition of hydrosulfite or carbon monoxide causes the 580 mμ band to disappear. Thus, both the position of the band and its spectroscopic behaviour indicate that it is the hemoglobin described by Keilin [5]. With this strain of yeast, no band at 580 mμ has been observed in aerobic cultures grown in the absence of antimycin "A". The effect of antimycin "A" is independent of the age of the culture, one- and four-day-old cultures showing the same spectroscopic appearance.

Since certain chemical compounds specifically induce a cytoplasmically inherited cytochrome deficiency in yeast [3], it was necessary to check whether the effect of antimycin "A" on aerobically growing cultures could be of this nature. Thirty-nine colonies were isolated by plating from an antimycin "A" containing aerobic culture. After subculturing in an antimycin "A" free medium, 38 had a normal cytochrome spectrum and one was of the "petite colonie" type. This is a normal composition for this strain and indicates that antimycin "A" does not have any specific mutagenic effect which would explain the absence of cytochrome *a*.

DISCUSSION

As shown above, antimycin "A" suppresses the synthesis of cytochrome *a* and enhances that of hemoglobin only if it acts on cells simultaneously growing and exposed to oxygen. Even if the inhibitor is present throughout, aerobic growth followed by exposure to oxygen in a nitrogen-free medium does not result in an inhibition of "adaptive" cytochrome formation of all three components. The following tentative hypothesis may be offered to account for the above facts. Growth under anaerobic conditions results in the synthesis of either a precursor or an enzyme system which, on subsequent exposure to oxygen, forms cytochrome *a*. Antimycin "A" inhibits the synthesis of such precursors or enzyme systems, but acts only if oxygen is present and has no effect on the transformation of precursors already formed to cytochrome *a*. Its lack of effect on adaptive synthesis would thus be explained. The increase of hemoglobin appears to be associated with an absence or reduction of cytochrome *a*. This could be explained either if hemoglobin were on a biosynthetic pathway alternative to cytochrome *a*, or if the heme of hemoglobin were a precursor of the prosthetic group of cytochrome *a*. Pending further study, of course, such hypotheses can have only heuristic value.

Whatever the detailed explanation of the effect of antimycin "A" on cytochrome *a* synthesis may prove to be, the results do suggest that the regular absence of cytochrome *a* in various cytochrome-deficient mutants of yeast and *Neurospora* might well be a secondary result of inability to respire. The "petite colonie" mutants, for example, could be regarded as primarily deficient in ability to synthesize cytochrome *b*, the enhancement of hemoglobin content and suppression of cytochrome *a* being a secondary antimycinlike effect. The cytochromes thus need not necessarily be an exception to the one gene, one enzyme hypothesis.

SUMMARY

Antimycin "A" suppresses the formation of cytochrome *a* and enhances the synthesis of hemoglobin by yeast cells growing in the presence of oxygen. It has no effect on "adaptive" cytochrome synthesis by resting cells.

REFERENCES

1. Ahmad, K., Schneider, H. G., and Strong, F. M., *Arch. Biochem.* **28**, 281 (1950).
2. Chen, S. Y., Ephrussi, B., and Hottinguer, H., *Heredity* **4**, 337 (1950).
3. Ephrussi, B. and Hottinguer, H., *Nature* **166**, 956 (1950).
4. Ephrussi, B. and Slonimski, P. P., *Biochim. et Biophys. Acta* **6**, 256 (1950).
5. Keilin, D., *Nature* **172**, 390 (1953).
6. Keilin, D. and Tissières, A., *Biochem. J.* **57**, XXIX (1954).
7. —— *Nature* **172**, 393 (1953).
8. Mitchell, M. B., Mitchell, H. K., and Tissières, A., *Proc. Natl. Acad. Sci.* **39**, 606 (1953).
9. Potter, V. R. and Reif, A. E. *J. Biol. Chem.* **194**, 287 (1952).
10. Raut, C., *Exptl. Cell Research* **4**, 295 (1953).
11. Slonimski, P. P. and Ephrussi, B., *Ann. Inst. Pasteur* **77**, 47 (1949).
12. Yčas, M. and Starr, T. J., *J. Bacteriol.* **65**, 83 (1953).

SERIAL TRANSFER OF EHRLICH MOUSE ASCITES CANCER IN FEMALE HAMSTERS

C. G. AHLSTRÖM and ULLA ISING

Institute of Pathology, University of Lund, Sweden

Received November 10, 1955

In the course of investigations of the intraperitoneal growth and serial transfer of Ehrlich mouse ascites cancer in hamsters it was noticed that the results obtained varied with the sex of the hosts. The observations made in the male series were accounted for in previous papers [1–3]. The present paper is concerned with serial transplantation of the cancer through *female* hamsters. As before, the cancer was transmitted from hamster to hamster at three-day intervals.

METHODS AND MATERIAL

The Ehrlich mouse ascites cancer used in the experiments is of tetraploid or nearly tetraploid type and has been maintained at the Institute for several years by serial intraperitoneal transfer through mice of an inbred but not pure strain.

Ascitic fluid collected from mice inoculated six to eight days earlier with 0.1 ml of ascites cancer was used for transplantation to the hamster. The first hamster in every series was inoculated with 2 ml of ascitic fluid. The hamster was killed three days later. The ascitic fluid was then collected and measured, after which 2 ml of it was transferred intraperitoneally to a new hamster. In this way the cancer was transmitted at three-day intervals through a series of hamsters. In some passages the inoculum was smaller because the amount of fluid available from the preceding animal in the series was less than 2 ml.

The number of cancer cells was determined in a haemocytometer. Smears from the ascitic fluid were stained according to Papanicolaou. The number of non-neoplastic cells in the ascitic fluid was assessed by the number found in the smears. 1000–3000 cells were counted and the number of non-neoplastic cells was correlated with 100 cancer cells. The number of cancer cells in mitosis per 100 cancer cells was taken as the mitotic index. For this purpose 1000–2000 cancer cells were counted.

The hamsters used were Syrian golden hamsters and weighed 100–120 g. They were brought up on a standard diet.

RESULTS

The ascites cancer was carried through three female series. The passage through each series was started with ascites cancer from different batches of mice. The results are apparent from Tables I, II and III, in which the left

TABLE I

(Series 1)

Serial transfer of Ehrlich mouse ascites cancer at three-day intervals through a series of female hamsters. The left part of the table contains data about the ascitic fluid each hamster received, the right part gives information on the ascitic fluid when the hamster was killed.

Passage	Volume of inoculated ascitic fluid in ml	Number of cancer cells $\times 10^6$ per ml	Total number of inoculated cancer cells $\times 10^6$	Volume of ascitic fluid after 3 days in ml	Number of cancer cells $\times 10^6$ per ml	Total number of cancer cells $\times 10^6$ after 3 days	Mitotic index	Yield of cancer cells per cent
1	2.0	115.9	231.8	6.0	2.6	15.6	0.7	6
2	2.0	2.6	5.2	0.3	32.5	9.7	0.8	186
3	0.3	32.5	9.7	0.15	79.6	11.9	2.2	123
4	0.15	79.6	11.9	1.8	3.1	5.6	2.3	47
5	1.8	3.1	5.6	1.6	133.8	214.1	1.0	3823
6	1.5	133.8	200.7	5.3	55.8	295.7	1.2	147
7	2.0	55.8	111.6	10.3	14.6	150.4	1.7	135
8	2.0	14.6	29.2	5.0	14.8	74.0	1.2	253
9	2.0	14.8	29.6	1.5	57.9	86.9	1.4	294
10	1.2	57.9	69.5	2.5	3.9	9.8	2.5	14
11	2.0	3.9	7.8	2.0	49.8	99.6	0.4	1277
12	2.0	49.8	99.6	3.5	10.8	37.8	2.0	38
13	2.0	10.8	21.6	5.0	24.5	122.5	1.0	567
14	2.0	24.5	49.0	5.6	61.3	343.3	1.0	705
15	2.0	61.3	122.6	3.6	51.4	185.0	1.4	151
16	2.0	51.4	102.8	7.2	107.9	776.9	0.4	756
17	2.0	107.9	215.8	3.7	60.8	225.0	1.7	104
18	2.0	60.8	121.6	16.6	29.1	483.1	1.0	397
19	2.0	29.1	58.2	2.5	164.6	246.9	1.3	424
20	1.5	164.6	246.9	12.0	73.5	882.0	1.3	357
21	2.0	73.5	147.0	0.5	58.4	29.2	3.1	20
22	0.5	58.4	29.2	2.0	65.3	130.6	1.8	447
23	1.7	65.3	110.0	3.0	104.5	313.5	2.2	285
24	2.0	104.5	209.0	9.5	57.5	546.2	0.7	261
25	2.0	57.5	115.0	6.2	75.0	460.0	0.9	400
26	2.0	75.0	150.0	2.6	84.5	219.7	1.9	146
27	1.0	84.5	84.5	9.5	34.9	331.6	1.4	392
28	2.0	34.9	69.8	3.3	90.4	298.3	1.1	427
29	2.0	90.4	180.8	9.0	42.5	382.5	0.2	212
30	2.0	42.5	85.0	5.0	79.3	396.5	1.1	466
31	2.0	79.3	158.6	6.5	83.6	544.4	0.8	343
32	2.0	83.6	167.2	10.5	40.0	420.0	1.1	251
33	2.0	40.0	80.0	3.0	94.5	283.5	1.7	354
34	1.0	94.5	94.5	6.5	79.0	513.5	0.5	543

TABLE II

(Series 2)

Serial transfer of Ehrlich mouse ascites cancer at three-day intervals through a series of female hamsters. The left part of the table contains data about the ascitic fluid each hamster received, the right part gives information on the ascitic fluid when the hamster was killed.

Passage	Volume of inoculated ascitic fluid in ml	Number of cancer cells $\times 10^6$ per ml	Total number of inoculated cancer cells $\times 10^6$	Volume of ascitic fluid after 3 days in ml	Number of cancer cells $\times 10^6$ per ml	Total number of cancer cells $\times 10^6$ after 3 days	Mitotic index	Yield of cancer cells per cent
1	2.0	94.6	189.2	9.3	72.8	677.0	0.8	361
2	2.0	72.8	145.6	12.5	73.4	917.5	1.5	623
3	2.0	73.4	146.8	6.2	95.3	590.9	1.5	402
4	2.0	95.3	190.6	11.5	63.3	727.9	1.1	382
5	2.0	63.3	126.6	2.9	15.4	30.8	0.8	35
6	2.0	15.4	30.8	4.6	4.4	20.2	2.1	66
7	2.0	4.4	8.8	1.75	23.0	40.3	1.8	457
8	1.75	23.0	40.25	3.5	13.5	47.3	2.1	116
9	2.0	13.5	27.0	3.0	5.0	15.0	0.5	56
10	2.0	5.0	10.0	0.6	75.4	45.2	0.9	452
11	0.5	75.4	37.7	2.0	115.8	231.6	1.2	614
12	2.0	115.8	231.6	4.5	129.3	581.9	1.8	251
13	2.0	129.3	258.6	5.5	64.9	356.9	1.1	130
14	2.0	64.9	129.8	11.0	42.1	463.1	0.2	356
15	2.0	42.1	84.2	5.0	55.6	328.0	1.1	389
16	2.0	55.6	111.2	9.6	20.8	199.7	1.0	179
17	2.0	20.8	41.6	1.5	10.4	15.6	1.7	38
18	1.3	10.4	13.5	2.5	35.6	89.0	2.4	652
19	2.0	35.6	71.2	5.0	40.9	204.5	1.9	287
20	2.0	40.9	81.8	4.0	79.3	317.2	1.3	388
21	2.0	79.3	158.6	8.2	30.8	252.6	1.0	159

half of the tables contains data about the ascites fluid each hamster received. The right half gives information on the ascitic fluid when the animal was killed three days later. The yield of cancer cells per hundred injected was taken as a measure of the growth of the cancer. The yield from each animal is given in the last column of the tables.

Diagram 1 *a*, which is based on the figures in this column, gives a graphical representation of the growth of the cancer during the successive passages in the three series.

It is evident that the growth of the cancer varied considerably from one

TABLE III

(Series 3)

Serial transmission of the Ehrlich mouse ascites cancer through a series of 13 hamsters; the first eleven hamsters were females, the last two were males.

Passage	Volume of inoculated ascitic fluid in ml	Number of cancer cells $\times 10^6$ per ml	Total number of inoculated cancer cells $\times 10^6$	Volume of ascitic fluid after 3 days in ml	Number of cancer cells $\times 10^6$ per ml	Total number of cancer cells $\times 10^6$ after 3 days	Mitotic index	Yield of cancer cells per cent
1	2.0	33.0	66.0	2.8	100.0	280.0	1.8	424
2	2.0	100.0	200.0	13.5	7.3	98.6	0.7	49
3	2.0	7.3	14.6	3.5	99.1	346.9	1.2	2376
4	2.0	99.1	198.2	11.0	63.6	700.0	0.4	399
5	2.0	63.6	127.2	2.75	3.8	10.8	3.0	8
6	2.0	3.8	7.6	2.0	7.9	15.8	2.0	208
7	2.0	7.9	15.8	2.4	25.0	60.0	1.8	380
8	2.0	25.0	50.0	3.8	89.1	338.6	1.1	677
9	2.0	89.1	178.0	8.8	50.5	444.4	0.3	249
10	2.0	50.5	101.0	6.0	70.0	420.0	1.1	415
11	2.0	70.5	141.0	7.0	68.6	480.2	1.1	340
12	2.0	68.6	137.2	3.2	10.1	32.3	1.7	23
13	2.0	10.1	20.2	—	—	—	—	—

animal to another. In the first hamster in series 1 the yield was poor, while that of the first passage in series 2 and 3 was three or four times more than the number of cells injected. During the third passage in series 3 the increase in the number of cancer cells was still more conspicuous. In the fourth passage and in the fifth the yield was poor in all three series, but afterwards it improved, and during the fifth passage in series 1 it increased to about forty times the number injected. In this series the number of cancer cells increased markedly also in the eleventh passage. On the other hand, the yield from some of the passages was poor. Usually, however, it was two to threefold the number of cells injected.

Also the amount of ascitic fluid varied widely from one animal to another. Most of the animals had two days earlier received 2 ml of ascitic fluid from the preceding animal in the series. The increase in ascitic fluid was sometimes considerable: the amount collected from the eighteenth and from the twentieth animal in series 1 was 16.6 ml and 12.0 ml, respectively; from the fourth and fourteenth animal of the same series it was about 11.0 ml, and from the

second animal in series 3 it was 13.5 ml. On the other hand, in some of the animals the amount of fluid had diminished to 0.15–0.30 ml, i.e. to such a small quantity that the cancer appeared to be dying. The ascitic fluid was grey-white or grey-red and varied in viscosity with the number of cancer cells.

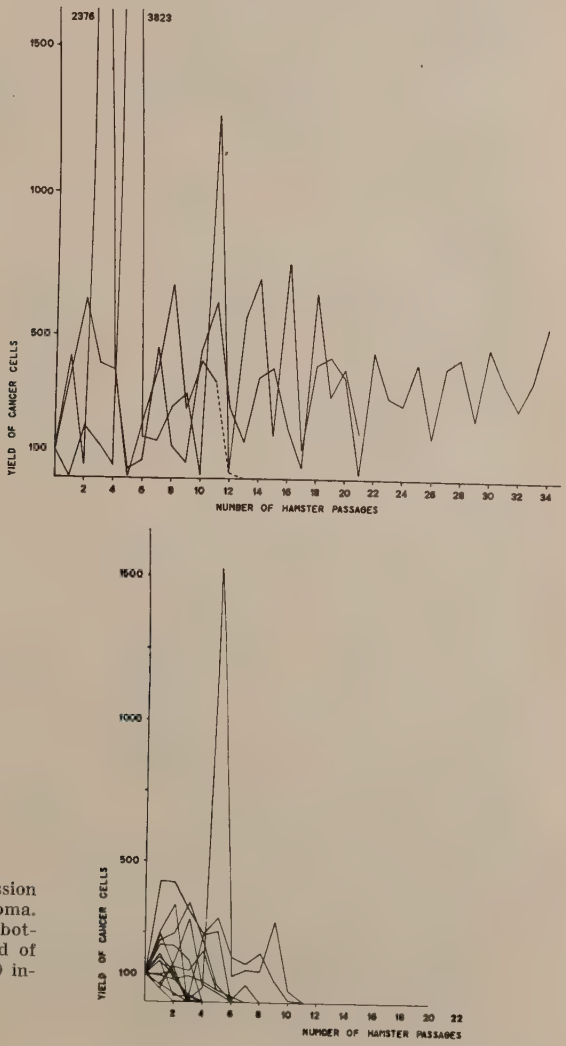

Diagram 1 *a* and *b*. Serial transmission of Ehrlich mouse ascites carcinoma. *a* (top), in female hamsters; *b* (bottom), in male hamsters. The yield of cancer cells is calculated per 100 injected cancer cells.

After transfer to the hamster the cancer cells increased conspicuously in size (Figs. 1 *a–c*). The nuclei became larger and showed distinct chromatin granules, the nucleoli appeared to be enlarged, the cytoplasm, which was sometimes vacuolated, was more abundant than during passage of the cancer through the mice. However, monstruous cells, which were seen in the male

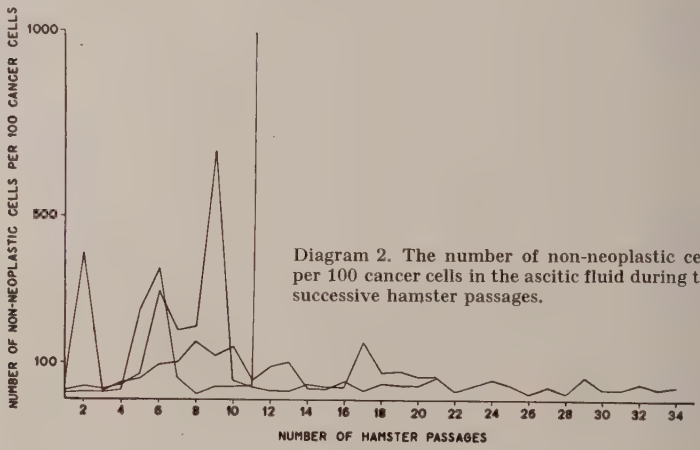

Diagram 2. The number of non-neoplastic cells per 100 cancer cells in the ascitic fluid during the successive hamster passages.

hamsters before the final death of the cancer, were not observed during the passage of the cancer through females. Not all of the cancer cells were enlarged, some of them being of the same size as those in the ascitic fluid in the mice.

On transfer of the cancer to hamsters the mitotic index decreased during the first passage and as a rule continued to be fairly low during subsequent passages. In hamsters with poor cancer growth the mitotic index was sometimes relatively high, probably because of a retardation of the cellular division and consequent accumulation of mitoses.

The ascitic fluid from our strain of mice showed an admixture of 10–20 per cent inflammatory cells. After transfer to the hamster females the proportion of inflammatory cells increased (Diagr. 2), just as it did in the male hamsters, and was particularly pronounced in passages in which the cancer showed poor growth, and thereby suggested an inverse relationship between

Fig. 1. Ascites cancer cells during successive passages in female hamsters (Series 1). *a*, The donor mouse; *b*, the first hamster passage; *c*, the thirty-fourth hamster passage. Magnification × 880. Papanicolaou-staining.

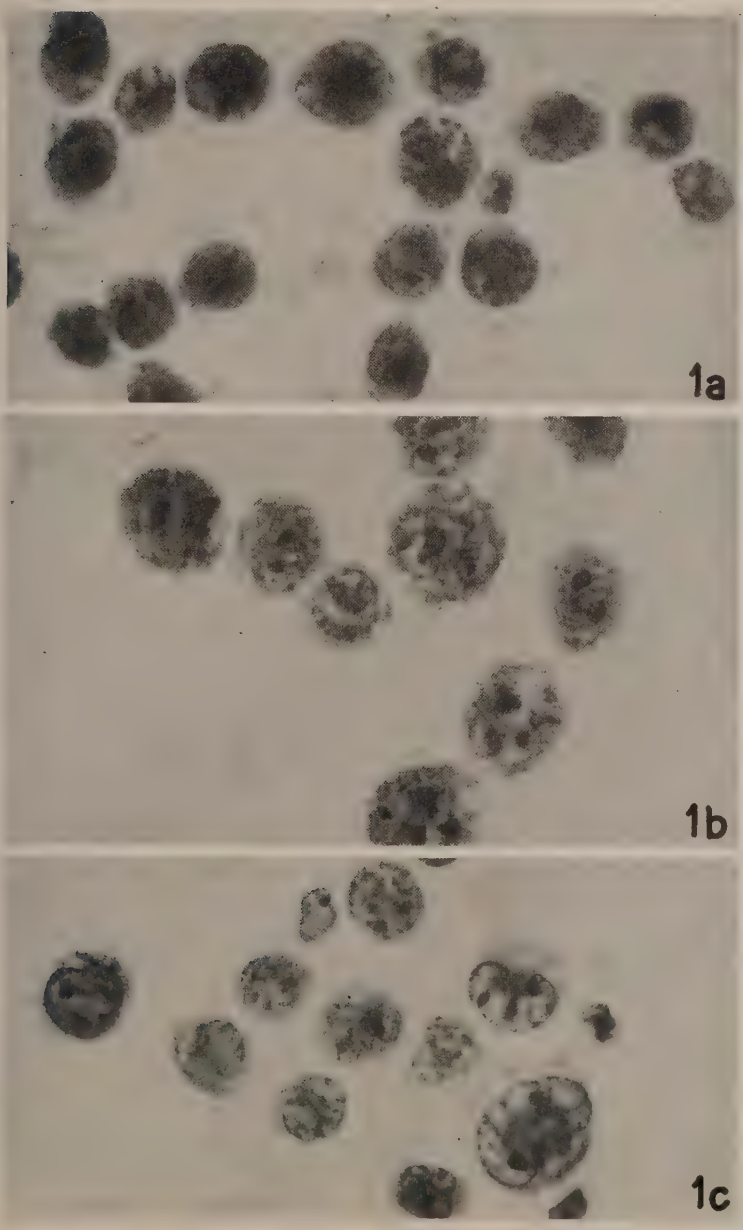
1a
1b
1c

the proliferation of the cancer cells and the number of non-neoplastic cells. It is remarkable that, generally speaking, the inflammatory reaction gradually decreased during the successive passages. During the latter part of series 1 it was of roughly the same degree as in the mice.

In series 1 the ascites cancer was carried through thirty-four hamsters, and in series 2 through twenty-one, and was interrupted since prolongation of the experiment could hardly be expected to give further information. By then the mouse cancer had been in alien environments for 102 and 63 days, respectively. In both series the cancer showed good vitality, and nothing spoke against its being possible to transfer the cancer *ad infinitum*. In series 3 the first eleven animals were females. During those passages the cancer had been transferred without difficulty. Owing to lack of the female hamsters the cancer was then transferred to a male. It was interesting to note that the yield of cancer cells now suddenly decreased, and during the next passage—also in male hamster—the cancer died. The decrease in the number of cancer cells was accompanied by a marked increase in the number of non-neoplastic cells (Fig. 2, Diagr. 2).

DISCUSSION

The results obtained in the present investigation should be considered against the background of those obtained in male hamsters. In the previous investigations [2, 3] a total of fifteen experiments had been carried out on male hamsters, and the results are summarised in Diagr. 1 *b*. In thirteen of those series the cancer could be carried through three to six passages; in one through seven passages; and in another through eleven passages. In the present investigation (Diagr. 1 *a*), however, the cancer was carried through as many as thirty-four passages in series 1 and through twenty-one passages in series 2 and could probably have been continued *ad infinitum*. In the third series the cancer was carried through 11 female passages but died when it was then transferred to males.

Though growth of the cancer in some of the animals was poor, it was, as a rule, better than that observed in the male hamsters. Only in one of the fifteen males series, and then only on one occasion, was the number of cancer cells collected ten times the number injected, an increase found for at

Fig. 2. Ascites cancer cells during successive passages in hamsters (Series 3). *a*, the donor mouse; *b*, the eleventh hamster passage, female; *c*, the twelfth hamster passage, male. Magnification × 880. Papanicolaou-staining.

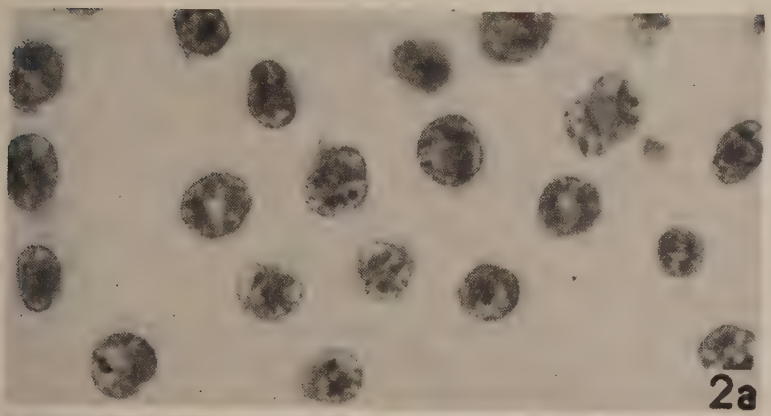
2a

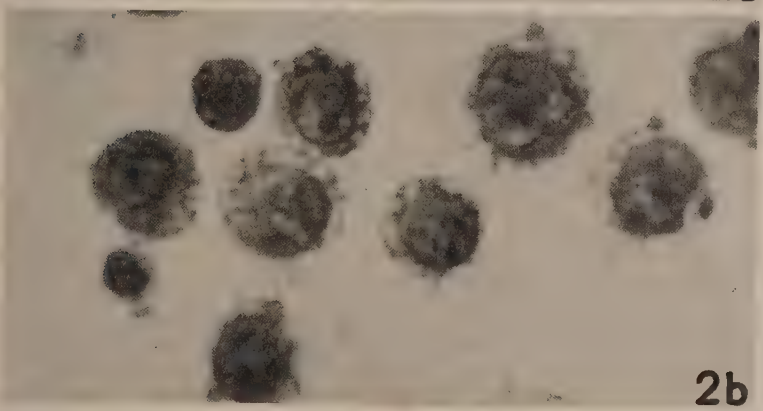
2b

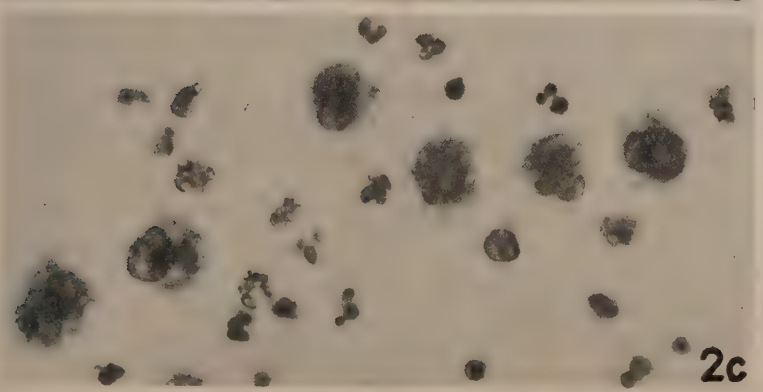
2c

least one of the animals in each of the three series of female hamsters. Only relatively seldom did the number of cells collected from the male hamsters reach twice that injected: in the females, however, an increase of at least this order was common.

That the environmental conditions in females were more favourable for growth of the cancer was also reflected by the appearance of the cancer cells, several monstruous degenerated specimens occurring already after a few passages through males, but never in the female series, where the cells were of fairly uniform appearance and only moderately enlarged (Fig. 1). In the male series the regression and death of the cancer was accompanied by a pronounced increase in the number of non-neoplastic cells. In the female series, however, this number was relatively low and showed a tendency to diminish during the successive passages (Fig. 4). In series 3, transfer of the cancer to male hamsters resulted in a rapid increase in the number of non-neoplastic cells and death of the cancer (Fig. 2).

That the results of transplantation sometimes vary with the sex of the hosts is known. Bittner [4] and Strong [10] demonstrated a difference in the incidence of takes in male and female mice inoculated subcutaneously with transplantable carcinomas. Gross [7] showed that small interdermal or intraperitoneal inoculations of sarcoma did not grow so well in females as in males. Greene [6] found the susceptibility to a papillary mammary carcinoma transplanted to the anterior chamber of the rabbit's eye to be lower in females than in males. Foulds [5] also found a sex difference in susceptibility, but in the opposite direction. However, according to Snell [9], the difference between the sexes with regard to susceptibility to most tumours is only slight or negligible.

A search of the literature failed to reveal any report of the growth of the Ehrlich mouse ascites tumour varying with the sex of the mouse. Heterologous transplantation thus revealed a latent property of the tumour and might suggest a possibility influencing the growth of the cancer. However, when the cancer has been transplanted through a sufficient number of hamster passages, its growth is no longer influenced by the sex of the hamster [3]. Once the cancer had become "hamster-adapted", it could also be carried through an apparently indefinite number of male hamsters. By that time the cancer had also undergone certain chromosomal changes, which might be responsible for the changed growth [8]. Series 3 showed that 11 hamster passages are not sufficient to produce such "hamster adaptation".

As yet, no explanation can be offered for the difference in growth of the cancer in males and females. It might be due to inherent properties of the

cancer cells or to hormonal factors stimulating growth in females and/or inhibiting growth in males. The variation in the growth of the cancer from one animal to another suggests that any such stimulation or inhibition varies cyclically and that the variation in growth might then be ascribed to the animals having been in different stages of the cyclic phase at the time of the transplantation of the cancer.

SUMMARY

In an investigation of Ehrlich mouse ascites cancer in female hamsters, in which the cancer was transmitted at three-day intervals through three series of female hamsters, the following observations were made.

1. In two series the cancer showed good vitality through thirty-four and twenty-one passages, respectively, and could apparently have been carried through an unlimited number of female hamsters. In the third series the cancer was carried through eleven female passages: it was then transferred to a male hamster and died during the subsequent male passage.

2. The cancer cells tolerated the serial transmission through *female* hamsters much better than they did in an earlier investigation on *males*, in which the yield of cancer cells successively decreased and the cancer survived only a few passages.

REFERENCES

1. Ahlström, C. G. and Ising, U., *Acta Pathol. et Microbiol. Scand.* **36**, 415 (1955).
2. —— *Lunds Universitets Årsskrift, N. F. Avd.* 2, **50**, nr 18 (1955).
3. —— *Brit. J. Cancer* (in press).
4. Bittner, J., *Am. J. Cancer* **16**, 322 (1932).
5. Foulds, L., *Brit. J. Cancer* **1**, 362 (1947).
6. Greene, H. S. N., *J. Exptl. Med.* **71**, 305 (1940).
7. Gross, L., *Proc. Soc. Exptl. Biol. Med.* **49**, 67 (1942).
8. Ising, U., *Brit. J. Cancer* (in press).
9. Snell, G. D., "Transplantable tumors" *in* Homburger and Fischman: The Physio-pathology of Cancer. Hoeber, New York, p. 338, 1953.
10. Strong, L. C., Hill, R. T., Pfeiffer, C. A., and Gardner, W. U., *Genetics* **23**, 585 (1938).

CONTRIBUTION A L'ÉTUDE DU CYTOPLASME PAR LA MICROSCOPIE A FORT GROSSISSEMENT AVEC LE DISPOSITIF ANOPTRAL

(PHOTOGRAPHIES SUR LE VIVANT ET APRÈS FIXATION OSMIQUE DE CELLULES CULTIVÉES *IN VITRO*)

J. FREDERIC

Institut d'Histologie, Université de Liège, Belgique

Reçu le 25 Novembre, 1955

Avant 1938, on concevait la substance fondamentale du cytoplasme de la manière suivante : amorphe en lumière transmise, optiquement vide à l'ultramicroscope (Mayer et Schaeffer, Levi, Lewis, etc.), elle a cependant une structure submicroscopique en trame ou en réseau, due à l'orientation particulière de certaines de ses molécules (Frey-Wyssling; Monné; Peters; etc.). Deux techniques ont apporté une contribution importante aux recherches sur cet important problème : la *centrifugation différentielle* et la *microscopie électronique*. Grâce à la première, Claude [13] a pu isoler un nouveau constituant cytoplasmique sous la forme de fins granules, les « microsomes », que de nombreux auteurs considèrent depuis comme de véritables organes cellulaires. Cette conception est cependant discutée à l'heure actuelle. Par son pouvoir élevé de résolution, le microscope électronique a permis de vérifier la présence de fines granulations microsomiales dans différents types de cellules [17, 32, 33 etc.]. On a décrit aussi un système réticulaire lâche, le « *réseau endoplasmique* », formé de filaments anastomosés [29, 31], ainsi que des structures lamellaires, appelées par certains « *ergastoplasme* ». Celles-ci ont été observées surtout dans des coupes ultrafines de cellules de foie, de pancréas et de muqueuse gastrique [18, 20, 3, 34 etc.].

Incontestablement, la microscopie électronique et la centrifugation différentielle ont apporté une contribution intéressante au problème de l'ultrastructure du cytoplasme; il faut néanmoins remarquer que ce sont des techniques assez brutales. A la première, notamment, on peut reprocher de ne permettre l'étude que de cellules fixées, déshydratées ou incluses dans une substance d'enrobage, celle-ci, à elle seule, constituant déjà une source possible d'artéfacts.

Cependant, par la *microscopie en lumière ordinaire* dans des conditions optiques favorables, Chèvremont [8] a pu distinguer une structure granuleuse dans le cytoplasme de macrophages et de fibroblastes étalés en cultures de tissus, fixés à l'osmium et colorés par l'hématoxyline ferrique. Comme le

souligne cet auteur, il est possible que le dépôt de la laque d'hématoxyline et de fer sur des structures submicroscopiques ait augmenté leur diamètre et les ait ainsi rendues décelables par les meilleurs systèmes optiques en lumière ordinaire.

L'ensemble des faits brièvement résumés ci-dessus tend donc à faire admettre qu'une structure submicroscopique existe dans le cytoplasme. Mais ces faits ont été établis par l'examen de cellules fixées. Bien que les fixateurs utilisés dans ces recherches soient pour la plupart à base d'acide osmique et que celui-ci soit considéré comme le plus fidèle [36, 8, 9, 28], la question se pose cependant de *savoir si ces structures existent dans les cellules intactes, ou encore de savoir dans quelle mesure elles ont été modifiées par la fixation.*

Plusieurs auteurs [6, 38, 8] ont étudié, par la *microscopie en contraste de phase*, le cytoplasme de cellules vivantes; même dans les conditions optiques les plus favorables, la substance fondamentale du cytoplasme intact leur est apparue homogène. Dans quelques cas, cependant, le contraste de phase négatif laissait «deviner» une certaine structure (Chèvremont — communication personnelle).

La question reste donc posée. Il nous a paru intéressant de la reprendre, à la suite de l'invention par Wilska [37] du *microscope à dispositif ANOPTRAL*, instrument nouveau qui s'est révélé supérieur, pour le problème qui nous occupe, aux systèmes habituels de contraste de phase. Il s'en distingue notamment par une réduction sensible du phénomène de halo et par son pouvoir de définition remarquablement élevé, grâce à son optique apochromatique et à sa grande ouverture numérique. Par ailleurs, la série de photographies publiée par Wilska laissait entrevoir des résultats intéressants.

Nous avons étudié et photographié à forts grossissements, avec le dispositif Anoptral, *sur le vivant ou après fixation osmique*, des cellules étalées de cultures de tissus, matériel particulièrement favorable pour l'étude fine du cytoplasme. Plusieurs fois, une même cellule a été photographiée vivante et repérée, puis fixée et photographiée à nouveau. Nos observations ont porté sur des cellules de l'embryon de Poulet : fibroblastes, myoblastes à un seul noyau et cellules épithéliales de l'intestin, ainsi que sur des cellules tumorales humaines de la souche HeLa.

MATÉRIEL ET TECHNIQUE

Cultures. Fragments de tissu conjonctif sous-cutané, de muscles squelettiques et d'intestin grêle, prélevés sur des embryons de Poulet (9-11^{e} jour d'incubation), et cultivés en goutte pendante suivant une technique que nous avons utilisée dans des recherches antérieures. Milieux nutritifs : plasma (coq) 10 %, sérum (coq) 10 %,

extrait embryonnaire 10 %, glycosol 70 % (dans le glycosol que nous utilisons, la quantité de bicarbonate de sodium a été portée à 0.5 g/litre). Les explants, de petite taille, sont disposés dans le caillot étalé en couche très mince sur des lamelles fines. Le 2e ou 3e jour après l'explantation, les cultures, vivantes ou fixées, sont montées dans du liquide de Ringer ou du glycosol (ou encore dans de l'eau distillée, pour quelques cultures fixées) et examinées immédiatement. Seules des cellules en parfait état de croissance sont observées et microphotographiées. Outre les différents types de cellules de Poulet mentionnés plus haut, nous avons étudié les cellules tumorales humaines de la souche HeLa, cultivées sur lamelles à partir d'une souche aimablement mise à notre disposition par le Prof. Nihoul (Université de Gand), à l'occasion d'un travail en collaboration avec cet auteur et J. Boddaert. Milieux utilisés : solution de Hanks, hydrolysat de lactalbumine 0,5 % et sérum (Poulain) 10 %.

Fixation soit aux vapeurs d'acide osmique, soit par le liquide de Bensley (bichromate de potassium-acide osmique 2 %, sans acide acétique, tel qu'il a été conseillé par Chèvremont; pH 5,8–6) précédé ou non de l'exposition aux vapeurs d'iode, soit encore à l'acide osmique tamponné selon Palade [28] (pH 7,2; tampon acétate de sodium-véronal sodique).

Observations directes et photographies avec le dispositif Anoptral (Reichert objectif 100 ; O.N. 1,30). Ce dispositif, inventé par Wilska [37], rappelle celui du contraste de phase; il s'en distingue cependant par plusieurs particularités dont voici brièvement l'essentiel. Comme dans le contraste de phase habituel, la lumière pénètre dans le condensateur par une ouverture annulaire mince, mais cette ouverture est ici de grand diamètre. Entre les deux dernières lentilles de l'objectif, qui est apochromatique et de grande ouverture numérique, est aussi disposé un anneau; ce dernier a ceci de particulier qu'il est fortement absorbant, contrairement à ceux des systèmes de contraste de phase, ou l'effet recherché est non pas une absorption élevée, mais essentiellement une modification de phase de la lumière. De plus, dans l'Anoptral l'anneau est constitué par une couche de substance analogue à de la suie, c'est-à-dire peu susceptible de produire des phénomènes gênants de réflexion; ceux-ci, par contre, peuvent apparaître dans les anneaux de phase habituels réalisés très souvent,

---

Fig. 1 à 3 : Images agrandies de fibroblastes vivants en culture de tissus et photographiés avec le dispositif Anoptral. Dans l'ensemble, elles se présentent comme si elles avaient été obtenues par la microscopie en contraste de phase négatif, mais avec un pouvoir de définition meilleur.
Fig. 1. Vue générale d'un fibroblaste étalé. Dans le cadre *a*, la zone de Golgi et le noyau avec deux nucléoles; en *b*, une portion de la zone moyennement étalée du cytoplasme et en *c* une portion de la zone périphérique étalée à l'extrême; il n'a pas été tenu compte de celle-ci dans nos recherches (voir texte). Les mitochondries sont bien visibles en gris clair; les quelques taches très blanches sont des enclaves lipidiques, les points noirs des vacuoles. (Gross. final : 2.400 ×.)
Fig. 2. Partie agrandie du cytoplasme d'une autre cellule. A gauche : une portion du noyau, avec sa membrane; il est entouré de chondriosomes en boules, comme c'est généralement le cas au début de la croissance *in vitro*. La substance fondamentale du cytoplasme, bien visible surtout à droite, se présente comme un ensemble de plages et de traînées d'aspect ouaté; on y voit des grains, isolés ou en groupes, et quelques très fins filaments. Les petites taches très claires sont quelques gouttelettes lipidiques. (3.400 ×, après agrandissement).
Fig. 3. Portion du cytoplasme dans une autre cellule. Une structure de la substance fondamentale y apparaît nettement sous la forme de traînées; à gauche et en haut, petite plage plus réfringente contenant quelques granulations fusionnées. Plusieurs mitochondries sont visibles dans le champ, dont une assez fine (en haut) à proximité de laquelle on distingue deux petites enclaves lipidiques. (Gross. final : 3.700 ×.)

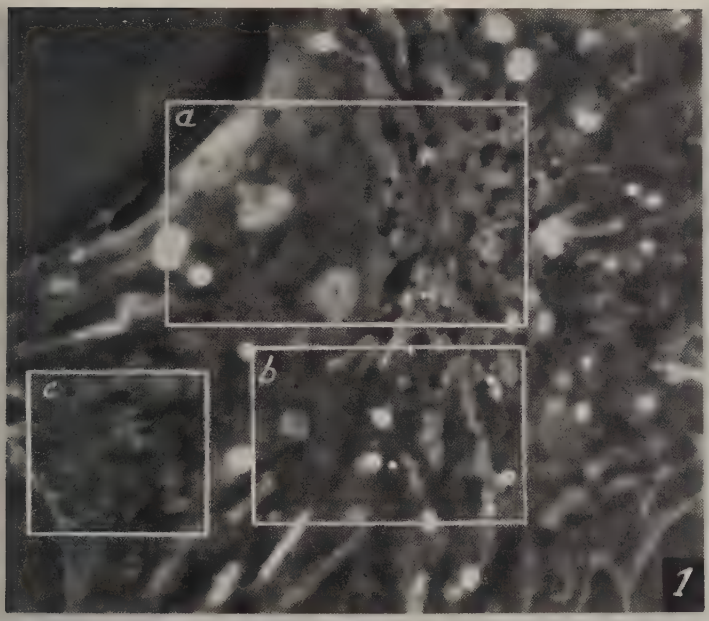
a
b
c
1

2

3

4

5

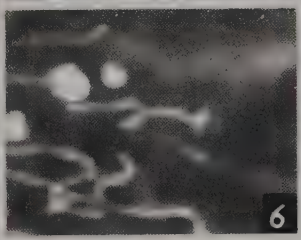
6

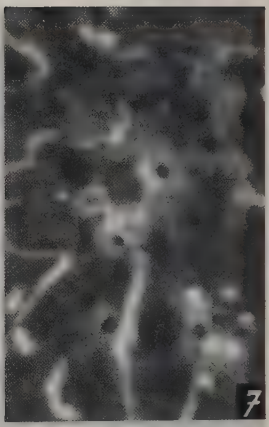
7

8

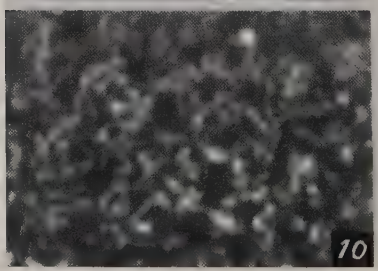
10

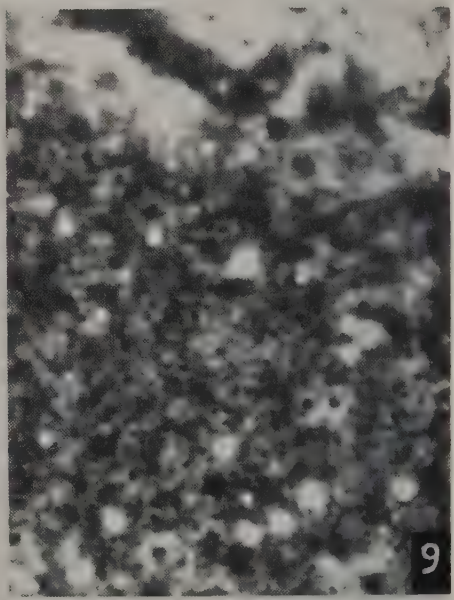
9

comme on le sait, par un dépôt métallique. Le pouvoir de définition de l'Anoptral est remarquablement élevé, les phénomènes de halo sont réduits et les images fournies très contrastées. Pour nos recherches, les photographies ont été prises sur plaques à haute définition, en lumière monochromatique et avec des temps de pose très courts; elles ont été secondairement agrandies de 2 à 5 fois, la plupart des détails et des fines structures n'étant pas visibles directement.

RÉSULTATS

Observations sur le vivant

Seule la substance fondamentale du cytoplasme sera étudiée ici; la microscopie par le dispositif Anoptral ne nous ayant révélé rien de nouveau qui mérite d'être ajouté aux descriptions antérieures de mitochondries, de membrane nucléaire et de nucléoles, avec les systèmes ordinaires de contraste de phase. Nous envisagerons successivement le cas de fibroblastes et de myoblastes ensuite celui des cellules épithéliales de l'intestin et des cellules de la souche HeLa.

Fig. 4 à 10 : Photographies de cellules vivantes (mêmes conditions que Fig. 1 à 3). Fig. 4 à 8 : fibroblastes de Poulet; figs. 9 et 10 : cellules tumorales humaines de la souche HeLa.

Fig. 4. Même aspect de la substance fondamentale que celui représenté Fig. 3. Par endroits, notamment vers le haut à droite, et à gauche vers le bas, on distingue une structure grumeleuse (3.700 × après agrandissement).

Fig. 5. Portion du cytoplasme d'une autre cellule. En-dessous du chondriosome occupant le milieu de l'image, on voit une petite formation plus réfringente, dont l'aspect rappelle celui d'un chondriosome réduit dans toutes ses dimensions. En haut (et dans la longueur de l'image), se trouve un filament très ténu et à peine visible. (3.700 ×, final.)

Fig. 6. Mêmes conditions que pour la figure précédente, mais dans une autre cellule. Noter, en haut et à droite : une zone plus réfringente de la substance fondamentale, dans laquelle on remarque des granulations à contours flous. A droite aussi, mais plus bas : un filament très fin, comparable à celui visible Fig. 5. A gauche, chondriosomes filamenteux et trois gouttelettes lipidiques très brillantes. (3.700 ×, après agrandissement.)

Fig. 7. Partie de la zone de Golgi photographiée à fort grossissement. (Le noyau se trouvait dans la partie immédiatement supérieure de l'image). Noter la présence, dans la substance fondamentale, de nombreuses granulations isolées ou plus ou moins fusionnées en petites plages plus réfringentes. On voit aussi quelques courts bâtonnets semblables à de très petites mitochondries. A gauche : chondriosomes filamenteux; un autre chondriosome, au centre de l'image, semble être plus ou moins confondu avec des groupes de grains. A droite et en bas : petit groupe de fines gouttelettes lipidiques. (Gross. final : 3.700 ×.)

Fig. 8. Vue générale de la zone de Golgi dans une autre cellule. Elle se présente comme un ensemble de petites plages plus réfringentes appuyé contre le noyau (qu'on voit en partie, à gauche, avec sa membrane). Elle est entourée de chondriosomes dont certains y pénètrent et paraissent y devenir plus flous. (3.000 ×.)

Fig. 9. Cytoplasme d'une cellule tumorale de la souche HeLa. Tout en haut, partie de la région périnucléaire, assez opaque, contenant notamment des mitochondries, peu distinctes ici. Dans la zone étalée du cytoplasme, on voit un réseau serré, à petites mailles; par endroits, ce réseau est plus dense, notamment vers le haut et vers le bas de l'image. Les petites taches brillantes sont de fines gouttelettes lipidiques. (Gross. final : 4.000 ×.)

Fig. 10. Portion plus périphérique d'une autre cellule de la souche HeLa. De haut en bas, le réseau tend à devenir plus lâche et certains de ses éléments paraissent s'isoler, en même temps qu'ils semblent devenir plus épais (voir notemment au centre de l'image). (4.000 ×.)

Fibroblastes et myoblastes.—Lorsque ces cellules sont peu ou moyennement étalées (Fig. 14), la substance fondamentale du cytoplasme se présente sous un aspect assez homogène, comparable, d'une manière générale, à celui que révèle l'optique à contraste de phase négatif. Cependant, outre la zone de Golgi dont il sera question plus loin, on y voit, par places, de petites plages légèrement plus claires, sans contours précis et dans lesquelles on ne peut que deviner une structure.

Lorsque les cellules sont bien étalées (Fig. 1), on peut y distinguer trois zones : une zone centrale assez épaisse (Fig. 1 *a*) contenant le noyau, la zone de Golgi et parfois quelques vacuoles; une zone moyenne (Fig. 1 *b*) plus transparente, assez homogène à première vue, dans laquelle se trouvent la plupart des mitochondries; et enfin une zone périphérique (Fig. 1 *c*) extrêmement mince et transparente, ne contenant pratiquement pas d'éléments figurés du cytoplasme. Dans cette portion périphérique, on distingue, tranchant nettement sur le fond, des fines bandes et des lignes parfois disposées en une sorte de réseau dont les branches principales seraient radiaires par rapport à la cellule. Il s'agit vraisemblablement, nous en avons acquis la conviction en observant l'émigration de ces cellules, de minces bandes de substance fondamentale faisant saillie dans une portion du cytoplasme étalée à l'extrême. En effet, l'aspect et la disposition de ces formations subissent d'incessants remaniements qui vont de pair avec les mouvements de déplacement de la cellule et les modifications de forme de sa portion périphérique. Par contre, la zone moyenne reste apparemment plus rigide : son aspect général ne change que peu et lentement, indépendemment, semble-t-il, des mouvements d'émigration. C'est sur cette zone moyenne que nous avons porté notre attention, notamment parce qu'il nous a paru qu'en cet endroit, l'épais-

---

Fig. 11. Photographie à très fort grossissement, avec le dispositif Anoptral, des débris cytoplasmiques d'un fibroblaste tué par écrasement pendant l'observation. La substance fondamentale s'est altérée et s'est répandue dans le milieu environnant, sur une surface assez grande; seule, une petite partie de cette dernière est représentée ici. On aperçoit une multitude de très fins grains assez réfringents, disposés en ligne ou par petits groupes; le diamètre de ces particules est compris entre 0,1 et 0,2μ. (4.800 ×, après agrandissement.)

Fig. 12. Partie du cytoplasme d'un fibroblaste étalé, fixé aux vapeurs d'acide osmique et photographié avec l'Anoptral. La substance fondamentale n'a plus le même aspect que sur le vivant; on y voit un réticulum dont les branches, courtes, sont d'épaisseur sensiblement régulière. Les chondriosomes paraissent assez bien conservés; leur structure semble cependant être devenue légèrement granuleuse. (3.700 ×, après agrandissement.)

Fig. 13. Zone de Golgi, après fixation par les vapeurs d'acide osmique, photographiée avec le dispositif Anoptral. Dans la zone de Golgi, au centre de l'image, est apparu un réticulum assez semblable à celui du cytoplasme environnant, mais plus réfringent, et à plus grosses mailles. (Comparer avec l'aspect sur le vivant, Fig. 8.) Le noyau, visible à gauche avec son nucléole, semble assez bien conservé. (3.400 ×, final.)

seur du cytoplasme correspondait aux conditions optiques optimales du dispositif Anoptral.

Si l'observation directe révèle assez peu de détails, les agrandissements photographiques, par contre, mettent en évidence une nette hétérogénéité de la substance fondamentale (Fig. 2 à 6). Celle-ci apparaît comme formée

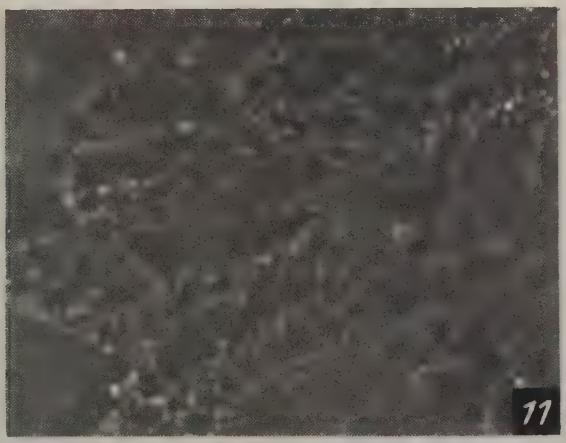

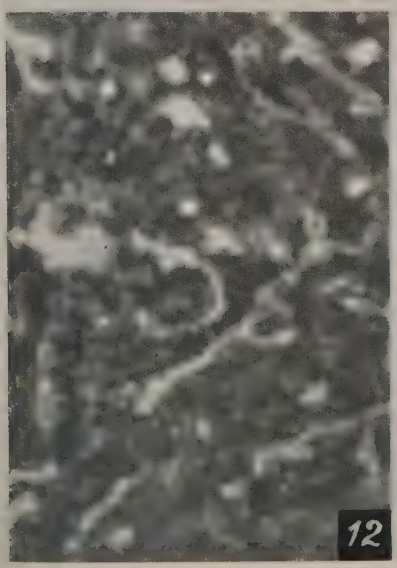

d'un ensemble de traînées ou de plages d'aspect ouaté et à contours imprécis, se détachant sur un fond moins réfringent. Ces formations, qui ne paraissent pas avoir de direction privilégiée, sont souvent disposées en réseaux à mailles assez lâches (Fig. 3). Leur constitution ne semble pas homogène; par endroits, en effet, on peut y distinguer des filaments (Fig. 2) et des grains. Certains de ces filaments, un peu plus épais et mieux visibles que les autres (Fig. 5 et 6) prennent l'aspect de chondriosomes dont le diamètre serait fortement

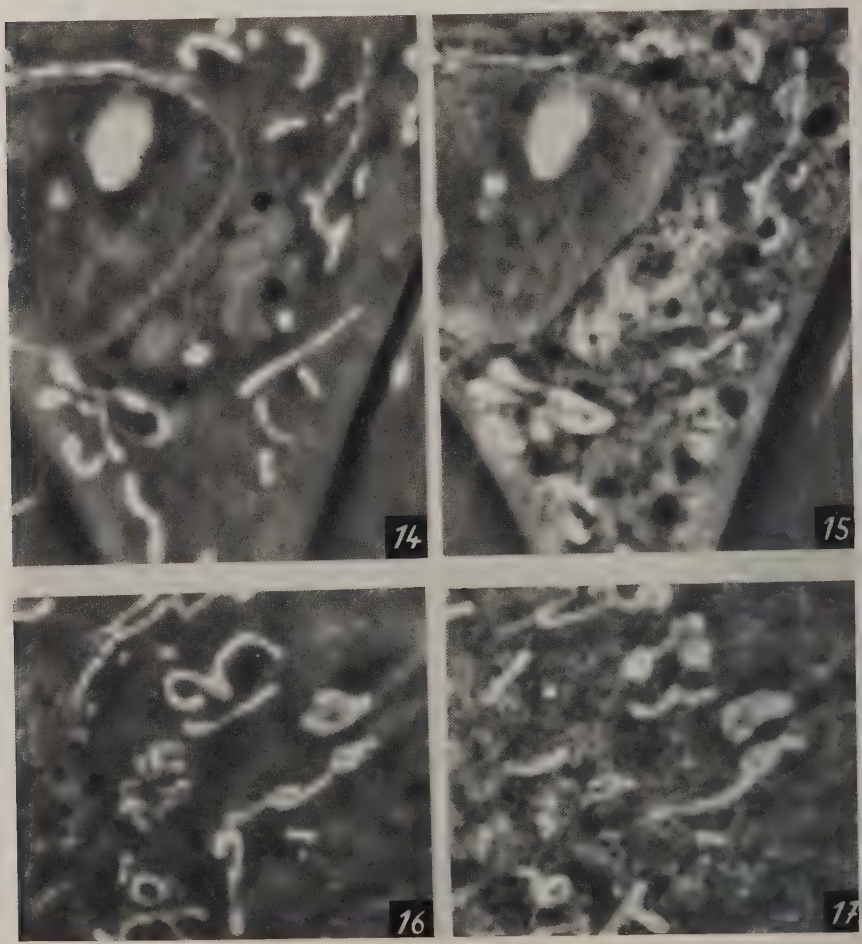

réduit. Quant aux grains, ils sont de taille variable, très souvent groupés et plus ou moins fusionnés (Fig. 3 et 6), donnant par place un aspect grumeleux; plus rarement, ils apparaissent mieux individualisés (Fig. 2). Ils ne peuvent être, dans ce cas, confondus avec les fines et rares enclaves lipidiques éventuellement présentes dans le cytoplasme; celles-ci s'en distinguent par leur taille plus grande et leur réfringence notablement plus élevée [Fig. 3]. Les chondriosomes, bien reconnaissables sous les différentes formes que nous avons décrites dans des publications antérieures avec M. Chèvremont [11, 13], sont fréquemment en rapport direct avec ces structures cytoplasmiques, soit qu'ils se trouvent en leur sein, soit encore qu'ils entrent en contact avec elles en plusieurs points (Fig. 3 à 6).

Plusieurs fois, en écrasant la cellule pendant l'observation, nous avons pu voir le cytoplasme être détruit et s'épandre dans le milieu environnant; le phénomène est extrêmement rapide. Des photographies à très forts grossissements des débris cytoplasmiques (Fig. 11) montrent une quantité de très fins grains, de dimensions assez uniformes, disposés en ligne ou par petits groupes. Mesuré sur les agrandissements photographiques, le diamètre de ces grains serait compris entre 0,10 et 0,20 micron; par leur petite taille, ils semblent se distinguer des granulations que nous avons signalées plus haut (comparer la Fig. 2, grossissement 3.400 ×, avec la Fig. 11, grossissement 4.800 ×).

Dans la cellule intacte, la *zone de Golgi* se voit particulièrement bien avec le dispositif Anoptral. Elle se présente comme un ensemble de petites plages de forme irrégulière, nettement plus réfringentes que la substance fondamentale (Fig. 8). Ces petites plages sont groupées dans une aire entourée de chondriosomes et très souvent appuyée contre le noyau. A forts grossissements

---

Fig. 14 à 17. Deux fibroblastes photographiés (dispositif Anoptral) sur le vivant, puis fixés à l'osmium et photographiés à nouveau (dans du Ringer).

Fig. 14. Aspect sur le vivant. La cellule est moyennement étalée. Outre le noyau, à gauche, et les mitochondries, on voit la zone de Golgi (au centre de l'image) sous la forme d'un ensemble de petites plages claires. Le cytoplasme n'étant pas suffisamment mince, la structure de la substance fondamentale n'est pas bien visible ici; par places, cependant, on distingue des traînées un peu plus réfringentes et d'aspect ouaté.

Fig. 15 La même cellule après fixation au liquide de Bensley (sans acide acétique). Il y a un peu de rétraction cellulaire; les chondriosomes et le noyau paraissent bien conservés, bien que ce dernier ait perdu sa transparence. Le cytoplasme est devenu plus réfringent dans l'ensemble et on y voit une sorte de réseau assez grossier; quelques vacuoles y sont apparues (taches noires). La zone de Golgi est devenue plus compacte et semble être maintenant formée d'une masse composée de grosses granulations accolées. (3.400 ×, après agrandissement.)

Fig. 16. Aspect d'une portion de cytoplasme dans un fibroblaste vivant, quelques minutes avant la fixation.

Fig. 17. La même région après fixation à l'acide osmique tamponné selon Palade. La substance fondamentale a pris un aspect réticulé. (3.500 ×, final.)

et dans les cellules bien étalées, elles montrent une structure nettement granuleuse (Fig. 7). Par leur forme et leur aspect, elles se présentent comme s'il s'agissait aussi de petites traînées de substance fondamentale cytoplasmique, telles que nous les avons décrites plus haut, mais qui seraient rendues mieux visibles par le nombre de granulations plus réfringentes. Certains chondriosomes qui pénètrent dans la zone de Golgi, semblent s'y fondre et se confondre avec les amas de grains. En outre, on peut observer la présence de courts bâtonnets très réfringents, fort semblables à de très petits chondriosomes (Fig. 7).

Cellules épithéliales de l'intestin grêle.—Au point de vue optique, ce matériel est moins favorable pour le problème qui nous occupe. Le cytoplasme de ces cellules manifeste moins de tendance à s'étaler et reste toujours relativement épais. Cependant, nous avons pu y distinguer et photographier les mêmes structures que celles décrites plus haut dans les fibroblastes, bien que moins nettement visibles.

Cellules de la souche HeLa.—Le cytoplasme revêt ici un aspect très différent de celui présenté par les fibroblastes. Il est bien observable surtout dans les parties minces de la cellule, où les mitochondries sont absentes; celles-ci, assez grosses, sont souvent groupées dans la région nucléaire. Outre quelques petites granulations lipidiques assez dispersées, on y voit (Fig. 9) une sorte de dispositif réticulé à petites mailles tranchant nettement sur un fond fort peu réfringent et à peine visible. Les mailles paraissent être formées de bâtonnets de 0,1 à 0,2 micron de diamètre (mesuré sur agrandissement photographique). Par endroits, le réseau devient plus dense et prend alors la forme de masses plus compactes, notamment dans la zone entourant la région nucléaire. Parfois, au contraire, et surtout dans la zone périphérique du cytoplasme, les mailles du réseau s'élargissent; certains éléments de celui-ci paraissent mieux isolés, plus longs et légèrement plus épais; ils ont alors la forme de filaments plus ou moins onduleux, avec des branches latérales (Fig. 10). Bien que, par leur forme, ces éléments puissent faire songer à des chondriosomes, ils s'en distinguent cependant par leur taille très nettement inférieure ainsi que par leur abondance.

Observations après fixation a l'acide osmique

Les trois fixateurs à base d'acide osmique que nous avons utilisés (acide osmique sous la forme de vapeurs; en solution tamponnée; ou selon la formule de Bensley, mais sans acide acétique) donnent des images sensiblement équivalentes, sauf peut-être le liquide de Bensley lorsqu'il est précédé de l'expo-

sition aux vapeurs d'iode. Celui-ci donne, semble-t-il, des résultats un peu plus grossiers.

Les altérations que provoque la fixation par l'acide osmique sont bien mises en évidence par les expériences où une même cellule a été photographiée vivante, avec le dispositif Anoptral, puis re-photographiée ensuite dans les mêmes conditions, mais après fixation (Fig. 14 à 17). D'une manière générale, il y a peu de rétraction cellulaire, et le chondriome est assez bien conservé, sinon qu'il prend parfois un aspect grumeleux; le noyau perd sa transparence et donne une image granulaire. Mais c'est surtout le cytoplasme qui change d'aspect (Fig. 12); dans l'ensemble, il devient sensiblement plus réfringent, phénomène particulièrement net lorsque les cellules sont peu ou moyennement étalées (Fig. 14 et 15). Dans tous les cas, la substance fondamentale se présente sous l'aspect d'un réticulum dont les branches sont courtes et d'épaisseur sensiblement régulière. C'est ce réticulum, plus ou moins lâche suivant les endroits mais en général assez serré, qui confère au cytoplasme une réfringence plus élevée après fixation. La zone de Golgi, elle aussi, change d'aspect. Elle se transforme soit en une masse d'apparence compacte, mais en réalité formée par un ensemble de gros grains accolés, soit en une sorte de réseau irrégulier, assez semblable à celui qui est apparu dans le cytoplasme, mais mieux marqué, à plus grosses mailles et surtout plus réfringent (Fig. 13). On y observe parfois aussi quelques vacuoles de taille variable, le plus souvent assez petites, qui n'existaient pas avant la fixation.

DISCUSSION

De l'ensemble de nos observations avec le dispositif Anoptral sur le matériel particulièrement favorable que représentent des cellules étalées de cultures de tissus, on peut affirmer qu'une certaine structure de la substance fondamentale du cytoplasme intact est visible sur le vivant. Grâce aux propriétés remarquables de ce système optique, surtout lorsqu'il est utilisé en lumière sensiblement monochromatique, l'analyse a pu être poussée presque jusqu'aux limites théoriques de résolution du microscope optique, puisque nous avons pu distinguer nettement des particules dont le diamètre est de l'ordre de 0,10 à 0,20 micron.

Mais il est encore difficile à l'heure actuelle d'interpréter les images que nous avons décrites dans les cellules vivantes et de les mettre en relation avec ce qu'on connaît de la structure submicroscopique du cytoplasme d'après les résultats apportés par la centrifugation différentielle et la microscopie électronique. Après que Claude [13, 14], et d'autres auteurs ensuite, eurent

isolé les microsomes sous la forme de fins granules cytoplasmiques, par la centrifugation de cellules hépatiques, la question s'est posée de savoir si ces particules correspondaient bien à une entité morphologique de la cellule vivante en bon état. Les microsomes seraient reconnaissables au microscope à fond noir sous un intense éclairage latéral [16, 20], mais invisibles dans des cellules vivantes intactes examinées en lumière transmise ou en contraste de phase [8, 38]. Par contre, ils ont été retrouvés sur des microphotographies électroniques de différents types de cellules [16, 17] et sur des microphotographies en lumière ordinaire de macrophages et de fibroblastes étalés de culture de tissus, fixés à l'osmium et colorés à l'hématoxyline ferrique [8, 10]. Signalons enfin que la vitesse de centrifugation généralement choisie pour l'isolement des microsomes paraît assez arbitraire; en utilisant des vitesses successives et rapprochées, plusieurs auteurs [7] ont montré qu'on obtenait des «granules» différents non seulement par leur taille, mais aussi par leurs propriétés biochimiques. Récemment, Bernhard, Gautier et Rouiller [4], en comparant les résultats obtenus par la centrifugation différentielle et ceux apportés par la microscopie électronique, pensent que les microsomes ne correspondent pas à une entité morphologique préexistante et qu'ils sont un mélange d'éléments cytoplasmiques partiellement altérés. Nous apportons un argument à cette hypothèse puisque en observant la destruction, par écrasement, de fibroblastes vivants, on voit apparaître une multitude de très fins grains dont le diamètre serait compris entre 0,10 et 0,20 micron, ce qui correspond aux dimensions généralement admises pour les microsomes (0,05 à 0,20 μ). Sans vouloir nier l'existence de granulations d'ordre submicroscopique dans la cellule vivante en bon état, on peut se demander si les petits grains observés après écrasement de la cellule ne sont pas le résultat de l'altération de la substance fondamentale consécutive à la mort cellulaire. Peut être donc les « microsomes » ne seraient-ils que la transformation en grains du cytoplasme altéré, tout au moins dans les fibroblastes. Cela n'exclut pas qu'ils puissent exister réellement dans certains types de cellules, les macrophages étalés, par exemple, ainsi qu'on peut le voir sur les microphotographies publiées par Chèvremont [8]. On peut se demander encore si les très petites particules que nous avons vu apparaître après destruction de la substance fondamentale n'y étaient pas préexistantes. Nous ne le pensons pas. Les granulations, que nous avons signalées par endroits dans la substance fondamentale, se distinguent des microsomes par leur nombre réduit et surtout par leur taille sensiblement plus grosse; leur signification sera discutée plus loin.

D'autre part, malgré l'excellent pouvoir de résolution du dispositif Anoptral,

nous n'avons pu retrouver dans les fibroblastes et les cellules intestinales examinées vivantes, aucune image superposable aux structures submicroscopiques mises en évidence par la microscopie électronique et dont les plus grosses, au moins, pourraient être visibles avec l'Anoptral. Nous n'avons pu y voir ni le réticulum endoplasmique, système de filaments anastomosés tel qu'il est décrit par Porter et ses collaborateurs [31] dans des cellules normales et tumorales, ni les structures lamellaires (ergastoplasme) signalées dans des coupes ultra-fines de cellules glandulaires ou non [18, 19, 3, 34]. Mais il faut remarquer que ces structures ont été décrites dans des cellules fixées (nécessairement pour la microscopie électronique), par l'acide osmique en particulier. Comme on le sait, l'acide osmique a été reconnu, jusqu'à présent, comme le fixateur donnant des images sensiblement équivalentes, à l'échelle microscopique, à celles appréciables sur le vivant en fond noir [36] ou en contraste de phase [6, 8, 10]. C'est encore le même fixateur qui s'est révélé le meilleur pour la microscopie électronique [32, 30, 2], surtout lorsqu'il est utilisé en solution tamponnée [28]. Cependant, d'après nos photographies à forts grossissements de fibroblastes fixés par l'acide osmique dans différentes conditions, et surtout d'après les images comparées d'une même portion de cytoplasme avant et après fixation, il semble bien que le traitement par l'acide osmique modifie la structure submicroscopique de la substance fondamentale. Notamment, il y rend décelable, par le dispositif Anoptral un système réticulaire qui n'était pas visible sur le vivant. On peut se demander jusqu'à quel point il n'y a pas analogie entre le réseau que nous avons vu apparaître lors de la fixation à l'acide osmique et les dispositifs réticulés observés sur des photographies électroniques de cellules traitées par le même fixateur. D'ailleurs, on n'observe pas de structures réticulaires ou en lamelles dans des microphotographies électroniques effectuées sur des coupes non fixées de foie traité par la méthode du freezing-drying [24].

Dans la substance fondamentale vivante et intacte, nous avons signalé la présence, par endroits, de granulations le plus souvent groupées, à contours peu nets et plus ou moins fusionnées, ainsi que celle de très fins filaments réfringents assez semblables à des chondriosomes dont le diamètre serait fortement réduit. Peut-être s'agit-il là, du moins en partie, d'une forme d'ultrachondriome [26, 27] ou encore de matériaux figurés submicroscopiques à partir desquels s'édifierait la "matière" mitochondriale lorsque le chondriome augmente de volume, soit spontanément [23] soit expérimentalement [21, 22]. Des recherches en cours apportent un argument à cette hypothèse. Comme l'ont montré Chèvremont et Chèvremont-Comhaire [11], l'adrénochrome ajouté à des cultures de tissus provoque, outre une inhibition préprophasique

de la mitose, la formation et l'accumulation dans la cellule d'un nombre élevé de chondriosomes globuleux. En reprenant ces expériences par l'observation avec l'Anoptral, nous avons pu constater que, dans de telles cellules, la substance fondamentale était devenue invisible autour des masses de chondriosomes accumulés, comme si elle avait été «épuisée» par la formation d'un nombre surabondant de mitochondries. Inversement, on peut se demander si les grains et fins filaments de la substance fondamentale ne constituent pas aussi la forme submicroscopique sous laquelle passent les chondriosomes lorsqu'on les voit disparaître à l'observation au contraste de phase (dans des cellules intercinétiques [23]; au cours des premières phases de la mitose [12]).

La *zone de Golgi* se voit particulièrement bien sur le vivant avec l'Anoptral. Dans l'ensemble, nos observations concordent avec celles qui ont été données antérieurement par la microscopie en contraste de phase (voir notamment Chèvremont [10]); cependant, nous avons pu y ajouter quelques points de détail intéressants. Il semble bien, d'après nos photographies, que la zone de Golgi ne se différencie morphologiquement du cytoplasme environnant que par une réfringence plus élevée, due notamment à la présence de grains eux-mêmes plus réfringents, au sein de la substance fondamentale. Nous ne pouvons préciser la nature de ces particules, mais peut-être y a-t-il un rapprochement à faire avec les «Golgi bodies» que Baker [1] a reconnus sur le vivant dans des cellules intestinales, ou encore avec les «grains de Golgi» décrits par Sjöstrand et Hanzon [35] sur des microphotographies électroniques de cellules pancréatiques. Un fait intéressant est la présence, outre les granulations, de petits bâtonnets réfringents comparables à de très courtes mitochondries, ainsi que celle de formations dont l'aspect serait celui de mitochondries, mais moins nettes de contours et plus ou moins confondues avec des groupes de grains. Rappelons aussi la présence constante de chondriosomes autour de la zone de Golgi; certains même y pénétrant et paraissant s'y fondre. Ces images suggèrent à nouveau l'existence de rapports étroits entre les chondriosomes et le matériel de Golgi. Des microphotographies électroniques récentes [35, 25] n'ont fourni aucun renseignement à ce sujet; mais les observations sur le vivant ont l'avantage de porter sur un espace à trois dimensions que ne peuvent envisager des coupes ultra-fines non sériées. En outre, se pose le problème de la fixation déjà évoqué plus haut et qui s'applique aussi à la zone de Golgi, puisque l'acide osmique modifie la structure de celle-ci, comme nous avons pu le voir avec le dispositif Anoptral.

Nous ne pouvons expliquer, jusqu'à présent, les très fines formations d'aspect réticulé observées dans les cellules tumorales vivantes de la souche

HeLa. Il est possible qu'il s'agisse de formations comparables à celles décrites par Porter et Thompson [33] dans des microphotographies électroniques de sarcome de rat et que Oberling et son école [26, 27] considèrent comme l'ultrachondriome, celui-ci étant, comme on le sait, très abondant dans des cellules en croissance rapide. Il y a en effet une analogie assez frappante entre les images publiées par Porter et Thompson et les nôtres. Enfin, on ne peut exclure l'hypothèse que ces formations soient de nature virusale.

RÉSUMÉ

1. La substance fondamentale cytoplasmique de différents types de cellules (fibroblastes et cellules épithéliales de l'intestin de Poulet; cellules tumorales humaines de la souche HeLa) a été étudiée avec le dispositif optique Anoptral. Celui-ci s'est révélé supérieur au contraste de phase, notamment par son pouvoir de définition plus élevé. Les cellules ont été observées et photographiées à forts grossissements, *vivantes* ou *après fixation à l'acide osmique* dans différentes conditions (sous forme de vapeurs; en solution tamponnée; associé à du bichromate de potassium). Plusieurs fois, une même cellule a été photographiée vivante et repérée, puis fixée et photographiée à nouveau.

2. Dans les fibroblastes et myoblastes *vivants* et en bon état, la substance fondamentale paraît hétérogène. Elle se présente comme formée d'un ensemble de traînées ou de plages d'aspect ouaté et à contours imprécis se détachant sur un fond moins réfringent. Ces formations contiennent, par endroits, des granulations souvent groupées et plus ou moins fusionnées, ainsi que des filaments dont l'aspect rappelle celui de chondriosomes dont le diamètre serait fortement réduit. L'aspect de la substance fondamentale, tel que nous l'avons observé, ne semble pas correspondre avec ce qui a été décrit au microscope électronique après fixation et déhydratation.

Il est possible que les grains et filaments constituent le matériel submicroscopique à partir duquel s'édifient les chondriosomes, ou la forme sous laquelle passent ceux-ci lorsqu'ils disparaissent à l'observation en contraste de phase habituel.

Les mêmes aspects peuvent être retrouvés dans les cellules épithéliales de l'intestin. Par contre, le cytoplasme des cellules tumorales de la souche HeLa se présente d'une manière différente. On y voit une sorte de dispositif réticulé à petites mailles, de densité variable, tranchant nettement sur un fond peu réfringent et à peine visible. Par endroits, certains éléments du réseau apparaissent mieux isolés; ils prennent alors la forme de filaments courts, assez

onduleux et ténus. Peut-être est-ce là une forme d'ultrachondriome, particulièrement abondant dans des cellules en croissance rapide.

3. Dans les fibroblastes vivants et bien étalés, la *zone de Golgi*, nettement visible, ne semble se distinguer morphologiquement du cytoplasme environnant que par la présence de grains et de bâtonnets plus réfringents dans la substance fondamentale. On y voit aussi des formations dont l'aspect serait celui de mitochondries, mais moins nettes de contours et plus ou moins confondues avec des groupes de grains. Les images observées suggèrent à nouveau l'existence de rapports étroits entre les chondriosomes et le «matériel» de Golgi.

4. Lorsque des fibroblastes vivants sont détruits par écrasement pendant l'observation, on voit apparaître une multitude de très fins grains de 0,1 à 0,2μ de diamètre. Il est possible que ces grains correspondent aux «microsomes» et que ceux-ci ne constituent, tout au moins pour les fibroblastes, qu'une transformation en grains de la substance fondamentale altérée.

5. La *fixation par l'acide osmique*, dans toutes les conditions étudiées, semble modifier la structure de la substance fondamentale, notamment en y rendant décelable par l'Anoptral, un réseau qui n'était pas visible sur le vivant. On peut se demander jusqu'à quel point il n'y a pas analogie entre ce réseau et les dispositifs réticulés ou lamellaires observés sur des microphotographies électroniques de cellules traitées par le même fixateur, considéré jusqu'ici comme le meilleur.

SUMMARY

1. In various cell types, the cytoplasmic ground substance has been studied and photographed in the living condition and after fixation, with a new optical system (Anoptral) superior to ordinary phase contrast by its high resolving pover.

2. In living chick fibroblasts and intestinal epithelial cells, the ground substance does not appear homogenous; trails of cloudy material are seen on a less refringent background. Thin filaments and granulations are also visible; these may be the "submicroscopic" material from which mitochondria are built. This configuration does not seem to correspond to what has been described with the electron microscope.

3. In the Golgi zone, the observations suggest close relationships between mitochondria and the Golgi material.

4. When living ground substance is destroyed by crushing, a large number of very fine grains (0.1 to 0.2μ) appear. These grains may correspond to iso-

lated "microsomes"; they may represent a form taken by altered ground substance.

5. Cytoplasm of the HeLa cancer strain has an appearance very different from that of normal fibroblasts.

6. Fixation by osmium tetroxide, even under the best conditions, seems to modify the structure of the ground substance, inasmuch as it is followed by the appearance of a network not visible in the living cell.

REFERENCES

1. Baker, J. R., *Quart. J. Microscop. Sci.* **90**, 293 (1949).
2. Bernhard, W., *Bull. microscop. appl.* **5**, 12 (1955).
3. Bernhard, W., Gautier, A., et Oberling, Ch., *Compt. Rend. Soc. Biol.* **145**, 566 (1951).
4. Bernhard, W., Gautier, A., et Rouiller, C., *Arch. Anat. microscop.* **43**, 236 (1954).
5. Bernhard, W., Haguenau, F., Gautier, A., et Oberling, Ch., *Z. Zellforsch.* **37**, 281 (1952).
6. Buchsbaum, R., *Anat. rec.* **102**, 19 (1948).
7. Chantrenne, H., *Biochim. et Biophys. Acta* **1**, 437 (1947).
8. Chèvremont, M., *Bull. Acad. Med. Belg.* **15**, 29 (1949–50).
9. —— Notions d'Histologie. Desoer ed., Liège, 1947.
10. —— Notions de Cytologie et Histologie. Desoer ed., Liège, 1955–56.
11. Chèvremont, M. et Chèvremont-Comhaire, S., *Arch. Biol.* **64**, 399 (1953).
12. Chèvremont, M. et Frederic, J., *Arch. Biol.* **63**, 259 (1952).
13. Claude, A., *Science* **87**, 467 (1938).
14. —— *Science* **91**, 77 (1940).
15. —— *Biol. Symposia* **10**, 111 (1943).
16. —— *J. exptl. Med.* **84**, 51 (1946).
17. Claude, A., Porter, K. R., et Pickels, G., *Cancer Research* **7**, 421 (1947).
18. Dalton, A. J., *Am. J. Anat.* **89**, 108 (1951).
19. Dalton, A. J. et Felix, M. D., *Am. J. Anat.* **92**, 277 (1953).
20. Dalton, A. J., Kahler, H., Striebich, M. J., et Lloyd, B., *J. Natl. Cancer Inst.* **11**, 439 (1950).
21. Frederic, J., *Compt. Rend. Ass. Anat.* 40e réunion (1953).
22. —— *Ann. N.Y. Acad. Sci.* **58**, 1246 (1954).
23. Frederic, J. et Chèvremont, M., *Arch. Biol.* **63**, 109 (1952).
24. Gersh, I., Bondareff, W., Finck, H., Isenberg, I., et Stephenson, J. L., *Compt. Rend. Congr. Internatl. Anat.*, Paris, 82 (1955).
25. Haguenau, F., *Bull. Microscop appl.* **5**, 18 (1955).
26. Oberling, Ch., Bernhard, W., Fevre, H., et Harel, J., *Rev. Hematol.* **6**, 395 (1951).
27. Oberling, Ch., Bernhard, W., Guerin, M., et Harel, J., *Bull. Cancer* **37**, 97 (1950).
28. Palade, G. E., *J. exptl. Med.* **95**, 285 (1952).
29. Palade, G. E. et Porter, K. R., *Anat. Rec.* **112**, 370 (1952).
30. Policard, A., Bessis, M., et Bricka, M., *Bull. Microscop. appl.* **2** (3–4), 29 (1952).
31. Porter, K. R., *J. exptl. Med.* **97**, 727 (1953).
32. Porter, K. R., Claude, A., et Fullam, E., *J. exptl. Med.* **81**, 161 (1945).
33. Porter, K. R. et Thompson, H. P., *Cancer research*, **7**, 431 (1947).
34. Sjöstrand, F. S. et Hanzon, V., *Exptl. Cell Research*, **7**, 393 (1954).
35. — *Exptl. Cell Research*, **7**, 415 (1954).
36. Strangeways, T. P. S. et Canti, R. G., *Quart. J. Microscop. Sci.* **71**, 1 (1927).
37. Wilska, A., *Mikroskopie*, **9**, 1 (1954).
38. Zollinger, H. U., *Mikroskopie*, **3**, 1 (1948).

MICROAQUARIA FOR TIME-LAPSE CINEMATOGRAPHIC STUDIES OF MORPHOGENESIS IN SWIMMING LARVAE AND OBSERVATIONS ON SEA URCHIN GASTRULATION

T. GUSTAFSON and H. KINNANDER

The Wenner-Gren Institute for Experimental Biology, University of Stockholm, Sweden

Received November 27, 1955

The purpose of a developmental physiologist is often to map the biochemical and cell physiological processes in embryos of different stages of development and to follow the manner in which these "molecular" processes are translated into morphological terms at the level of cells, tissues, organs, and whole organisms. At present much attention is given to the former part of this program, but, on the other hand, little is known about the mode in which the biochemical processes operate in moulding the shape of the embryo. This disproportionately large difference is no doubt due to our incomplete knowledge of the morphological events themselves, e.g., of the morphological behaviour of individual cells during the process of gastrulation. The work of Holtfreter [1], for instance, demonstrates that much can be learned in this field from experimental work with fragmented blastema or isolated and recombined individual cells. Time-lapse cinematography of intact, transparent larvae offers another means of attacking problems of morphogenesis, and it has successfully been used in a number of cases.

The transparency of the sea urchin larva, as well as many other marine larvae, makes them well suited for a time-lapse cinematographic analysis of gastrulation, but their rapid axial spin and other swimming movements offer serious obstacles to this mode of approach. The present paper describes a method which largely overcomes these obstacles, and by means of which the larvae can be kept in a more or less constant position for at least 12 hours.[1]

Microaquaria for Continuous Study of Larvae in a Fixed Position

The device consists of a strip of nylon net ("Nytal", obtained from Swiss Silk Bolting Mfg. Co. Ltd., Thal, Switzerland) inserted between the coverglass and the slide. The meshes together with the slide and the coverglass

[1] A brief note on this subject was published by these authors in *Experimental Cell Research* **10**, 733 (1956).

form a series of "microaquaria" for single larvae. If a drop of a blastula suspension is placed on the wetted nylon net, supported by a slide, the larvae will be individually caught in the microaquaria when the coverglass is placed in position.

The number of the nylon net used in the present study was "10/130", i.e., it has a mesh opening of 130 μ. Nylon nets with other mesh openings, from 1130 down to 85 μ, are also commercially available from the same manufacturers. The mesh opening chosen was wide enough to permit the slight expansion of the blastula which takes place during gastrulation. In order to prevent swimming movements of the larvae, crystals of calcium carbonate were deposited on the nylon threads, which thereby attained the appearance of barbed wire (Fig. 1). The crystals caused slight local depressions in the blastula without seriously disturbing its general volumetric expansion or ciliar movements, and kept the larva in a more or less constant position for many hours (cf. Figs. 5, 6, 8). The device permitted the larva to exhibit slow or occasional movements connected with its volumetric changes. In this way abnormal tensions in the blastula were generally kept at a minimum. If the expansion of the larva was great, the object was partially pressed out from the microaquarium into the narrow spaces between the net and the glass surfaces, formed by crystals protruding from the net plane. It remained, however, close to its previous position, the mesh serving as an "egg-cup" which pressed the larva against the glass. In all these cases, the movements of the larvae were so slow that the time-lapse record was not seriously disturbed.

The crystals were obtained by boiling a piece of net (10×25 mm) in calcium bicarbonate-rich water, e.g., in a solution of pure $CaCl_2$ and $NaHCO_3$, or even in Ca-rich tap water (0.0006M Ca). In order to obtain good crystals, the beaker has to be washed with acid between the different preparations. Otherwise the crystals will form mainly on the crystal germs on the beaker instead of on the nylon net. The net should be put into the water already from the beginning of the heating. Factors determining the rate of crystallization evidently determine the shape of the crystals, which can thus be obtained in a more or less predictable form. Rapid crystallization, e.g. in vigorously heated 40 ml 0.05M $CaCl_2$ 0.05M $NaHCO_3$ solution, gave rise to a crust of short crystals on the threads. Slow heating, starting, e.g., with 60 ml 0.016M reagents, gave separate long crystals of needle-like appearance. Very often both short and long crystals complexes were formed. After the net was prepared, it was gently washed in a stream of sea water and then stored in sea water until use.

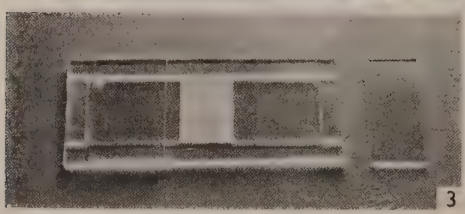

Figs. 1–3. Device for keeping marine larvae in a constant position for time-lapse studies of their development.
Fig. 1. Nylon net for the microaquaria, with crystals of calcium carbonate. Mesh opening 130 μ. Fig. 2. Device for continuous change of water in the microaquaria. To the left (*a*) the filter paper strip for off-flow, to the right (*b*) the water cuvette and the filter paper strip for on-flow.

Fig. 3. Slide with net and coverglass. Additional glass strips keep the ends of the filter paper strips in steady contact with the ends of the coverglass. For convenience, the glass strip on the right is unfixed so that it can be placed in position above the wetted filter paper on-flow strip. The glass strip on the left is fixed, and the off-flow filter paper strip is inserted below it, while still dry and rigid.

As both the size of the mesh opening and the shape of the crystals can be varied with great amplitude, this technique can be used for the study of objects of various dimensions.

In order to insure a continuous supply of oxygen and a drainage of waste products in the microaquaria, a stream of sea water was gently passed between the slide and the coverglass. The water came from a cuvette fixed to the right end of the slide by means of modelling clay. The water in this cuvette was automatically maintained at a constant level by the water supply from a Mariotte flask (Fig. 4). A strip of thick porous filter paper with the dimensions of 20 × 80 mm siphoned the water from the cuvette to the edge of the coverglass (Fig. 2, right), and another strip, usually a double one, insured a continuous off-flow from the other end of the coverglass into a beaker (Fig. 2, left) cf. [2]. The strip for on-flow was carefully washed by siphoning with sea water before use, and was protected from evaporation by means of pieces of coverglasses placed above and below, but never in direct contact with it. The distance between the slide and the coverglass played a large role in regulating the rate of water flow and could be varied by pressing the coverglass against the net, thereby breaking crystals protruding from the net plane. An excessive water flow moves the larvae from their fixed positions, or in some cases causes their general deformation. Six to nine ml water per hour passing through the net of 25 mm breadth was quite satisfactory, but 2–3 ml was insufficient for normal larval development. These figures will of course vary with the number of larvae caught by the net.

If an ordinary slide is used, air may invade the space below the coverglass, and disturb the circulation in the microaquaria. This difficulty was overcome by mounting glass strips (Fig. 3), by means of paraffine wax, along the edges of the slide. The longer ones of these strips were in contact with the coverglass. The width of the piece of net was further exactly adjusted to the width of the coverglass.

Technical Data on Time-Lapse Microcinematography and Film Analysis

The device described above made it possible to use time-lapse cinematography for studying morphogenesis in post-hatching marine larvae, which was hitherto impossible owing to their rapid movements. Concerning the technical details for the cinematography and the film analysis, the following data from our work may be of interest. The equipment described (Fig. 4) is very simple and easily transportable.

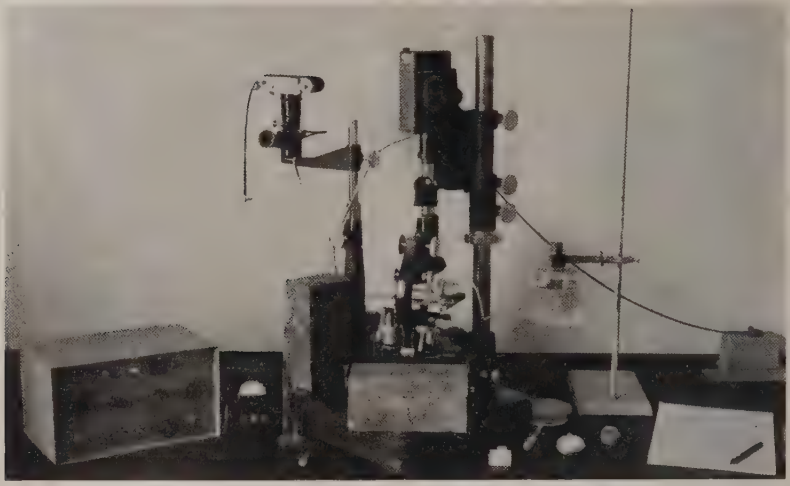

Fig. 4. Device for time-lapse cinematography used in the present work. Electronic timer to the left, Mariotte flask, solenoid, and cable for release to the right.

Microscope: Leitz, Stand B with large square mechanical stage.

Objectives and substage: Leitz achromat 45/0.65, fluorite 42/0.85 and apochromate 40/0.95. Leitz Two-diaphragm condenser. Phase contrast microscopy, Leitz objective achromat Pv 20/0.45 with the Heine condenser, was also used, but this equipment did not reveal more details than the ordinary one.

Source of light: Reichert Universal Micro-Illuminator "Lux E" with a low voltage filament bulb, 6 volt 5 amp. An "Osram" lamp survived more than 45,000 switches on at 3.5–4.0 amp. No filter was used.

Stand: A heavy vertical Siemens stand for micro-cinematography to which the micro-illuminator was attached with clamps. The stand was loaded with lead pigs as an additional security against vibrations.

Camera: 16 mm Bell & Howell Auto-Load, a clockwork-driven magazine camera. The actual instrument was especially adapted for cable release. Exposure time for single frame $^1/_{40}$ sec. This camera can be loaded in a few seconds, e.g. in a 10-second interval between two exposures.

Film: Kodak Super X, a reversal film.

Micro-cineadaptor: Reichert Kinekonnex, consisting among other things of an observation eyepiece, a micro-cine objective as a substitute for the normal camera objective, and a photo-ocular. Film frame magnification 1.2×microscope objective magnification.

Timer: A specially manufactured simple electronic timer with a frame counter. In order to avoid excessive illumination of the developing larva, the light was only switched on two seconds before each exposure and switched off a fraction of a second

Figs. 5–6. Stages in the migration of the primary mesenchyme cells and the early invagination of the archenteron in *Psammechinus miliaris*. Pictures from a 16 mm time-lapse film. Magnification 430 ×. Relative ages in hours and minutes, zero indicating the start of the two individual experiments.

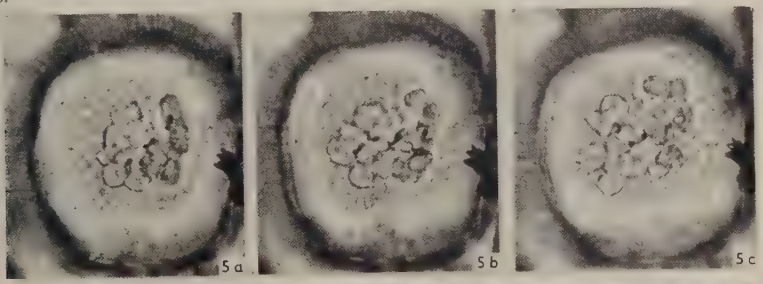

Fig. 5. Mesenchyme blastula seen from the animal pole. Relative ages: *a*, 0; *b*, 15′; *c*, 40′; *d*, 1 h 12′; *e*, 1 h 42′.

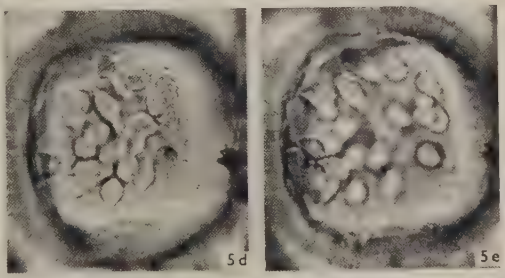

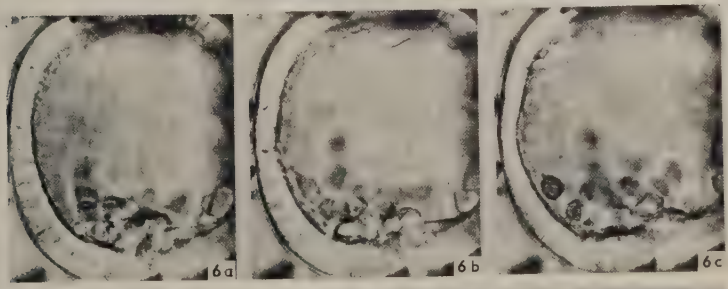

Fig. 6. Mesenchyme blastula and early gastrula seen from the side. Note the decrease in the thickness of the wall. Relative ages: *a*, 0; *b*, 17′; *c*, 1 h 7′; *d*, 2 h 30′; *e*, 3 h 20′.

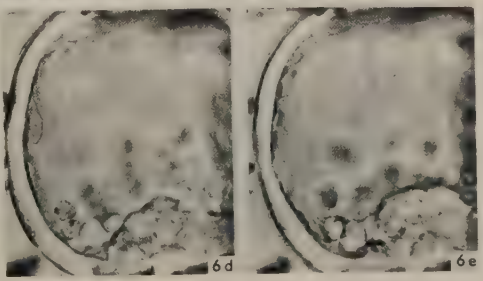

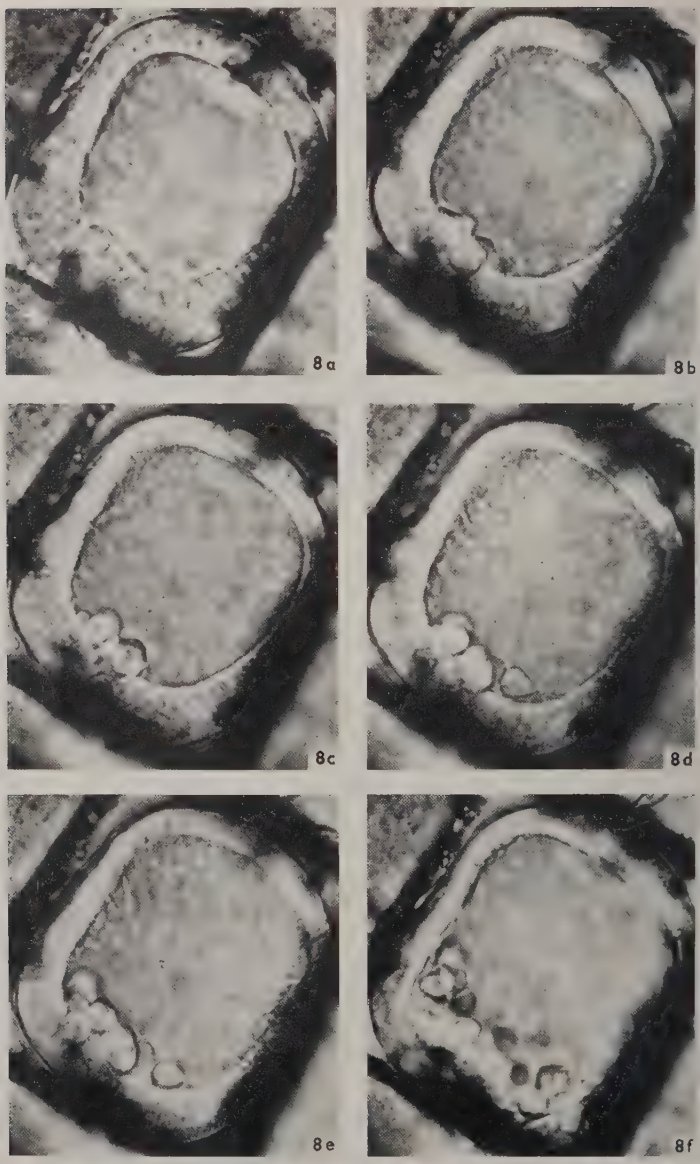

Fig. 8. The formation of the primary mesenchyme and the archenteron in *Psammechinus miliaris*. The second phase of invagination is mediated by contractions of pseudopodia from the tip of the archenteron (*l*-*m*). *a f*, The relative age in hours and minutes, zero indicating the start of the

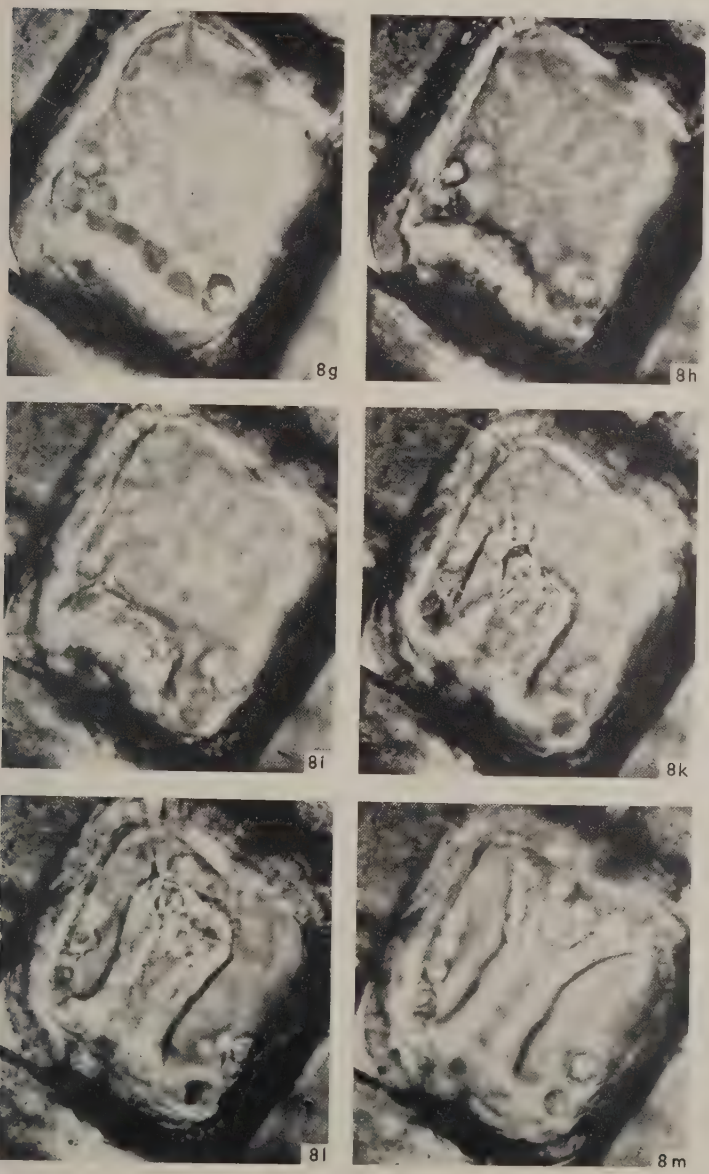

experiment: *a*, 0; *b*, 21′; *c*, 35′; *d*, 53′; *e*, 1 h 10′; *f*, 2 h 41′; *g*, 4 h 19′; *h*, 4 h 57′; *i*, 5 h 39′; *k*, 6 h 32′; *l*, 6 h 48′; *m*, 7 h 42′. Picture series from a 16 mm time-lapse film. The series corresponds to Fig. 9*e*. Magnification 430 ×.

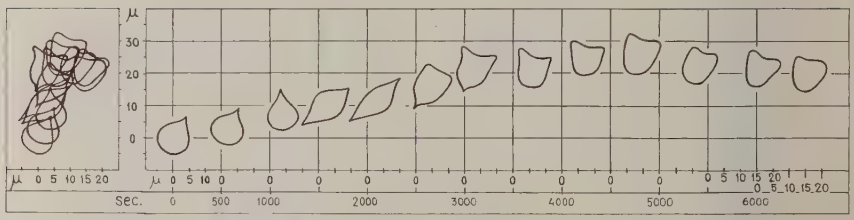

7a

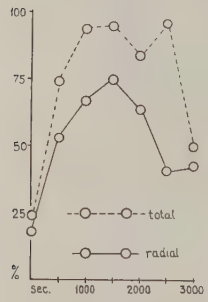

7b

7c

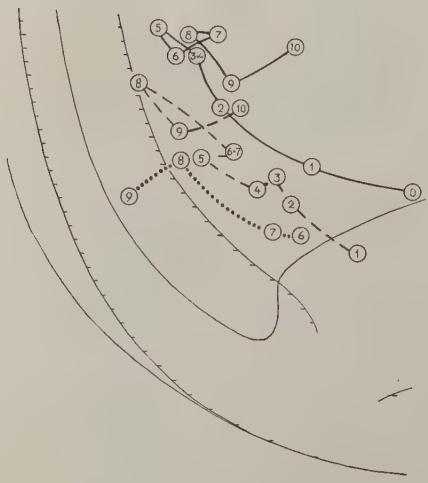

7d

Fig. 7. Diagram of the migration and shape changes of the primary mesenchyme cells in *Psammechinus miliaris*.

a. The migration of a single primary mesenchyme cell. The cell was drawn with regular time intervals. The superposed figures to the left is dissected into the components in the frames to the right, each representing a single stage. Interval 500 sec.

b. The percentage of spindle shaped primary mesenchyme cells (total and with radial orientation respectively) in different stages of the mesenchyme blastula. Intervals 1000 sec.

c. The radial migration of three primary mesenchyme cells, the identity of which could be followed throughout the analysis. The positions of the individual mesenchyme cells indicated by open circles where the figures enclosed indicate the relative stage of development. A sector of the vegetal region is seen from the animal pole. The inner border of its wall is represented by the curved line. Interval between each stage 500 sec.

d. The radial migration of three primary mesenchyme cells as in c. Blastula in side view. The contours of the blastula wall at the relative time 0 and 10 are represented by the spiny and the smooth lines respectively. Intervals 1000 sec.

afterwards. The rate preferred in the present case was one exposure every 10th second (in a few cases every 18th second). This frequency was generally sufficient for the study of gastrulation in *Psammechinus miliaris* at a temperature of 22°C.

Release: Cable release, actuated by a solenoid, mounted separately in order to avoid shaking of the camera.

Device for analysis: 16 mm G. B.-Bell & Howell projector, model 613, especially adapted for time and motion analysis with special heat filter, permitting prolonged single frame analysis, frame counter, and hand crank. The projector was fixed on a heavy iron plate, mounted on two optical benches. In order to facilitate the making of drawings, the pixtures were reflected by means of two surface plated mirrors down onto a horizontal drawing-table.

Application of the Technique to Studies of the Cellular Basis of Sea Urchin Gastrulation

By means of the technique described, it was possible to follow the whole process of gastrulation in individual sea urchin larvae (*Psammechinus miliaris*) from the time of hatching to the early prism stage. The whole process was repeatedly recorded by means of time-lapse cinematography, generally with exposure every 10th second. 350 meters of film were taken. The development of the larvae was generally not disturbed by their fixed positions. In several cases the net contained hundreds of larvae which developed synchronously and normally, even at a normal rate. In certain cases, when the mechanical stress was considerable in the meshes, e.g., due to deformation by carbonate crystals, abnormalities occurred which are of interest for the analysis of the mechanism of invagination.

The photographs used as illustrations for the following text were obtained from the time-lapse films. It is to be noted that no series of single photographs can give the same information as motion pictures. Single details which in the photographs appear indistinct, clear up as soon as they become united by a common motion against an immobile background.

A detailed presentation of the results will be given in later papers, when the analysis of the films is completed. Some results with bearing on the mechanism of gastrulation will be reported below.

Even before the primary mesenchyme appears in the blastocoele, it can often be seen as a collection of rounded apolar cells, distinctly delineated from the truncated cells in the blastula wall. The intercellular cement between these presumptive primary mesenchyme cells is evidently weakened, as a slight pressure on the blastula can force some of the cells out of the wall. The decrease in cellular adhesion often results in ruptures and funnel formations in the vegetal blastula wall (Fig. 8*a*). Finally the cells appear to

be passively squeezed out of the wall into the blastocoele. A swelling of the cells in the vegetal region may create a lateral pressure in the blastula wall, operative in this squeezing. The rigidity of the migrating cells is apparently low. When leaving the wall, the cells are strongly deformed by the adjacent cells; when arriving halfway into the blastocoele, they are generally pear-shaped with their blunt ends located centripetally, but as soon as they have become free, they attain a more or less spherical shape. The low mechanical rigidity of the migrating primary mesenchyme cells can be correlated with a high internal fluidity, witnessed by rapid movements of cytoplasmic granules.

Upon entering the blastocoele, the spherical cells generally remain more or less passive for a period of time. They are only pushed aside by new mesenchyme cells squeezed into the blastocoele from the subjacent blastula wall. The cells appear to be covered by a sticky substance, maybe remnants of the intercellular cement. The stickiness may contribute to the stabilization of the collection of mesenchyme cells in the blastocoele, which can attain rather peculiar shapes, e.g., a mushroom shape, in which the shaft is composed of the youngest mesenchyme cells. Finally, the cells begin to disperse. New primary mesenchyme cells may still appear in the center of the cell population. In its periphery the cells begin to form pseudopodia which attach themselves to the blastula wall. The contractions of the latter cause the cells to move (Figs. 5, 6, 7). The migrating cells are generally pear- or spindle-shaped (Figs. 5, 6, 7 *a, b*), probably as a result of the pull by the pseudopodia. The pseudopodia are to a great extent radially directed, with reference to the vegetal pole, and as a consequence the cells move more or less centrifugally (Figs. 5, 6, 7 *c, d*).

The surface stickiness and the pseudopodia connect the individual cells to some extent and restrict their independent movements. A real tug-of-war between individual cells and cell groups is therefore frequently observed. Cells which become free from this obstacle may migrate very rapidly. The mutually connected cells and their pseudopodia, on the other hand, form a ring around the vegetal plate. Analysis of the behaviour of single cells in this ring reveals a far-reaching reorganization in an early phase of invagination of the archenteron (Fig. 7 *d*). The individual cells migrate farthest toward the animal pole before invagination has started, but then descend and lie around the base of the early archenteron. In this site they appear to attach themselves more or less permanently, being connected to each other and to the ectoderm by strands (pseudopodia?) in which the skeletal rods later appear.

It is tempting to ascribe to the ring of primary mesenchyme cells a mechanical function in an early phase of invagination, especially as exogastrulation in vegetalized larvae can be correlated with a ring level far displaced in the animal direction. The trend of the ring cells to advance in the animal direction, opposed by their mutual connections, may result in a relaxation of the blastula wall below the ring plane. This may favour the onset of invagination. This contribution of the mesenchyme ring is, however, not in accord with the fact that the cells are lacking in many other types of larvae with invagination of the archenteron.

The initiation of invagination appears rather abruptly and gives rise to an archenteron rudiment with thick walls. This process is evidently autonomous, as the vegetal plate exhibits the same changes in an isolated fragment of the blastula wall [3]. The mechanism behind the primary invagination is still obscure. An active change of shape of the individual cells in the vegetal plate is suggested by observations of flattened larvae. In addition, the time-lapse films reveal rapid oscillations and a high fluidity in the cells of the archenteron tip, which should be further analyzed at a higher frequency of frames.

Whatever factors are responsible for the early invagination, they are not sufficient to carry the archenteron tip much further in the animal direction. Invagination is thus slowed down or even stagnates completely, cf. Fig. 9. A new important component of invagination comes into play when the archenteron tip has advanced about $^1/_4$ to $^1/_3$ through the blastocoele. Cells at the archenteron tip now begin to show an intense activity. Long pseudopodia, often very thin, are now rapidly formed by the cells (cf. Fig. 8 *i-m*), crossing the body cavity and attaching themselves to the animal region of the ectoderm. The pseudopodia exhibit contractility, and pull the archenteron tip in the animal direction. They sometimes break, but are replaced by new ones. Measurements of the life-time of the pseudopodia have given values of a couple of hours down to 15 minutes, cf. Fig. 9. The farther the invagination proceeds, i.e., the shorter the distance between the archenteron tip and the animal pole, the more frequent become the pseudopodia, or the thicker they are, and the more permanent. This contributes to an acceleration of invagination. The basal parts of the archenteron look completely passive during the whole process. The walls only become thinned out, probably as a consequence of the pull.

The causal role of the pseudopodia in the second phase of invagination is evident from the correlation between the first appearance of the pseudopodia and the onset of invagination after a period of stagnation, cf. Fig. 9.

In addition, different larvae show different time–space characteristics of invagination which in each case can be correlated with the actual behaviour of the pseudopodia. In one case (Fig. 9*f*), where the blastula wall was inflated in the equatorial region on one side, the pseudopodia attached themselves to the inflated area, probably because the distance was shorter in this direction than in other directions. The eccentric position of the pseudopodia was followed by an invagination directed toward the inflated area of the wall. In another case (Fig. 9*e*) where the pseudopodia formation was delayed, but very intense when it finally occurred, invagination stagnated for an abnormally long period of time, but then continued with an unusually high speed.

Finally, the archenteron does not respond at a sufficient rate to the pull of the pseudopodia. As a consequence, the pseudopodia forming cells pull themselves out from the tip of the archenteron. These cells are the so-called secondary mesenchyme cells. The process can take place in different stages of invagination. In one case (Fig. 9*d*), they were pulled out after about $^2/_3$ invagination had occurred. As the cells to a great extent lost their connections with the archenteron tip, there was a decrease in the rate of invagination.

After completed invagination, there is a period of apparently low activity around the archenteron tip, but soon the secondary mesenchyme cells begin to migrate along the archenteron or along the body wall in various directions. This type of migration differs from that of the primary mesenchyme cells. The cells apparently have longer pseudopodia, they are more irregular in shape and more clearly multipolar, and also migrate at a higher rate and more solitarily than the primary mesenchyme cells. It is an important task to follow the way in which these cells build up the delicate network of musculature of the intestinal wall and many other mesodermic structures.

The migration of the secondary mesenchyme cells appears to be directed by "long-range forces". A secondary mesenchyme cell can thus migrate back and forth along the archenteron wall, "eagerly" stretching a pseudo-

---

Fig. 9. Diagrams of the course of invagination in six larvae of *Psammechinus miliaris*. Inner height of the archenteron in microns is plotted against the relative age in hours, the first stage arbitrarily called 0 hours. The pseudopodial activity is symbolized by the horizontal lines below the curve to the right, each line representing one visible pseudopodium, dashed lines indicating periods where the pseudopodium was undistinct or only intermittently visible. The wavy line indicates direct contact between the secondary mesenchyme and the ectoderm, which makes observations of the pseudopodia difficult. The schematic drawing to the left of the curves gives the appearance of the larva in three different arbitrarily chosen stages, corresponding to the marks below the abscissa. The smooth contour refers to the stage of departure; the dashed and dotted lines mark the external border of the archenteron with pseudopodia and secondary mesenchyme cells. Curve 9*e* corresponds to the larva in Fig. 8.

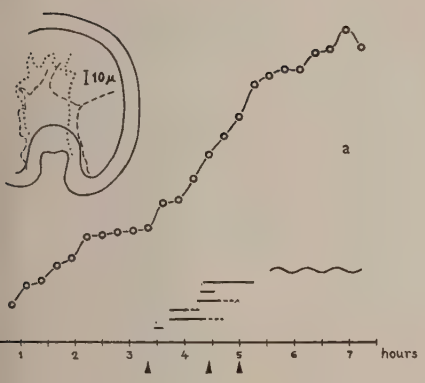
10μ
a
hours

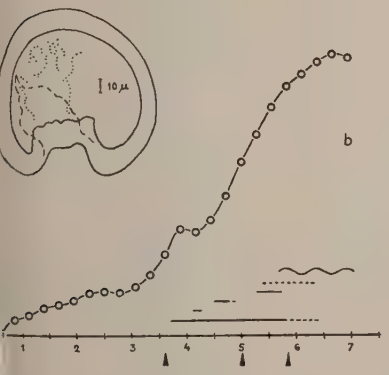
10μ
b
hours

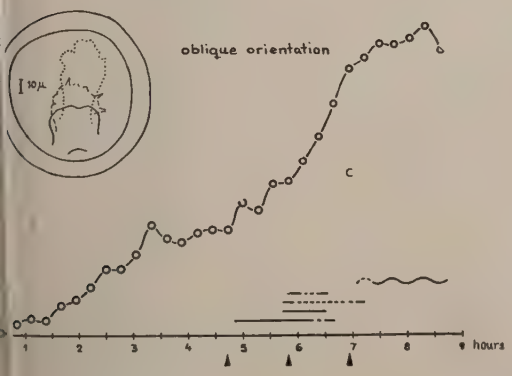
oblique orientation
10μ
c
hours

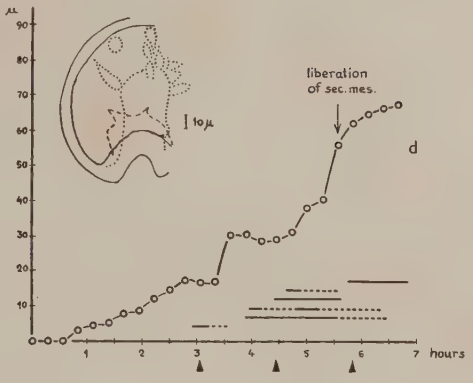
liberation of sec. mes.
10μ
d
hours

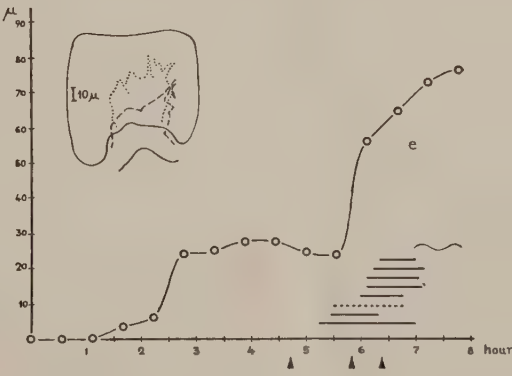
10μ
e
hour

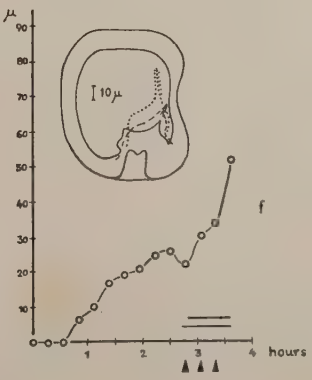
10μ
f
hours

podium in the direction of the ectoderm which may be rather distant. The "long-range forces" may correspond to diffusion gradients of metabolites emanating from cells with an intense metabolism, e.g., yolk breakdown. It can be assumed that the same directive agent is active in guiding the pseudopodia in the archenteron tip against the ectoderm, and that they even induce their formation. It is, finally, suggested that the same type of directive agent also guides the primary mesenchyme cells in their migration centrifugally from the vegetal pole in the animal direction during the formation of the primary mesenchyme ring.

The question then arises as to why the primary mesenchyme cells migrate so far into the animal direction in a lithium larva, and why invagination as a whole fails in this case. One may assume that the ectoderm is the source of the directive agent, and that the primary mesenchyme cells migrate to a level where the concentration is above a certain value. In a lithium larva, this level is probably shifted in the animal direction corresponding to the reduced size of the ectoderm. The failure of the invagination may be the immediate result of a disturbed formation of pesudopodia in the archenteron tip. Perhaps this area does not come inside the radius of action of the directive agents. Further studies on vegetalized larvae will be done to elucidate this question.

The preceding section may be sufficient to illustrate the usefulness of time-lapse studies of individual larvae. Observations alone are often considered to be unable to solve problems of causality. Time-lapse cinematography, however, introduces a moment of experimentation in the process of pure observation, i.e., the immediate results of singular processes are registered. In many cases, however, time-lapse cinematography should be supplemented with observations on experimentally treated larvae, e.g., larvae treated with lithium, iodosobenzoic acid, heat, cold, enzymes, antisera, antimetabolites, etc. These agents could be added during the course of time-lapse cinematography by means of the filter paper strips carrying water through the microaquaria. Some experiments of this kind have already been performed.

SUMMARY

A technique is described which permits a time-lapse cinematographic analysis of morphogenetic processes of sea urchin larvae and other marine larvae, the rapid swimming movements of which normally prohibit the use of time-lapse recording. The method has been applied to the gastrulation

of the sea urchin *Psammechinus miliaris* in time-lapse experiments on single larvae for periods up to 12 hours with little disturbance of the normal development. A preliminary analysis of the film focuses attention on contractile pseudopodia as operative units in gastrulation. Such pseudopodia mediate the migration of the primary mesenchyme cells. Pseudopodia are also active in a second phase of invagination of the archenteron. During this phase, pseudopodia are formed by the cells in the tip of the archenteron rudiment. By the contraction of these pseudopodia, which attach themselves to the ectoderm, the archenteron tip is pulled in the animal direction.

This work was mainly carried out at Kristinebergs Zoologiska station, Fiskebäckskil. The authors wish to express their most cordial thanks to the station authorities, Professor John Runnström and Fil. Dr. Gunnar Gustafson, for never failing generosity. The work has been supported by the Swedish Research Council.

REFERENCES[1]

1. Holtfreter, J., *J. Exptl. Zool.* **129**, 623, (1955).
2. Klercker, O., *Z. Wiss. Zool.* **6**, 145 (1889).
3. Moore, A. R., and Burt, A. S., *J. Exptl. Zool.* **82**, 159 (1939).

[1] *Note added in proof:* An article by K. Dan and K. Okazaki, dealing with the problem of invagination has appeared in *Biol. Bull.* **110**, 29 (1956). This article, too, underlines the importance of pseudopodia as operative units in the process of invagination in the sea urchins.

SOME EFFECTS OF A PARTIALLY PURIFIED TOXIN OF *MICROCOCCUS PYOGENES* VAR. *AUREUS* ON CHICKEN ERYTHROCYTES[1]

W. D'AGUANNO[2] and F. R. HUNTER[3]

Department of Physiology, Florida State University, Tallahassee, Florida, U.S.A.

Received November 27, 1955

A number of experiments describing some effects of bacterial toxins on cell suspensions have been reported previously. This work was designed not only to elucidate the mechanism of bacterial action *in vivo* but also to add to an understanding of certain aspects of the functioning of cells.

One of the toxins previously studied was prepared from *Staphylococcus aureus* (*M. pyogenes* var. *aureus*).[4] This crude toxin had an initial accelerating effect on the respiration of chicken and dogfish erythrocytes and on the respiration of *Arbacia* and *Asterias* eggs [11, 12]. The toxin had no effect on the time for hemolysis of dogfish erythrocytes suspended in ethylene glycol but the rate of swelling of chicken erythrocytes in a solution of glycerol in Ringer-Locke was altered [13]. A further analysis of this last mentioned effect showed that chicken erythrocytes exposed to the crude toxin became more fragile but their permeability to glycerol was unaltered. Washing the cells following a 10-minute exposure to the toxin failed to prevent eventual hemolysis [8].

Since some of these previously reported effects may have been the result of substances in the crude preparation other than the toxic material produced by these bacteria, the present experiments were performed using a partially purified toxin. Christie and Graydon [4] demonstrated the presence of a lipase in this toxin and because of the possible action of this enzyme on the lipids in the erythrocyte membrane, this was the fraction we were interested in studying.

[1] This work was supported in part by a grant R.G. 2977, from the U. S. Public Health Service.

[2] Taken from a dissertation presented to the Faculty of the Graduate School, Florida State University, in partial fulfillment of the requirements for the degree of Ph.D., in the Department of Physiology. Present address: Division of Pharmacology, Food and Drug Administration, Department of Health, Education and Welfare, Washington D.C., U.S.A.

[3] Present address: University of Illinois Medical School, Chicago, Illinois.

[4] The authors are indebted to the Lederle Laboratories for supplying this material. It was Lot No. 2529-103 containing 15,000 dermonecrotic doses per cc.

EXPERIMENTAL

Purification and assay of toxin.—A modification of the method described by Fulton [6] for obtaining the alpha toxin was used. This consisted of dialysis of the crude toxin against distilled water at 5°C for 48 hours with periodic changing of the water. The protein was then precipitated at an acid pH in 20 per cent acetone (by weight). Following centrifugation at 2500 × *g* for 10 minutes, the precipitate was dried *in vacuo* and stored in a refrigerator. This material lost little activity when kept in this way for longer than one year.

An assay method similar to that described by van Heyningen [18] was set up to test the hemolytic activity of various preparations. For convenience, human erythrocytes were used. One hundred Hemolytic Units is that amount of toxin which will cause 50 per cent hemolysis of a 0.01 per cent suspension of human red cells incubated for 5 hours at 37°C. Table I compares the weight and lytic activity of several preparations.

The lipolytic activity of the purified material was tested by demonstrating the production of acid following incubation at 37°C of a toxin-olive oil suspension [22].

General procedures.—Chicken blood was obtained by cardiac puncture and heparin

TABLE I

Weights and hemolytic activities of various toxic fractions.

Procedure	Weight (mg per 10 cc of crude toxin)	% Change	Hemolytic assay (per 0.5 cc of crude toxin)		
			Dilution	Time exposed (hrs.)	% Hemolysis
Crude toxin	278.0	0	1 X	5	62.5
			1 : 1	5	50.5
			1 : 2	5	42.0
			1 : 5	5	37.5
Dialyzed	84.0	69.9	1 X	5	62.5
			1 : 1	5	2.0
			1 : 2	5	0.0
10 per cent acetone .	1.0	99.6	2 X	1	2.0
20 per cent acetone. .	1.6	99.4	2 X	1	61.0
	1.9	99.3	1 X	5	62.5
	2.8	99.0	1 : 1	5	52.0
	2.9	99.0	1 : 2	5	42.0
			1 : 5	5	25.0
30 per cent acetone. .	7.1	97.4	2 X	1	55.0

was added. The blood was centrifuged at 2500 $\times g$, plasma and leucocytes were removed by aspiration and for most of the measurements, the erythrocytes were washed at least once with Ringer-Locke solution. Experimental suspensions contained cells, toxin and Ringer-Locke solution, while the controls contained cells and Ringer-Locke solution only. These suspensions were incubated at 37°C for varying lengths of time, care being taken to avoid bacterial contamination. Sterility was checked

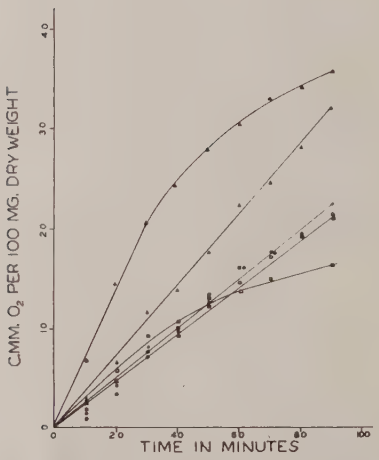

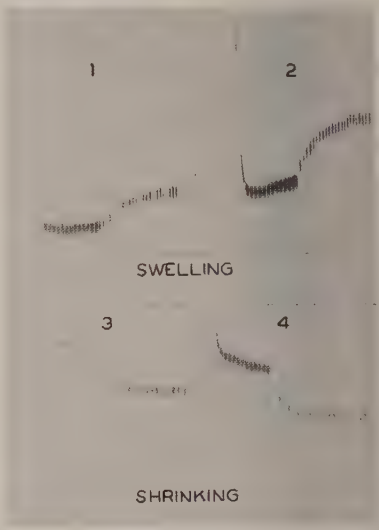

Fig. 1 (left). The effect of toxins of *Staph. aureus* on the rate of oxygen consumption of chicken erythrocytes. △ commercial toxin; ▲ dialysate; ○ Ringer-Locke control; □ dialyzed toxin; ● acetone control; ■ acetone precipitate.
Fig. 2 (right). The effect of a partially purified toxin of *Staph. aureus* on the rates of swelling and shrinking of chicken erythrocytes. Upper curves—swelling in 0.3*M* glycerol in Ringer-Locke. Lower curves—shrinking of cells in 1.75 × Ringer-Locke following equilibration in 0.6*M* glycerol in Ringer-Locke. Curves 1 and 3—controls, 2 and 4—experimentals.

by inoculation in fluid thioglycolate medium. These cultures were incubated at 37°C for 24 hours and then observed.

A dilution of toxin was selected which would hemolyze a small percentage of the cells during the period of incubation. It was believed that in this way the analyses were made on a population of cells which included a large number of altered cells, some of which were about to hemolyze.

Hematocrits spun on an air turbine [14] gave measurements of cell volumes. The amount of hemolysis in the control and experimental solutions before and after incubation was determined by the method of Parpart *et al.* [17].

Respiration.—Oxygen consumption was measured at 37°C using the conventional Warburg technique. One cc of the material to be tested was added to 2 cc of a washed

erythrocyte suspension in Ringer-Locke solution in the Warburg vessels. Measurements of oxygen consumption were begun after 10 minutes for temperature equilibration. Fig. 1 shows the acceleration in the presence of the commercial toxin as previously reported [12]. The material on the outside of the membrane following dialysis also accelerates but to a lesser extent. The dialyzed toxin inhibits while the acetone precipitate (purified hemolytic agent) has no effect on the respiration of the cells.

Lipid analyses.—Erythrocytes were incubated for 4–8 hours in the presence of toxin or Ringer-Locke solution. Upon removal from the incubator, hematocrits were taken and the samples were centrifuged, the supernatant aspirated and the cells were washed once with Ringer-Locke solution. The cells were then hemolyzed with approximately an equal volume of water and the ghosts were extracted for total lipids by the cold alcohol–ether (3:1) method of Boyd [3]. The alcohol-ether extract was evaporated to dryness at 50–65°C and a petroleum ether extract was made of the dry residue. Aliquots of this extract were used to measure the lipid content of the red cell membranes by means of the Van Slyke manometric apparatus [19, 20].

Table II compares the lipid content in the membranes of control and treated cells. Each value in the table is the average of at least 5 combustions and has been corrected for the amount of carbon in a blank, containing reagents only. In all cases but one it can be seen that the controls contain less lipid than the experimental cells.

TABLE II

Some effects of a partially purified toxin of *Micrococcus pyogenenes* var. *aureus* on lipids of plasma membrane of chicken erythrocytes.

Control mg. C/cc	Experimental mg. C/cc	Change mg. C/cc	% Change
2.431	3.271	+0.840	+34.9
3.086	2.259	−0.827	−26.8
1.491	2.371	+0.880	+58.8
2.098	2.468	+0.370	+17.6
1.974	2.282	+0.308	+15.6
1.859	2.378	+0.519	+27.8

Non-electrolyte permeability.—The permeability to glycerol was measured using the methods previously described [7, 10]. Typical results, shown in Fig. 2 are the same as those previously reported when the commercial toxin was used [8]. The upper two curves show the rate of swelling of control and experimental erythrocytes incubated at 37°C for 8–10 hours in Ringer-Locke solution and Ringer-Locke plus 800 H.U. of toxin respectively. To obtain such records, 0.05–0.08 cc of cells were added to 20 cc of 0.3*M* glycerol in Ringer-Locke solution in the chamber of the photoelectric apparatus.

To obtain the lower two curves, equal volumes of control, or toxin-treated cells, and 0.6*M* glycerol in Ringer-Locke solution were mixed. After standing for 10–15 minutes at 37°C 0.08–0.15 cc of this suspension were added to 20 cc of 1.75 × Ringer-Locke solution. As the glycerol left the cells, they shrank with a subsequent downward deflection of the galvanometer. Both the swelling and shrinking measurements

show that the erythrocytes which had been exposed to the toxin are no more permeable to glycerol than the control cells.

Cation shifts.—The sodium and potassium contents of control and toxin-treated cells were measured by the internal standard method using a Perkin-Elmer flame photometer, model 52-C [9]. Following a period of incubation of from 0–10 hours, the cell suspension was packed in an air turbine [16]. One half cc of packed cells was added to 15 cc of a weak barium hydroxide solution (pH 9–10) to hemolyze the cells. The ghosts were removed by centrifugation and 10 cc of this hemolysate were added to 2 cc of 20 per cent trichloracetic acid to precipitate the protein. Following centrifugation, 10 cc of 50 parts per million of lithium were added to this supernatant and this mixture was used for analyses. The values for Na and K were calculated on the basis of the volume of the cells in Ringer-Locke solution at zero time. This method of calculation compensates for any movement of water into or out of the cells during incubation. The data are presented in Table III including volume and per cent hemolysis measurements. It can be seen that the experimental cells tend to be a little larger and a few more of them hemolyze than in the control suspensions. Both control and experimental cells gain Na and lose K, during the period of incubation. The experimental cells gain Na and lose a small amount of K almost immediately, before the zero hour reading could be obtained.

TABLE III

The changes in Na, K, volume and per cent hemolysis in chicken erythrocytes incubated at 37°C in the presence of a toxin of *Micrococcus pyogenes* var. *aureus*

		Hours incubated			
		0	6	8	10
Na	Control	15.2	18.9	18.7	20.4
MEq/L	Expt'l	25.7	28.7	28.2	35.0
K	Control	117.4	127.4	108.3	110.9
MEq/L	Expt'l	114.1	123.5	103.7	110.3
% Hemolysis	Control		1.3	1.3	3.4
	Expt'l		5.4	7.5	12.9
% Volume	Control		5.5	8.6	7.1
Increase	Expt'l		8.2	12.8	16.2

DISCUSSION

Using a partially purified preparation obtained from a commerical toxin of *M. pyogenes* var. *aureus*, most of the observations previously reported by one of us (FRH) were repeated. The purified fraction retained most of the hemolytic activity of the original material and also contained lipolytic activity. The respiratory accelerator which was present in the crude toxin was separated from the hemolytic agent by dialysis. This, then, suggests that the

metabolic action previously reported results from small molecules present as an impurity in the crude preparation.

The action of the lipase in this toxin resembles in some respects the action of a pancreatic lipase reported by Ballentine and Parpart [1]. They found that beef and rabbit erythrocytes exposed to pancreatic lipase lost no lipid from the cell surface. Beef cells hemolyzed more rapidly in solutions of non-electrolytes while rabbit cells hemolyzed less rapidly. They suggested that the enzyme broke certain bonds in the cell membrane which did not release any lipid but did alter the effective barrier to the penetration of non-electrolytes. It has previously been shown [8] that toxin-treated cells hemolyze more rapidly in ethylene glycol and glycerol solutions. This results from an increase in fragility without an increase in permeability as determined by osmotic volume changes. One might postulate, then, that the lipase of the toxin breaks certain bonds in the membrane but this does not result in loss of lipid. These altered cells swell slightly and are more fragile. The bonds which are broken do not let glycerol move into or out of the cell at a more rapid rate.

With such a subtle change in the cell membrane there still remains the question of why the cells eventually hemolyze. The simplest explanation and one consistent with the suggestions of Bernheimer [2] and Wilbrandt [21] would be to assume that the Na and K data indicate that a few of the cells have lost their capacity to maintain the cation gradients across their membrane. Such cells would hemolyze as soon as the Na and K had diffused to the point where their osmotic effect across the membrane was negligible. As the toxin continues to act on the remaining cell population, the next least resistant cells would have their membranes changed sufficiently to allow the net change in cations and so they would hemolyze, and so on. One might speculate that a lipase acting on a red cell membrane might alter lipids involved in maintaining the structure of the membrane or the enzyme might alter non-structual lipids. If the movement of Na and/or K into or out of the cell does involve carriers and, if these are lipid in nature, a lipase might conceivably alter the carriers sufficiently to bring about colloidal osmotic hemolysis.

The significance of the apparent increase in the lipid content of the toxin-treated cells is not clear. If the toxin does break bonds in the membrane one might suggest that the alcohol-ether extraction of such membranes would be more complete. That this is unlikely is suggested by Parpart and Ballentine [15] who state that with mammalian erythrocytes, at least, this method of extraction removes all of the lipid. Another suggestion would be that some of

the toxin remains combined with lipid in the membrane and is extracted with the lipids. The fact that the hemolytic action of this toxin cannot be stopped by washing the cells [8], would be consistant with this hypothesis. Forssman [5] moreover, has shown in a series of articles that some forms of staphylolysin are firmly bound to erythrocytes, while others are not. If the toxin used in the present experiments fell in the former category, this could explain the lipid values.

SUMMARY

1. A partially purified hemolytic fraction was obtained from a crude preparation of *M. pyogenes* var. *aureus* toxin by dialysis and precipitation with 20 per cent acetone.

2. A respiratory acceleration previously reported in the crude toxin was removed by dialysis.

3. Prior to hemolysis there is no loss of lipid from the membranes of chicken erythrocytes exposed to this toxin.

4. The permeability of these cells to glycerol is unaffected.

5. The present data are not incompatible with the hypothesis that these cells hemolyze in the presence of this toxin by colloidal osmotic hemolysis.

REFERENCES

1. Ballentine, R. and Parpart, A. K., *J. Cell Comp. Physiol.* **16**, 49 (1940).
2. Bernheimer, A. W., *J. Gen. Physiol.* **30**, 337 (1946).
3. Boyd, E. M., *J. Biol. Chem.* **115**, 37 (1936).
4. Christie, R. and Graydon, J. J., *Austr. J. Exptl. Biol. and Med. Sci.* **19**, 9 (1941).
5. Forssman, J., *Acta. Pathol. et Microbiol. Scand.* **16**, 335 (1939).
6. Fulton, F., *Brit. J. Exptl. Pathol.* **24**, 65 (1943).
7. Hunter, F. R., *Science*, **109**, 119 (1949).
8. —— *Proc. Soc. Exptl. Biol. and Med.* **74**, 697 (1950).
9. —— *J. Biol. Chem.* **192**, 701 (1951).
10. —— *J. Cellular Comp. Physiol.* **41**, 387 (1953).
11. Hunter, F. R., Bullock, J. A., and Rawley, J., *Biol. Bull.* **97**, 57 (1949).
12. Hunter, F. R., Marker, M. J., Bullock, J. A., Rawley, J., and Larsh, H. W., *Proc. Soc. Exptl. Biol. and Med.* **72**, 606 (1949).
13. Hunter, F. R., Rawley, J., Bullock, J. A., and Larsh, H. W., *Science* **112**, 206 (1950).
14. Parpart, A. K. and Ballentine, R., *Science* **98**, 545 (1943).
15. Parpart, A. K. and Ballentine, R., *in* Modern Trends in Physiology and Biochemistry. Edited by E. S. Guzman Barron, Academic Press, Inc., 1952.
16. Parpart, A. K. and Green, J. W., *J. Cellular Comp. Physiol.* **38**, 347 (1951).
17. Parpart, A. K., Lorenz, P. B., Parpart, E. R., Gregg, J. R., and Chase, A. M., *J. Clin. Invest.* **26**, 636 (1947).
18. van Heyningen, W. E., *Biochem. J.* **35**, 1246 (1941).
19. Van Slyke, D. D. and Folch, J., *J. Biol. Chem.* **136**, 509 (1940).
20. Van Slyke, D. D., Page, I. H., and Kirk, E., *J. Biol. Chem.* **102**, 635 (1933).
21. Wilbrandt, W., *Pflüger's Arch. ges. Physiol.* **245**, 22 (1941).
22. Young, J. H. and Hartman, R. J., *Proc. Indiana Acad. Sci.* **48**, 79 (1939).

THE KINETICS OF GLUCOSE TRANSPORT THROUGH THE HUMAN RED CELL MEMBRANE

W. WILBRANDT, S. FREI and TH. ROSENBERG

Department of Pharmacology, University of Berne, Switzerland, and Biochemistry Department, Nordisk Insulinlaboratorium, Denmark

Received July 30, 1955

In a preceding paper [14] various models of cell membrane penetration involving both chemical reactions and diffusion have been discussed and their steady state kinetics calculated. It was found that the general function relating v, the rate of transport, to $(S)_I$ and $(S)_{II}$, the substrate concentrations on the two sides of the membrane, is complex. Since, however, under all conditions studied, it contains the term $[(S)_I-(S)_{II}]$ as numerator, it is possible to characterize the kinetics by the quotient

$$\frac{(S)_I-(S)_{II}}{v} \equiv F \tag{1}$$

which was termed "transport resistance". For free diffusion F is a constant. For most of the models treated it is a function of $(S)_I$ and $(S)_{II}$ containing terms of the types indicated in Table I. Under special conditions any one of these terms may become limiting, which then leads to the corresponding simpler types of kinetics also given in Table I.

Table I

Term	Type	Kinetics
$\frac{1}{K_D}$	D	$v=K_D[(S)_I-(S)_{II}]$
$\frac{(S)_I}{K_{Z1}}$	Z_1	$v=K_{Z1}\frac{(S)_I-(S)_{II}}{(S)_I}$
$\frac{(S)_{II}}{K_{Z2}}$	Z_2	$v=K_{Z2}\frac{(S)_I-(S)_{II}}{(S)_{II}}$
$\frac{(S)_I(S)_{II}}{K_E}$	E	$v=K_E\left[\frac{1}{(S)_{II}}-\frac{1}{(S)_I}\right]$

K_D, K_{Z1}, K_{Z2} and K_E are constants composed of the parameters of the system considered, e.g. enzyme concentrations, reaction velocity constants, diffusion coefficients, dissociation constants.

Type D represents the well-known kinetics of "simple" diffusion. It was shown, however, that this type will also prevail in the more complex systems considered, if the substrate concentrations are low. "Saturation values" of the rate of transport (constant maximal rate at high substrate concentration) as frequently observed in cell penetrations appear in the types Z_1 and E.

In this paper a kinetic analysis along these lines shall be given for the penetration of glucose across the human red cell membrane.

Deviations from "simple" diffusion for this special case have been found by numerous workers [1, 2, 3, 4, 6, 7, 8, 9, 12, 13, 15, 18]. Attempts have also been made repeatedly to replace the usual diffusion equations by more adequate basic kinetic equations. Wilbrandt and Rosenberg [21] as well as Widdas [15] found, that the most appropriate equation for this purpose is that of type E, whereas LeFèvre [10] arrived at relations representing types Z_1 and Z_2.

In this paper we present new experimental results which were obtained by improved methods and strengthen our previous conclusions.

METHODS

The penetration of glucose was followed by osmotic methods described previously [18, 20]. Briefly, the principle of the "indirect" method (which was used exclusively) is the following. The cells are suspended in a large (usually 20-fold) volume of salt solution containing glucose in a known concentration. At intervals curves of osmotic fragility are run on samples of the suspension, using photoelectric opacimetry. The change in the amount of internal glucose (by entrance or exit) is then calculated from the shift of these curves, assuming osmometer behaviour. Details have been given previously. Recent experience has shown that it is necessary to perform the fragility determinations at low temperature (2–6°C) in order to minimize errors due to the loss of sugar from the cells before the final degree of hemolysis is established.

From S, the amount of internal glucose thus determined, its internal concentration $(S)_i$ is calculated using the relation

$$(S)_i = \frac{S}{S+1}[(N)_0 + (S)_0] \tag{2}$$

in which $(S)_0$ and $(N)_0$ are the external concentrations of glucose and of non-penetrating solutes, respectively. This equation is derived from the condition for osmotic equilibrium:

$$\frac{S+1}{V} = (N)_0 + (S)_0 \tag{3}$$

where V is the volume of the cell [18]. In these and the following relations, "cell units" as introduced by Jacobs [5] are used: unit volume = initial volume of the cell in isotonic salt solution; unit concentration = isotonicity.

RESULTS

In Fig. 1 the experimental results are given on which the present evaluations are based. They include experiments on both entrance and exit of glucose and are representative for a large amount of experimental evidence.

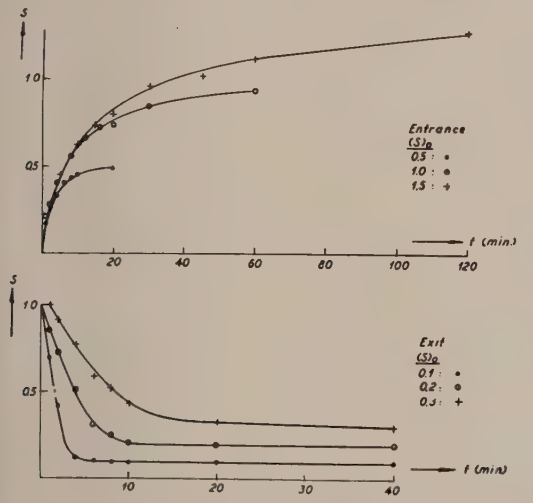

Fig. 1. Observed penetration of glucose into and out of human red cells. S = amount of glucose in the cell in cell units.

For the evaluation two methods were used which may be called the *differential* and the *integral* method. In using both methods it proved necessary occasionally to correct for deviations from the theoretical equilibrium and for time lags. Such deviations have also been noted by other workers.

The *differential* method implies graphical determination of the rate of transport $v = dS/dt$[1] for various values of S and the penetration time t. The dependence of the rate on substrate concentration might be presented by means of a direct plot of v against $(S)_i$ or $(S)_0$, the internal and external concentrations. It proved more suitable however, to use the "transport resistance" F, because it is a linear function of substrate concentration with clear-cut characteristics for the different kinetic types. Instead of the types

[1] v has here positive sign for entrance, negative for exit. Equations (1) and (7)–(10) are then valid in the same form for both entrance and exit.

Z_1 and Z_2, it is most convenient here to use the corresponding types Z_i and Z_0 characterized by the equations

$$Z_i: \qquad v = K_{Zi} \frac{(S)_0 - (S)_i}{(S)_i}, \tag{4}$$

$$Z_0: \qquad v = K_{Z0} \frac{(S)_0 - (S)_i}{(S)_0}. \tag{5}$$

In Fig. 2 the dependence of F on $(S)_i$ is shown schematically for the different kinetic types.

As Fig. 3 shows for both exit and entrance experiments, F is proportional to $(S)_i$. A comparison with Fig. 2 rules out types D, Z_i, and Z_0.

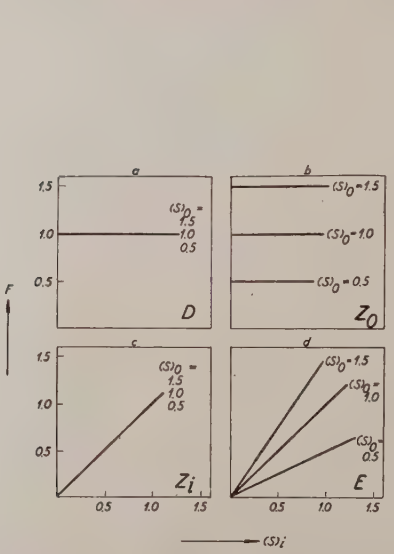

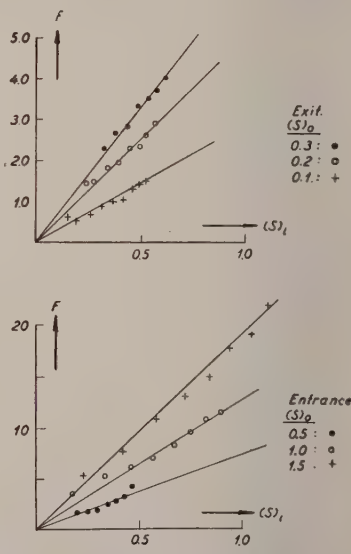

Fig. 2 (*left*). Schematical plots of the penetration resistance F against the internal glucose concentration $(S)_i$ for the different kinetic types. The constants K_D, K_{Z_0}, K_{Z_i} and K_E have arbitrarily been chosen as unity. Curves are given for $(S)_0 = 0.5$, 1.0, and 1.5.

Fig. 3 (*right*). Plot of the observed transport resistance F against internal glucose concentration $(S)_i$ for various values of $(S)_0$.

Evaluation of Fig. 3 shows that the dependence of the slopes on $(S)_0$ is linear in accordance with the equation for type E:

$$F = \frac{1}{K_E}(S)_i(S)_0. \tag{6}$$

The values obtained for $K_E = 7.5 \times 10^{-2}$ for entrance and 4.3×10^{-2} for exit.

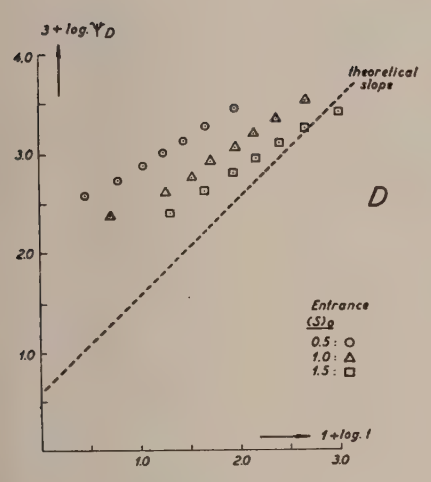

Fig. 4 a.

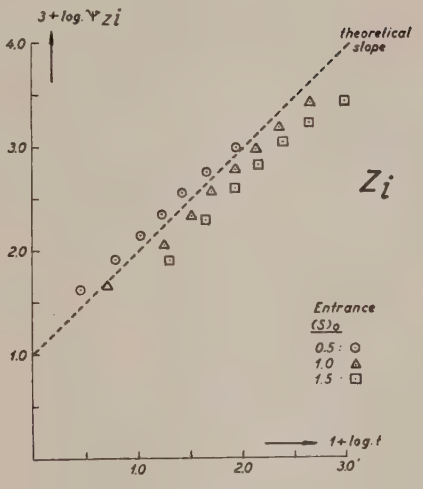

Fig. 4 b.

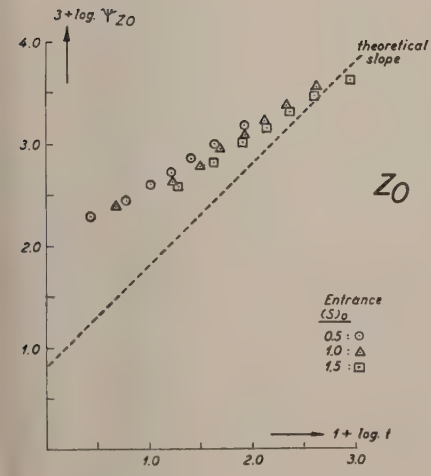

Fig. 4 c.

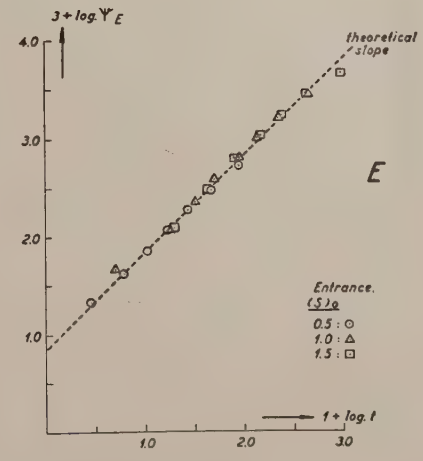

Fig. 4 d.

Fig. 4, a–d. Double-logarithmic plots for the different kinetic types of ψ, as defined by equations (7)–(10), against time. Entrance experiments.

In the *integral* method, which was also used by Widdas [17], the kinetics of penetration into or out of the cells is calculated by methods similar to those used by Jacobs [5] and others in cell permeability studies assuming penetration to occur by simple diffusion. Instead of Fick's diffusion equation, equivalent to our type *D*, the equation for the kinetic type under consideration (Z_i, Z_0, or E) is used as the basic differential equation, and the volume changes due to the simultaneous transfer of water are taken into account. The resulting integrated equations are:

$$K_D t = \frac{(N)_0 + (S)_0}{(N)_0^2} A + \frac{(N)_0 S_{t=0} - (S)_0}{(N)_0^2} a \equiv \psi_D, \tag{7}$$

$$K_{Z0} t = \frac{(N)_0 + (S)_0}{(N)_0^2} (S)_0 A + \frac{(N)_0 S_{t=0} - (S)_0}{(N)_0^2} (S)_0 a \equiv \psi_{Z0}, \tag{8}$$

$$K_{Zi} t = \frac{(N)_0 + (S)_0}{(N)_0^2} (S)_0 A + \frac{(N)_0 S_{t=0} - (S)_0}{(N)_0^2} [(N)_0 + (S)_0] a \equiv \psi_{Zi}, \tag{9}$$

$$K_E t = \frac{(N)_0 + (S)_0}{(N)_0^2} (S)_0^2 A + \frac{(N)_0 S_{t=0} - (S)_0}{(N)_0^2} [(N)_0 + (S)_0] (S)_0 a \equiv \psi_E. \tag{10}$$

In these equations a is the penetration fraction $(S_{t=0} - S)/(S_{t=0} - S_{t=\infty})$, where the amount of intracellular substrate is S at time t, $S_{t=0}$ at time 0, and $S_{t=\infty}$ at time ∞. A is $\ln [1/(1-a)]$. $(N)_0$ is again the external concentration of non-penetrating substances and $(S)_0$ that of the substrate.

The evaluation is carried out by plotting log ψ against log t. If the correct kinetic type has been chosen, all the experimental points regardless of substrate concentrations will lie on one straight line of 45° slope (ordinate intercept = log K). Figs. 4 a–d show plots of this kind for entrance experiments. Exit experiments yielded very similar results, agreeing best with type *E*, and nearly as well with type Z_0. (Z_0 however, was ruled out for these experiments by the differential method in Fig. 3.) The values obtained for K_E were 7.0×10^{-2} for entrance and 4.3×10^{-2} for exit, in good agreement with those obtained by the graphical method.

DISCUSSION

The two methods of evaluation of the experimental results used here have different and complementary points of merit. The results of the *differential* method are largely independent of influences from previous phases of the

experiment, particularly from lag phenomena.[1] Furthermore, this method appears to yield a better differentiation of the kinetic types at low external substrate concentrations. The *integral* method on the other hand, is less sensitive to experimental error.

The results represented in Figs. 3 and 4 reveal that the transport of glucose across the human red cell membrane follows the kinetic type *E*. They confirm our previous conclusions from similar experiments and agree with the analysis made by Widdas [17] with widely different methods.

It was shown in the preceding paper that a number of different transport systems and conditions may lead to type *E* kinetics. A condition common to all of these cases is that at least two of the substrate-binding sites involved in the transport shall approach saturation, and that these saturations are effected from different sides of the membrane. Both enzymes and carrier molecules have been discussed as saturable sites. On the basis of the results reported here, one cannot differentiate between these possibilities. However, in view of the inhibitory effect of enzyme poisons upon the transport the participation of enzymes is highly probable [7, 8, 19]. A kinetical analysis of such inhibitions which is in progress may shed more light on the details of the transport mechanism.

The values of the constants K_E in the experiments discussed above, according to both methods of evaluation, are approximately 7×10^{-2} for entrance and 4×10^{-2} for exit (37°C, "cell units"). The observed difference, in our opinion, is real, since it was found in all experiments with entrance and exit under comparable conditions. Such a difference, however, would not be expected from the kinetical equations of type *E*, since here exchanging $(S)_i$ and $(S)_0$ should affect the sign of the rate of transport only and not its numerical value. These findings therefore raise the suspicion that the transport mechanism contains more elements or more complex elements than has been assumed.

SUMMARY

Because of the well-known deviations from predictions assuming penetration by simple diffusion, and the conflicting interpretations in the literature, the transport of glucose in both directions across the human red blood cell membrane was studied using improved osmotic methods.

[1] Time lags are encountered not infrequently in both entrance and exit experiments. They will be discussed in greater detail elsewhere.

A kinetic analysis was carried out in two ways; (1) by graphical evaluation of the penetration rate as a function of substrate concentration (*differential* method), (2) by testing the fit of experimental data to the integral equations representing the time course of penetration for various basic types of transport kinetics (D, Z_1, Z_2, E) discussed previously (*integral* method).

Both methods of evaluation showed agreement with type E, characterized by the relation

$$\frac{dS}{dt} = v = K_E \left[\frac{1}{(S)_i} - \frac{1}{(S)_0} \right].$$

The result is discussed with respect to the transport mechanism, particularly as regards special conditions of saturation.

The values found for the constants K_E differ for entrance (7×10^{-2}) and exit (4×10^{-2}). This result may point to additional elements of the transport.

REFERENCES

1. Bang, O. and Ørskov, S. L., *J. Clin. Invest.* **16**, 279 (1937).
2. Ege, R., *Biochem. Z.* **111**, 189 (1920).
3. ——— *Biochem. Z.* **114**, 88 (1921).
4. Guensberg, E., Inaugural-Dissertation Bern, 1947.
5. Jacobs, M. H., *Biol. Bull.* **62**, 178 (1932).
6. Kozawa, S., *Biochem. Z.* **60**, 231 (1914).
7. LeFèvre, P. C., *Biol. Bull.* **93**, 224 (1947).
8. —— *J. Gen. Physiol.* **31**, 505 (1948).
9. —— *J. Gen. Physiol.* **34**, 515 (1951).
10. —— *Symposia Soc. Exptl. Biol.* **8**, 118 (1954).
11. LeFèvre, P. G. and LeFèvre, M. E., *J. Gen. Physiol.* **35**, 891 (1952).
12. Masing, E., *Arch. ges. Physiol.* **149**, 227 (1913).
13. —— *Arch. ges. Physiol.* **156**, 401 (1914).
14. Rosenberg, Th. and Wilbrandt, W., *Exptl. Cell Research* **9**, 49 (1955).
15. Widdas, W. F., *J. Physiol.* **118**, 23 (1952).
16. —— *J. Physiol.* **120**, 23 (1953).
17. —— *J. Physiol.* **125**, 163 (1954).
18. Wilbrandt, W., *Arch. ges. Physiol.* **241**, 289 (1938).
19. —— *Helv. Physiol. Acta* **5**, C64 (1947).
20. —— *Arch. ges. Physiol.* **250**, 569 (1948).
21. Wilbrandt, W. and Rosenberg, Th., *Helv. Physiol. Acta* **9**, C86 (1951).

ELECTRON MICROSCOPY OF GOLGI ELEMENTS IN SEA URCHIN EGGS

B. A. AFZELIUS

The Wenner-Gren Institute for Experimental Biology, University of Stockholm, and the Department of Anatomy, Karolinska Institutet, Stockholm, Sweden

Received December 1, 1955

The sea urchin egg has been the subject of a vast number of cytological investigations, and it is often taken as a typical example of the animal cell. Nevertheless, no clear picture can be obtained from the literature on the Golgi apparatus or its homologue in the sea urchin egg—in contrast to the Golgi apparatus of the vertebrate tissue cell, which has been well described in phase contrast and electron microscope studies. Observations on the Golgi apparatus in living cells with phase contrast microscopy make it hard to consider the Golgi apparatus as a fixation artefact, as has often been stated earlier. Electron microscope investigators like Dalton and Felix [4], Sjöstrand and Hanzon [28], Rhodin [24], and Haguenau and Bernhard [10] have demonstrated the same ultrastructural components of the Golgi apparatus in many mammalian cell types. These components are Golgi membranes, Golgi vacuoles, and Golgi "granules". As pointed out first by Sjöstrand and Hanzon these elements are embedded in a homogeneous substance called the Golgi ground substance.

Homologues of the Golgi apparatus of the vertebrate cell exist in the invertebrate cell. The generally accepted term for one of these bodies is dictyosome. The high resolution of the invertebrate dictyosome has not been studied before, and the only work so far dealing with germ cell dictyosomes is that of Beams and Tahmisian in 1953 [2]. These authors observed that the shape of the dictyosomes in their electron micrographs was the same as that of the dictyosomes in the living cell studied with phase contrast microscopy, but the resolution of their pictures was not sufficient to allow a correct interpretation of the submicroscopic morphology.

The Golgi techniques, first developed in 1898, were not applied to studies of the sea urchin egg until 1926, when Wilson published a short note on the components in the cytoplasm of the sea urchin egg. He stated that the appearance of the dictyosomes differed in the stages of oogenesis, that the dictyo-

somes appeared as flakes, crescents or rods, and that these were not removed by centrifugation. These components were misinterpreted by Just in a paper published in 1927 [16]. The same year the school of Parat published studies performed on sea urchin eggs [6, 20, 21], which for many years confused the conception of the Golgi apparatus, not only in the sea urchin egg but in all cell types. After introducing a neutral red technique Parat studied the distribution in living eggs of what he called the vacuome. He suggested that the distribution of the vacuome was identical with the distribution of the dictyosomes demonstrated with the classical Golgi techniques in the sea urchin oogenesis and development. The vacuome studied in living but vitally stained cells was considered to give a more life-like picture of the actual cell component than the dictyosomes obtained with Golgi methods. The shape of the single elements, on the other hand, was not the same and the identification of the vacuome with the dictyosomes was later shown to be doubtful [5, 7, 12, 15]. Parat [22] subsequently changed the nomenclature once more, giving the name of "chondriome actif" to the Golgi elements and suggesting a transformation from mitochondria to these elements. In spite of these and other confusions, Parat's papers contained much information about the distribution of the dictyosomes in sea urchin eggs and embryos. The developmental stages of the dictyosomes during echinoderm oogenesis were also dealt with by Harvey [11, 12], Tennent, Gardiner and Smith [31], and Subramaniam [29, 30]. The behavior of the dictyosomes was described by Hovasse [14, 15] and Motumura [17].

Following osmium techniques the Golgi elements appeared as discrete bodies in the sea urchin oocyte. In the smallest oocyte only one element was seen and this was situated near the nucleus. This juxta-nuclear element was reported to appear as one [32], or a few crescents [11, 12], or as a compact granule [29], or when demonstrated with the neutral red technique as many small vacuoles [20]. In later stages the juxta-nuclear complex was broken and the cytoplasm contained scattered dictyosomes. These have been studied in the living oocyte of the primitive echinoderm *Antedon* with the dark field microscope [11]. Here the dictyosomes usually appeared as crescents or scales. These were thought to divide repeatedly and to give rise to an increasing number of dictyosomes in the growing oocyte [11, 32]. According to most authors [21, 29, 31], the number of dictyosomes is reduced during egg maturation, but some dictyosomes probably persist. No increase of the dictyosome number was said to occur upon fertilization or during the cleavages until the late blastula stage [14, 20]. Considerable changes appeared, on the other hand, in the neutral red vacuome after fertilization and during

the mitotic divisions [21]. The dictyosomes of the gastrula cell were no longer scattered but collected in a Golgi zone as is the case in the very small oocyte [14, 20].

The role of the dictyosomes in the sea urchin egg is naturally even less clearly understood than its morphology, although some hypotheses have been suggested. In oogenesis the dictyosomes were said to give rise to oil drops [32]. The yolk granule formation was considered by Parat [20] to be a deposition of yolk in the vacuome, which then dehydrates and disappears. Subramaniam [29, 30] stated that the yolk deposition occurred in mitochondria. Harvey [12] reported that a yolk deposition took place in the ground cytoplasm. Both authors noted that this happened in the immediate vicinity of one or a few dictyosomes. During the first cleavages, according to Motomura [17], basophilic vacuoles stainable with Golgi techniques formed the new cell surfaces. The dictyosomes were also said to form the so-called "parabasal bodies" of the flagella in the blastula [14, 15, 22].

This paper deals with the dictyosome fine structure in sea urchin oogenesis and development and the problem of yolk formation in this material.

MATERIAL AND METHODS

Sea urchins collected on the Swedish west coast and the Norwegian north coast were used: *Echinus esculentus*, *Psammechinus miliaris* and *Strongylocentrotus droebachiensis*. Fixation was performed by various methods. Fresh eggs were immersed in 1 per cent osmium tetroxide in sea water, in a drop of pure osmium tetroxide at 40°C, or in a solution of 1 per cent osmium tetroxide and 1 per cent potassium dichromate in sea water. The fixed eggs were washed in sea water, dehydrated with ethyl alcohol and embedded in methacrylate, principally according to Newman, Borysko and Swerdlow [18]. The sections were made with the ultra-thin technique worked out by Sjöstrand [25, 27] using a microtome designed by him [26]. As a cutting edge, highly polished Schick razor blades were used mounted in a curved position. The sections were floated on a liquid surface of 20 per cent ethyl alcohol according to Gettner and Hillier [9], transferred to formvar-coated specimen grids, and examined in the electron microscope without dissolving the methacrylate. An RCA EMU 2c electron microscope was used, equipped with compensated objective pole piece, an objective aperture of 50 microns, three apertures in the projector lens and a reduced condensor lens aperture.

OBSERVATIONS

Oocyte juxta-nuclear apparatus.—Near the nucleus of the young oocyte there is a structure with a total diameter of approximately 3μ (Fig. 1). Its interior is composed of small vesicles with a diameter varying from 0.04 to

near 0.2μ. The boundaries of this formation seem to consist of lamellae. The lamellae consist of paired membranes with a total thickness of about 240 Å. About six double membranes are applied closely to each other to form a slightly curved bundle. In the plane of the section about five to seven such bundles may be seen surrounding the inner vesiculate area. The enclosure is not complete and some vesicles of the same appearance as that of the vesiculate area are seen in the cytoplasm outside the formation. This resembles the structures described in the centrosome region of mammalian leucocyte [23].

The constituent single membranes in a membrane pair join together at their ends, completely enclosing areas of a less osmiophilic substance. Where the membranes in a pair join each other there is often an enlargement of the inner area to a club-like vesicle. These may have the same dimensions as the free vesicles surrounding them. The cytoplasm of the oocyte at this stage contains a few yolk granules and mitochondria but no dictyosomes apart from those in the described juxta-nuclear formation.

Oocytes dictyosomes.—The typical dictyosome is scale-shaped as seen in the living oocyte by Harvey [11]. In the present study the dictyosomes are easily recognized in the oocyte cytoplasm. Their size and shape correspond to Harvey's data and the ultrastructural organization is very similar to that of the Golgi apparatus of the vertebrate cell [28]. The scale-like bodies appear in a perpendicular section as straight or curved rodlets with lengths of between 1 and 2μ. Their thickness is about 0.2μ. Fig. 5 can be taken as an illustration of the finer organization. The main components of the Golgi apparatus in the mammalian cell, the double membranes, vacuoles and "granules", are all present. At the same time it is evident that no sharp distinction can be drawn between these parts in the present material. The Golgi "granules" have a diameter of about 400 Å and consist of an osmiophilic wall of about 60 Å and a less dense inner substance and thus appear vesicular. These Golgi "granules" or vesicles may also be larger and are then elongated in the plane of the dictyosome. In extreme cases such a closed vesicle can extend from one end of the dictyosome to the other. Then its sides lie fairly parallel to each other and the structure is called a Golgi double membrane. When the large vesicles are more or less rounded they are called Golgi vacuoles. The wall of all these components has the same thickness. The orientation of the walls between two double membranes or one double membrane and one vacuole is more parallel than the orientation within one double membrane system. The Golgi ground substance reported in vertebrate Golgi apparatus [28] is faintly discerned in the present material. Dimensions of

Golgi membranes are reported in Table II (p. 83). In many dictyosomes no conspicuous vacuoles are present, all double membranes following straight courses (Fig. 4).

The growing oocyte offers a favourable subject for the study of the multiplication of the dictyosome. The dictyosome is sometimes seen larger than normal—around 2.4μ—and the structure is bisected. The break is near the center and the membranes of a pair join near this – a few Golgi "granules" are sometimes present in the center (Fig. 2). Table I (p. 83) indicates that the largest percentage of dictyosome breaks occurs in the growing oocyte.

A few Golgi vacuoles of the oocyte dictyosome may have a granulated mass in the interior (Fig. 5 and the semi-diagrammatic interpretation of this, Textfig. 1). This is in contrast to Golgi vacuoles at other stages, which have

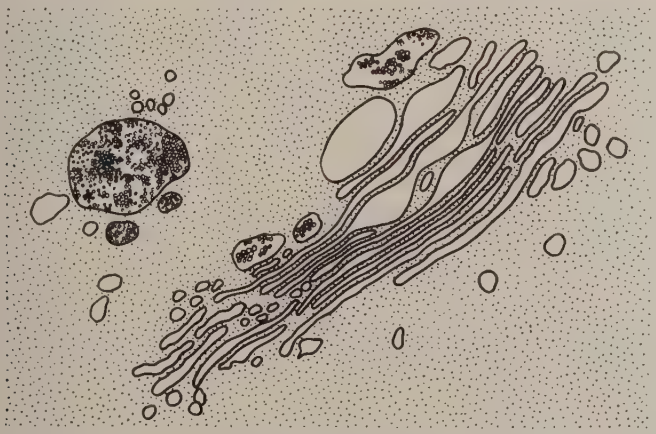

Textfig. 1. Semi-diagrammatic interpretation of Fig. 5 from a *Strongylocentrotus* oocyte. The cytoplasm outside the Golgi double membrane is intentionally dotted, in order to stress the fact that no anastomoses exist between the double membrane interspaces. A misconception of a reticulum is easily arrived at when the single membranes of two pairs are interpreted as a double membrane. See also Figs. 5, 3 and 4 for this particular characteristic. An expanded vesicle, which is filled with a granular material, associates with a cluster of smaller vesicles. This is thought to be a stage in yolk granule formation. Magnification 58,000 ×.

a non-osmium-impregnated content, giving an "empty" appearance. Most morphological stages from "filled" Golgi vacuoles to yolk granules have been found. The mature yolk granule is a spherical particle with a mean diameter of approximately 1μ depending upon the species. In the present material the ultrastructure of the yolk granule can be described as an outer

single membrane of about 65 Å enclosing a granular and osmiophilic inner substance.

Dictyosomes in the mature egg.—Egg maturation in the species examined is accompanied by a strong reduction of the dictyosome number. For several reasons the degree of this reduction is difficult to establish. The immature oocyte may have a diameter of nearly 100μ and contains some hundreds of morphologically separate dictyosomes. Only a fraction of these, which are cut perpendicularly and lie within the area of a thin section, can be demonstrated. As there are other membrane systems of different kinds in the egg [1], it is often necessary to inspect photographed parts of the cytoplasm to distinguish the dictyosomes. The photographed cytoplasm samples of immature oocytes and mature eggs definitely show a much smaller number of typical dictyosomes after maturation. In some eggs this reduction may be nearly complete, but generally a careful inspection of the egg cytoplasm reveals at least a few typical dictyosomes.

An attempt was made to concentrate the dictyosomes in a certain zone of the eggs by centrifugation. *Psammechinus* eggs were centrifuged at 3300 *g* in 8 minutes and *Strongylocentrotus* eggs at 3300 *g* in 15 minutes, and then fixed immediately. Light microscopical inspection showed the egg cytoplasm to be stratified in sharply defined zones. With electron microscopic examination of thin sections from these stratified eggs it was seen that the dictyosomes were not removed to a specific zone but could be found in both the light and the heavy poles. Another attempt to demonstrate the dictyosomes was performed with the Dalton technique.[1] However, in the examined eggs of *Psammechinus* and *Strongylocentrotus* not only the dictyosomes but also yolk granules and other cell components were impregnated by osmium, rendering the dictyosomes still more difficult to detect.

It is a notable feature of some oocyte dictyosomes that not all double membranes are equally spaced. The outermost double membrane may be

---

Fig. 1. *Strongylocentrotus droebachiensis*, very young oocyte. The nucleus, *N*, is at the bottom of the picture and the free cell surface, *C*, at the top. The central part of the figure shows the centrosome region, which consists of a vesiculated area surrounded by dictyosomes. *Y* = yolk granule. Magnification 25,000 ×.

Fig. 2. *Echinus esculentus*, oocyte. A dictyosome with a break of all double membranes at the same level. Magnification 39,000 ×.

[1] After a fixation in osmium tetroxide and potassium dichromate for 1 hour, the eggs were washed with sea water and impregnated at 40 °C in a 1 per cent osmium tetroxide solution in sea water for 16 hours. In order to keep the eggs at the same tonicity the fixed eggs were washed with sea water; the success of the Dalton technique, however, might depend upon the slightly oxidizing power of chlorine in the tap water. (Dalton, personal communication.)

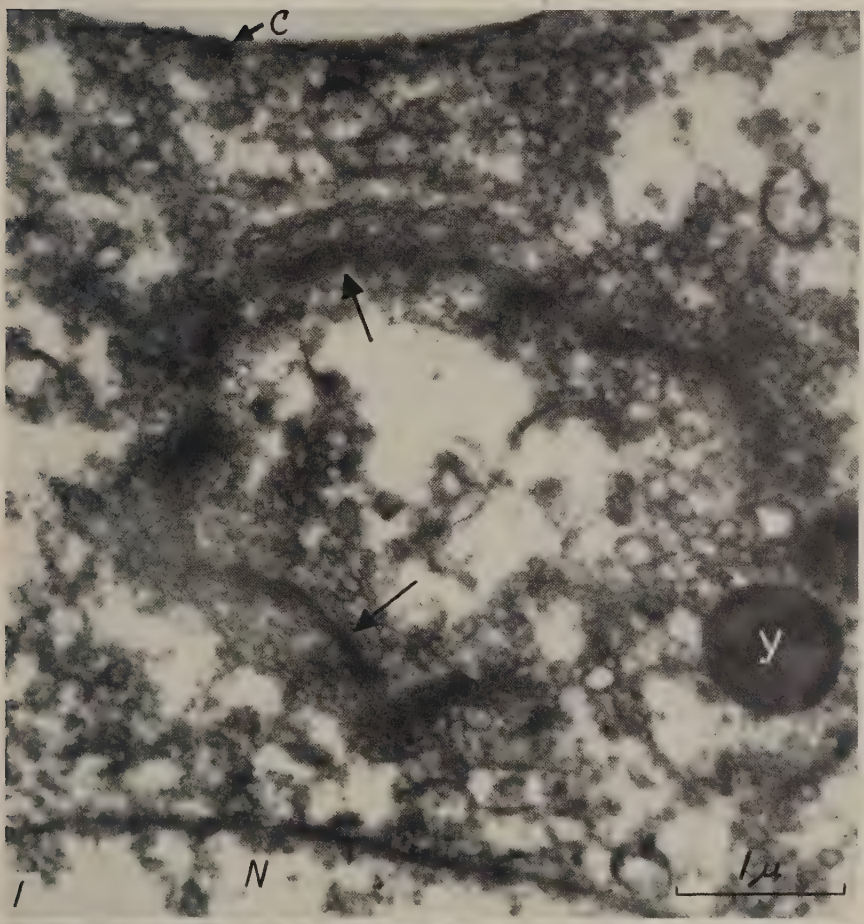
C
y
N
1μ
1
1μ
2

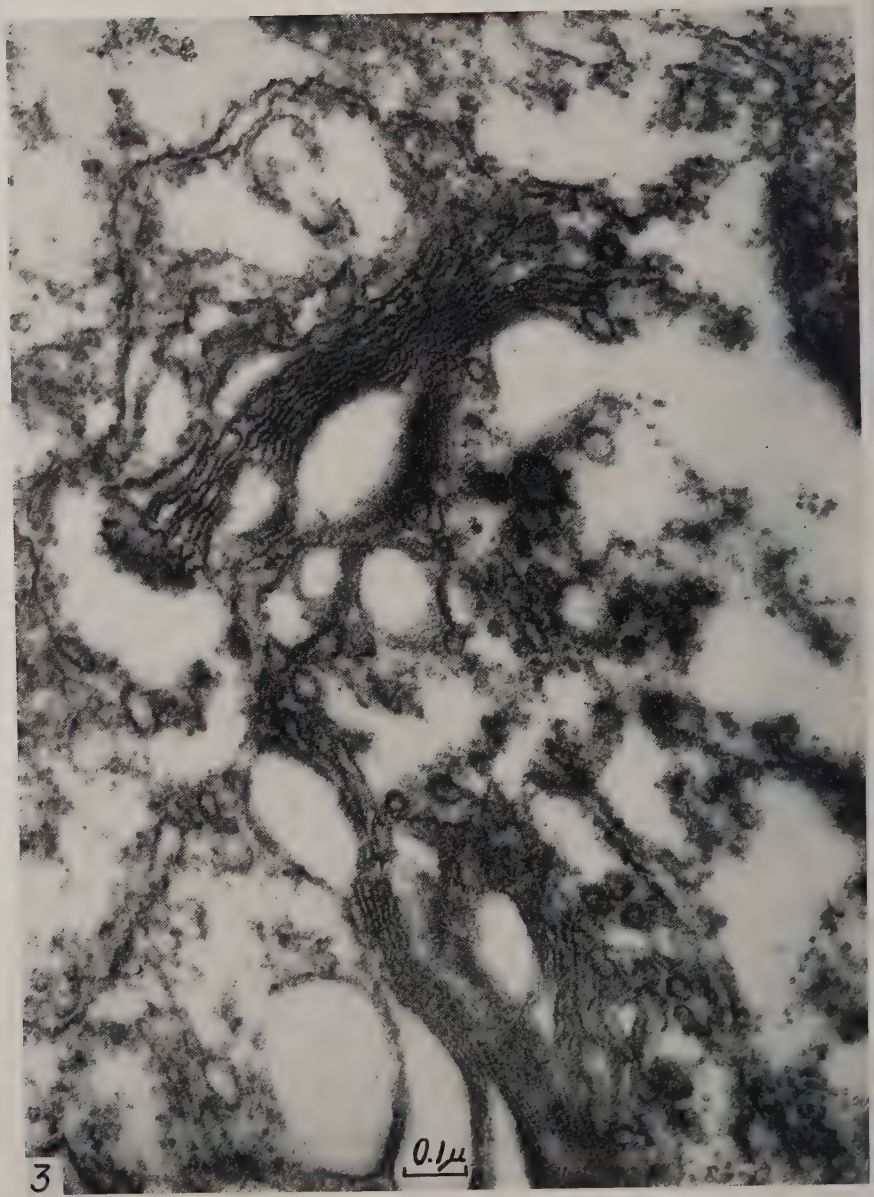

Fig. 3. Two dictyosomes of an *Echinus esculentus* oocyte. The lower dictyosome shows many swollen vesicles. The upper dictyosome has a vesicle separated from the others. Magnification 94,000×.

Fig. 4. Dictyosome from an *Echinus esculentus* oocyte. Magnification 130,000 ×.

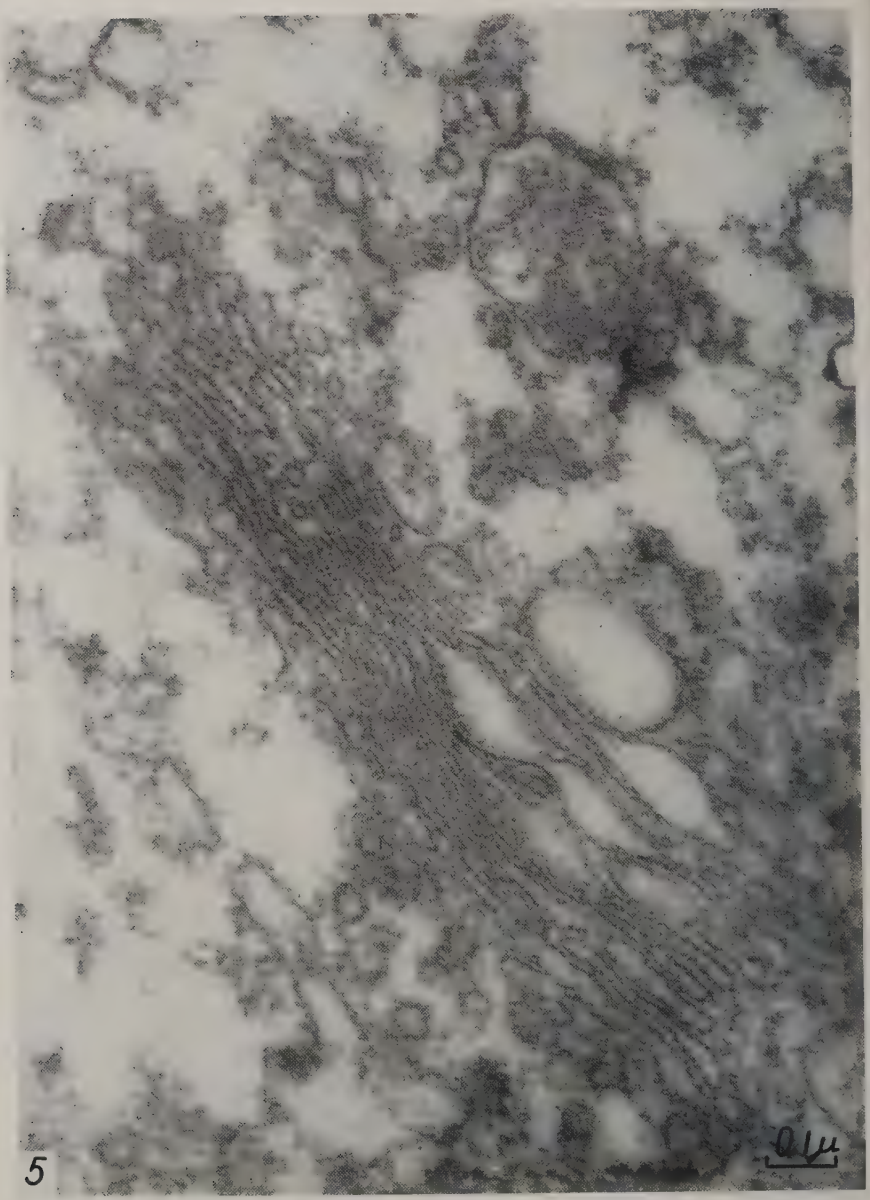

Fig. 5. *Strongylocentrotus droebachiensis*, oocyte. Dictyosome with a granular vacuole, which is intermediate in structure between the vesicle and the yolk granules. Magnification 105,000 ×.

separated from the others by greater distance. The walls of this double membrane are of a normal thickness, but the inner non-dense area is broader and more irregular than the inner area of the aggregated double membranes. An example of a partly isolated double membrane of this type is shown in the upper dictyosome in Fig. 3. In extreme cases all double membranes, which are more or less isolated from each other, have an irregular shape. Such "dispersed dictyosomes" are rare in the oocyte, but may be regarded as typical of the mature egg. (Fig. 6.) The ground cytoplasm, in which all particulate components of the egg are found, appears finely granulated after fixation with osmium. This non-specific granulation (particle size approximately 150 Å) is also seen on the outside of the double membranes, in a "dispersed dictyosome". The "dispersed dictyosome" is composed of 7 double membranes; the same number found in a normal dictyosome. The total size of a dictyosome is considerably larger in the "dispersed" than in the "aggregated" condition (see Table II, p. 83). The dictyosomes of the mature egg, which have tightly aggregated double membranes, are commonly smaller than those of the oocyte. Fig. 6 is therefore representative of the two dictyosome types existing in the mature egg.

Dictyosomes in the fertilized and developing egg.—Some preliminary observations on the dictyosomes of the fertilized and developing egg may be mentioned. The dictyosomes are scattered in the cytoplasm and exist in larger numbers in the fertilized than in the unfertilized egg. The size of a dictyosome in the fertilized egg and embryo is about the same as in the oocyte. The fine structure of a dictyosome appears to be identical before maturation and after fertilization. (See Table II.) In the gastrula stage there is a change as far as the distribution of the dictyosomes is concerned. The dictyosomes are no longer randomly scattered in the cytoplasm, but are found near the outer surface in the ectoderm cells. They are arranged here in a complex of a few dictyosomes, which gives an appearance similar to the Golgi apparatus of a vertebrate cell (Fig. 7). In the center of this zone sometimes a structureless, osmiophilic particle is seen with a diameter of 0.16μ. This is probably the centriole.

No observations have been made on the relationship between the dictyosomes and the astral rays during division, nor has the formation of the new cell wall been studied.

The flagellated cells of blastulae and gastrulae have a dictyosome in the immediate vicinity of the base of their flagella. Thin strands connect the flagellar basal granule and the dictyosome. This notable combination is illustrated in Fig. 8.

DISCUSSION

One characteristic of the Golgi apparatus is its morphological variability in various cells and, in the same cell type, at different functional states. Another feature of the Golgi apparatus is that its chemical composition probably varies between different cell types resulting in a varied behavior towards the chemicals used in the Golgi technique. As the function of the Golgi apparatus is poorly understood, it is no wonder that the nature of this cell structure has often been regarded with great scepticism. A clear morphological definition of the vertebrate cell Golgi apparatus was not given until the electron microscopic investigations of Dalton and Felix [4] and Sjöstrand and Hanzon [28] were published. Embedded in the Golgi ground substance are Golgi membranes, Golgi vacuoles, and Golgi "granules". The Golgi apparatus varies in appearance according to the relative amounts of these components [3, 10].

The present study deals with the dictyosome morphology in sea urchin oogenesis and development. At least five main stages can be distinguished with regard to the dictyosomes. In the first stage, in the very young oocyte and in the final stage found in many gastrula cells, the dictyosomes are found adjacent to the centrosome. Between these two stages are phases characterized by a rapid multiplication, by a disappearance, and then a reappearance of most of the dictyosomes.

The best defined dictyosome structure is found in the growing oocyte (Figs. 4 and 5). As pointed out above (p. 77), no fundamental difference is found between this dictyosome stage and the Golgi apparatus of the vertebrate cell. Even the dimensions of the Golgi membranes are identical. As there may be few or no vacuoles formed by the membranes, the organization is easily interpreted. In pictures of sufficient resolution it is easy to follow Golgi membranes around interspaces forming Golgi double membranes or Golgi vacuoles. *No anastomoses connect the interspaces of adjacent double membranes or vacuoles.* This is in contrast to what has been stated to be the case with the Golgi apparatus of neurones, as reported by Palay and Palade [19]. These authors described anastomoses between the double membranes of the Golgi apparatus, which was therefore called the agranular reticulum. Thus a similarity existed between the Golgi apparatus and the so-called endoplasmic reticulum and they suggested that the former was a precursor of the latter. Anastomoses in the non-dense interspaces of the Golgi apparatus

Fig. 6. *Strongylocentrotus droebachiensis*, mature egg. A "dispersed dictyosome" appears at the upper part of the picture and a small aggregated dictyosome at the bottom. Magnification 40,000 ×.
Fig. 7. *Strongylocentrotus droebachiensis*, gastrula ectoderm cell. The dictyosomes are found in a Golgi zone. *C* = cell border. Magnification 44,000 ×.

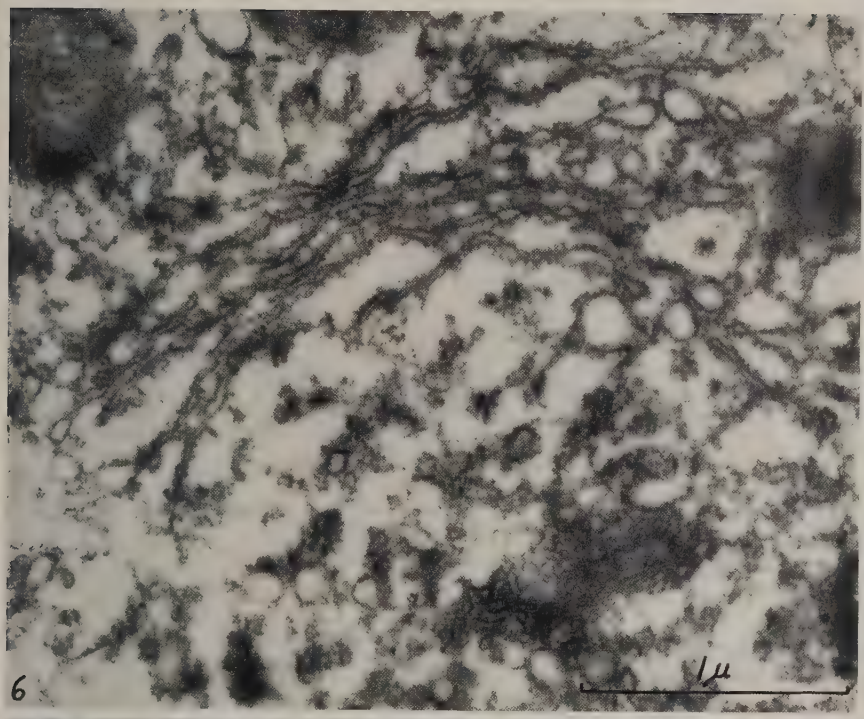
6
1μ

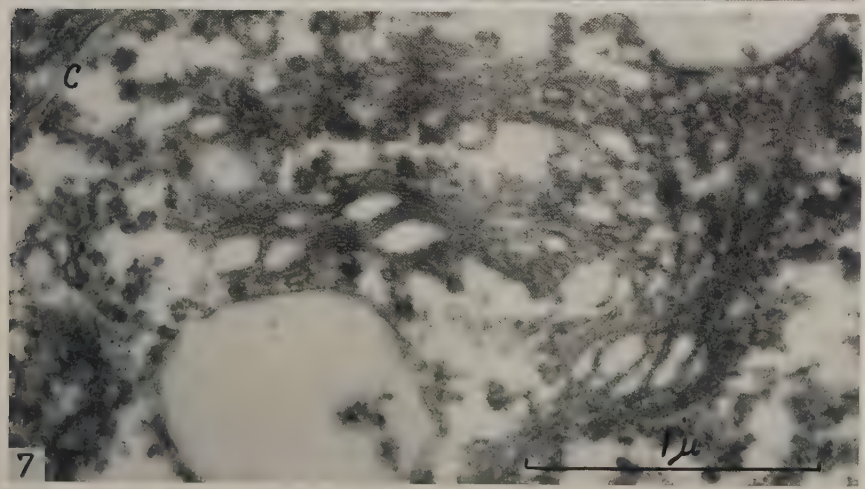
C
7
1μ

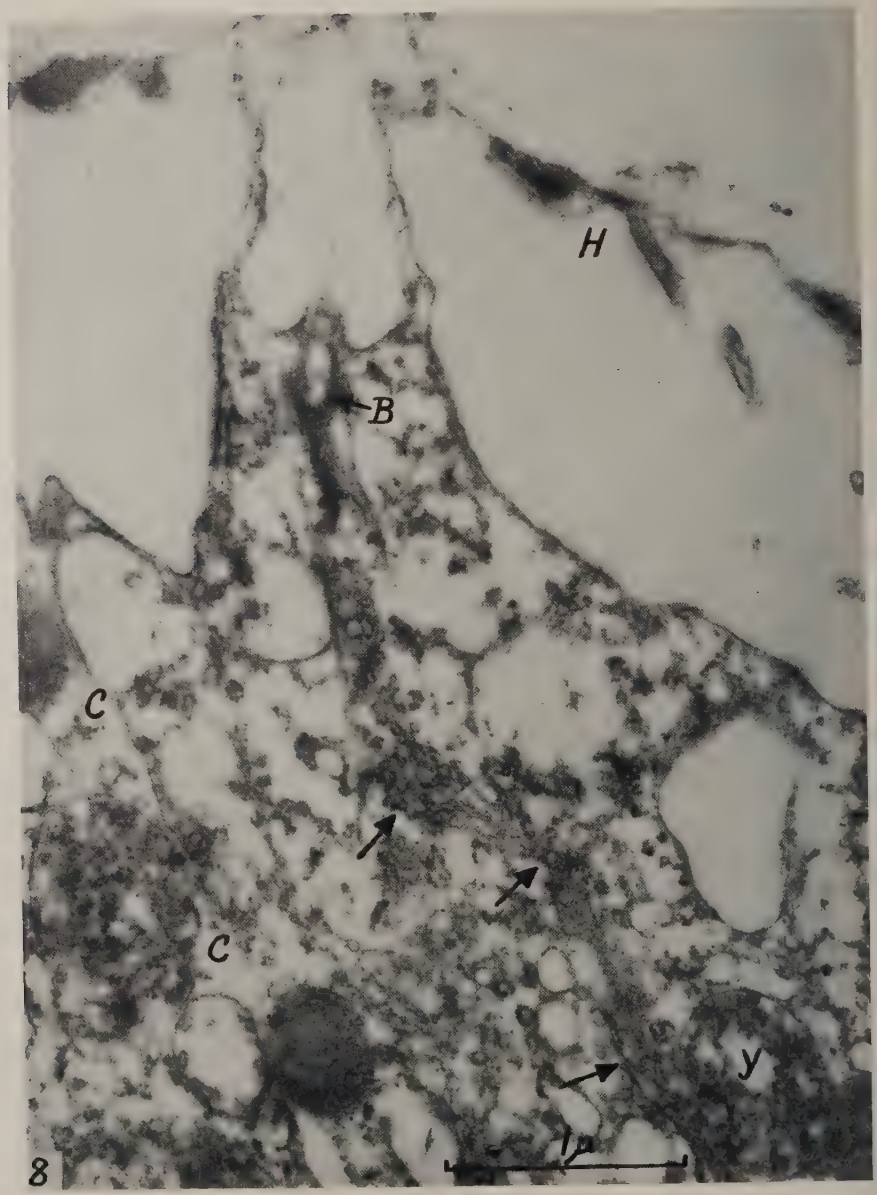
H
B
C
C
y
1μ
8

were not shown in their micrographs, and it seems certain from other studies that such anastomoses do not exist, e.g. pancreas excretory cells [28], kidney proximal tubule cells [24], and intestinal epithelial cells [33]. On the other hand, *a network can be formed by the walls* of adjacent Golgi vacuoles, as pointed out by Haguenau and Bernhard [10]. This network may be similar to that described by light microscopists with the classical Golgi techniques and may be an artefact or a true representation.

The Golgi double membranes, vacuoles, and "granules" all have the same wall thickness, namely 60 Å. As all intermediate forms exist, there are probable transformations among these three structures, and therefore they may be composed of the same material. The influence of the fixation fluid is difficult to estimate, as no applicable control method is known. The same structure is, however, seen when fixed with pure and liquid osmium tetroxide of 40°C, with 1 per cent osmium tetroxide solution in sea water and with a mixture of osmium tetroxide and potassium dichromate in sea water. Fixation in 1 per cent osmium tetroxide solution in distilled water gives an essentially similar picture of the dictyosome, which is therefore probably insensitive to hypotonic swelling.

The growing oocyte is a favourable cell for the study of dictyosome multiplication and development. Divisions are often found and occur regularly across the double membranes. Although a splitting of the double membranes would seem to be more easily performed, this is not the case. A break of all double membranes occurs at the same level (Figs. 2 and 3), which seems to be the mode of multiplication. The number of parallel double membranes is therefore constant, approximately 7 in dictyosomes of all diameters.

It is known that rapidly synthesizing cells have a large and scattered Golgi apparatus. This is also true for the growing oocyte. The sea urchin egg is unusual in that a resting phase is intercalated between maturation and fertilization. This cell is therefore suitable for a study of the Golgi apparatus in a resting stage. With regard to the dictyosomes this resting phase is characterized by a much reduced dictyosome number, the aggregated dictyosomes being smaller and more compact than in the oocyte stage. Light microscopy has not revealed a clear picture of the dictyosomes in this resting stage. This might be due to difficulties encountered in the application of the Golgi staining techniques. Attempts to impregnate fresh sea urchin eggs with osmium

---

Fig. 8. *Strongylocentrotus droebachiensis*, gastrula ectoderm cell. A flagellum (not in the level of the section) originates from the basal granule, *B*. Thin strands connect this region with the dictyosome, which is marked with three arrows. *Y* = yolk granule, *C* = cell border, and *H* = hyaline layer on the outside of the cell cortex. Magnification 36,000 ×.

were made by the author. No specific staining was obtained, and the method of extracting excess colour with turpentine did not give the desired result. Light and electron microscopy seem to indicate that osmium impregnation methods are not applicable to certain cell types.

The mature unfertilized sea urchin egg is characterized also by the appearance of a cell component, here called a "dispersed dictyosome". That this component is derived from a dictyosome of a normal type is naturally impossible to state; such is the case with all dynamic processes studied by electron microscopy. Some morphological similarities make such a transformation from the disappearing dictyosomes to the appearing "dispersed dictyosomes" seem plausible. This would then be a process very similar to that suggested in neurones by Palay and Palade. The Nissl bodies may have much the same appearance in sections as the "dispersed dictyosome" of the sea urchin egg; compare Figs. 4 and 8 in the quoted work [19] and Fig. 6 in the present.

The function of the Golgi apparatus has not been essentially clarified by electron microscopic studies. The conception that it participates in an obscure manner in secretory processes [7, 13] appears to be confirmed by the intimate topographical associations with Golgi and zymogen granules which were demonstrated by Sjöstrand and Hanzon [28]. The possible role of the oocyte dictyosome in yolk granule formation can also be assumed for similar reasons. The yolk granule formation takes place during a long period and without synchronization between the different granules, and therefore no distinct intermediate stages can be obtained by sectioning oocytes of different sizes. Even in the smallest oocyte studied there are some particles which appear to be yolk granules and these bear no topographical relationship to the dictyosomes. This indicates that all yolk granules do not arise by the same mechanism; for example, some may arise in the follicle cells and then be introduced into the oocyte. Two slightly different mechanisms are suggested for the condensation of secretion products in the Golgi apparatus. One consists of a coalescence of several Golgi "granules" which seems to be the manner in which zymogen granules appear [28]. The other mechanism is characterized by the appearance of a substance within a Golgi vacuole. These two mechanisms probably co-operate to form a yolk granule as judged by the intermediate structures. Other cell types in which osmiophilic material fills the Golgi vacuoles are the liver cells [10] and the epithelial cells of the duodenum [33].

The presence of the Golgi apparatus in practically every type of animal cell indicates that it may have more than a secretory function. The yolk granules of the oocyte and the acrosome of the spermatozoa remain within

TABLE I

Absolute and relative numbers of dictyosomes photographed from cytoplasm samples of sea urchin oocytes, mature eggs, and fertilized eggs (fixed 25 30 minutes after sperm addition). The dictyosomes are classified in three groups according to their distance from the neighbouring dictyosome in the plane of the section. In the first group the neighbouring dictyosome is at a distance of 0.1μ or less, in the second at a distance of between 0.1 and 1μ, and the third group may be said to consist of isolated dictyosomes.

	Distance 0–0.1μ		Distance 0.1–1μ		"Isolated"		Total number	
	Number	Per cent	Number	Per cent	Number	Per cent	Number	Per cent
Oocyte	18	46	6	15	15	39	39	100
Mature egg .	2	10	2	10	16	80	20	100
Fertilized egg	8	33	4	17	12	50	24	100

TABLE II

Dimensions of the dictyosomes, their membranes and the yolk granule outer membranes. All values have been calculated from 10 mean values from approximately 5 eggs. Each mean value in the three columns to the right is obtained from *c.* 10 separate measurements.

	Dictyosome diameter in μ		Dictyosome thickness in μ		Dictyosome single membrane in Å		Adjacent single membranes of two pairs and their intermediate space in Å		Yolk granule outer membrane in Å	
		σ		σ		σ		σ		σ
Echinus esculentus, oocyte	1.32±0.05	0.13	0.22±0.01	0.03	58±4	10	162± 5	15	66±3	9
Psammechinus miliaris, oocyte	1.02±0.09	0.27	0.26±0.03	0.07	64±4	11	190±13	39	68±3	9
Strongylocentrotus droebachiensis, oocyte . .	1.20±0.11	0.33	0.24±0.02	0.06	64±5	14	182± 7	23	67±3	10
Strongylocentrotus droebachiensis, mature egg*	2.78±0.31	0.98	0.55±0.05	0.16	71±3	9	242±16	50	—	
Strongylocentrotus droebachiensis, fertilized egg	1.19±0.09	0.28	0.21±0.02	0.04	66±3	7	179± 7	22	—	

* In the mature *Strongylocentrotus* eggs the values of the "dispersed dictyosomes" have been calculated; the fourth column indicates the total thickness of the double membrane in a "dispersed dictyosome".

the cell. The contractile vacuole of parazoa and protozoa seems to be of Golgi nature [8], and so is the so-called "parabasal apparatus" in some flagellated cells [15, 22]. The latter observation is confirmed in the present study.

SUMMARY

The ultrastructure of the Golgi element (dictyosome) in sea urchin oogenesis and development has been studied by means of electron microscopy in ultrathin sections prepared according to the technique of Sjöstrand.

1. The dictyosome of the growing oocyte and the fertilized egg is a stack of aggregated flattened vesicles in approximately 7 parallel rows. A few vesicles of a dictyosome may be swollen. The vesicles are closed and do not anastomose. Generally, smaller vesicles are found at the edges of the dictyosome. This structural organisation of Golgi membranes, vacuoles and "granules" is similar to the Golgi apparatus from a vertebrate cell. These Golgi components have the same membrane thickness—60 Å. A Golgi ground substance is barely discerned.

2. In the growing oocyte many dictyosomes have a break of all vesicles, which bisects them at the same level. This probably represents a divisional stage. Dictyosomes of all diameters—0.2 to 2.4μ—have approximately the same thickness—0.2μ.

3. In the very young oocyte the dictyosomes are collected into a circular formation near the nucleus. The gastrula cell also has the dictyosomes in the Golgi zone, whereas the other stages studied have the dictyosomes scattered in the cytoplasm. The mature egg has only a few dictyosomes, and these are of relatively small diameter.

4. It is not possible to stratify the dictyosomes within the sea urchin egg by centrifugation. The classical method of visualizing the Golgi apparatus by osmium impregnation did not result in specific staining.

5. Some dictyosome vacuoles of a growing oocyte contain a granular component. Most morphological stages from the granular vacuoles to yolk granules can be found, which suggests that yolk granules may originate in the dictyosomes.

6. In the mature egg there appears a cell component consisting of a stack of flattened, closed vesicles in approximately 7 parallel rows. The thickness of the membrane is 60 Å; the total thickness of the vesicle, where its sides are parallel, is approximately 240 Å. The vesicles are not aggregated, and the total size of the component (*c.* 3 × 0.5μ) is larger than that of an aggregated dictyosome. This formation has been called a "dispersed dictyosome".

7. A dictyosome is found at the base of the flagellum in the flagellated cells of a gastrula.

The author wishes to express his sincere gratitude to Dr. F. Sjöstrand, Associate Professor of the Department of Anatomy, for the privilege of working in his laboratory, and to Professor J. Runnström, the Wenner-Gren Institute, for his unfailing support and interest. To Dr. G. Gustafson, Kristineberg Zoological Station of Royal Academy of Sciences, and to Konservator T. Soot-Ryen, Tromsö Museum, Norway, the author wishes to record his thanks for generous help and supply of material. Financial support from the Swedish National Research Council and the Hierta-Retzius' stipendiefond is gratefully acknowledged. A part of the expenses for material was defrayed by a grant from the "Swedish Cancer Society" awarded to Professor J. Runnström.

REFERENCES

1. Afzelius, B. A., *Exptl. Cell Research* **8**, 147 (1955).
2. Beams, H. W. and Tahmisian, T. N., *Cytologia* **18**, 159 (1935).
3. Clermont, Y. and Haguenau, Françoise, *Compt. rend. Acad. Sci.* **241**, 708 (1955).
4. Dalton, A. J. and Felix, Marie, *Am. J. Anat.* **94**, 171 (1954).
5. Douglas, Hilda, Duthies, E. S., and Gatenby, J. B., *Z. wissenschaftl. Zool.* **144**, 211 (1933).
6. Ephrussi, B. and Parat, M., *Compt. rend. Soc. Biol.* **96**, 1360 (1927).
7. Gatenby, J. B., *J. Roy. Microscop. Soc.* **75**, 134 (1955).
8. Gatenby, J. B. and Dalton, A. J., *Nature* **176**, 301 (1955).
9. Gettner, M. E. and Hiller, J., *J. Appl. Phys.* **21**, 889 (1950).
10. Haguenau, Françoise and Bernhard, W., *Arch. Anat. microscop. Morphol. Exptl.* **44**, 27 (1955).
11. Harvey, L. A., *Proc. Roy. Soc. London Ser. B.* **107**, 417 (1931).
12. —— *Proc. Roy. Soc. London Ser. B.* **107**, 441 (1931).
13. Hirsch, G. C., Form- und Stoffwechsel der Golgi-Körper. Berlin, 1939.
14. Hovasse, R., *Compt. rend. Soc. Biol.* **118**, 450 (1935).
15. —— *Compt. rend. Soc. Biol.* **119**, 1001 (1935).
16. Just, E. E., *Anat. Rec.* **37**, 158 (1927).
17. Motomura, I., *Sci. Repts. Tohuko Univ.* (4) **18**, 255 (1950).
18. Newman, S. B., Borysko, E., and Swerdlow, M., *J. Research Natl. Bur. Standards* **43**, 183 (1949).
19. Palay, S. L., and Palade, G. E., *J. Biophys. Biochem. Cytol.* **1**, 69 (1955).
20. Parat, Marguerite, *Compt. rend. Soc. Biol.* **96**, 1360 (1927).
21. Parat, Marguerite and Parat, M., *Compt. rend. Soc. Biol.* **96**, 1363 (1927).
22. Parat, M., *Compt. rend. Acad. Sci.* **188**, 1517 (1929).
23. Policard, A. and Bessis, M., *Exptl. Cell Research* **8**, 583 (1955).
24. Rhodin, J., Correlation of Ultrastructural Organization and Function in Normal and Experimentally Changed Proximal Convoluted Tubule Cells of the Mouse Kidney. Stockholm, 1954.
25. Sjöstrand, F. S., *Nature* **168**, 646 (1951).
26. —— *Experientia* **9**, 114 (1953).
27. —— Electron Microscopy of Cells and Tissues, Physical Techniques in Biological Research, III. New York, 1956.
28. Sjöstrand, F. S. and Hanzon, V., *Exptl. Cell Research* **7**, 415 (1954).
29. Subramaniam, M. K., *Proc. Indian Acad. Sci. Bangalore* **1**, 219 (1934).
30. Subramaniam, M. K. and Gopala, A. R., *Z. Zellforsch. mikroskop. Anat.* **24**, 576 (1936).
31. Tennent, D. H., Gardiner, M. S., and Smith, Dorothy, E., *Publ. Carneg. Inst.* **27**, 413 (1931).
32. Wilson, E. B., *Am. Naturalist* **60**, 105 (1926).
33. Zetterqvist, H., The ultrastructural organization of the columnar absorbing cells of the mouse jejunum. Stockholm 1956.

RELATION BETWEEN CELL GROWTH AND CELL DIVISION

II. THE EFFECT OF CELL SIZE ON CELL GROWTH RATE AND GENERATION TIME IN *AMOEBA PROTEUS*[1]

D. M. PRESCOTT[2]

Department of Zoology, University of California, Berkeley, Calif., U.S.A.

Received December 1, 1955

In the preceding paper of this series [8] the growth in volume, protein, and reduced weight of *Amoeba proteus* over the complete cell cycle were described. The growth rate in this cell is at a maximum level immediately following cytoplasmic division and thereafter falls off steadily until, 4 hours before the first recognizable sign of cell division (prophase), growth virtually ceases. With the normal growth pattern for this cell thus established, it became possible to investigate further the relationships between initial cell size, final cell size, growth rate, and cell generation time. Specifically, the experimental approaches used here were as follows: (1) dividing cells were experimentally induced to undergo unequal division, the post-telophase cell sizes determined, and the length of the subsequent generation for each of these abnormally large or small post-telophase cells recorded; (2) the patterns of growth for an abnormally large and for an abnormally small post-telophase amoeba were determined and then analyzed with respect to the normal growth pattern.

MATERIALS AND METHODS

Amoeba proteus was stock-cultured exclusively on *Tetrahymena geleii* as described [9, 10]. All cultures were initiated from a single clone. In following the history of individual amoebae or small groups, a dividing amoeba (or amoebae) was selected from a stock culture, and one or more of the daughter cells cultivated on *Tetrahymena* in a small petri dish bottom-layered with one per cent non-nutrient agar (Difco). Both stock cultures and experimental cultures were kept in complete darkness at 23°C unless otherwise noted.

Unequal division.—The division of amoebae kept in weak light or complete darkness gives rise to two daughter cells of nearly equal size (cf. below, Table I). However,

[1] Supported by a grant to Prof. Daniel Mazia from the American Cancer Society, recommended by the Committee on Growth, National Research Council.

[2] Present address: University of California Medical Center, Department of Anatomy, School of Medicine, Los Angeles 24, California.

if a dividing amoeba is exposed to strong light (sunlight or the beam from a microscope lamp), the division is likely to be unequal (see Results). Taking advantage of this, a number of abnormally large and small post-telophase cells were produced, and their reduced weights (weight when submerged in the inorganic amoeba medium) determined on the Cartesian diver balance [8, 11].

Growth curves.—Growth curves in reduced weight for an abnormally large post-telophase cell and for an abnormally small post-telophase cell were determined on the Cartesian diver balance in the same manner as has been described for normal-sized cells [8]. As mentioned in [8], any particular *absolute* value for a reduced weight determination is only accurate to $\pm$ 0.1 mμg (millimicrogram) owing to inaccuracies of the standard used for calibration of the balance. However, in comparing the weight of one amoeba with that of another, or the weights of the same amoeba at different growth stages, the relative error is always less than $\pm$ two per cent.

The sister abnormal-sized post-telophase cells used for the growth studies were cultured on *Tetrahymena* at 23°C in the dark. Every several hours each amoeba was removed from the culture dish and weighed on the diver balance to determine the progress of growth. The last weight determinations were made as the amoebae entered division stages.

RESULTS

Unequal division.—To illustrate the effect of light on the division of amoebae, 27 dividing amoebae were exposed to the light beam from a microscope lamp; the reduced weights of the daughter cells produced in each case, as determined on the diver balance, are listed in Table I. In the same Table are listed the reduced weights of 8 daughter cell pairs which resulted from division allowed to proceed in complete darkness. The temperature was kept at 23°C for both groups. In this latter group the largest size difference is 10 per cent, and the mean is 5 per cent. In the group exposed to light, with the exception of three pairs, the size difference is much greater than 10 per cent; the mean difference is 40 per cent. In 4 cases the division was so unequal that the one daughter cell was two times or more the size of the other. In a few cases, cytoplasmic divisions were completely inhibited with exposure to light, giving rise to binucleated cells. Otherwise, the amoebae appeared to be in no way damaged by the light treatment, and, following the unequal division, the daughter cells fed and grew actively and later divided regardless of whether or not the light exposure was continued. Binucleated amoebae grew and divided cytoplasmically at the next nuclear division (coming after 24 hours or more); usually the division was into 4 uninucleated individuals, but occasionally into one binucleated and two uninucleated cells. Cytoplasmic division has never been observed to occur without accompanying nuclear division.

The data in Table I illustrate one further point. By adding the two daughter cell weights in each pair, the weights of the 35 amoebae just before cytoplasmic division are obtained. The mean division size is 20.1 mμg $\pm$ 0.1 mμg with a standard deviation of only 0.7 mμg. Therefore, it is not surprising that the 8 cases of equal division (Table I) produced a group of 16 amoebae of nearly uniform size (9.9 $\pm$ 0.1 mμg, with a standard deviation of 0.4 mμg).

TABLE I

The data illustrate the effect of light on the equality of cell division in *Amoeba proteus*.

Exposed to light during division. Resultant post-telophase cell pairs			In darkness during division. Resultant post-telophase cell pairs		
mμg reduced weight		% difference	mμg reduced weight		% difference
8.1	13.0	61	9.4	10.0	6
6.5	13.1	101	10.2	10.6	4
9.8	10.8	10	9.0	9.9	10
8.6	11.4	33	9.8	9.9	1
6.9	12.0	74	9.7	10.6	9
8.2	11.0	34	9.9	10.6	7
7.9	12.0	52	9.5	9.8	3
8.6	10.3	20	9.9	10.1	2
9.1	11.0	21	Mean 9.7	10.2	5
9.0	10.7	19			
8.6	11.8	37			
8.9	11.0	24			
7.8	13.3	70			
7.1	13.5	90			
6.9	14.3	101			
6.2	14.4	132			
6.4	13.6	112			
7.0	13.1	87			
9.5	10.5	11			
9.6	11.0	15			
9.5	10.5	11			
9.4	11.5	22			
10.1	11.5	14			
9.7	10.3	6			
9.6	10.0	4			
10.0	12.0	20			
7.2	12.0	67			
Mean 8.4	11.8	40			

This uniformity in the size of amoebae in the same growth stage can be credited in large part to control and standardization of culture conditions [9, 10]. Such size uniformity is not to be found in the wild, infusion type of *Amoeba proteus* culture. The availability of a complete nutrient medium for this amoeba undoubtedly would further reduce individual variations through increased standardization of culture conditions.

Unequal division and subsequent generation time. –The abnormal-sized post-telophase amoebae of Table I were cultured on *Tetrahymena* at 23°C, and the length of the subsequent generation time was recorded for each amoeba. In Fig. 1 the weights of the individual post-telophases (the values given in Table I) are plotted against the number of hours required to reach the next division. Included in Fig. 1, for comparison, are the generation times for the 16 normal-sized post-telophase amoebae of Table I. A normal post-telophase cell (9.5 to 10.5 mμg) under the culture conditions employed here, doubles in size (see curve I, Fig. 2) by approximately 20 hours and divides at the end of 23.5 to 25.0 hours.

The amoebae represented in Fig. 1 have been divided into three groups: group one, normal-sized post-telophases with a reduced weight range of 9.5 to 10.5 mμg; group two, abnormally small post-telophases with reduced weights of less than 9.5 mμg; group three, abnormally large post-telophases with weights greater than 10.5 mμg. As will be seen below (Fig. 2) the weight reached by the abnormal-sized post-telophase amoebae at the next division is normal. Thus, knowing the weight gained by each normal- or abnormal-sized post-telophase cell by the next division, and knowing the generation time in each case, it becomes possible to calculate average growth rates for the individual amoebae for the complete cell cycle. Group one has a *mean* growth rate of 0.41 ± 0.01 mμg/hour; group two (small post-telophase), 0.44 ± 0.01 mμg/hour; group three (large post-telophase), 0.35 ± 0.01 mμg/hour. It appears then that the large post-telophase amoebae grow more slowly and divide before the normal, and the small post-telophase amoebae grow more rapidly but still divide later than the normal. In general, the generation times for the amoebae in groups two and three are not equally affected by a given variation from the normal post-telophase cell weight. In group two, a size which is three mμg below normal results in approximately a 6-hour (25 per cent) increase in generation time. In group three, a size increase of three mμg over normal results in a shortening of the generation time of roughly three hours only (12 per cent).

Growth curves.—Curves II and III in Fig. 2 show the growth patterns for two amoebae which were produced by a single unequal division. The post-

telophase weights in this case were 7.2 and 12.0 mμg, representing a size difference of 67 per cent. Curve I in Fig. 2 is the mean of 4 growth curves in [8] and shows the growth pattern followed by a normal-sized post-telophase

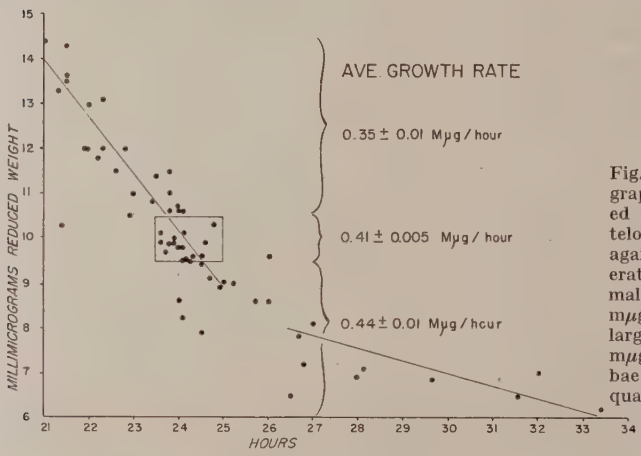

Fig. 1. Each point in the graph represents the reduced weight of a single post-telophase amoeba plotted against its subsequent generation time. The abnormally small (less than 9.5 mμg) and the abnormally large (greater than 10.5 mμg) post-telophase amoebae were produced by unequal divisions.

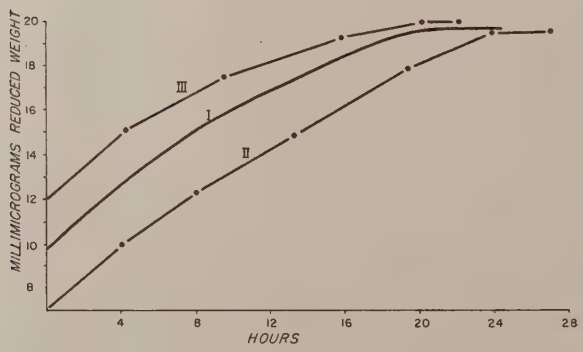

Fig. 2. Growth curves for three post-telophase cells, each of a different size: Curve I, growth of a cell of normal zize; Curves II and III, growth of an abnormally small and an abnormally large cell respectively.

amoeba. The large post-telophase amoeba increased in size by 65 per cent in 22 hours. The small post-telophase amoeba grew to 170 per cent of its initial weight in 27 hours. Both reached approximately the normal division size at the end of the cycle. Again, the large post-telophase cell grows more slowly and divides earlier; the small post-telophase cell grows more rapidly and divides later. The growth pattern for the normal-sized post-telophase (curve III) is intermediate.

DISCUSSION AND CONCLUSIONS

Effect of light on cytoplasmic division.—Clearly, the effect of light on dividing *Amoeba proteus* is directly related to the known negative phototrophic reaction of this organism. Amoebae kept in the dark and under favorable growth conditions usually take the form of a flat, fringed disc and do not show motility. A few seconds of light exposure induce a change to the typical streaming form. Even enucleated amoebae, which normally show only sporadic and weak motility, can be induced to more active movements by light exposure [1]. The movement is always away from the light. There are some indications that light of shorter wave-lengths, and perhaps ultra-violet light, may be the most effective stimulator [3, 5]. In *Amoeba proteus* nuclear division slightly precedes cytoplasmic division so that late telophase is reached before cytoplasmic division is completed. During the events of nuclear division the amoebae completely lose motility, detach from the substrate, and become spherical. At this stage of division even very strong light is *not* sufficient to induce streaming in the amoebae. Shortly *before* the completion of cytoplasmic division, when the daughter nuclei have begun to reconstitute, the amoebae reattach to the substrate and, if exposed to light at this time, begin cytoplasmic streaming; in this situation cytoplasm may flow from one to the other of the incompletely separated daughter cells. The direction and intensity of this cytoplasmic re-apportioning most likely depend on the orientation of the daughter cells with respect to the light source. Because of the negative phototropism, the daughter cell closer to the light would be expected to lose cytoplasm to the second daughter cell and thus be smaller.

The wide variation in the degree of inequality of divisions (Table I) apparently reflects various orientations of the dividing amoebae to the microscope beam. If the division plane lies parallel to the direction of light, then each daughter cell should be identically affected, and the division, therefore, should be an approximately equal one. A few of the light-treated amoebae (Table I) did divide into nearly equal parts. The binucleated amoebae, which result from a failure of cytoplasmic division, probably occur when the plane of the cell division is perpendicular to the direction of the light; under these conditions, it is conceivable that all of the cytoplasm (and nucleus) of one daughter cell flows into the other daughter cell. In the majority of cases, however, the division goes to completion despite the light-induced streaming of the cytoplasm.

Control of cell size and growth rate.—In view of the non-growth predivision period we cannot say that final cell size is controlled by dividing at a critical

mass; growth ceases, and cell size remains fixed during several hours preceding division. Secondly, the final size attained by *A. proteus* at division is independent of initial cell size; large and small daughter cells attain the same mass by the next division (Fig. 2). It appears then that final cell size may be under some sort of genetic control. This is certainly not a new idea, but the present studies lend experimental evidence.

The control of cell size means, of course, that there is also control or limitation of cell growth in some manner. The growth curves (Fig. 2) indicate that, as the cell increases in size and proceeds toward division, there must be a mechanism for slowing and, eventually, halting growth. Following this, growth can be re-initiated in three different situations: (a) In the normal course of events growth begins again immediately following cell division. (b) Under certain conditions of light exposure the nucleus divides, but cytoplasmic division is inhibited, and a binucleated cell is produced. In this case growth is resumed following reconstitution of the two daughter nuclei. (c) If, before the cell enters prophase, its size is reduced by the artificial amputation of cytoplasm, mitosis is delayed until the cell has again grown to full division size. The latter experiment will be discussed in detail in another paper of this series. In these three situations there is a common condition; the amount of cytoplasm *per nucleus* has been drastically reduced. Conceivably this means that the amount of cytoplasm which the single nucleus is capable of supporting has a definite limit, and, as this size limit is approached, growth becomes progressively slower and finally stops completely. This idea is consistent with the data of Fig. 1; the larger the cell, the lower the rate of growth.

Stated in the above manner, "limitation of growth" is perhaps a more appropriate term than "control of growth." Under this scheme, when a cell has reached the predivision period, further growth would depend upon the reorganization of the nuclear material (synthesized during interphase) into two functional units (nuclei) at mitosis. This suggests that the growth limitation mechanism resides in some function of the nucleus. The nucleus of *A. proteus* is now known to synthesize at least part of the ribonucleic acid found in the cytoplasm [2, 4] and, in addition, to control directly a significant part of the cell's protein synthesis [6]. It is in nuclear functions such as these that we should probably seek some key to growth regulation. Ultimately, however, the problem must be carried down to specific genetic machinery.

Cell size, growth rate, and generation time.—There are two points which discourage consideration of cell size as an important factor in the actual initiation of cell division. One of these, the presence of the predivision period,

has been mentioned above and discussed elsewhere [8]. Secondly, even amoebae which are prevented from attaining full division size by means of starvation will still divide, but the division is considerably delayed [7]. If growth (and therefore size) is limited too severely, the cell dies in two or three weeks without undergoing division. Cell size then, although not involved directly in the division stimulus, affects the length of the cell cycle and, in this general way, the time of division.

The relationship is again indicated in Fig. 1; the larger the cell at the beginning of its life cycle, the more rapidly it reaches division. Post-telophase cells below normal size have generation times longer than normal. There is perhaps nothing unexpected in this, and indeed, it emphasizes the role of cell size in the rapidity with which a cell proceeds toward division. A closer examination of the data in Fig. 1, however reveals an interesting qualification concerning this relationship. If a post-telophase cell were permitted to begin the cell cycle with the full amount of cytoplasm normally contained in a dividing amoeba (20 mμg), we can see by extrapolating the upper left part of the curve in Fig. 1 that an amoeba of this size would still require about 16 hours to reach division. The events occupying the terminal part of such a 16-hour period of no growth would supposedly be the same events which are responsible for the existence of the 4-hour predivision period occurring in the course of normal growth. However, the discrepancy between the expected generation time for a 20 mμg post-telophase cell, i.e., a 4-hour predivision period, and the calculated (by extrapolation) generation time, i.e., 16 hours, may be a measure of the time required for the limiting processes other than growth of the predivision events. Perhaps "limiting processes" might better be expressed as "the biochemical differentiation of the cell over its life cycle." As a specific example, desoxyribonucleic acid synthesis (and perhaps RNA synthesis) would be expected to form part of such a process. Completion of this biochemical differentiation presumably results in mitosis.

As mentioned above, amoebae which are kept well below division size by starvation may still divide after a greatly extended interphase. In this case the completion of biochemical differentiation must go on endogenously and thus proceed more slowly than if the process were permitted to draw on a continued nutrition.

SUMMARY

1. Exposing dividing *Amoeba proteus* to strong light results in an unequal division. The effect is explainable on the basis of the negative phototropism of this organism.

2. Normal and abnormally large and small post-telophase amoebae produced by unequal division were weighed on the Cartesian diver balance, and the subsequent generation times for these cells were recorded. Growth curves by weight for a large post-telophase cell and a small post-telophase cell were also determined. A large cell grows more slowly but still has a shorter than normal generation time. A small cell grows more rapidly and divides later than the normal. In all cases the post-telophase cells reach the normal division size at the next division, and a pre-division period of "no growth" is always apparent. As cell size increases, the growth rate drops.

3. Cell size and growth appear to be under nuclear control.

The author wishes to express his gratitude to Professor Daniel Mazia for his interest and encouragement during the course of this work and for criticism concerning the manuscript.

REFERENCES

1. Cohen, A. I., unpublished.
2. Goldstein, L. and Plaut, W., personal communication.
3. Harrington, N. H., and Leaming, E., *Am. J. Physiol.* **3**, 9 (1900).
4. James, T. W., *Biochim. et Biophys. Acta* **15**, 367 (1954).
5. Mast, S. O., *J. Exptl. Zool.* **9**, 265 (1910).
6. Mazia, D. and Prescott, D. M., *Biochim. et Biophys. Acta* **17**, 23 (1955).
7. Prescott, D. M., unpublished.
8. —— *Exptl. Cell Research* **9**, 328 (1955).
9. —— *Compt. rend. Lab. Carlsberg, Sér. chim.*, in press.
10. Prescott, D. M. and James, T. W., *Exptl. Cell Research* **8**, 256 (1955).
11. Zeuthen, E., *Compt. rend. Lab. Carlsberg, Sér. chim.* **26**, 243 (1948).

III. CHANGES IN NUCLEAR VOLUME AND GROWTH RATE AND PREVENTION OF CELL DIVISION IN *AMOEBA PROTEUS* RESULTING FROM CYTOPLASMIC AMPUTATIONS[1]

From one division to the next in *Amoeba proteus* the nucleus and the cytoplasm each double in volume, and cell division occurs approximately every 24 hours at 23°C under the culture conditions described in [9]. If the growth of an amoeba is stopped at some advanced point in the cell cycle by transfer to non-nutrient conditions, such an amoeba will nevertheless divide without further increase in size, although the generation time is considerably extended. The length of this extension depends upon the size of the amoeba at the time at which growth was halted [6]. Thus it appears that limiting cell growth through starvation does not prevent cell division but only delays its onset.

[1] Supported by a grant to Professor Daniel Mazia from the American Cancer Society, recommended by the Committee on Growth, National Research Council.

On the other hand, if an amoeba is kept under favorable growth conditions and a portion of its cytoplasm amputated periodically, it will continue to grow but will not divide as long as the amputation treatment is repeated regularly. This latter experiment was reported by Hartmann in 1928 [3]. In one case, using *Amoeba proteus,* division was inhibited for several months before the experiment was voluntarily discontinued. During the same period the control amoeba went through 65 cell divisions.

Since the experiments in [6] and [7] indicate that a given cell size is not so important for the direct initiation of cell division, the inhibition of cell division in Hartmann's cutting experiments cannot be credited simply to a *limitation* of cell size. This experimental treatment, however, might reasonably be expected to interrupt those differentiations within the amoeba which are associated with the cell cycle. Readjustments following each cutting may involve a set-back for the cell with respect to progress through the life cycle.

In the work described below, Hartmann's experiments have been repeated. Besides the division inhibition, however, two other effects of cytoplasmic amputation were noted and measured. The results obtained here permit a better understanding of the division inhibition and bear generally on the problems of the relations between cell growth, size, and division.

MATERIALS AND METHODS

Amoeba proteus was stock-cultured on *Tetrahymena* as previously described [9]. The experiments involved following the history of individual amoebae; these were cultured separately in small petri dishes at 18°C in complete darkness.

A fine glass needle was used for the periodic amputations of cytoplasm from the amoebae. The volumes of the amputated pieces of cytoplasm and of whole amoebae were determined by a compression chamber method described in [7].

An approximation of nuclear volumes in living amoebae was achieved by measuring nuclear length, width, and thickness and calculating the volume of flat, slightly elongated discs with these dimensions. The nucleus of *Amoeba proteus* approaches this shape, but no great accuracy can be claimed for these particular volume determinations.

RESULTS

A dividing amoeba was picked from a stock-culture and the two daughter cells cultured separately at 18°C. At this temperature the time between divisions is about 40 hours. Periodically one quarter to one half of the cytoplasm of one of these amoebae was cut off, and the volume of the removed piece measured. The other amoeba (control) was permitted to grow and divide, but at each division one of the daughter cells was fixed and its volume

measured. By this procedure the control always consisted of one normal, growing amoeba. The volume measurements on the amputated pieces of cytoplasm and the daughter amoebae permitted the determination of growth rates for the experimental and control amoebae (see below).

Five such experiments were attempted, but the first three were terminated at 3, 7, and 6 days respectively because the treatment (cutting away cyto-

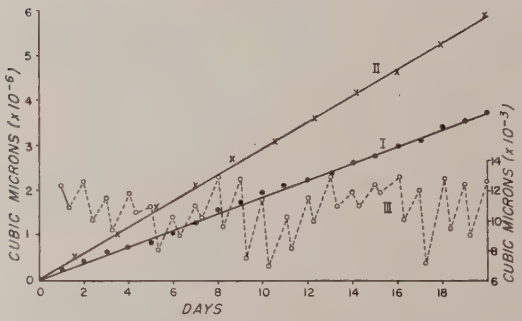

Fig. 1. Curve I, growth of a non-dividing amoeba. Division prevented by periodic amputation of cytoplasm. Curve II, growth of a normal, dividing amoeba. Curve III, changes in nuclear volume resulting in periodic loss and regaining of cytoplasm.

plasm every 36 hours) was not sufficiently severe to delay division until the next scheduled cutting. In the two successful experiments, the cuts were performed about every 24 hours and division prevented for 20 days, at which time both experiments were voluntarily ended. During the experimental period each of the control amoebae divided 11 times. Within 38 hours after the last cutting both experimental amoebae divided.

The two experiments gave essentially the same results, and the data for only one of these are plotted in Fig. 1. The volume of each amputated piece of cytoplasm has been added to the total volume for all pieces previously cut so that the last point, for example, in Curve I (Fig. 1) represents the total volume of cytoplasm removed in the 20 amputations. In a similar manner Curve II in Fig. 1 was constructed by adding together the volumes of daughter cells as they were produced by the control amoeba. Curves I and II represent, then, the growth of the experimental and the control amoebae over the 20-day period. In both experiments the growth rate for the cut amoeba was slightly, but significantly, below the rates for the control.

As part of one of the cutting experiments nuclear volume was measured immediately before each amputation and again 6 to 8 hours following the operation. These data are given by Curve III in Fig. 1; the nuclear volume scale is marked on the right ordinate. In spite of a probable large error involved in nuclear volume measurements, the trend is consistent; with each

reduction of cytoplasmic volume of the cell (points on Curve I, Fig. 1) the nuclear volume decreases. As the cut cell grows and approaches its pre-operative size, the nucleus increases in volume. With each operation the nuclear volume cycle is repeated.

DISCUSSION AND CONCLUSIONS

Cytoplasmic amputation in a growing amoeba results in these detectable effects: (1) a decrease in nuclear volume, (2) a delay in cell division, and (3) a general reduction in the cell's growth rate. The decrease in nuclear volume is a direct indication of readjustment processes taking place within the cell during the several hours following the amputation. The specific nature of this volume change is as yet unknown although there are three major possibilities any one of which may be involved: (a) a simple dehydration of the nucleus, (b) transfer of protein from the nucleus to the cytoplasm, and (c) transfer of ribonucleoprotein to the cytoplasm.

The first of these possibilities cannot be discounted although logically it appears unlikely. That the sudden loss of cytoplasm has marked effects on the synthetic activities of the cell is illustrated by the delay in division and decrease in growth rate. Since the nucleus undoubtedly contributes to the maintenance of these activities of the cell, it reasonably follows that the nucleus must also play some part in the recovery following cytoplasmic loss. Simple dehydration of the nucleus may be classified as a passive response, but hardly as an active contribution. From other experiments with this same amoeba it is now certain that the nucleus carries on, or at least controls, a significant part of the cell's protein synthesis [5], and, secondly, that the nucleus synthesizes at least part of the RNA found in the cytoplasm [2, 4]. Possibly the protein synthesis which is nucleus-associated represents the protein part of the ribonucleoprotein contribution of the nucleus to the cytoplasm. This finding [2, 4] adds circumstantial support to the hypothesis which assigns to RNA a central role in the transfer of genetic specificity from the chromosomes to the cytoplasmic proteins; certainly RNA has been strongly implicated in the synthesis of cytoplasmic proteins [1]. Whatever the function of RNA, we could reasonably expect that the amputation of cytoplasm might alter either the rate of synthesis of RNA by the nucleus or rate of transfer of this material to the cytoplasm, or both.

The delay in cell division and reduction in the cell's growth rate are effects of a more general nature and might be predicted on the basis of the readjustment activity following cytoplasmic loss. These effects do, in them-

selves, demonstrate the occurrence of major readjustments. If the amputation treatment is repeated with the proper frequency, cell division is repeatedly delayed, i.e., completely prevented. However, as previously pointed out, limitation of cell size by starvation delays, but does not inhibit, cell division. It follows from this that limitation of cell size by amputation of cytoplasm does more than simply slow down the events leading to division; for if such were not the case, division would occur eventually in spite of the operations. More likely, each division "delay" indicates that the cell has suffered a reversion to an earlier stage of its division-to-division life cycle.

With respect to the decrease in growth rate, the experiments in [8] demonstrate that smaller-sized amoebae grow at a slightly faster rate. From this it might be predicted that an amoeba in which size is kept small by repeated amputations of cytoplasm would have an average growth rate higher than normal. Curves I and II in Fig. 1 show the situation to be just the reverse. The decreased growth rate cannot be accounted for on the basis of a size limitation. During the period of readjustment following cytoplasmic amputation, growth most likely falls to such a low level that the over-all growth rate is brought below the control.

SUMMARY

The experiments of Hartmann in which division in *A. proteus* can be prevented by periodic amputation of cytoplasm were repeated. The growth rate of such growing, non-dividing amoebae was measured and found to be slightly, but significantly, below the rate for a normal growing, dividing amoeba. Following each cytoplasmic amputation nuclear volume falls and later, as the cell regrows to its pre-operative size, rises again. The decrease in nuclear volume, prevention of cell division, and the lower average growth rate are reflections of a period of readjustment following the loss of cytoplasm.

Each operation results in a reversion for the cell to an earlier point of the cell life cycle.

REFERENCES

1. Gale, E. F. and Folkes, J. P., *J. Biochem.* **59**, 661 (1955).
2. Goldstein, L. and Plaut, W., personal communication.
3. Hartmann, M., *Zool. Jahrbuch* **45**, 973 (1928).
4. James, T. W., *Biochim. et Biophys. Acta* **15**, 367 (1954).
5. Mazia, D. and Prescott, D. M., *ibid.* **17**, 23 (1955).
6. Prescott, D. M., unpublished.
7. —— *Exptl. Cell Research* **9**, 328 (1955).
8. —— *ibid.* submitted for publication (1955).
9. Prescott, D. M. and James, T. W., *ibid.* **8**, 256 (1955).

"PERSPEX" SLIDES FOR ROLLER CULTURE OF HUMAN CELLS

R. J. V. PULVERTAFT, J. A. HAYNES and J. T. GROVES

Westminster Hospital, Department of Pathology, London, England

Received December 13, 1956

The use of serum agar squares for slide culture of pathological material previously described [2] has proved very satisfactory, particularly for bone marrow. The optical properties, especially with long working distance phase contrast condensers, are excellent. One disadvantage is that although fluid culture medium can be inserted and withdrawn by making a hole in the wax seal, it is easy to damage the specimen in the process. In spite of this, material from cases of human carcinoma has been maintained with active cell division for up to six weeks.

Harris [1] has described a chamber which can be mounted on a roller; we have experimented with this and confirm its value. However, the depth of fluid involved destroys some of the definition at high powers.

A simple Perspex slide chamber has given optimal results with bone marrow and malignant tissue. In the standard slide a moat 3 mm deep is made in Perspex, thus leaving a central pillar 6 mm in diameter. Two holes are bored through the edge of the slide to communicate with the moat. The slide is sterilised by boiling. The standard culture medium is human serum (heated at 56°C for 30 minutes) 50 parts, Earle's solution 48 parts, chick embryo extract 2 parts; 100 units per cc of penicillin and streptomycin are added.

Cells for culture may be mounted in culture fluid directly on to the pillar; a cover slip is applied and sealed on with paraffin wax. One of the orifices is then plugged with wooden spigots impregnated with wax, and the moat is half filled with culture medium. The other hole is then plugged. It is important to wait until the wax is firmly set before running in fluid; otherwise an emulsion of wax is formed. For the same reason silicone seals are useless.

Cultures are fed at any required interval after removing both spigots, and withdrawing the old medium.

We find it preferable in many cases to have an agar base. For this purpose the pillar is recessed one mm below the slide level, and molten serum agar is dropped on to it. A cover slip is immediately applied, and the agar sets with

a plane surface. With care and practice the coverslip can be slid off; the standard technique is then followed. Chicken clot cultures can also be made by standard technique.

The slides are mounted on a specially designed roller; but any rotating device, such as an alarm clock will suffice, as speed of rotation may vary widely.

That fluid from the outer moat travels over the pillar can be shown by adding Indian ink to the fluid; transference to the pillar is almost instantaneous.

Text-fig. 1. Roller slide.

All photographs are by Phase Contrast, Cooke, Troughton & Simms.

Fig. 1 (top). Ascitic fluid, carcinoma of pylorus, centrifuged deposit—48 hr. culture × 560.
Fig. 2 (bottom). "Leng" cells, seminoma testis, laboratory strain—72 hr. culture × 1160.
Fig. 3 *a* and *b*. Bone marrow, monocytic leukaemia. Fibroblasts; living cells—7-day culture × 1160.
Fig. 4 (top). Bone marrow, monocytic leukaemia; living cells—72 hr. culture × 1160.
Fig. 5. Bone marrow, pernicious anaemia. Mitosis of megaloblast—24 hr. culture × 1160.

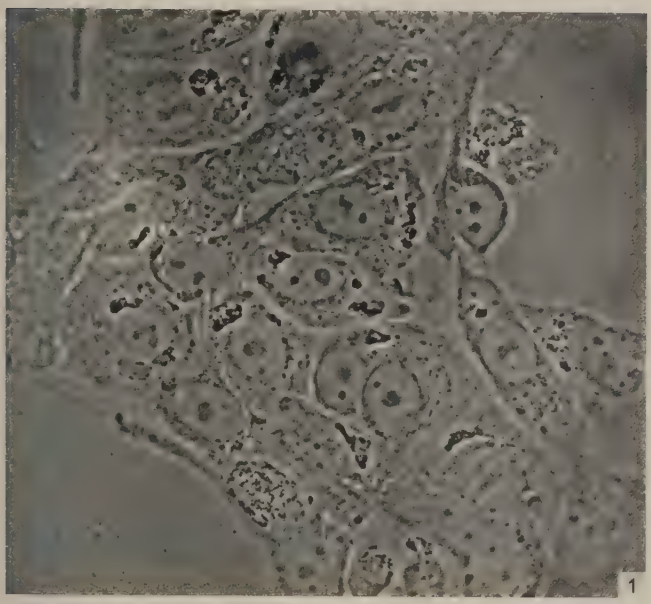

1

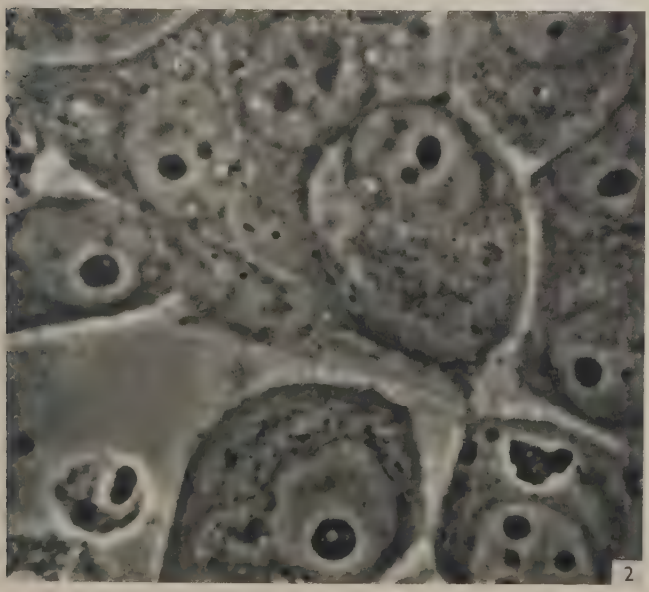

2

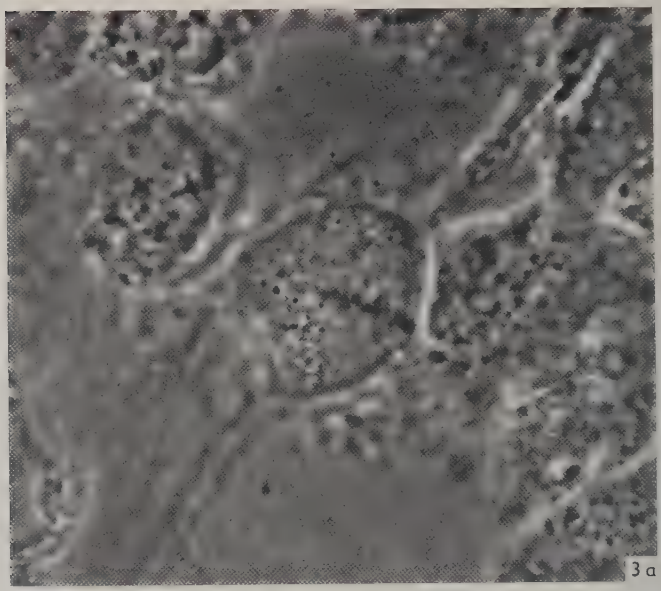

3 a

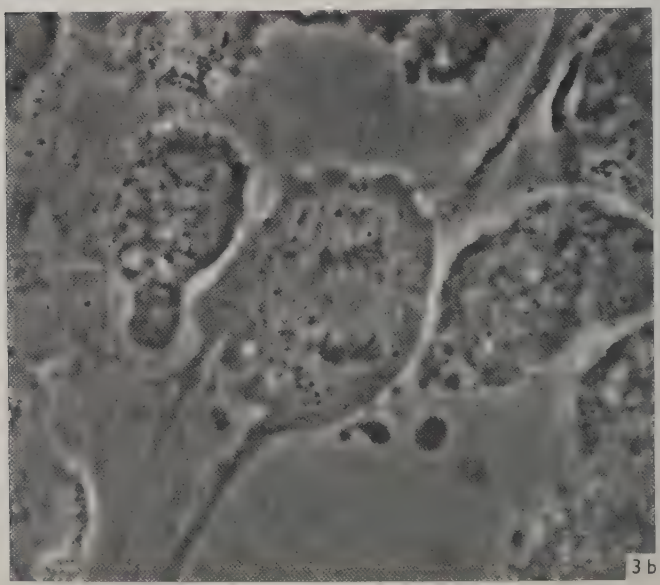

3 b

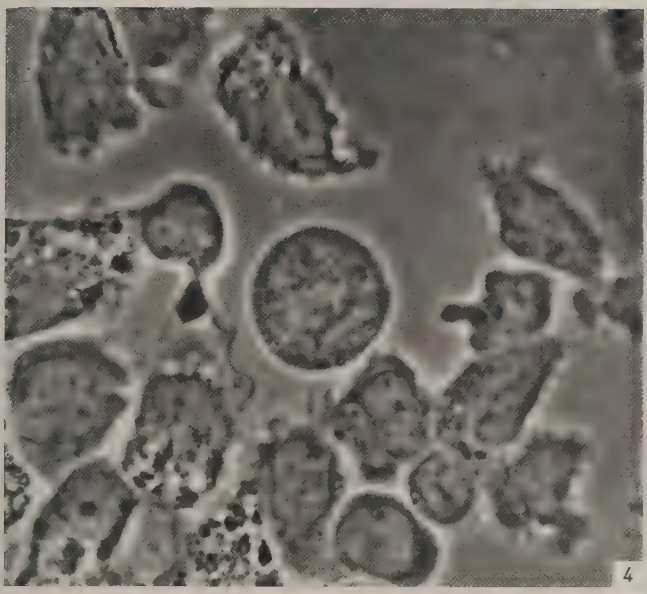

4

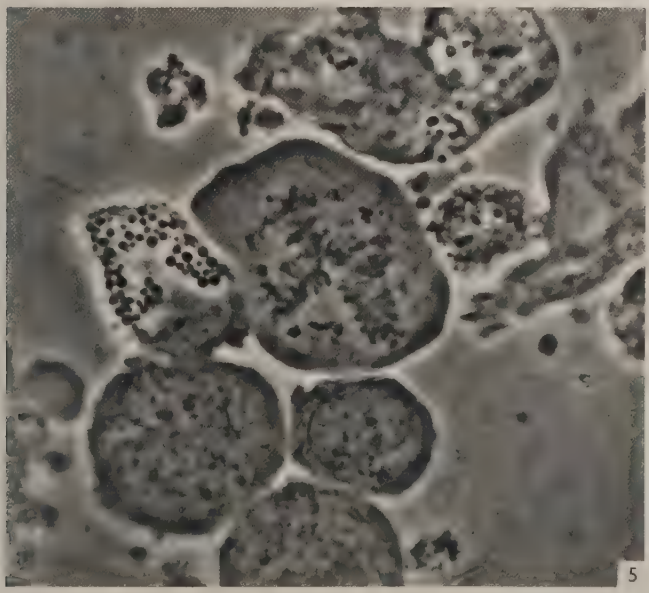

5

For photographic purposes the slides can be removed from the rollers for many hours without damaging the cultures. If the phase contrast condenser has a short working distance thinner Perspex slides are used, but are more difficult to work on a lathe; they could be moulded very easily. Coverslips can be removed, as much of the culture adheres to them; fixation and staining follow standard technique.

The slides and roller were made for us by Mr. N. Pierce for whose constant help we are grateful. The photographs were processed by Mr. David Floyd.

The expenses of this work were covered by a generous grant from the Board of Governors, Westminster Hospital.

Our thanks are due to Dr. J. G. Humble and Lt. Col. P. D. Stewart, Royal Army Medical College, Millbank, for providing material.

REFERENCES

1. Harris, H., *Brit. J. Exptl. Pathol.* **XXXVI**, 10 (1955).
2. Pulvertaft, R. J. V. and Jayne, W. H. W., *Ann. R. C. S.* **12**, 161 Mar. (1953).

A NEW ULTRAMICROTOME FOR ELECTRON MICROSCOPY

S. CLAESSON and A. Å. SVENSSON

Institute of Physical Chemistry, University of Uppsala, Sweden

Received December 15, 1955

During the last fifteen years many attempts have been made to modify the well-known technique of cutting sections for ordinary light microscopy to fulfil the demand in electron microscopy for sections $<0.1\mu$ in thickness. The first was made by von Ardenne [1] in introducing the wedge sectioning method whereby sections $<1\mu$ could be obtained. Another line was followed by O'Brien and McKinley [13] and by Fullam and Gessler [4] in applying high speed sectioning but it was not until Pease and Baker [15] modified the standard Spencer microtome by simply diminishing the mechanical advance and changing the embedding technique, that a reproducible section thickness of $\sim 0.2\mu$ was reached.

In an extensive analysis of the Pease and Baker method Hillier and Gettner [7] showed that artefacts and variations in thickness of the sections were due to the following imperfections of the instrument: static friction, variable thickness of lubricating oil films, thermal drift, defects of the knife edge and external vibrations. During recent years several authors have succeeded in eliminating some or all of the above-mentioned irregularities either by changing conventional microtomes [3, 5] or by designing entirely new ones. Another advance in microtome technique was the introduction of the plastic embedding method of Newman, Borysko and Swerdlow [12].

Watson [19] and Kobayaski and Shimadzu [11] used a rotary disc and Sjöstrand [17] a rotary wheel for giving the specimen block a reproducible single pass motion relative to the cutting edge. Sjöstrand also applied a well-controlled thermal feed for the advancement of the block. For the single pass motion Hodge, Huxley and Spiro [8] used the principle of a flexibly suspended expanding rod driven eccentrically by a wheel. On the other hand Porter and Blum [16] used a rigid rod suspended at one end in two pairs of pivots while Cocks and Schwartz [2] used a cantilever suspension for the specimen block but did not extend it to a single pass motion. Recently Haanstra [6] showed that contact between the knife and the specimen block at the back stroke could be avoided by magnetostriction of a nickel core carrying the object.

With these designs serial sections $< 0.1\mu$ have been cut, by some instruments even of the order 200 Å, a thickness permitting the full utilization of the resolving power of modern electron microscopes.

Design

In designing a new microtome we aimed at a simple construction without high precision components. From previous experience it was evident that many constructional difficulties could be evaded simply by not using bearings that could interfere with the precise motion. We have therefore obtained the movements by using elastic deformation of a cantilever system. The good mechanical properties of such systems were pointed out to us by Mr. Folke Widegren of Svenska Kullagerfabrikerna, Gothenburg. To obtain a single pass motion it was necessary to make a double cantilever system by arranging two cantilevers at right angles to each other.

The simple cantilever principle was previously used for microtome construction by Cocks and Schwartz [2] to obtain a double pass movement of the specimen relative to the knife and they refer to Jones [10] who had shown the mechanical advantages of such a system. Jones got a very precise motion of a moving member by fixing it between a pair of parallel leaf springs, the center portions of which were clamped between two metal plates.

We have found it possible to construct a microtome according to the double-cantilever principle without any difficult mechanical problems. In order to keep the mechanical construction simple, the thermal feed was applied to the knife. The construction is as follows (Figs. 1 and 2).

The reproducible circular motion of the specimen block was obtained by attaching it to the deflectible double cantilever system which was rotated by a motor via balance wheel, a shaft and an eccentric. The continuous feed of the microtome knife against the specimen is accomplished by mounting the former at the end of a heatable bar screwed to a fixed support (Fig. 1).

A drawing of the moving system of our construction is given in Fig. 2. Two thin parallel steel leaf springs (*A*) of equal length are fixed at one end to the inner sides of the branches of a vertical U-formed support (*B*) screwed to a base plate (*C*). The other ends of the springs are fastened to the vertical sides of a square frame (*D*) which on its horizontal sides carries another pair of leaf springs (*E*). It may be noted that the square frame (D) is freely suspended in the sense that it is only supported by the two spring pairs (*A* and *E*). The horizontal springs are somewhat longer than their vertical companions and are screwed to a solid square block (*F*) which functions as a carrier for

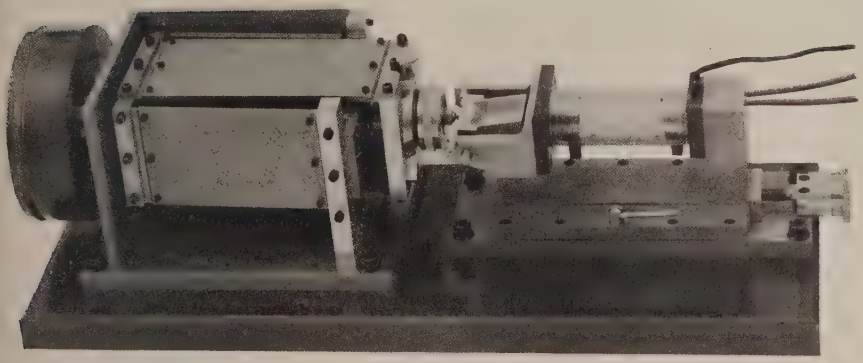

Fig. 1. Over-all view of the microtome showing to the left the "rotor" and to the right the knife holder with its thermal feed. One of the sideplates of the frame and the plexiglass cover of the "rotor" have been taken away.

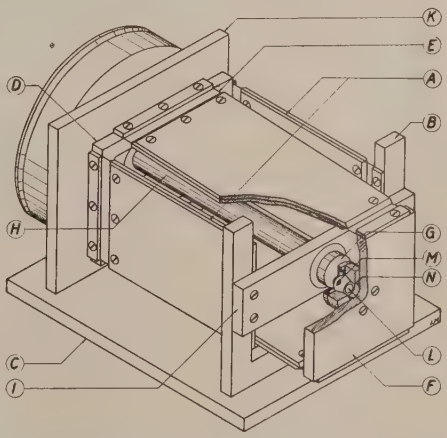

Fig. 2. Diagram of "rotor". *A*, vertical leaf springs; *B*, U-shaped support; *C*, base plate; *D*, movable hollow square block; *E*, horizontal leaf spring; *F*, movable front square block; *G*, eccentric; *H*, shaft; *I*, transverse frame; *K*, back piece screwed to the base plate; *L*, pivot of the eccentric; *M*, ball bearing; *N*, holder of the bearing.

the specimen holder. Furthermore, the vertical and horizontal springs are so spaced from each other that when bent the horizontal pair can pass in between the vertical one. The springs are clamped on both sides by flat iron plates over their whole length except for half a centimeter at each end. They can thus only be bent perpendicular to their surface.

The specimen holder is given a continuous circular motion by an eccentric (*G*) attached to the front end of a shaft (*H*) the axis of which is supported by slide bearings in the transverse arm (*I*) of the U-formed support and in the solid back piece (*K*). The pivot (*L*) of the eccentric is supported by a

pivoting ball bearing (M) the outer part of which is attached by a holder (N) to the back side of the front square block.

By this arrangement of the springs great advantages are gained. By using two pairs of perpendicular leaf springs a single pass motion is obtained since the motion of the specimen holder is only directed by the eccentric. Furthermore, the arrangement of the springs is such that the moving system

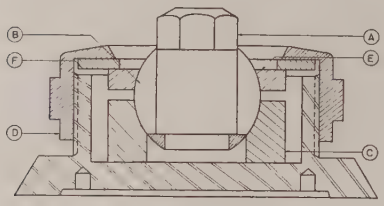

Fig. 3. Diagram of specimen holder. A, clutch for the specimen; B, elastic steel ball; C, cylindrical block; D, outer screw ring; E, spherical ring; F, flat ring.

becomes rather insensitive to external thermal effects. This is due to the fact that any change in temperature around the springs will cause about the same extension or retraction but in opposite directions. Since the springs are clamped between plates over almost all their length they cannot twist or buckle, but only bend in the narrow free area parallel to their short ends. This makes each pair of springs work as perfect hinges. When the specimen holder has been rotated one cycle by the eccentric in a quasi-circular path it comes back to the same point longitudinally, for the springs are fastened to the front support and are in the same state of deformation as one cycle before. The only possible longitudinal variation may come from a play of the bearings in a direction perpendicular to the shaft. However, since the springs have been chosen fairly long the corresponding longitudinal variation is negligibly small. No static friction can interfere with the smooth movement since there are no parts of the rotor that come to rest at any point of the revolution.

The cylindrical specimen is fitted into a clutch (Fig. 3A) which is clamped in a steel ball collet (B). This ball, resting in the spherical groove of a cylindrical block (C), can be turned 30° in all directions. One thus has the possibility of cutting the specimen at different angles. To compensate for the ensuing lateral shift of the specimen, the block (C) can be moved on the bottom of the holder and be fixed by letting the outer screw ring (D) press onto the collet via the flat inner ring (F) and the spherical ring (E). By this arrangement the top of the specimen always has the same position in the holder and since

Fig. 4. Electron micrograph of a longitudinal section of *Bacillus megaterium*. Magnification 68,000 ×.

0.5 μ

the latter is clamped to the front block in a three-point suspension (Fig. 1 and Fig. 2 *F*) it always has the same position relative to the knife edge. The knife edge is so adjusted that the specimen block is cut at right angles to the knife.

The knife holder shown (Fig. 1) is of a modified Hillier type [9] and functions also as a liquid trough for collecting the sections. Similar knife holders have been made for other knives. The holder is suspended in a fork-shaped carrier attached to a stiff hollow brass bar which is surrounded by a coil of resistance wire for the thermal expansion. The brass bar is fixed to a strong vertical support that is part of the sliding base which for the longitudinal adjustment of the knife can be moved in its guide on the polished base plate by the screw at the extreme right in Fig. 1. The sliding base may be locked in a chosen position by pressing the guide against the slide by a long handled screw. To be able to make several runs in rapid sequence the hollow feed bar can be rapidly cooled by allowing tap water to run through it.

For completeness the following details of the construction are given.

The three base plates, the largest of which has the dimensions $70 \times 25 \times 3.5$ cm, have been made of forged iron giving weight and rigidness to the construction. The different parts of the frame (in Fig. 1, one of the side pieces has been taken away) carrying the moving system, are all of 0.8 or 1.5 cm duraluminium and secured to each other with Allen screws. The steel leaf springs are of a commercial type. Their dimensions are: length 25 and 20.5 cm respectively, width and thickness 10 cm and 0.15 mm respectively while the iron plates giving them stability are 2 mm thick and 1 cm shorter than the springs. The horizontal springs are placed 10 cm apart and the vertical ones 13 cm apart. No methodical study has been made of the influence of spring dimensions or of the method of clamping the springs on the rigidness of the system. The results obtained, however, showed that the precautions taken were adequate. The parts of the instrument requiring most precise construction are the steel shaft, its bearings and the eccentric. The ends of the shaft carrying the bearings were 1.5 cm thick while the rest of it was 2 cm in thickness. These dimensions were large enough for carrying the 12 kg driving wheel without any deformation of the shaft. The choice of so heavy a wheel was dictated by the fact that it was considered to be of utmost importance that possible vibrations at the instant of cutting should be minimized. The flat cylindrical eccentric (30 mm diameter) made of hardened steel had its cylindrical pivot (7.5 mm diamter) 7.5 mm from the center, thus giving a circular motion of diameter 15 mm to the specimen holder. The pivot engages a steel ball bearing which is clamped by means of a brass ring into a holder, the latter being attached to the back of the specimen block (2 *F*). This construction allows the ball bearing to be turned slightly in the holder, thus preventing the pivot from being clamped in the bearing due to slight dissymmetries in the installation.

Fig. 5. Longitudinal section through two adjacent tracheid cells of summer wood of Swedish spruce, *Picea abies*. Magnification 51,000 ×.

A cylindrical brass rod 12 cm long and 4 cm wide was used for the expanding bar. Water could be circulated through a hole drilled along its longitudinal axis. The heating coil, an 80Ω Nichrome wire, was wound on the outside of the bar under a band of glass fabric and the whole isolated by a 2 mm thick lucite sheath cover with a 3 mm free air space in between. At its end the bar was isolated from the vertical support and the knife holder by two 1.5 cm thick bakelite pieces so that all metal contact was avoided. The screw was capable of producing movements of the slide down to 5μ which made the instrument also suitable for cutting sections for light microscopy. The knife holder could be laterally moved 18 mm, thus permitting a large part of the knife to be used during the same experiment. The razor blade used as a knife was clamped between two plates with a radius of curvature of 12 cm and screwed to the trough. In its normal position the knife forms an angle of 30° against the vertical plane but the trough is easily turned to other cutting angles.

The current for the heating coil was taken from a low power transformer the output of which was variable between 7 and 25 volts. The driving motor was equipped with a wormgear and transmission for different speeds. For avoiding vibration the motor was placed on a separate table. The sections cut were viewed through a 40× binocular microscope in reflected light.

Performance

The rotor gave no indication of vibrations either transmitted from the motor and wormgear or from the bearings. This could be inferred by the absence of any striation or wavy structure of the sections at 40 × magnification on the water surface of the trough. Also, when investigated in the electron microscope striation observed in the sections was always due to knife imperfections, as shown by the fact that the marks were directed in the sections perpendicular to the knife edge. When deciding what periphery speed of the specimen would be best, both the influence of the cutting speed on the quality of the sections and the wish to let the bar extend as far as possible per unit of time were considered. With the latter precaution the effect on section thickness of sudden temperature changes was reduced. Cutting speeds between 2 and 5 cm per sec. did not influence the quality of the sections but below 2 cm per sec. the sections were imcompletely cut and only broken away from the specimen block. Usually a speed of 2.5 cm per sec. was chosen. This corresponded to 32 revolutions of the specimen per minute.

The rate of expansion of the brass bar, as measured by a microkator, model nr 510, C. E. Johansson, Eskilstuna, Sweden, set against the trough, was strictly proportional to the square of the applied voltage but decreased slightly as its temperature was raised. The decrease of the rate of expansion after 15 min. for different initial rates of expansion did not exceed 20 per cent of the value at the start. This was consideredsa tisfactory since usually 32 sections were cut per minute and thereby about four hundred sections

could be collected during this time interval. Normally 350–400 Å serial sections were cut, the thickness being calculated from the calibration experiments. However, sections as thin as 250 Å were obtained with the best knife edges. Due to difficulties in collecting the sections a maximum of ten consecutive sections could be investigated in a series where the sections varied in thickness between 300 and 400 Å as determined by shadowing the sections and measuring the length of their shadow.

The greatest problem of ultramicrotomy is to get a satisfactory knife edge. In our case Schick razor blades as recommended by Sjöstrand [18] were clamped and polished on a rotating mirror glass plate with Linde B powder in soap solution. The holder was pivoted on a metal bar above the glass plate, in such a way that only the knife edge came in contact with the glass plate. Thereby scratches in the plate due to the holder were avoided and the knife was in contact with the glass plate along its whole edge. The polished blades were viewed at 1000 × magnification in a light microscope, in itself a crude method when determining the quality of a knife edge in connection with electron microscopy. Those showing imperfections were discarded. By raising or lowering the glass plate different facet angles of the edge could be obtained. A facet angle of 50° and a cutting angle of 30° were mostly preferred but cutting angles up to 50° could be used. A 25 per cent alcohol water solution functioned as collecting surface for the sections. When collecting serial sections by lowering against them a wire hoop covered with a formvar membrane, it was important that the water surface was slightly convex at the knife edge in order to avoid damage to the membrane. The specimen block was trimmed to a pyramid giving sections about 0.1 mm² large at the top.

The specimens were always embedded according to the technique of Newman, Borysko and Swerdlow [12] in butylmethacrylat with varying amounts of methylmethacrylat depending on the hardness of the specimen cut.

The electronmicroscope used was a Siemens, type ÜM 100, with 40μ objective aperture and a compensated objective pole piece. The microscope was operated at a magnification of 8500 ×.

Cells of a culture of *Bacillus megaterium*, strain KM in the phase of declining growth rate were chosen as a first test object for the capacity of the microtome. The cells were fixed in OsO_4 according to the method of Palade [14] and embedded in the usual way. Fig. 4 shows a longitudinal section through a cell which has just been divided into two by a transverse growing cell wall that has split up into two. In the lower part of the picture the beginning of a centripetally growing transverse wall is seen. The main constituent of cytoplasm is small dense particles of the order of 40 Å. In the cytoplasm

are embedded both "empty" vacuoles and vacuoles containing electron optically dense threads and spheres. At the lower right side of the picture part of an oblique transverse section is seen where also these dense bodies appear. A more detailed study of these results will be published elsewhere.

Among other things, the microtome has been used for investigating the submicroscopic structure of the cells of Swedish spruce, *Picea abies.* Small chips of wood were extracted with 18 per cent sodium hydroxide for dissolving the hemicellulose. The chips were embedded as mentioned above and after cutting, the embedding medium was dissolved from the sections and the latter shadowed with Pd. Fig. 5 shows a longitudinal section through two adjacent tracheid cells of summer wood. In the center is seen the heavily lignified ($\sim 0.1\mu$) middle lamella and at its side the primary wall, which clearly has a different structure from the adjacent secondary wall.

This microtome has now been in continuous use for more than one year. During this time it has functioned satisfactorily and no readjustment or replacement of any components has been required.

SUMMARY

A new ultramicrotome, with thermal feed of the knife against the specimen and with a rotor based on the double cantilever principle is described. The instrument which is of simple construction and requires no precision parts has been working reliably for a year giving serial sections of the order of 350 Å and single sections of the order of 250 Å. Two sections are shown, one of *Bacillus megaterium* and one of tracheid cells of Swedish spruce, *Picea abies.*

REFERENCES

1. Ardenne, M. von, *Z. wiss. Mikroskop.* **56**, 8 (1939).
2. Cocks, G. G. and Schwartz, C. M., *Rev. Sci. Instr.* **23**, 615 (1952).
3. Eaves, G. and Flewett, T. H., *Exptl. Cell Research* **6**, 155 (1954).
4. Fullam, E. F. and Gessler, A. E., *Rev. Sci. Instr.* **17**, 23 (1946).
5. Geren, B. B. and McCulloch, D., *Exptl. Cell Research* **2**, 97 (1951).
6. Haanstra, H. B., *Philips Tech. Rev.* **17**, 178 (1955).
7. Hillier, J. and Gettner, M. E., *J. Appl. Phys.* **21**, 889 (1950).
8. Hodge, A. J., Huxley, H. E., and Spiro, D., *J. Histochem. and Cytochem.* **2**, 54 (1954).
9. Hillier, J. and Gettner, M. E., *Science* **112**, 520 (1950).
10. Jones, R. F., *J. Sci. Instr.* **28**, 38 (1951).
11. Kobayashi, K. and Shimadzu, S., *J. Electronmicroscopy* **2**, 40 (1954).
12. Newman, S. B., Borysko, E., and Swerdlow, M., *J. Research Natl. Bur. Standards* **43**, 183 (1949).
13. O'Brien, H. C. and McKinley, G. M., *Science* **98**, 455 (1943).
14. Palade, G. E., *J. Exptl. Med.* **95**, 285 (1952).
15. Pease, D. C. and Baker, R. F., *Proc. Soc. Exptl. Biol. Med.* **67**, 470 (1948).
16. Porter, K. R. and Blum, J., *Anat. Rec.* **117**, 685 (1953).
17. Sjöstrand, F. S., *Experientia* **9**, 114 (1953).
18. —— *J. Cellular Comp. Physiol.* **42**, 15 (1953).
19. Watson, M. L., *Biochim. et Biophys. Acta* **10**, 1 (1953).

ALKALINE PHOSPHATASE IN OSTEOBLASTS AND FIBROBLASTS CULTIVATED *IN VITRO*

E. HENRICHSEN

Biological Institute, Carlsberg Foundation, Copenhagen, Denmark

Received December 19, 1955

Levander [15–20], Annersten [1] and Bertelsen [3] made the interesting observation that bone tissue may be produced by the injection of an alcoholic extract of bone or bone marrow into the muscles of rabbits. Bertelsen [3] attempted to bring about the same transformation *in vitro* by cultivating fibroblasts from heart and muscle of chicken embryos in the presence of extracts of bone or bone marrow. He did not succeed, however, in maintaining the cells *in vitro* in the presence of the alcoholic extracts, which seemed to damage the cultures.

Wilmer [34], Chèvremont and Firket [5] and Rodova [30] who made use of the Takamatsu-Gomori staining procedure, have shown that the cytoplasm of fibroblasts cultivated *in vitro* contains no or only small amounts of alkaline phosphatase. The enzyme is present in the nuclei, particularly during mitosis [5]. In osteoblasts, on the other hand, considerable amounts of the enzyme were also found in the cytoplasm [30].

The present study was undertaken in the hope that the appearance of alkaline phosphatase in the cytoplasm could be used as an indication of the transformation *in vitro* of the indifferent heart fibroblast into an osteoblast. However, a study of calcification in tissue cultures [2], together with preliminary estimations of alkaline phosphatase, made evident that heart fibroblasts maintained *in vitro* under certain conditions produced alkaline phosphatase in their cytoplasm. In other words, it seemed doubtful whether osteoblasts could be identified merely by the presence in the cytoplasm of alkaline phosphatase.

In view of this situation a detailed investigation of alkaline phosphatase activity of heart fibroblasts and osteoblasts was found necessary. The results, which differ considerably from those of the above-mentioned investigators, are reported here.

METHODS

Most of the tissue cultures were made according to the hanging drop technique, the medium being composed of equal parts of adult chicken plasma and embryo extract. Embryo extract diluted 1:1 with Tyrode's solution was used in cultivating heart fibroblasts. Since osteoblasts are known to be unfavourably influenced by a high concentration of embryo extract [29], they were given an extract diluted 1:2 with Tyrode's solution. In some cultures an air bubble was introduced into the medium before coagulation in order to produce a thin film [11], which greatly facilitated examination of the cells.

In some experiments the cultivated tissues were transferred to new media every second day. With every third change of medium, the original explants or older parts of the culture were removed, and only the peripheral parts, i.e., the migration zones of the preceding two passages, were transferred to a new medium. In other series of experiments the tissues were transferred to new media every third to fourth day, the original explants and older parts of the cultures being preserved. Tissues were also cultivated in Carrel flasks in a clot consisting of 0.5 ml adult chicken plasma, 1 ml Ringer's solution, and one drop of embryo extract. To this was added a fluid phase consisting of 0.4 ml adult chicken serum, 0.3 ml Tyrode's solution and 0.1 ml embryo extract.

The term "fibroblast culture" is used throughout this paper to designate cultures made from hearts of 9-day chicken embryos. "Osteoblast cultures" are those made from the frontal bones of 11-day chicken embryos.

Histological methods.—The cultures were washed in Ringer's solution for 5 minutes and then fixed in 80 per cent alcohol for 20 minutes. Some were brought to water via alcohol, stained and mounted whole in glycerol jelly. Of other cultures serial sections were made in the manner described by Enghusen [9].

Alkaline phosphatase was demonstrated routinely by means of the Manheimer-Seligman [22] method using the calcium salt of β-naphtyl phosphate as a substrate. The liberated β-naphtol is coupled with naphtyl-diazonium-1.5-disulfonate. The preparations were incubated at about 10°C for 20 minutes at pH 9.3.

For comparison a few cultures were stained by means of the improved method of Grogg and Pearse [12, 28] in which the sodium salt of α-naphtyl-phosphate is used as a substrate and the α-naphtol formed is coupled with diazotized 5-chloro-*o*-toluidine. The incubation time was 1 hour or less at pH 9.3 and room temperature. The results were identical with those obtained by the original Manheimer-Seligman method, on which the present investigation is chiefly based.

In histochemical demonstration of alkaline phosphatase, the diazo methods are much to be preferred to the Takamatsu-Gomori method, since misinterpretations due to absorption of calcium phosphate to structural elements in the cells are avoided. It is also important to avoid the difficulties caused by the presence of calcium phosphate deposits when investigating the relationship between alkaline phosphatase and calcification.

The incubation for only a short time at low temperature required in the original technique described by Manheimer and Seligman makes this method not a particulary sensitive one. The method has since been improved by introduction of stable

diazo compounds with no inhibitory action on the enzyme [28]. However, it is my experience that even slight amounts of phosphatase can be detected by means of the Manheimer-Seligman method. By this technique a precipitate of tiny dye granules is formed, which in dark ground illumination appear as yellow shining points. When the phosphatase activity is low, too few granules are formed to be seen as a red staining in ordinary transmitted light, but dark ground illumination shows clearly every single granule precipitated in the preparation (Figs. 1–2). The Heine condensor (Leitz), which makes possible a rapid change from ordinary transmitted light to dark ground illumination or phase contrast, was found very useful in this kind of work, as has already been emphasized by Wundrig [35].

EXPERIMENTAL RESULTS

Osteoblasts.—Zones of migrating cells were produced around the explants of frontal bone tissue after 3 days of cultivation *in vitro*. Phosphatase staining of such cultures reveal two types of cells. The cells located close to the original explant showed positive phosphatase reaction. The cells in the peripheral part showed no phosphatase staining. (Figs. 1–2.)

In the central part of the cultures a strong phosphatase reaction was produced by the periosteum of the original bone explant. Under favourable conditions, i.e. when a thin layer of medium has been produced by introduction of an air bubble, it can be seen that the staining of the cells in the neighbourhood of the explant is caused by a precipitation of the dye in or very close to the migrated cells (Fig. 1). The intense staining of this particular part of the culture is clearly not due to diffusion of enzyme or dye liberated in the central explant.

The cell layer covering the bone piece, the periostium, can be completely removed by scraping with a knife. After such treatment no migration of cells will take place. An extensive migration of cells containing phosphatase will be seen after less thorough scraping of the bone surface. This reaction is undoubtedly due to removal from the bone of the outer layer of indifferent fibroblasts. It occurred frequently that the phosphatase staining after scraping was unevenly distributed on the surface of the bone explant. Cells containing phosphatase were seen only close to and obviously migrating out from the phosphatase staining parts of the periostium.

In some cultures the original explant was removed after a while as described by Rodova [30]. Cells then migrated out into the empty area and osteoblasts formed a thin layer similar to that produced in the "bubble cultures". Contrary to the findings by Rodova [30], who used the Gomori method, no phosphatase staining of fibrils was seen.

Mixed cultures of osteoblasts and fibroblasts were maintained *in vitro*

through 21 passages for 7 weeks. At the first transfer to new medium—after 3 days of cultivation—only the tissue close to the original explant, where most of the osteoblasts were located, was cut out and transferred to the new medium. The peripheral parts of the migration zones which contained most of the phosphatase-free fibroblasts, were thereby removed. The phosphatase reaction in the cells had decreased considerably towards the end of the 7-week period. The presence of phosphatase was usually indicated only by yellow granules visible in dark ground illumination, but areas of brightly stained red cells could sometimes be seen. Thus phosphatase staining could still be observed in normally cultivated osteoblast cultures after 7 weeks of cultivation.

Heart fibroblasts.—No phosphatase activity was ever encountered in the cytoplasm or nuclei of the cells migrating out from the heart explants during the first three days of cultivation. Nor did the original explants contain active enzyme at this stage (Fig. 3). As mentioned above, this observation confirms results previously obtained by Wilmer [34], Chèvremont and Firket [5], and Rodova [30] concerning the cytoplasm of fibroblasts *in vitro*.

When the tissue was transferred to a new medium every 2–3 days, only the marginal zones being preserved for further cultivation every third transfer, no trace of phosphatase was seen when the tissue was examined in ordinary transmitted light (Fig. 4). However, when dark ground illumination was used, a slight phosphatase staining was occasionally present. This phosphatase staining was seen along the cut edges of the culture, which are formed by transfer of the cultures to new medium.

When older parts of the cultures were preserved and the transfer to a new medium took place at an interval of 3–4 days, the phosphatase staining along

---

Fig. 1. Cells in outgrowth from piece of frontal bone. Note the phosphatase-stained osteoblasts in the central part of the migration zone and the phosphatase-free fibroblasts in the periphery.
Fig. 2. Same culture as Fig. 1 seen in dark ground illumination. Note the red phosphatase staining of the cells with the most intense phosphatase activity and the yellow shining staining of the areas with weak phosphatase activity. The fibroblasts in the periphery of the culture do not contain yellow shining dye granules.
Fig. 3. Cellophane culture of heart fibroblasts after 2 days of cultivation. No phosphatase staining is seen in the piece of heart or in the migrated heart fibroblasts.
Fig. 4. Heart fibroblast culture in 5th passage. The culture has been transferred to new media second day. No phosphatase staining is seen.
Fig. 5. Heart fibroblast, 5th passage. The culture has been transferred to new media every 3–4 day. Intense phosphatase staining along the cut edge from the last transfer.
Fig. 6. Culture of heart fibroblasts grown on perforated cellophane in a fluid medium for 4 days. Note the intense red phosphatase staining of the fibroblasts compared to Fig. 3.
Fig. 7. Photograph in natural size of heart fibroblast cultures in the second passage showing the phosphatase staining after 2, 3, 4, and 5 days of cultivation.

(Color plate reproduced by Thorell & Thomsen Bogtryk, Copenhagen.)

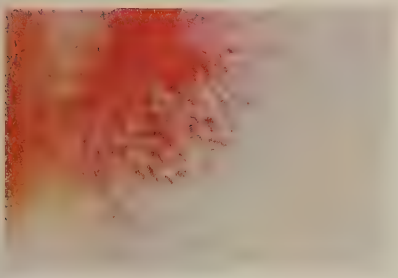

Fig. 1

Fig. 2

Fig. 3

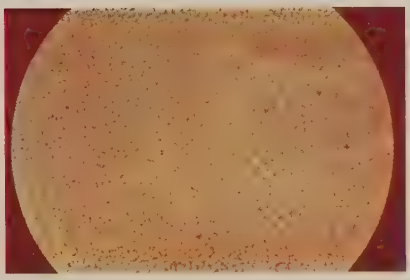

Fig. 4

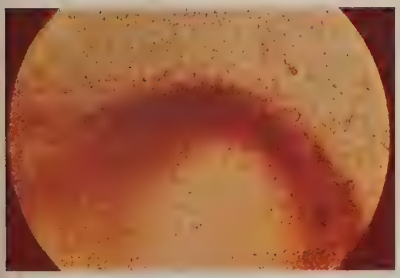

Fig. 5

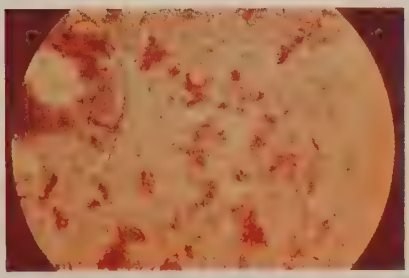

Fig. 6

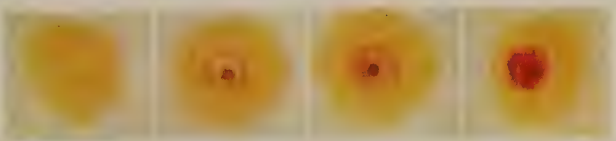

Fig. 7

the cut edges was more pronounced, appearing bright red macroscopically and by ordinary microscopy (Fig. 5). Red phosphatase staining of the original explants of chicken heart also appeared after 4–5 days of cultivation. When a culture had been maintained for 4–5 days in the same medium, even the peripheral cells of the migration zone showed a positive phosphatase reaction, which as a rule could only be seen in dark ground illumination, but which sometimes formed a red ring in the periphery of the culture (Fig. 7). The dye indicating alkaline phosphatase activity was always found in or very close to the cells. No sign of any dye stuff was ever found in the cultivating medium.

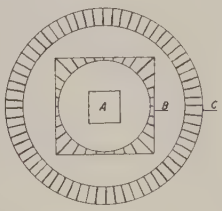

Fig. 8. Diagram of heart fibroblast culture at the 4th day of the second passage. *A* is the explant of chicken heart, *B* the cut edge of the first passage, *C* the peripheral limit of the second passage. The hatched areas indicate areas with alkaline phosphatase activity.

When seen macroscopically the phosphatase-stained cells were located in the areas indicated in the schematic drawing, Fig. 8, of a culture in the second passage. However, when seen in the microscope, the cut edge is no sharp borderline. Some cells just outside the cut edge are stained too, obviously because some phosphatase-containing cells have been able to migrate. The ability to migration, however, seems to be reduced for those cells as compared with the phosphatase-free fibroblasts which form the peripheral part of the migration zone. At a later stage the cells located in the periphery could also be seen phosphatase-stained, but not as a result of migration of phosphatase-containing cells from the more central part of the culture.

It was previously found [2] that a circular zone of calcification appears in heart fibroblast cultures maintained in Carrel flasks in the presence of organic phosphates. In the course of the present investigation it was further noticed that the cells in the same circular zone always contained alkaline phosphatase as indicated by the staining reaction.

By cultivating heart fibroblasts on perforated cellophane as described by Evans and Earle [10] in a medium composed of chicken serum, 30 per cent, Tyrode solution, 60 per cent, and embryonic extract (diluted 1:1 with Tyrode solution), 10 per cent, the same change of the phosphatase staining of the fibroblasts could be observed. Phosphatase-staining fibroblasts appeared after about 3 days of cultivation without changing the medium (Fig. 6).

In some cultures fibrils were seen as tracks left behind the creeping cells. Where the cells which had formed the fibrils were phosphatase-negative, the fibrils also appeared phosphatase-free, but when the collection of cells to which the fibrils were attached were phosphatase-positive, the fibrils too showed a very distinct red phosphatase staining.

It has been suggested that alkaline phosphatase could be absorbed to phosphatase-free cells when these cells were in a state of degeneration [13]. The observations described here do not support this theory, as the medium gives no reaction for alkaline phosphatase. If this should be due to a very low concentration of the enzyme in the substrate, it then seems difficult to explain as an absorption phenomenon the very strong phosphatase reaction which appears in some of the cultures after 4–5 days of cultivation. In order to prove that the alkaline phosphatase which appears in the heart fibroblasts, as described here, is not caused by an absorption phenomenon, the following experiment was carried out. Heart fibroblasts were cultivated on perforated cellophane as described above, but the medium had been heated to 60°C for half an hour in order to destroy all alkaline phosphatase. The cells hardly migrated out from the explant in this medium in most of the cultures, because the heating procedure destroys many of the growth-promoting substances. In some cultures however, cells migrated out from the explant forming a small migration zone. After 5 days of cultivation a red staining for alkaline phosphatase could be seen in some of the migrated cells and in some parts of the original explant. This result can only be interpreted by assuming that the enzyme is produced by the cells during the period of cultivation.

The relation of the precipitated dye to cell structure.—Cells showing a very weak phosphatase reaction, i.e., those showing very few granules in dark ground illumination, indicate when seen in phase contrast, that the precipitated dye is localized in the cytoplasm. The nucleus and the area just outside the nucleus is free of the dye granules (Fig. 9).

When the cells were more heavily stained, the cell structure could not be seen in phase contrast. In these cases an interesting relationship was observed between the appearance of alkaline phosphatase in heart fibroblasts and the state of the cell nucleus.

Phase contrast microphotographs were made of cells with and without phosphatase staining. Cells situated in the thin layer of bubble cultures were used. The dye was then extracted by means of absolute alcohol, the cultures were again mounted in glycerol jelly, and the same cells were again photographed. From a comparison of the pictures taken before and after the extrac-

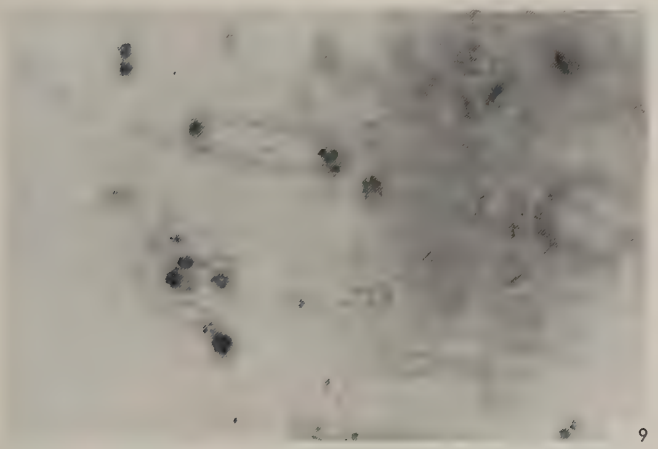

Fig. 9. Photomicrograph of heart fibroblasts with weak phosphatase activity. The dye granules are precipitated in the cytoplasm only.

tion of the dye it became evident that the cells which did not show any phosphatase reaction were of normal morphological appearance. They were spindle-shaped and contained an oval nucleus with two nucleoli, and no cytoplasmic granules were present. On the other hand, cells containing alkaline phosphatase differed markedly in their morphology from the normal cells just described. The cells were larger and had lost their spindle shape. The nuclei were of a more or less circular shape, the two nucleoli were sometimes fused into one mass. In many cases the nucleus was very indistinct or could not be seen at all, so that one would assume that karyolysis had taken place (Figs. 10–12). Granules appeared in the cytoplasm as tiny black bodies, when seen in dark phase contrast. These granules were found only when a definite change in the structure of the nucleus had taken place. It must be emphasized that no phosphatase reaction of the cytoplasm or nuclei was ever seen in the cells during mitotic division which is in opposition to that found by Chèvremont and Firket [5], who used the Gomori method. Cells filled with lipid droplets—often described as degenerated cells in the literature—did not show any phosphatase reaction when the nuclei were of normal appearance.

Muscle fibroblasts.—Cultures of striated muscle tissue from chicken embryos 9 days of age showed the same phosphatase reactions as heart fibroblasts.

Figs. 10–12. Photomicrographs (*a* and *b*) of heart fibroblasts showing alkaline phosphatase activity before (*a*) and after (*b*) extraction of the dye by alcohol.

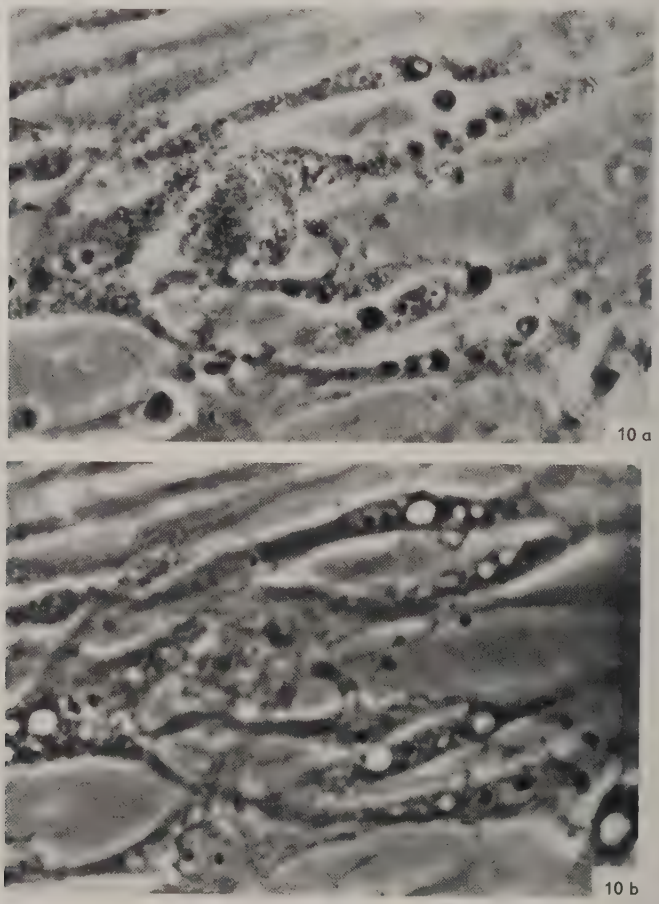

Fig. 10 *a* and *b*. Note the normal nuclei of the phosphatase-free cells, the granular precipitation of the dye and the condensation of the cromatin substance.

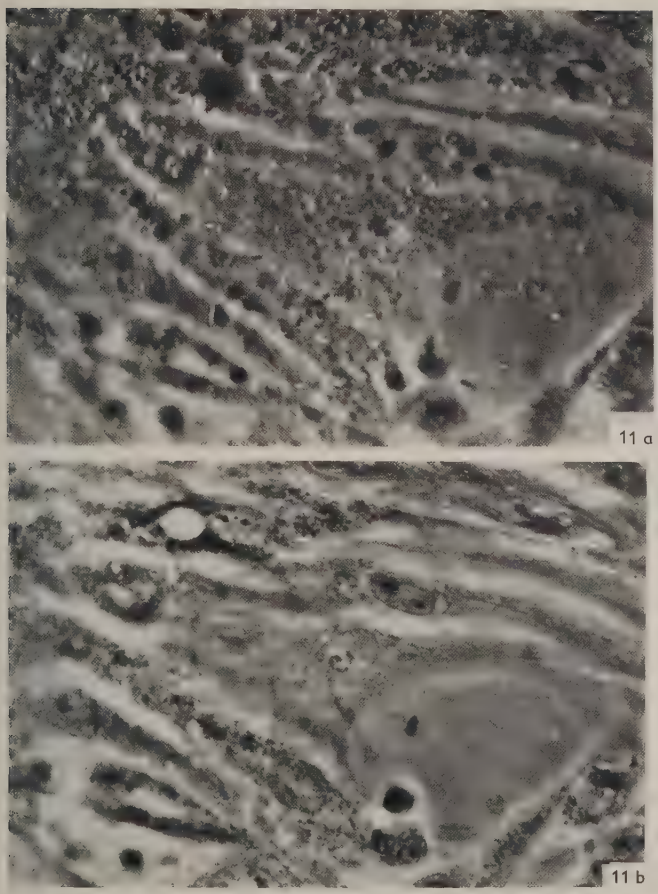

Fig. 11 *a* and *b*. Note the spherical appearance of the nucleus of the phosphatase-containing all.

DISCUSSION

The fact that a positive phosphatase reaction was never seen in the nucleus when the Manheimer-Seligman method was employed, is a confirmation of results obtained by previous authors who based their findings on diazo-methods [24, 7, 22, 25]. It is now generally agreed that the black nuclei obtained by the Gomori method are artefacts [23, 31, 6, 36, 26, 15]. The absence of positive reactions during mitosis, as described in this paper, may

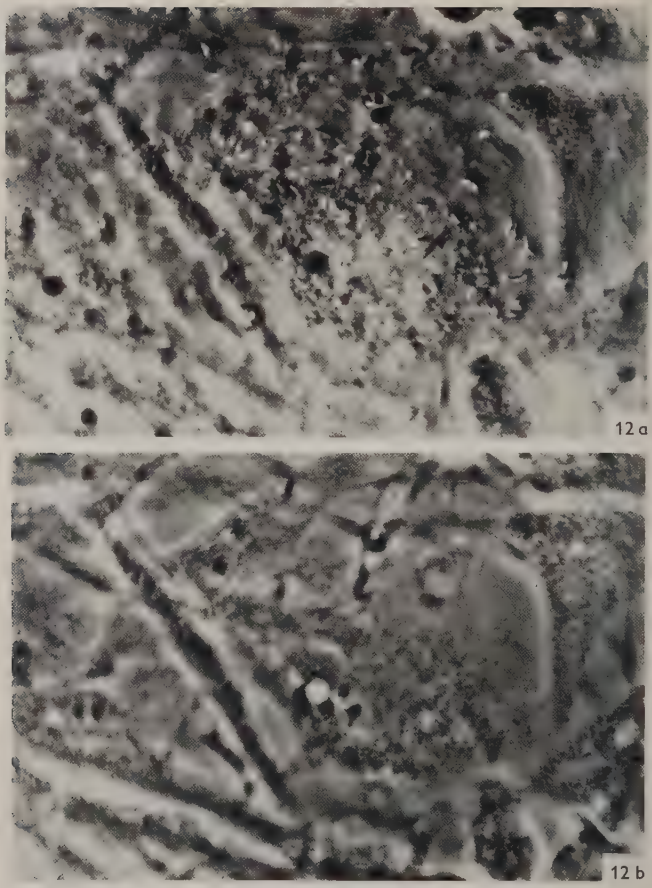

Fig. 12 *a* and *b*. The nucleus is here barely visible.

in the same way be interpreted as absence of phosphatase activity in chromosomes. This was also in opposition to the results obtained when the older Gomori technique was used.

The presence of alkaline phosphatase in the cytoplasm of normal osteoblasts must be considered an indication of cell differentiation. Histochemical methods have thus revealed cytological differences, which were not observed by Policard [29], who assumed that osteoblasts were ordinary fibroblasts

migrating from the periostium. During adaptation to tissue culture the osteoblasts show decreasing phosphatase activity. However, the enzyme could be found even after 7 weeks of cultivation. There seems no reason to assume that a true dedifferentiation takes place during cultivation. Hence these enzyme studies are in accordance with experiences of other authors concerning dedifferentiation in tissue cultures [4, 33].

We have good reason to assume that alkaline phosphatase is not found in normal heart fibroblasts *in vivo*. Heart fibroblasts do not show positive phosphatase reaction, when they leave the fresh explants *in vitro*. When the fibroblasts *in vitro* are in a "normal" state, they never contain alkaline phosphatase in their cytoplasm such as was seen in osteoblasts. This is in accordance with the results of Wilmer [34], Chèvremont and Firket [5], and Rodova [30].

It seems of considerable interest that a relationship was found between the presence of the alkaline phosphatase activity and what is commonly called cell degeneration. The changes of the structure of nuclei of the phosphatase-positive cells as seen in phase contrast resemble the changes described by Zollinger [37, 38] during "hydropic degeneration". The granules seen in the cells under the same conditions seem to be identical with the granules (dead granules or *d*-granules) which Lewis and Lewis [21], using dark ground illumination, saw in degenerated cells *in vitro*. Zollinger [38] using phase contrast saw the same granules in degenerated cells.

We have no reason to believe that the fixation in alcohol and mounting in glycerol jelly will change the structure of nuclei in such a manner that the changes described above are produced (cf. [39]).

The phosphatase reaction of degenerated fibroblasts has probably also been observed by Chèvremont and Firket [5] who in some cases found a blackening of the cytoplasm, which they assumed to be an artefact. They write: "Il arrive parfois que dans une ou quelques cellules étalées cytoplasme et noyau présentent un noircissement plus intense et plus homogène, mais ces images, qu'on distingue aisément d'une réaction normale, sont peu fréquentes et nous ont paru correspondre à un artéfact."

The origin of the alkaline phosphatase which appears in the fibroblasts during degeneration is not known. It has already been pointed out that the presence of alkaline phosphatase in the nucleus has not definitely been demonstrated histochemically. The validity of the demonstration of the enzyme in isolated nuclei [8] has been questioned by Novikoff [26], and Stern *et al.* [32] conclude from their investigations with isolated nuclei that alkaline phosphatase occurs "in low concentration, if at all in the nuclei". It is there-

fore of interest that the present investigation showed that whenever the precipitation of the dye was sufficiently distinct the precipitation was found only in the cytoplasm.

These observations suggest that alkaline phosphatase originates in the cytoplasm. However, at the present time we can only demonstrate that the enzyme appears in the cytoplasm during the transition from "normal" to dead fibroblast, but it is still not possible to explain the formation or liberation of the phosphatase. Whether or not the process is reversible is equally unknown. Preliminary work on phosphatase activity and calcification in heart fibroblast cultures indicates that the process in tissue cultures goes on irreversibly until the cell is dead.

SUMMARY

The presence and localisation of alkaline phosphatase in osteoblasts and heart fibroblasts cultivated *in vitro* was studied with the Manheimer-Seligman staining method.

Osteoblasts contained a considerable amount of alkaline phosphatase in their cytoplasm. No enzyme was present in fibroblasts under normal conditions. Phosphatase was absent from the nuclei of resting or dividing cells.

Phosphatase activity appeared in the cytoplasm of heart fibroblasts coincident with degenerative changes in cytoplasm and nuclei.

This investigation was supported by grants from Landsforeningen til Kræftens Bekæmpelse and from Statens almindelige Videnskabsfond. Thanks are due to Dr. Albert Fischer for his interest in this work. The helpful advice of Dr. Tage Astrup and Dr. Audrey Fjelde in preparing the English manuscript is gratefully acknowledged.

REFERENCES

1. Annersten, S., *Acta chir. scand. Suppl.* **60** (1940).
2. Astrup, T. and Henrichsen, E., *Exptl. Cell Research* **6**, 151 (1954).
3. Bertelsen, A., *Acta ortopæd. scand.* **15**, 139 (1944).
4. Bloom, W., *Physiol. Revs.*, **17**, 589 (1937).
5. Chèvremont, M. and Firket, H., *Arch. Biol.* **60**, 441 (1949).
6. Cleland, K. W., *Proc. Linnean Soc. N.S. Wales.* **75**, 54 (1950).
7. Danielli, J. F., *J. exptl. Biol.* **22**, 110 (1946).
8. Dounce, A. L., *J. biol. Chem.* **147**, 685 (1943).
9. Enghusen, E., *Exptl. Cell Research* **3**, 611 (1952).
10. Evans, J. and Earle, W. R., *J. Natl. Cancer Inst.* **8**, 103 (1947).
11. Fischer, A. and Schlabayzius, M., *Acta Anat.* **9**, 420 (1950).
12. Grogg, E. and Pearse, A. G. Everson, *Nature* **170**, 578 (1952).
13. Gomori, G., *Am. J. Pathol.* **19**, 197 (1943).
14. —— *J. Lab. Clin. med.* **37**, 526 (1951).

15. Levander, G., *Nord. Kir. Foren. Forhandl.* p. 48 (1933).
16. —— *Nord. Kir. Foren. Forhandl.* p. 65 (1935).
17. —— *Nord. Kir. Foren. Forhandl.* p. 546 (1939).
18. —— *Nord. Kir. Foren. Forhandl.* p. 299 (1943).
19. —— *Acta chir. scand.* **83**, 1 (1939).
20. —— *Acta chir. scand.* **83**, 545 (1940).
21. Lewis, H. W. and Lewis, M. R., "Behavior of cells in cultures", *in* General Cytology, Ed. Edmund v. Cowdry, Chicago 1924.
22. Manheimer, L. H. and Seligman, A. M., *J. Natl. Cancer Inst.* **9**, 181 (1948).
23. Martin, B. F. and Jacoby, F., *J. Anat.* **83**, 351 (1949).
24. Menten, M. L., Junge, J., and Green, M. H., *J. Biol. Chem.* **153**, 471 (1944).
25. Novikoff, A. B., *Science* **113**, 320 (1951).
26. —— *Exptl. Cell Research Suppl.* **2**, 123 (1952).
27. Parker, R. C. and Fischer, A., *Proc. Soc. Exptl. Biol. med.* **26**, 580 (1929).
28. Pearse, A. G. E., Histo-Chemistry. Theoretical and Applied. Ed. Little, Brown & Co., Boston, U.S.A., and J. A. Churchill, London, 1953.
29. Policard, A. et Boucharlat, M., *Compt. Rend. Soc. Biol.* **93**, 533 (1925).
30. Rodova, H., *J. Anat.* **82**, 175 (1948).
31. Ruyter, J. H. C. and Neumann, H., *Biochim. et Biophys. Acta* **3**, 125 (1949).
32. Stern, H., Allfrey, V. G., Mirsky, A. E., and Saetren, H., *J. Gen. Physiol.* **35**, 559 (1952).
33. Weiss, P., "Differential Growth", *in* The Chemistry and Physiology of Growth. Edited by A. K. Parpart. Princetown University Press 1949.
34. Wilmer, E. N., *J. exptl. Biol.* **19**, 11 (1942).
35. Wundrig, G., Studien aus dem Institut für natur- und geistenwissenschaftliche Anthropologie Berlin-Dahlem **1**, 42 (1952).
36. Yokoyama, H. O., Stowell, R. E., and Mathews, R. M., *Anat. Rec.* **109**, 139 (1951).
37. Zollinger, H. U., *Schweiz. Z. allgem. Pathol. u. Bakteriol.* **11**, 276 (1948).
38. —— *Am. J. Pathol.* **24**, 1039 (1948).
39. —— *Am. J. Pathol.* **24**, 797 (1948).

A DIFFERENCE BETWEEN SPERMATOGONIA AND SOMATIC TISSUES OF MICE IN THE INCORPORATION OF [8-^{14}C]-ADENINE INTO DEOXYRIBONUCLEIC ACID

S. R. PELC and ALMA HOWARD[1]

Medical Research Council, Experimental Radiopathology Research Unit, Hammersmith Hospital, London, England

Received December 21, 1955

Published data on the ejaculation of sperm in mammals [9] allow of an approximate calculation of the deoxyribonucleic acid (DNA) content of a single ejaculate, which in the horse may be 4–8 per cent of the total amount of DNA in the testis. This figure, which may reasonably be applied to other mammals, together with the well-known histological evidence of frequent cell division in the testis, make it certain that new DNA must constantly be made in, or supplied to, the testis on a considerable scale. A number of investigators, however, have reported very low figures for the incorporation into DNA in the testis of labelled substances which in other organs are readily used in DNA synthesis. For example, Furst *et al.* [4] fed N^{15}-labelled adenine to rats and found after 24 hours no incorporation into the mixed nucleic acids of the testis, in contrast to liver, kidney, intestine, etc. Goldthwait and Bendich [6] injected ^{14}C-formate and found 24 hours after injection activities of 213 counts/min./micromole of DNA adenine of the small intestine compared with 7 counts for the testis. Similar values are reported by these authors for incorporation of formate into guanine and thymine of the respective organs. Marrian [10] injected [8-^{14}C]-adenine into rats and found after 2 hours that the specific activity of ADP and AMP of the testis was one sixth or less of that of the liver and the intestine.

Hevesy and Ottesen [2], however, killing rats 4 days after injection of ^{32}P, found significant incorporation into testis DNA and calculated a renewal of 10 per cent in 4 days. The discrepancy between these results and those of other authors indicates a difference in DNA synthesis between somatic tissues and the testis. To elucidate these differences, we have compared, in testis and somatic tissues, the number of cells whose DNA has become labelled at various times after i.p. injection of [8-^{14}C]-adenine. Previous work on DNA synthesis in the testis has been done by biochemical methods which in-

[1] Now at B.E.C.C. Research Unit in Radiobiology, Mount Vernon Hospital, Northwood, Middlesex, England.

volved averaging over the various stages of spermatogenesis. In the experiment reported here, autoradiography, which allows the incorporation of labelled precursors into DNA to be observed in individual cell nuclei, is used. Two earlier experiments of similar design gave essentially the same results as those reported here.

MATERIALS AND METHODS

C_{57} Black × C_3H F_1 hybrid male mice about 5 months of age were injected intraperitoneally with 20 μC [8-^{14}C]-adenine-HCl in 0.4 ml water. The labelled adenine (specific acitivity 1 mC/mM) was obtained from the Radiochemical Centre, Amersham, England. It was dissolved immediately before use and all mice were injected at the same time from the same solution.

Mice were killed from 1 to 32 days after injection, and a part of one testis fixed for 1 hour in absolute methanol. Small amounts of tissue were squashed in 45 per cent acetic acid under coverslips, the coverslips were floated off in 10 per cent acetic acid, and the squashes thoroughly washed in running water. Another part of the testis, as well as other organs and tissues, were fixed for 1 hour in 3 parts absolute ethanol: 1 part glacial acetic acid, transferred to formol-saline (1:9) for 24 hours or more, dehydrated, embedded in paraffin and sectioned at 5μ. After removal of paraffin the slides were washed in running water. All sections and squashes were incubated for 40–60 mins at 37°C in 0.03 molar veronal buffer at pH 7 containing 0.029 to 0.037 mg ribonuclease per ml. The enzyme was obtained from Worthington Biochemicals Ltd., Freehold, New Jersey, U.S.A.

After ribonuclease extraction, slides were washed in water and autoradiographs prepared by the stripping film technique [3]. Low exposures were used. Consequently, the number of developed grains over a cell nucleus can be taken as proportional to the number of beta particles hitting the film, and therefore as proportional to the number of ^{14}C atoms incorporated, if the exposure time is taken into account. Special stripping film for autoradiography was obtained from Kodak Ltd., Harrow-Wealdstone, Middlesex, England. Autoradiographs were exposed for 28–64 days.

The unstained squashes were observed by phase contrast to identify cells, the phase plate being removed when photographic grains were counted. Sections were stained with carminic acid or Ehrlich's haematoxylin and observed with the conventional light microscope.

RESULTS AND DISCUSSION

Biochemical analyses of tissues of mammals injected with [8-^{14}C]-adenine have shown [2] that only adenine-containing compounds are labelled. Of these the important non-acid-soluble ones, which would be expected to remain in tissue after acid treatment, are ribonucleic acid (RNA) and DNA. In this experiment slides were incubated with ribonuclease before the photographic film was applied. We may therefore assume that the autoradiographs observed are due to ^{14}C which has been incorporated in DNA. This assump-

tion is supported by other experiments in which deoxyribonuclease was found to remove radioactivity remaining after ribonuclease digestion in mammalian cells labelled with [8-^{14}C]-adenine (Hornsey and Howard, in press).

Time of DNA labelling.—Observation of squash preparations, in which whole flattened cells or nuclei are well separated from one another, shows that some spermatogonia are labelled one day after adenine injection. Primary spermatocytes are unlabelled at 1, 2 and 4 days: some labelled ones appear at 6 days. Labelled secondary spermatocytes and spermatids first appear at 8 days. Sperm in the testis are unlabelled at 10 days, but labelled at 25 days. After 32 days labelled sperm is found in the epididymis (Fig. 2). We conclude that labelling takes place in spermatogonia only, and that the appearance of radioactivity in cells at later stages of spermatogenesis is due to the handing on of labelled material to the spermatocytes and its persistence during spermiogenesis. That increase in amount of DNA precedes the meiotic divisions and does not occur at later stages was observed by Swift [12] in the mouse. In plants also the increase in amount and labelling of DNA are not observed between early meiotic prophase and the interphase preceding the gametophyte mitoses [13, 11, 14, 15].

Timing of spermatogenic stages.—Our observations indicate that the time taken from the last period of DNA labelling in spermatogonia to prophase of primary spermatocytes is about 5 days; about two more days are occupied in the transformation to spermatids: and the whole process from spermatogonium to sperm takes 10–25 days. These estimates are in general agreement with those arrived at in two previous experiments in which labelled cells of mouse testis were studied by means of autoradiographs [8, 5] and with other published work.

Labelling of somatic tissues and of spermatogonia.—Several organs and tissues other than testis were fixed, sectioned and autoradiographed. These included intestine, oesophagus, skin, lymph node, cornea, epididymis, seminal vesicle, lung, trachea, thyroid, lower lip and pinna. Labelled cells were absent in thyroid, liver and epididymis. In all tissues in which mitosis is common some labelled cells were found (Fig. 3). On inspection of the slides it soon became clear that in labelled somatic tissues the percentage of labelled cells was as high or higher one day after the injection of adenine as at later times. For the cornea, this was confirmed by counts in the basal layer of the epithelium (Fig. 1, Table I, col. 7). Only nuclei of basal layer cells are labelled one day after injection; at later times the flat nuclei of fully differentiated cells become positive. The amount of ^{14}C per nucleus appeared to be the same at different times in some cells, indicating that little or no additional

labelled adenine was incorporated by labelled cells after the first day. As soon as flat nuclei become labelled, the content in the basal layer diminishes. Such a picture was to be expected if labelled adenine in a form available for incorporation into DNA disappears rapidly from body fluids after injec-

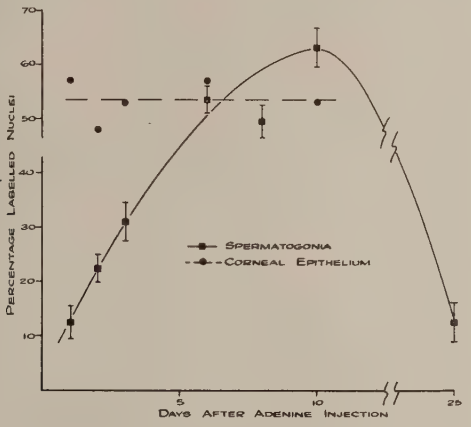

Fig. 1.

tion. That it does so is indicated in other experiments (Hornsey and Howard, in press).

The labelling of spermatogonia (Fig. 4) is, however, strikingly different from that shown by other mitotically active cells in the body. Table I and Fig. 1 summarize the results of counts of the percentage of labelled sperma-

TABLE I

Time after adenine injection (days)	Spermatogonia		Tubules		Number of grains above background per labelled spermatogonium (squashes)	Corneal epithelium
	Number counted	Percentage labelled	Number observed	Number containing 10% or more labelled spermatogonia		% labelled
1	989	12.3	13	3	34	57
2	1291	22.4	14	5	20	48
3	1049	30.4	16	16	48	53
6	1068	53.5	14	14	32	57
8	1064	49.5	14	14		53
10	880	63.3	12	12		
25	997	12.2	14	7		

All photomicrographs are of mice injected i.p. with 20 μC of [8-^{14}]C-adenine. 5μ sections were treated with ribonuclease, ARG's prepared and stained with carminic acid. Focussing on the photographic grains.

Fig. 2. Epididymis. Mouse killed 32 days after injection. Note the ARG over mature sperm and its absence over epithelial cells. 1250 ×.

Fig. 3. Skin epidermis. Mouse killed 1 day after injection. Note the ARG over cells of the basal layer; none over the flattened nuclei in the keratinizing region. 1250 ×.

Fig. 4. Testis. Mouse killed 6 days after injection. The dark nuclei are resting spermatogonia; the lighter ones are dividing spermatogonia in an adjacent tubule. 1250 ×.

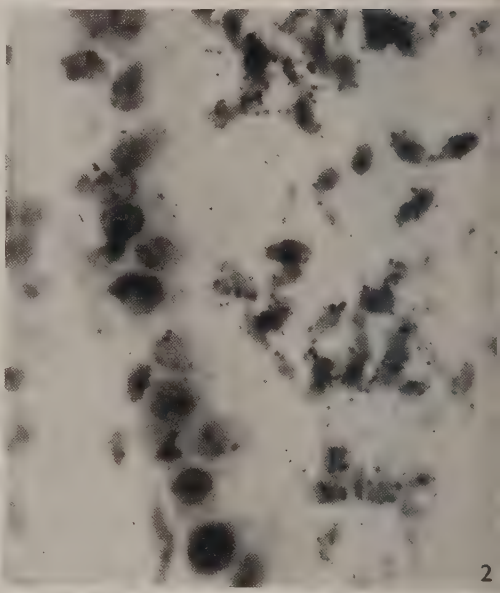

togonia seen in sections at different times after adenine injection. Only 12.3 per cent of all spermatogonia are labelled at 1 day: the percentage rises to 53.5 at 6 days and remains at about this level until 10 days.

That the increasing percentage of labelled spermatogonia is due to new labelling of additional cells at 2, 3 and 6 days after injection, and not to the division of cells labelled during the first day to produce two or more labelled daughter cells, is shown by the absence of a reduction in the degree of labelling of spermatogonia during the first 6 days, as shown by the number of photographic grains developed over them in squashes (Table I, col. 6). This number, although variable, shows no consistent downward trend with time. If increase in number of labelled cells were due to cell division, the degree of labelling would be expected to be halved at each division.

Table I, cols. 4 and 5, give the number of spermatogenic tubules in which at least 10 per cent of spermatogonia were labelled. At 1 day, 10 of 13 tubules contained no labelled cells in the section examined, while one contained 35 labelled out of 55 cells. At 2 days the values were from zero in 3 tubules to more than 60 per cent in 2 tubules. At 3 days and later the percentage of labelled cells in individual tubules was much more uniform, varying rather closely about the mean percentage for all the spermatogonia in the section. These observations are a further demonstration that additional cells become newly labelled after the first day, and suggest that spermatogonia enter in groups into a stage at which they become labelled, and that these groups are distributed along the tubules in a manner consistent with the spermatogenic wave [1]. Since a wave of spermatogonial divisions is known to exist, we conclude that there exists a wave of DNA synthesis associated with this mitotic activity.

Various reasons may be suggested for the striking difference in DNA labelling of spermatogonia and of somatic tissues as illustrated by the corneal epithelium. The observation that the amount of ^{14}C incorporated into DNA per newly-labelled spermatogonial nucleus is similar from 1 to 6 days after injection indicates that the specific activity of the DNA precursor available to these cells is reasonably constant during that period. This suggests that a DNA-precursor, either within the testis or elsewhere, becomes maximally labelled soon after injection, and is drawn upon by spermatogonia during the next 6 days. Cells of the corneal epithelium and other somatic tissues studied are apparently unable to draw upon this supply, at least after the first day. The possibility that the DNA of reproductive cells may be synthesized in a manner which differs from that of somatic cells is of sufficient genetic and biochemical interest to justify special mention.

SUMMARY

C_{57} black × C_3H F_1 hybrid male mice about 5 months old were injected intraperitoneally with 20 μC [8-^{14}C]-adenine-HCl and killed from 1 to 32 days later. Autoradiographs of squashes and sections of various organs were prepared after treatment with ribonuclease. The available evidence indicates that the autoradiographs obtained after this treatment are due to ^{14}C incorporated in deoxyribonucleic acid during synthesis.

Visual inspection and cell counts show that a maximal number of nuclei is labelled after 1 day in those somatic tissues in which cell division is frequent. In the testis only 12.3 per cent of the spermatogonia are labelled 1 day after injection, rising to 63.3 per cent after 10 days. Grain counts and the distribution of labelled spermatogonia in the tubules indicate that the increase in percentage is due to new labelling and not to redistribution of DNA through cell division.

Primary spermatocytes are unlabelled at 1, 2 and 4 days; some are labelled at 6 days. Labelled secondary spermatocytes and spermatids first appear at 8 days. Sperm in the testis are unlabelled at 10 days, but labelled at 25 days. After 32 days labelled sperm is found in the epididymis. The timing of spermiogenesis derived from these observations agrees with previous estimates.

At present no satisfactory explanation can be given for the difference in DNA labelling of spermatogonia and of somatic tissues. It is suggested that a DNA precursor, either within the testis or elsewhere, becomes maximally labelled soon after injection, and is drawn upon by spermatogonia but not by cells of somatic tissues.

REFERENCES

1. Curtis, G. M., *Am. J. Anat.* **24**, 339 (1918).
2. Davidson, J. N., The Biochemistry of the Nucleic Acids. Methuen, London, 1953.
3. Doniach, I. and Pelc, S. R. *Brit. J. Radiol.* **23**, 184 (1950).
4. Furst, S. S., Roll, P. M., and Brown, G. B., *J. Biol. Chem.* **183**, 251 (1950).
5. Glücksmann, A., Howard, Alma, and Pelc, S. R., *J. Anat.* **89**, 13 (1955).
6. Goldthwait, D. A. and Bendich, A., *J. Biol. Chem.* **196**, 841 (1952).
7. Hevesy, G. and Ottesen, J., *Acta Physiol. Scand.* **5**, **238** (1943).
8. Howard, Alma and Pelc, S. R., *Brit. J. Radiol.* **23**, 634 (1950).
9. Mann, T., The Biochemistry of Semen. Methuen, London, 1954.
10. Marrian, D. H., *Biochim. et Biophys. Acta* **13**, 282 (1954).
11. Plaut, W. S., *Hereditas* **39**, 438 (1953).
12. Swift, H. H., *Physiol. Zool.* **23**, 169 (1950).
13. Swift, H. H., *Proc. Natl. Acad. Sci.* **36**, 643 (1950).
14. Taylor, J. H., *Exptl. Cell Research* **4**, 164 (1953).
15. Taylor, J. H. and McMaster, R. D., *Chromosoma*, **6**, 489 (1954).

DISTRIBUTION DE L'ACIDE RIBONUCLÉIQUE ET INCORPORATION DE LA PHÉNYLALANINE-2-^{14}C DANS LES PROTÉINES

A. FICQ[1] et J. BRACHET

Laboratoire de Morphologie animale, Université libre de Bruxelles, Belgique

Reçu le 26 Décembre, 1955

La répartition et la localisation de l'acide ribonucléique (ARN) sont bien connues depuis les travaux cytochimiques initiaux de Caspersson [6, 7] et de Brachet [3, 4]. On sait que ces deux chercheurs sont arrivés, indépendamment l'un de l'autre et par des techniques différentes, à une même conclusion générale: l'ARN doit jouer un rôle important dans la synthèse des protéines. De très nombreux faits, qui ont éte passés récemment en revue par l'un de nous [5], plaident en faveur de cette hypothèse d'une intervention de l'ARN dans la synthèse des protéines; elle tend d'ailleurs de plus en plus à être acceptée par les biochimistes [1, 10] etc.

Il faut cependant admettre que l'interprétation proposée initialement par Caspersson [6] et par Brachet [3, 4] ne reposait qu'en partie sur des faits tangibles : seule, en effet, le teneur en ARN des cellules avait été suivie par des méthodes cytochimiques semi-quantitatives ou par des dosages biochimiques directs [4]. Par contre, l'importance réelle des synthèses protéiques dans les cellules étudiées n'était pas connue avec certitude : il était, certes, logique de penser que les cellules glandulaires sécrétrices de pepsine ou de trypsine, les cellules à divisions rapides des cryptes de Lieberkühn ou de la rate sont le siège d'importantes synthèses protéiques. On n'en avait toutefois pas fourni la preuve.

La mise au point par l'un de nous [8] d'une technique d'autoradiographie par traces, précise et commode, permet maintenant d'aller plus loin : grâce à cette méthode, il est possible de suivre, sur les mêmes coupes, la basophilie des cellules colorées au vert de méthyle-pyronine (Unna), et l'incorporation d'acides aminés dans les protéines de ces mêmes cellules. On sait que cette incorporation, si elle ne correspond pas nécessairement à une synthèse nette de protéines, se rapproche à maints égards d'une telle synthèse.

[1] Chargée de Recherches au Fonds national de la Recherche scientifique de Belgique.

MATÉRIEL ET MÉTHODES

Au cours de 3 expériences, 10 μC de phénylalanine-2-^{14}C ont été injectées dans la cavité péritonéale de souris blanches (dans 1 ml de Ringer). Les animaux ont été sacrifiés après, respectivement, 30 minutes, 1 heure 15 et 16 heures.

Les principaux organes (foie, rate, intestin, rein, poumon, cœur, utérus) ont été fixés par congélation-dissolution (freeze-substitution) dans de l'alcool méthylique à basse température. La technique histologique ultérieure et le processus autoradiographique employé ont été décrits récemment en détails par l'un de nous.

RÉSULTATS EXPÉRIMENTAUX

Le simple examen microscopique des autoradiographies montre que la corrélation entre l'intensité de la coloration à la pyronine (qui peut servir d'indice de la teneur en ARN) et la radioactivité est d'autant meilleure que le temps écoulé entre l'injection de la phénylalanine et le sacrifice de l'animal est plus court. Ce résultat n'est pas fait pour surprendre, puisque nous savons, par de nombreuses expériences faites sur le foie de rat et de poulet, que l'incorporation des acides aminés est particulièrement rapide et intense dans les microsomes; or, ces petits granules cytoplasmiques sont exceptionnellement riches en ARN [12, 2, 13, 18 etc.]. Mais il est à noter qu'il s'agit là d'un phénomène général, qui se produit dans tous les organes que nous avons étudiés et pas seulement dans le foie.

Nous passerons rapidement en revue l'aspect histologique des différents organes étudiés et nous examinerons ensuite les données quantitatives que fournit le comptage des traces individuelles.

Examen histologique des autoradiographies.

L'aspect des autoradiographies ne présente pas de différences importantes quand on compare les souris qui ont été sacrifiées respectivement 30 minutes et 1 h 15 après l'injection du précurseur radioactif : nous ne les décrirons donc pas séparément. Quant à l'animal dont les organes ont été fixés 16 heures après l'administration intrapéritonéale de phénylalanine, il manifeste, comme on pouvait s'y attendre, une nette tendance à une répartition plus uniforme de la radioactivité dans les différents tissus.

Pancréas.—C'est l'organe qui présente, après 30 minutes, la radioactivité la plus intense. Comme le montre la fig. 1, il existe une différence marquée entre les acini de la portion exocrine et les îlôts de Langerhans : la radioactivité de ces derniers est toujours beaucoup plus faible. On sait que les techniques cytochimiques utilisées par Caspersson [6, 7] et par Brachet [3] ont

permis à ces auteurs de démontrer que les îlots de Langerhans sont beaucoup plus pauvres en ARN que la portion exocrine; cette différence marquée entre les deux portions du pancréas constituant d'ailleurs, pour ces auteurs, un argument important en faveur d'une intervention de l'ARN dans les synthèses protéiques. Les observations présentes montrent que les protéines des cellules acineuses incorporent effectivement les acides aminés beaucoup plus activement que celles des cellules des îlots de Langerhans.

Signalons en passant que les différences de basophilie entre les deux parties du pancréas qui ont été décrites par Brachet [3] ne peuvent être retrouvées sur nos autoradiographies : en effet, les coupes de pancréas, après fixation par congélation-dissolution, ne prennent pas la pyronine : seuls leurs noyaux se colorent en vert à l'Unna. Mais il suffit de traiter les coupes, avant la coloration à l'Unna, par un fixateur énergique tel que le Zenker acétique pour obtenir les images classiques : îlôts de Langerhans clairs, cellules des acini colorées intensement en rouge au niveau de leur ergastoplasme. Il est clair que, dans le pancréas simplement fixé par fixation-congélation, l'ARN est combiné à une substance qui masque ses affinités tinctoriales; celles-ci ne se manifestent que si on rompt le complexe au moyen d'un fixateur acide énergique. Des observations, qui seront publiées ailleurs, nous ont montré que le complexe formé par la ribonucléase et l'ARN, dans des cellules intactes plongées dans de la ribonucléase (racines d'oignon, oocytes d'étoile de mer et de grenouille) présentent les mêmes particularités : elles ne sont pas ou guère basophiles après fixation par freeze-substitution, mais elles le deviennent fortement quand les coupes sont traitées au Zenker. Il est bien possible que, dans le pancréas qui est exceptionnellement riche en ribonucléase, cet enzyme forme un complexe intracellulaire avec l'ARN : un tel complexe ne fixerait la pyronine que s'il est rompu par un précipitant énergique des protéines et des acides nucléiques.

Foie.—Le parenchyme de cet organe montre également une forte radioactivité, qui n'atteint cependant pas celle du pancréas exocrine. Par contre, les cellules pauvres en ARN, qui se logent entre les lobules hépatiques (parois des vaisseaux, canalicules biliaires, tissu conjonctif, infiltration lymphocytaire), ne présentent qu'une faible radioactivité. La fig. 2 montre combien le contraste entre les deux zones est frappant, tant en ce qui concerne la radioactivité que la basophilie; ce contraste se retrouve, quoiqu'un peu atténué, dans la souris qui a été sacrifiée 16 h après l'injection de la phénylalanine.

Ajoutons que, comme l'ont déjà signalé Ficq et Errera [9] et Moyson [16] les noyaux des cellules du parenchyme hépatique présentent une très forte radioactivité, plus élevée que celle du cytoplasme.

Intestin.—Cet organe, en raison sans doute de sa richesse en protéases et en nucléases, présente, comme le pancréas, certaines difficultés après une fixation par congélation-dissolution : la coloration de Unna est difficile à réussir et il peut même arriver que les coupes attaquent la gélatine de l'émulsion photographique; on observe parfois aussi une diffusion du matériel radioactif aux abords de la coupe.

Lorsque ces ennuis peuvent être évités, la corrélation entre la basophilie et la radioactivité est, à nouveau, très satisfaisante : même dans l'animal sacrifié 16 h après l'administration de la phénylalanine, la musculeuse est beaucoup moins fortement radioactive que la muqueuse. Dans les souris sacrifiées plus tôt, on remarque (fig. 3) que les cryptes de Lieberkühn sont nettement plus actives que le restant de la muqueuse et que la sous-muqueuse; elles sont aussi beaucoup plus colorables à la pyronine.

Notons cependant que les cellules basophiles du plexus d'Auerbach ne tranchent pas, sur le fond que forme la musculeuse, par une radioactivité particulièrement intense.

Utérus.—Le muscle utérin, peu colorable à la pyronine, ne présente qu'une faible radioactivité, comparable à celle de la musculeuse de l'intestin. Dans la muqueuse utérine (endometrium), ce sont les glandes et la couche profonde (couche basilaire) qui offrent, à la fois, la plus forte basophilie et la radioactivité la plus intense. On ne trouve, à l'autoradiographie, qu'un petit nombre de traces dans la couche superficielle (couche fonctionnelle) de la muqueuse; elle tendait d'ailleurs à se desquamer dans les souris que nous avons examinées.

Il serait assurément intéressant de rechercher si le parallélisme que nous avons noté entre la radioactivité et la basophilie se retrouverait aux différentes étapes du cycle œstral.

Rate.—Les nodules lymphatiques de la pulpe blanche (corpuscules de Malpighi) tranchent nettement sur la pulpe rouge par leur coloration bleue à l'Unna : elle est due aux nombreux noyaux des lymphocytes, dont le cytoplasme est pauvre en ARN. Au contraire, les cellules réticulo-endothéliales des cordons de Billroth (pulpe rouge) attirent l'attention par leur forte coloration rouge à l'Unna. Comme le montre la fig. 4, l'autoradiographie révèle des différences considérables de radioactivité entre les diverses cellules qui constituent la pulpe splénique : les cellules basophiles de la pulpe rouge présentent une très forte activité, alors que les éléments lymphocytaires sont beaucoup moins actifs. Le contraste, à cet égard, entre des cellules voisines de basophilie très différentes est particulièrement frappant.

Nos observations concordent parfaitement avec celles qui ont été faites,

sur les ganglions lymphatiques du rat, par Gavosto et Ficq [11] au moyen de la même méthode.

Rein.—La radioactivité des glomérules de Malpighi est faible, surtout dans les animaux injectés depuis peu. Par contre, les tubes contournés présentent une très forte activité; elle est nettement supérieure à celle que montrent les segments grèles et les canaux de Bellini dans la médullaire.

L'examen cytochimique ordinaire à l'Unna montre que la corticale est plus colorable à la pyronine que la médullaire; il semble cependant que la radioactivité des tubes contournés soit plus forte qu'on ne l'aurait prévu, en se basant sur leur seule basophilie (fig. 5).

Poumon.—Dans tous les animaux étudiés, la radioactivité des alvéoles pulmonaires, qui sont pauvres en ARN, est très faible. Seul l'épithélium des bronches et des bronchioles, qui se colore beaucoup plus intensément à la pyronine, présente une radioactivité notable.

Cœur.—Cet organe se comporte comme la musculature lisse de l'intestin et de l'utérus : la basophilie et la radioactivité sont toujours très faibles (fig. 6).

Comptage des traces.

Afin d'obtenir des données plus quantitatives que celles que peut fournir un simple examen microscopique, nous avons procédé, dans le cas des 3 souris, à un comptage des traces émises par unité de surface (276 μ^2) dans différents organes. Les résultats de ce comptage figurent au tableau I.

TABLEAU I

Radioactivité spécifique de différents organes de souris exprimée en nombre de traces par unité de surface (276 μ^2).

	Pancréas		Foie		Rate		Intestin			Rein			Uterus			
							muqueuse									
	exocrine	endocrine	cell. parench.	lymphocytes	pulpe rouge	follic. lymphoc.	crypt. L.	lumière	musculeuse	tubes contournés	glomérules	médullaire	muqueuse	musculeuse	Poumon	Cœur
ris sacrifiée																
rès 30′ . . .	192,6	25,6	86,3	20,0	157,2	17,2	88,3	50,7	14,7	64,7	19,6	18,2	61,2	12,4	12,1	10,6
ris sacrifiée																
rès 75′ . . .	—	—	114,2	31,0	83,6	16,4	89,8	53,0	18,2	76,1	38,0	37,0	64,0	20,0	22,6	17,4
ris sacrifiée																
rès 16 h . . .	—	—	57,8	19,0	43,0	10,0	80,4	47,0	26,0	96,8	47				17,3	13,8

L'examen du tableau I confirme les impressions qu'on avait retirées du simple examen microscopique : on voit, tout d'abord, que la radioactivité approche déjà de son maximum une demi-heure après l'injection de la phénylalanine-2-^{14}C. Elle tend à baisser, sauf dans le cas du rein, dans l'animal sacrifié 16 h après l'injection de phénylalanine.

On notera aussi que les comptages démontrent qu'il existe réellement de grandes différences entre les zones basophiles et non basophiles des divers organes : par exemple, dans la souris sacrifiée 30 min. après l'injection, les acini pancréatiques sont, par unité de surface, près de 8 fois plus actifs que les îlôts de Langerhans; la différence est plus marquée encore (9 fois) quand on compare la pulpe rouge à la pulpe blanche de la rate; les musculeuses sont de 5 à 6 fois moins actives que les muqueuses, tant dans l'intestin que dans l'utérus. Ces différences tendent à s'atténuer dans la souris qui a été tuée 16 heures après l'injection de l'acide aminé radioactif : l'écart entre les 2 pulpes de la rate tombe de 9 à 4 fois, celui entre les cryptes de Lieberkühn et la musculeuse descend de 6,5 fois à 3 fois, lorsqu'on compare entre elles les souris sacrifiées 30 minutes et 16 heures après l'injection du précurseur dans la cavité péritonéale. Cette constatation est, répétons-le, dans la logique des choses, puisque nous savons que ce sont les protéines des microsomes qui se marquent en premier lieu : dans la souris sacrifiée après 16 h, les protéines qui ne sont pas associées à l'ARN ont eu amplement le temps de se marquer à leur tour. Il est même permis de penser que la corrélation entre la basophilie et l'incorporation de l'acide aminé dans les protéines serait encore meilleure si les animaux avaient été sacrifiés moins d'une demi-heure après l'injection de la phénylalanine radioactive.

DISCUSSION

L'emploi de la méthode autoradiographique apporte un argument nouveau en faveur de l'idée que l'ARN joue un rôle important dans le métabolisme des protéines : cette technique démontre, en effet, l'existence d'un parallélisme extrêmement étroit et constant entre l'incorporation de la phénylalanine radioactive dans les protéines (qu'il s'agisse de réactions d'échange ou de synthèse nette) et la basophilie cytoplasmique; celle-ci constitue, on le sait, un bon indice de la teneur en ARN.

Ce parallélisme ne se manifeste pas seulement quand on compare différentes portions, inégalement riches en ARN, d'un même organe; on le retrouve encore lorsqu'on range les divers organes que nous avons étudiés d'après leur radioactivité et qu'on compare le classement ainsi obtenu avec celui

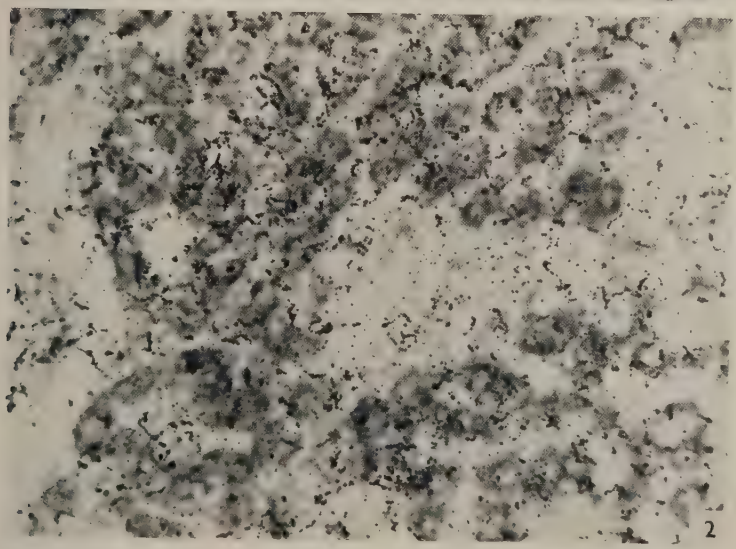

Fig. 1. Autoradiographie d'une coupe de pancréas marquée à la phénylalanine-2-^{14}C; la radioactivité intense que l'on observe dans la partie exocrine contraste avec celle, beaucoup moindre de l'îlôt de Langerhans dont on peut voir un quadrant, à droite de la microphoto.
Fig. 2. Coupe de foie; l'infiltration lymphocytaire que l'on observe au centre de la coupe est beaucoup moins active que les cellules parenchymateuses des travées qui l'entourent.

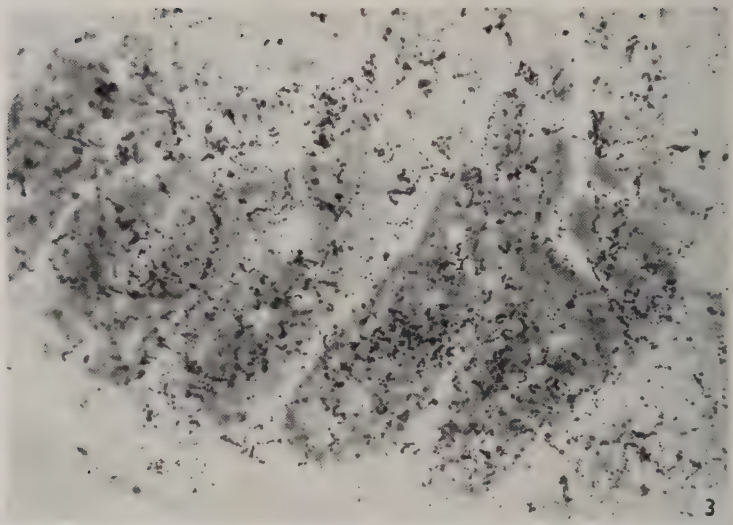

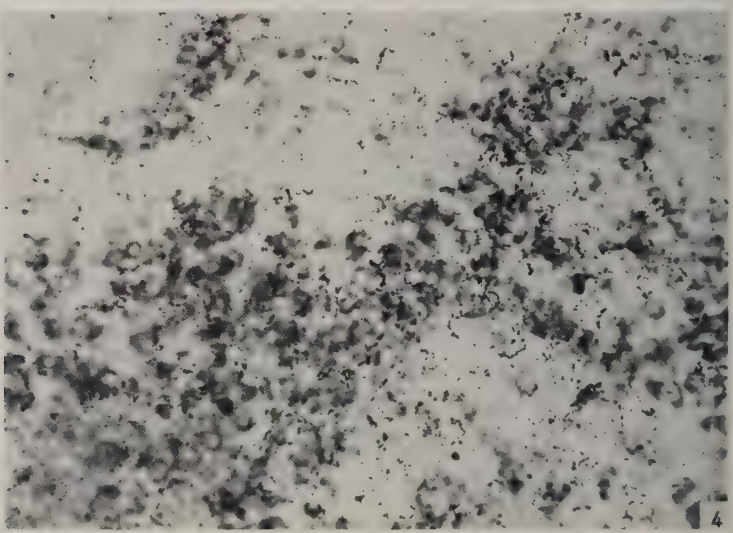

Fig. 3. Coupe d'intestin; les cryptes de Lieberkühn basophiles sont nettement plus actives que le reste de la muqueuse et surtout que la musculeuse.
Fig. 4. Coupe de rate; les cellules basophiles de la pulpe rouge présentent une radioactivité très élevée par rapport à celle des éléments lymphocytaires qui apparaissent en clair sur la microphoto.

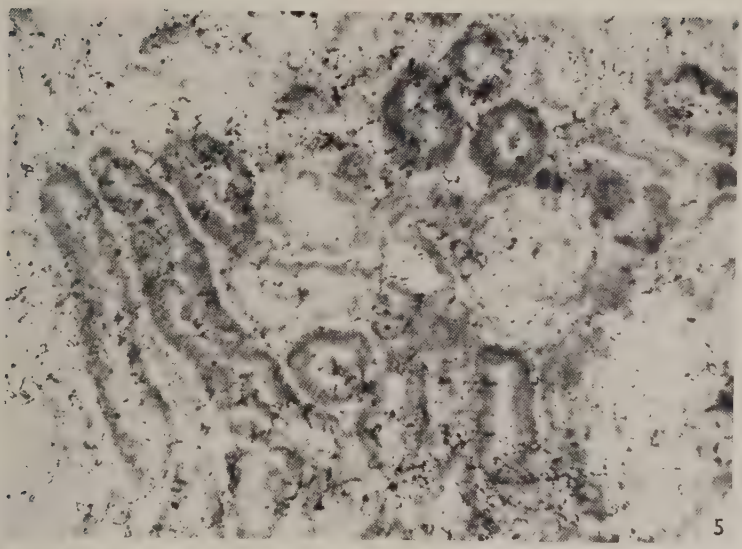

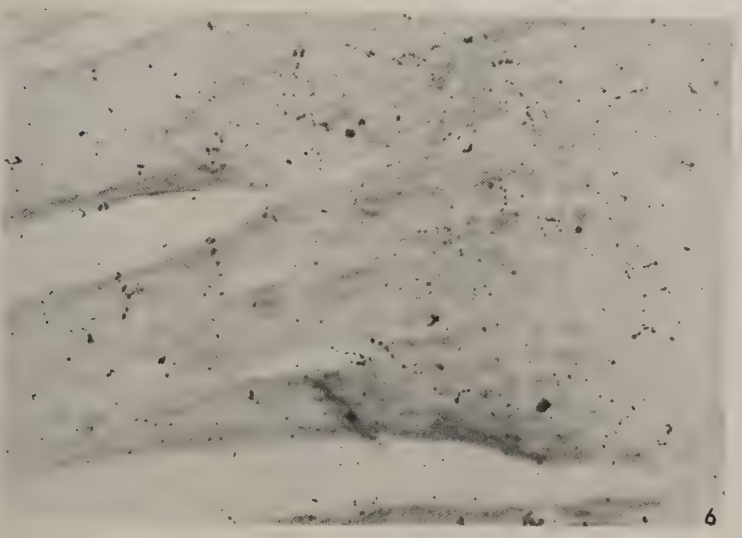

Fig. 5. Coupe de rein; on observe une radioactivité relativement élevée dans les tubes contournés; elle est beaucoup plus faible dans les glomérules de Malpighi.
Fig. 6. Coupe de cœur présentant une radioactivité très faible.

que donne leurs teneurs en ARN. En effet, la radioactivité des différents organes de la souris décroît, dans nos expériences, dans l'ordre suivant : pancréas > foie, rate > intestin > rein > poumon > cœur. En ce qui concerne la teneur en ARN, des divers organes de la souris, l'un de nous [4] a pu les classer de la manière que voici, après avoir dosé leur teneur en pentoses : pancréas > muqueuse intestinale > foie > rate > rein > poumon > cœur.

Ce classement est très voisin de celui qu'on peut établir, pour le rat, en utilisant les données qui ont été rassemblées récemment par Leslie [15] : pancréas > foie > intestin > rate > rein > poumon > cœur.

On voit que le parallélisme entre les données biochimiques et nos observations est excellent; la concordance est plus satisfaisante encore si on songe que le foie, la rate et l'intestin ont des teneurs en ARN très voisines. D'ailleurs, l'hétérogénéité marquée de la rate et de l'intestin, en ce qui concerne la radioactivité des différentes cellules, rend difficile leur classement exact.

Il serait cependant souhaitable de reprendre sur le plan strictement biochimique, les problèmes que nous avons étudiés par les techniques cytochimiques : il ne semble pas exister, en effet, de travaux où on a suivi simultanément l'incorporation d'un acide aminé dans les protéines (peu de temps après l'injection) et la teneur en ARN dans les divers organes d'un même animal. Le travail qui se rapproche le plus du nôtre, à cet égard, est celui de Lee *et al.* [14] : travaillant sur le rat et utilisant de la cytosine-^{35}S comme précurseur, ils ont constaté que l'activité spécifique des protéines décroît dans l'ordre suivant, après 8 h : muqueuse intestinale > rein > rate > foie > cœur. Ces résultats cadrent, en somme, avec les nôtres, si on tient compte des nombreuses différences existant dans les conditions expérimentales.

La forte activité du rein dans les expériences de Lee *et al.* [14] concorde avec les résultats que nous avons obtenus dans le cas de la souris sacrifiée 16 h après l'injection de phénylalanine : à ce moment, c'est la corticale du rein qui, dans nos expériences, présente l'activité la plus forte. Comme nous l'avons déjà noté en passant, des phénomènes particuliers se manifestent dans le rein : la radioactivité de la corticale est plus forte que ne le ferait prévoir sa basophilie modérée; en outre, l'incorporation de l'acide aminé semble s'accentuer, dans le rein, au moment où elle baisse dans les autres organes (16 h après l'injection). Ces anomalies sont vraisemblablement liées à la physiologie même du rein; la capacité que possède le tube contourné de résorber des protéines qui ont filtré à travers la paroi du glomérule [17] en fournit peut-être l'explication. L'application au rein de la méthode autoradiographique, après l'injection de protéines marquées au ^{14}C dans le sang ou la cavité péritonéale, permettrait sans doute de trancher la question.

Ajoutons, pour terminer, que le foie est le seul organe où l'incorporation de la phénylalanine soit nettement plus intense dans le noyau que dans le cytoplasme : la forte activité des noyaux, déjà signalée dans le foie par Ficq et Errera [9] et par Moyson [16], n'est donc pas nécessairement un phénomène général. Il serait imprudent d'en tirer des conclusions hâtives au sujet du rôle du noyau dans la synthèse des protéines.

RÉSUMÉ

On a suivi simultanément la basophilie (Unna) et l'incorporation de la phénylalanine-2-^{14}C (autoradiographie) dans les protéines de divers organes de la souris. On observe, dans ces conditions, une excellente corrélation entre la teneur en acide ribonucléique (ARN) des cellules et l'incorporation, surtout lorsque l'animal a été sacrifié peu de temps après l'injection du précurseur (30 min.).

Ces résultats sont en faveur d'une intervention de l'ARN dans la synthèse des protéines.

BIBLIOGRAPHIE

1. Borsook, H., Rapp. 3e Congrès intern. Biochimie. Bruxelles, p. 54, 1955.
2. Borsook, H., Deasy, C. L., Haagen-Smit, A. J., Keighley, G., et Lowy, P. H., *Federation Proc.* **9**, 154 (1950).
3. Brachet, J., *Arch. Biol.* **53**, 207 (1941).
4. —— *Enzymologia* **10**, 87 (1941).
5. —— Nucleic Acids. Academic Press, N. Y., p. 476, 1955.
6. Caspersson, T., *Naturwissenschaften* **29**, 33 (1941).
7. —— Cell Growth and Cell Function. Norton, New York, 1950.
8. Ficq, A., *Arch. Biol.* **66**, 509 (1955).
9. Ficq, A. et Errera, M., *Biochim. et Biophys. Acta* **16**, 45 (1955).
10. Gale, E., Rapp. 3e Congrès intern. Biochimie. Bruxelles, 71, 1955.
11. Gavosto, F. et Ficq, A., *Ann. Inst. Pasteur* **86**, 425 (1954).
12. Hultin, T., *Exptl. Cell Research* **1**, 376, 599 (1950).
13. Keller, E. B., *Federation Proc.* **10**, 106 (1951).
14. Lee, N. D., Anderson, J. T., Miller, R., et Williams, R. H., *J. Biol. Chem.* **192**, 733 (1951).
15. Leslie, I., Nucleic Acids. Vol. II, p. 8. Academic Press, New York, 1955.
16. Moyson, F., *Arch. Biol.* **66**, 149 (1955).
17. Moyson, F., Oliver, J., MacDowell, M., et Lee, Y. C., *J. Exptl. Med.* **99**, 589 (1954).
18. Smellie, R. M. S., McIndoe, W. M., et Davidson, J. N., *Biochim. et Biophys. Acta* **11**, 559 (1953).
19. Tyner, E. P., Heidelberger, C. H., et Le Page, G. A., *Cancer Research* **12**, 158 (1952).

THE EFFECTS OF MONOCHROMATIC ULTRAVIOLET LIGHT ON THE EGG OF *DROSOPHILA*

A. S. GOLDMAN[1] and R. B. SETLOW

Department of Zoology and Department of Biophysics, Yale University,[2]
New Haven, Conn., U.S.A.

Received January 4, 1956

It is of interest to determine the identity, the location, and the role of biologically important compounds in embryonic development. The following is an account of the results of an action spectrum analysis which was undertaken to obtain such information. This action spectrum depends on two fundamental properties of ultraviolet irradiation in its action on living systems. First, the energy of the radiation is quantized such that disrupting packets of energy can be delivered to sensitive compounds within the biological system. Second, only compounds which absorb the radiation can be affected. Thus, if the efficiency of various monochromatic wavelengths within the ultraviolet spectrum for causing a certain biological inactivation is plotted against the wavelength of irradiation, the resulting curve may display a wavelength of maximum efficiency. This wavelength will then correspond to the wavelength of maximum absorption of the sensitive compound [6]. This method is particularly suitable for differentiating between absorption by purine and pyrimidine containing compounds and that by tyrosine and tryptophan containing compounds. Davis [2] has obtained such an action spectrum for the process of neural tube formation in the chick.

The egg of *Drosophila* is a particularly suitable experimental material because the superficial cleavage of this insect type presents two early developmental stages in which radiation damage to the cytoplasm can be differentiated from that to the nuclei. Immediately after fertilization the zygote nucleus migrates to the center of the egg where it divides several times within the protection of large quantities of yolk and pigment. Since ultraviolet light has a limited penetration through protoplasm [6] an early stage is thus provided in which only the peripheral cytoplasm is exposed to the radiation. After the eighth nuclear division most of the daughter nuclei migrate to the cortical cytoplasm in which location all subsequent development occurs. This pro-

[1] Present address: State University of New York, College of Medicine at Syracuse, New York.
[2] Assisted in part by the U.S. Atomic Energy Commission.

vides a later stage in which the nuclei are then also subject to radiation damage.

The present investigation provides evidence that ultraviolet damage to the nuclei causes complete early inhibition of development. However, damage to the cytoplasm merely alters some morphogenetic movements in the larvae resulting in the appearance of totally differentiated larvae with herniated intestines or with eviscerated yolk. This cytoplasmic damage can be shown by action spectrum analysis to be due to light absorption by cytoplasmic compounds containing purine and pyrimidine bases. This finding is of interest since, if the affected cytoplasmic compound is nucleic acid (RNA), as seems quite probable, it provides a suitable method for studying the positive contribution or role of RNA in embryonic development.

MATERIALS AND METHODS

Eggs of *Drosophila melanogaster* Canton-S strain, kindly supplied by D. F. Poulson, were collected with an instrument described by Ulrich [7] which consists of a fly chamber suspended over a dish of medium. When the sliding bottom of the chamber is opened, the flies can oviposit on the exposed medium. About 30 to 60 females were allowed to oviposit for 60 minutes in this device so that large quantities of eggs of approximately similar age could be collected. In early experiments eggs were collected by allowing females to oviposit on small Syracuse dishes filled with yeast, corn meal, molasses, and agar medium. However, the Ulrich method was found to yield eggs in much higher mumbers and to reduce the total handling time of the eggs from 30 to 45 minutes to 5 to 10 minutes. This reduction in handling time was necessary in order to irradiate the eggs before the nuclei migrated to the periphery (90 minutes at 23–25°C).

Females prefer to oviposit on strips of blotting paper dipped in dilute acetic acid which are placed on fermenting yeast-agar medium. The eggs on the paper strips were individually oriented with the embryonic anlagen on the ventral sides exposed to the radiation. Preliminary tests indicated that the ultraviolet induced abnormalities were similar with eggs oriented with either ventral or dorsal sides exposed, but to make all results strictly comparable, eggs of all subsequent experiments were individually oriented such that their embryonic primordia on the ventral sides were exposed to the ultraviolet radiation. This orientation was carried out for both control and irradiated series.

After collection and orientation, the eggs were divided into control and experimental groups. Eggs of less than 90 minutes of age were irradiated with different doses of the available ultraviolet wavelengths to determine the spectral efficiency of the radiation in causing inactivation of normal development. These constituted the series of exposure of the cytoplasm. Eggs of 120–160 minutes of age having their nuclei at the periphery and thus vulnerable to radiation were irradiated with wavelengths of 2537 and 2894 Å. In all experiments eggs were allowed to develop at 25°C in a

constant temperature box except for the few minutes during which the eggs were irradiated.

In some early experiments, the eggs were dechorionated in 5 per cent chlorox solution and cultured in insect Ringer and the development of the control and irradiated embryos was observed at various intervals under a binocular dissecting microscope. In subsequent experiments, counts were made of the number of hatched and unhatched larvae. Abnormalities occurring in the unhatched embryos were then classified after dechorionation.

A water-prism monochromator described by Fluke and Setlow [5] was employed for irradiations. The apparatus is capable of delivering monochromatic wavelengths of high intensity with less than 1 per cent scattered light. A photocell, calibrated with a thermopile which in turn was calibrated against a standard lamp, was used to determine the intensity of the incident radiation.

In early experiments the monochromator was equipped with a low intensity U.V. source (250 watt Hg arc lamp), and the length of time to achieve the desired radiation dose occasionally exceeded the time of the desired experimental stage. Incident intensities were about 5×10^3 ergs/cm^2/min. Also, in these experiments the method of egg collection yielded a limited number of eggs. For these reasons, photoinactivating efficiencies of wavelengths, 2400, 2482, 2700 and 3023 Å were obtained from only one or two experimental doses.

Later experiments were performed with a 1000 watt, capillary, Hg arc as the light source. The average incident intensities were about 10^5 ergs/cm^2/min. except at 2300 Å at which wavelength the intensity was one-tenth this value. The results obtained for eggs irradiated at 2805 Å with low intensities for long periods of time were similar to those obtained at 2805 Å with higher intensities for shorter periods. The results depended only on the product of intensity and time. This demonstrates a reciprocity of time and intensity. Different radiation doses at other wavelengths were obtained by varying the time of irradiation.

RESULTS

Description of Abnormalities

Normally occurring developmental anomalies.—Both the extreme contractions and the intestinal herniations and yolk eviscerations produced by irradiation described below occur at a low frequency in normal, untreated embryos. Fig. 1 shows that in control embryos the abnormal contraction occurs at a frequency of about 3 per cent, and evisceration of yolk or herniation of intestine about 5 per cent. Since these defects occur normally, an experiment was undertaken to determine whether an unspecific environmental alteration, such as a temperature shock, could increase their frequency. Eggs were collected for a period of 4 hours and after orientation, 72 eggs were placed at 4°C for 2 hours and then returned to 25°C.

Fig. 1 also shows that such a cold shock treatment can increase the frequency of embryos showing extreme contraction to 20 per cent and that of

embryos showing evisceration of yolk and herniation of intestine to about 17 per cent. This indicates that the aberration of the developmental processes leading to these abnormalities may arise from non-specific agents. However, since ultraviolet radiation is capable of causing these abnormalities in proportion to the incident dose, quantitative analysis of the effects of the irradia-

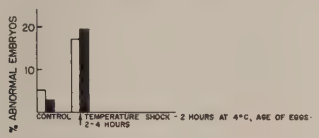

Fig. 1 (*left*). The effect of a cold shock on development of *Drosophila*.

☐ Embryos showing evisceration of yolk or herniation of intestine.
■ Embryos showing extreme contraction.

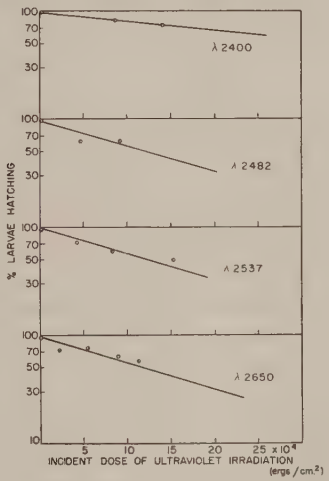

Fig. 2 (*right*). The per cent of larvae hatching after eggs were irradiated with cytoplasm exposed versus the incident dose of radiation.

diation was undertaken to determine the identification of the sensitive compound.

Radiation of eggs with nuclei exposed.—Fertilized eggs irradiated 120–160 minutes after oviposition either develop normally or show an abnormal retraction of the protoplasm from the anterior and posterior ends. The final appearance of this abnormality is a small, oval, and opalescent mass of protoplasm contracted within the vitelline membrane. Radiation of eggs at this stage, then, results in complete early inhibition of development.

Radiation of eggs with cytoplasm exposed.—Fertilized eggs radiated less than 90 minutes after oviposition fell into two categories: normal hatched larvae and abnormal unhatched larvae. Occasionally, a few embryos occurred which were abnormal in appearance with a characteristic dark brown coloration. These were discarded from consideration, because in preliminary experiments it had been observed that this coloration was characteristic of eggs which were radiated after being carried within the abdomen of the female for an abnormally long time. This was recognized because these eggs were at least 4 to 6 hours older in development than the rest. Consequently, these

eggs would have been irradiated at a stage much later than 90 minutes. The abnormal unhatched larvae recovered in these experiments were of two types: one showed masses of yolk of varying size, extruded either at the anterior or at the posterior end, or at both (designated as yolk evisceration). The second type showed sheets of intestine herniated over and above the larva, extending from a half to the whole of its long axis (designated as herniation of the intestine). In both cases normal movement of the embryo could be observed. These movements lasted for several hours after the larvae were fully differentiated. Preliminary histological studies of both abnormalities indicated that the differentiation of other organs and structures was apparently complete.

In some early experiments, the eggs were dechorionated shortly after irradiation, and the development of both control and irradiated embryos was observed under the binocular dissecting microscope. At about 9 hours of development when the head normally turns under and the gut closes over on the dorsal side, the irradiated embryos appear markedly different from the controls. The head of the irradiated embryos extends considerably farther posteriorly than the controls. Poulson has observed such anomalous development in some mutant strains of *Drosophila* (pers. comm.). These observations suggest that the two observed abnormalities are of similar qualitative nature, since both anomalies could be explained by the failure of the head to turn in properly. Thus, in some cases, the yolk could escape through the openings in the improperly closed membranes causing the yolk eviscerations, and in others, the whole intestine might herniate out of the embryo proper, giving rise to intestinal herniations. Therefore, both these abnormalities were considered together.

Eggs with cytoplasm exposed to irradiation at 2300 Å.—The few abnormal embryos developing from eggs irradiated at 2300 Å were completely different from any of those described above. The abnormal embryos contained a random mixture of differentiated parts and undifferentiated, opalescent protoplasm. Moreover, only from eggs irradiated at this wavelength did larvae hatch with some abnormal structures. The abnormal structures observed were soft and viscous tergites on the dorsum of the hatched larvae. This response to irradiation with 2300 Å light is probably attributable to denaturation of proteins (see below).

Response of Eggs to Ultraviolet Radiation

Irradiation of eggs with nuclei exposed.—Fertilized eggs irradiated 120–160 minutes after oviposition either develop normally or show extreme contrac-

tion of protoplasm. Table I gives a classification of eggs irradiated with various incident doses of wavelengths 2537 and 2894 Å. The data indicate that the nuclei are very sensitive to 2537 Å radiation with the maximum damage resulting with an incident dose of about 10×10^4 ergs/cm^2. The eggs irradiated at 2894 Å were from 80–160′ of age. Thus they contained both eggs with cytoplasm exposed and nuclei exposed. However, the contractions were interpreted to be damage when nuclei were exposed and the data were included with those of 2537 Å in which only eggs with nuclei exposed were irradiated.

TABLE I

Results of irradiation of eggs with nuclei exposed.

Wavelength Å	Dose in 10^4 ergs/cm^2	Total number eggs	Normal	Per cent normal	Yolk evisc.	Int. hern.	Contractions	Per cent contractions
Control	0	168	155	92	3	5	5	5
2537	5	5	2	40			3	60
	10	13	1	8			12	92
	15	4	1	25			3	75
2893	14	22	0	0	1	11	10	46
	21.9	18	0	0	1	3	14	82

Irradiation of eggs with cytoplasm exposed.—After collection and orientation, eggs of less than 90 minutes of age were irradiated with various doses at each of the following wavelengths: 2300, 2400, 2482, 2537, 2650, 2700, 2805, 2894, 2967, 3023, and 3131 Å. With the exception of eggs irradiated with 2300 Å radiation and very high doses of other wavelengths fertilized eggs irradiated with cytoplasm exposed fell into two categories: normal hatched larvae and abnormal unhatched larvae showing yolk evisceration and intestinal herniation. Table II gives typical data which show the response of the eggs to various doses of different incident wavelengths.

In order to obtain the spectral efficiency of these U.V. wavelengths in causing developmental alterations, an arbitrary means of comparing the effects of the various wavelengths must be made. The method employed is based on the fact that, within experimental error, as shown in Figs. 2, 3, and 4, the percentage of embryos surviving the irradiation entirely (i.e., percentage hatched larvae) depends exponentially on the incident dose of radiation. The analytical relation between percentage hatched, n/n_0, and the incident dose is

$$n/n_0 = e^{-SD}$$

TABLE II

Irradiation of eggs with cytoplasm exposed.

Wavelength Å	Dose in 10^4 ergs/cm²	Total number eggs	Normal	Per cent normal	Yolk evisc.	Int. hern.	Contractions	Per cent contractions
Control	0	168	155	92	3	5	5	2.8
2537	4.1	15	11	73		4		
	8.1	10	6	60	1	3		
	16.2	2	1	50		1		
2805	3.8	16	13	81		3		
	3.9	18	16	90	1	1		
	7.2	17	15	89		2		
	7.5	13	11	83	1	1		
	9.8	22	22	100				
	11.4	11	7	63	1	2	1	8
	12.8	15	5	33		7	3	20
	15	10	6	60	1	3		
	24.3	18	6	33		9	3	12
	38.4	12	1	8	5	3	4	33
	50.1	14	1	7	3	5	6	43
3131	49	15	14	93	1			
	98	10	8	87	1		1	1
	196	15	7	63	2	2	4	26
	980	13	1	20	4		8	62

where D is the incident dose of radiation in ergs/cm² or quanta/cm², S is the sensitivity parameter known as a cross section with dimensions of area/quantum, and e is the Naperian base of logarithms. Such an analysis was used because if the larvae hatched normally, the probability that no inactivating events have occurred in the irradiated material is high. Therefore, the dose required to give an arbitrary percentage survival provides a good means of comparison of the efficiencies of the wavelengths. The arbitrary survival taken was 37 per cent since, as is seen from the above equation when $n/n_0 = e^{-1} = 0.37$, then $S = 1/D$. In the present experiments, such an analysis provides a measure of the spectral efficiency in causing the developmental anomalies because the embryos could only fall in one of two categories: normal or abnormal. The spectral efficiencies can be compared by considering the incident dose only since the transmission of the chorion as measured in a Beckman spectrophotometer was found to be about 85 per cent at all wavelengths.

Since in irradiation of eggs with cytoplasm exposed, damage to the nuclei has no apparent relation to the cytoplasm, it was assumed that cytoplasmic damage would occur independently of the few nuclear abnormalities appearing at the higher doses of the longer wavelengths used. The cytoplasmic abnormalities cannot be scored in these cases since nuclear damage prevents

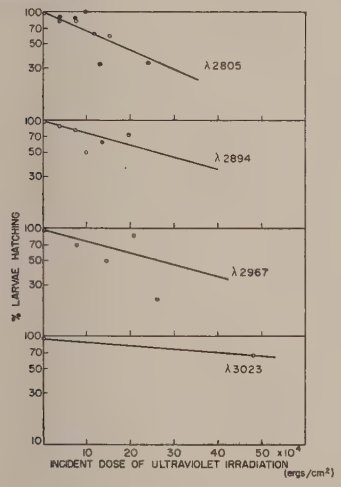

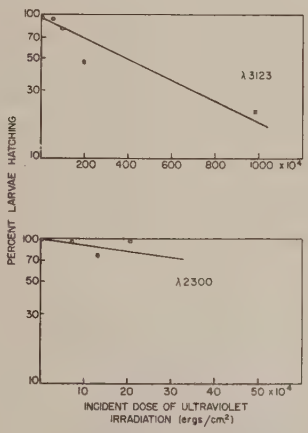

Fig. 3 (*left*). The per cent of larvae hatching after eggs were irradiated with cytoplasm exposed versus the incident dose of radiation. The solid points represent an incident intensity of 5×10^3 ergs/cm²/min., the open points an intensity of 10^5 ergs/cm²/min.
Fig. 4 (*right*). The per cent of larvae hatching after eggs were irradiated with cytoplasm exposed versus the incident dose of radiation.

the eggs from developing to the point where the cytoplasmic damage can be observed. We have assumed that all larvae not hatching after irradiation with cytoplasm exposed would have shown cytoplasmic damage. This is the justification for taking the percentage hatched as an indication of cytoplasmic damage. The assumption does not hold at longer wavelengths (see below). The percentage nuclear abnormalities appearing at the longer wavelengths was determined from the ratio of the number with nuclear abnormalities to the *total* number of fertilized eggs.

Fig. 2, 3, and 4 show semi-log plots of the percentage of hatched larvae against the dose of radiation in ergs/cm², for wavelengths 2400, 2482, 2537, 2650, 2700, 2805, 2894, 2967, 3023, and 3131 Å. The abscissa of Fig. 3 is twofold that of Fig. 2, whereas the first plot of Fig. 4 is some forty-fold that of Fig. 2. It can be seen from Fig. 2 that the slopes of the curves increase as

the wavelength increases from 2400 to 2650 Å. Fig. 3 shows that the slopes decrease from wavelengths 2805 to 3023 Å, while Fig. 4 demonstrates that eggs are highly insensitive to the radiation at 2300 or 3131 Å as indicated by the much higher doses required. There is a large scatter in the points for the determination at 2967 Å.

The few abnormal embryos developing from eggs radiated at 2300 Å showed random differentiation instead of yolk evisceration or intestinal herniation. The data given in Fig. 4 and in Table III, show the great insensitivity of eggs with cytoplasm exposed to radiation at this wavelength. Presumably this insensitivity is partially due to limited penetration of this wavelength through protoplasm. This response to irradiation at 2300 Å is probably attributable to the denaturation of proteins which, because of their high light absorption, are particularly sensitive to radiation of this wavelength (cf. Fig. 6). However, the data for the inactivation of development at this wavelength were included in the action spectrum.

TABLE III

Irradiation of eggs with cytoplasm exposed at 2300 Å.

Wavelength	Dose in 10^4 ergs/cm^2	Total number eggs	Normal	Per cent normal	Random abnormalities	Contractions	Per cent contraction
Control	0	168	155	92.5		5	2.8
2300	7.03	18	17	94		1	4
	13.1	25	19	76	6		
	20.1	15	14	94	1		

Determination of the Action Spectrum

To compare the photoinactivating efficiency of the various wavelengths of the ultraviolet spectrum, the reciprocal of the number of incident quanta/unit area required to give a 37 per cent survival must be plotted against the wavelength [6]. The efficiency has been calculated in terms of Å^2/incident quantum. Fig. 5 shows the inactivation spectrum for the early normal development of *Drosophila*. Fig. 5 also shows the absorption spectrum of nucleic acid and protein, plotted as optical density against wavelength. If the inactivation spectrum is compared with the absorption spectrum of nucleic acid, it can be readily inferred that these are quite similar. The maximum photoinactivating efficiency occurs at 2600 Å in the action spectrum, and the

maximum absorption of nucleic acid is also at 2600 Å. The action spectrum is relatively higher than the absorption spectrum for wavelengths above 2800 Å. For these wavelengths the incident light may penetrate the cytoplasm and cause damage to the nucleus, and less energy is needed to damage the nucleus than the cytoplasm (see Tables I and II). These results are consistent

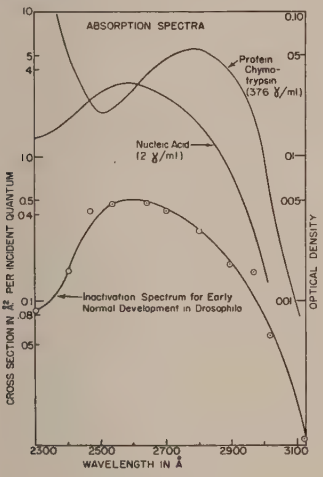

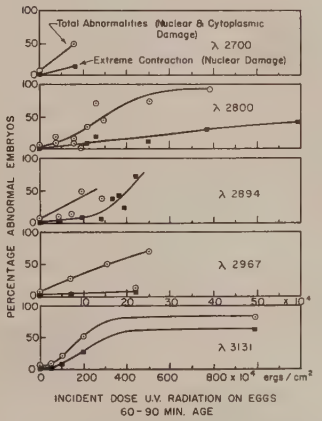

Fig. 5 (*left*). The action spectrum for the inactivation of early normal development (left scale). The absorption spectra of a protein, chymotrypsin, and nucleic acid are shown for comparison. The optical density scale represents log I_0/I for a 1 cm solution of indicated concentration.
Fig. 6 (*right*). The response of eggs irradiated with cytoplasm exposed to longer wavelengths of ultraviolet. Total abnormalities include those arising from cytoplasmic and nuclear damage.

with the hypothesis that the nucleic acids within the cytoplasm are the sensitive class of compounds. Furthermore, since preliminary results of biochemical fractionations, to be published elsewhere, indicated that the primary effect of radiation is on the nucleic acid fraction (RNA), it was assumed that the affected compound was most likely cytoplasmic nucleic acid, presumably RNA.

Confirmation of the Differential Irradiation of Cytoplasm and Nuclei

The irradiation of eggs with cytoplasm exposed with wavelengths from 2700 to 3131 Å gives rise to, at high doses, abnormal embryos showing extreme contraction. The penetration of light through cytoplasm increases with the wavelength from 2700 to 3131 Å [6]. A comparison, then, of the

energy required to give a certain frequency of yolk evisceration or intestinal herniation, with that of the extreme contractions should give a quantitative estimate of the degree of penetration of a particular wavelength. This estimate should also give the distance of separation between the sensitive component damaged at the periphery of the egg and the sensitive component damaged in the interior by higher doses of the longer wavelengths. Fig. 6 shows a comparison between the dose responses of the total per cent abnormality and per cent contraction for eggs irradiated with cytoplasm exposed. It may be seen that the extreme contractions begin to appear at much higher doses than do the other abnormalities. The difference between the two curves represents the cytoplasmic abnormalities. The response of contraction rises much faster at 2894 than at 2805 Å. Probably this can be best explained with the suggestion that although more energy is absorbed by either nucleic acid or protein at 2805 Å, more energy penetrates to the interior at 2894 Å. The rate of response of the extreme contraction at the other wavelengths is in agreement with both the degree of penetration of the energy of the wavelength and the degree of absorption of the wavelength.

The extent to which wavelength of 2805 Å penetrates the constituents of protoplasm is 80 per cent transmission at 10 micra, 50 per cent at 30 micra. On the assumption that this wavelength will penetrate through *Drosophila* eggs to a similar extent, an estimate of the increase of incident dose of U.V. radiation required to give the same percentage of both types of abnormalities should give the distance of penetration between the sensitive elements in the surface and those in the interior. It may be seen from the data for 2805 Å, shown in Fig. 6, that 37 per cent of the total abnormalities of which yolk eviscerations and intestinal herniations are the major part, are caused by an incident dose of about 10×10^4 ergs/cm^2 at the periphery of the egg, and that to get the same per cent contraction requires an incident dose of 40×10^4 ergs/cm^2. According to the data of penetration of 2805 Å through protoplasm, this four-fold increase in incident dose would imply a penetration to cause a similar amount of damage at 70μ within the interior of the egg. Since the normal embryo is an ellipsoid whose minor axis is 140μ, this calculation places the internal sensitive cellular components within the geometrical center of the minor axis, which is the location of the nuclei in the stage of the egg when irradiated.

There are obviously many simplifications involved in these calculations. The sensitivity to U.V. radiation of the nuclei within the interior of the egg was assumed equal to that of the cytoplasm, although the nuclei when irradiated at the periphery were considerably more sensitive than the cyto-

plasm. The greater light absorption by the yolk compared to cytoplasm has been ignored. The rather remarkable agreement of the calculated distance of penetration of this U.V. wavelength with the distance of separation of the cytoplasm from the nuclei can only mean a somewhat fortuitous cancellation of the inherent errors.

DISCUSSION

The present investigation indicates that damage to the nuclei is irreversible and completely inhibits normal development. Damage to the cytoplasm allows the completion of normal differentiation, but with some abnormal morphogenetic movements. The subsequent interaction of the damaged cytoplasm with the intact nuclei is incapable of completely compensating for the damage. Furthermore, if the absorbing cytoplasmic compound is RNA, as is most likely, then the evidence suggests that absorption of the energy of ultraviolet light by this compound leads to abnormal tissue movements and presumably to abnormal tissue interactions. Although the damage to the cytoplasm occurs very early in development, its morphological reflection occurs at a much later stage, at a time when the head tucks under in the embryo. Preliminary results of biochemical assays of the concentration of phosphorus and of purine and pyrimidine bases of the RNA fraction, indicate that there is a rapid increase of about two-fold the total amount of RNA immediately after irradiation with a subsequent decline to the control concentration. There is apparently little effect on the DNA-fraction concentration. This finding, if corroborated, is of interest in that it supports the hypothesis that RNA is the affected compound.

Our results demonstrate the suitability of an action spectrum analysis for determining the identity of biologically important compounds in development, provided that photoinactivation of a developmental process can be obtained. With refinements of the means of irradiation to a micro scale, the site of the sensitive compounds can be more precisely delineated. An action spectrum analysis may have the advantage of giving more specific information than other existing methods of interfering with chemical reactions in the embryonic system.

Davis [2] has obtained an action spectrum for the inhibition of the folding of the neural tube in the chick. The curve obtained displays a wavelength of maximum photoinhibiting efficiency at 2800 Å rising to a second maximum towards the shorter wavelengths at about 2450 Å. He interpreted these results to indicate a steroid as the sensitive compound. However, great caution should be exercised in the interpretation of action spectra data in the

absence of supplemental information from other methods. Because of the limited penetration of 2400 Å rays through protoplasm [6], it may very well be that Davis' secondary maximum at 2450 Å is spurious and that the efficiency of the inactivation should continue to rise with the shorter wavelengths (cf. Fig. 5) and that his inactivation curve most probably corresponds to absorption by proteins.

Von Borstel and Wolff [8] have shown that the nucleus and cytoplasm of habrobracon eggs can be damaged separately by irradiating the convex (nuclear) surface or the concave (cytoplasmic) surface with ultraviolet light. The nuclear inactivation results in an exponential hatchability curve which can be photoreactivated whereas the cytoplasmic inactivation results in a sigmoidal hatchability which could not be photoreactivated. They have also found (personal communication) that an action spectrum for nuclear damage looks like nucleoprotein absorption, whereas that for cytoplasmic damage resembles absorption by nucleic acids. In the latter case many yolk eviscerations and intestinal herniations are visible.

Antibodies or antimetabolites can interfere specifically with important biological compounds; however, there are difficulties in determining the site and mode of action within the cell of the specific proteins [9, 3], antibodies [3], or antimetabolites [1]. Furthermore, present results from the use of a variety of antimetabolites indicate only generalized effects or rate changes in development [1]. Differential enzyme inhibitors also seem to yield general effects on development with little information as to the distribution of the inhibited enzymes. Cytochemical methods largely describe the topical localization of chemical constituents during development and only rarely can a causal correlation be made between these localizations and developmental activities. Hence, it is particularly hopeful that an action spectrum in conjunction with other biochemical and biophysical methods can yield information as to the identity, location, size, shape and role of biologically important compounds in development.

SUMMARY

1. An action spectrum analysis was made in order to determine the identity, location and role of U.V. sensitive compounds in the early development of *Drosophila*. Because of its superficial cleavage, this egg presents two early stages in which radiation damage to the nucleus can be differentiated from radiation damage to the cytoplasm.

2. Eggs irradiated when the nuclei were exposed to U.V. damage either develop normally or show an abnormal retraction of their protoplasm. Eggs

damaged by irradiation in this stage result in complete early inhibition of their development.

3. Eggs irradiated at several wavelengths with cytoplasm exposed and nuclei shielded within the interior of the egg either develop normally or show evisceration of yolk or herniation of intestine. Differentiation of the rest of the larvae is apparently complete. Eggs are highly insensitive to light at λ 2300 Å but the few resulting abnormal embryos contain a random mixture of differentiated and undifferentiated, opalescent protoplasm. This response is most probably attributable to the high sensitivity of proteins to denaturation at this wavelength. Higher doses of the longer wavelengths also produce some abnormalities very similar to those produced by irradiation of eggs with nuclei exposed because of the increased transparency of the cytoplasm to these wavelengths.

4. An action spectrum for the production of abnormalities characteristic of eggs irradiated with cytoplasm exposed shows that the absorbing compounds affected contain purines or pyrimidines.

5. Quantitative data have provided evidence that the radiation damage to the cytoplasm can be differentiated from radiation damage to the nuclei. Furthermore, since the affected purine or pyrimidine containing compounds must be located in the cytoplasm, a working hypothesis is adopted that cytoplasmic nucleic acid, RNA, is the affected compound and that damage to this compound leads to the observed abnormal tissue movements and presumably to abnormal tissue interactions.

The authors wish to express their appreciation and sincere gratitude to Dr. D. F. Poulson for his kind assistance with the developmental analysis; to Dr. S. C. Shen for his helpful suggestions.

REFERENCES

1. Bieber, S., *Anat. Rec.* **117**, 521 (1953).
2. Davis, J. O., *Biol. Bull.* **87**, 73 (1944).
3. Ebert, J. D., *Ann. N. Y. Acad. Sci.* **55**, 67 (1952).
4. —— *Proc. Natl. Acad. Sci.* **40**, 337 (1954).
5. Fluke, D. J. and Setlow, R. B., *J. Opt. Soc. Amer.* **44**, 327 (1954).
6. Loofbourow, J. R., *Growth* **12** *Suppl.*, 77 (1948).
7. Ulrich, H., *Drosophila Inform. Serv.* **27**, 124 (1953).
8. von Borstel, R. C. and S. Wolff, **41**, 1004 (1955).
9. Weiss, P., *Science*, **115**, 487 (1952).

ON "CYTOFERTILIZIN" FROM SEA URCHINS

B. E. HAGSTRÖM

The Wenner-Gren Institute for Experimental Biology, University of Stockholm, Sweden

Received January 14, 1956

When sea urchin eggs are stored in sea water, they secrete a substance, which is manifested by its agglutinating action on the sperm of the same species. The agglutinating factor was termed "fertilizin" by Lillie [11, 12], who thought it essential for fertilization [12]. Lillie arrived at the opinion that fertilizin is continuously secreted by the egg and that the jelly layer surrounding the egg is saturated with fertilizin [11]. He furthermore claimed that the fertilizable condition of the egg is closely related to the presence of fertilizin; thus, when the production of fertilizin has ceased the eggs are no longer fertilizable [11].

However, Lillie's hypothesis was opposed by Loeb [14, 15] who pointed out that a complete dissolution of the jelly layer resulted in a cessation of the production of fertilizin (= sperm agglutinin) though the eggs were still fertilizable. Loeb [14] concluded that the sperm agglutinin and the jelly layer were synonymous. He also suggested that the loss in fertilizability observed by Lillie [11] was dependent upon the death of the egg and not upon the lack of fertilizin. Loeb's conception about the origin of fertilizin was later confirmed by Tyler *et al.* [26, 28, 29] and by Vasseur [31, 32]. The comprehensive literature concerning fertilizin was recently reviewed by Vasseur [31], cf. also [22, 27].

The present author, however, was able to demonstrate [6, 8] that it was no longer possible to maintain the "fertilizin theory" in the sense of Lillie and Tyler [12, 27]. It was observed that the removal of the jelly layer very much enhanced the fertilization rate [6, 8] instead of making the eggs unfertilizable. Furthermore, the addition of jelly solution to the eggs was found to cause a decrease in the fertilization rate both of normal eggs with jelly layers and of jelly-free eggs [6]. The only promoting action of "fertilizin" so far observed is the stimulation of sperm motility [31, 32, 33].

In 1950 Motomura [19] reported the existence of a new sperm agglutinating factor in the jelly-free sea urchin egg, which he called "cytofertilizin". This factor was not identical with jelly fertilizin because it was more soluble in alkaline than in acid medium, whereas jelly fertilizin is readily dissolved in

acid sea water. Furthermore, Motomura indicated that cytofertilizin is also secreted by the fertilized egg into the perivitelline space [19, 20, 21].

The present investigation is a study on the action of cytofertilizin in fertilization. Evidence is also presented about the origin of cytofertilizin. Throughout this paper cytofertilizin will be abbreviated *Cf.*

MATERIAL AND METHODS

The following species of sea urchins were used in this work: *Paracentrotus lividus* and *Arbacia lixula* from the Gulf of Naples and *Psammechinus miliaris* from Kristineberg, Swedish west coast.

The eggs were treated with HCl at pH 5.6–5.8, which treatment completely removes the jelly, cf. [6]. The jelly-free eggs were thoroughly washed by repeated sedimentation in filtered sea water.

The *Cf* was prepared by pouring 20 ml boiling sea water into a beaker containing 5 ml jelly-free eggs. The mixing of the hot sea water and the eggs resulted in a final temperature of 75–80°C and after 1–3 minutes the beaker was rapidly cooled down to about 10°C in ice water. Eggs and liquid were separated by sedimentation or by filtering. In this investigation only unfertilized eggs were used to prepare *Cf.*

The influence on fertilization was measured according to the fertilization rate method (for details cf. [7]).

Cf was also prepared by ageing a dense suspension of unfertilized jelly-free eggs in sea water [19]. The secretion of *Cf* was from time to time tested by studying the effect of the overstanding liquid on sperm agglutination. The agglutination experiments were performed according to the 3-drop method [32].

RESULTS

The production of Cf by eggs aged in sea water.—Motomura [19] showed that jelly-free eggs are still capable of producing a sperm agglutinating factor after a storage of about 20 hours in sea water. As a rule jelly fertilizin showed a higher titer of agglutinin than did the *Cf* [19].

The present writer has made similar experiments in order to investigate the origin of *Cf* and to get information about the possible morphological changes concerned with the secretion of *Cf.*

Eggs obtained in the usual manner [7] were thoroughly washed in filtered sea water, which treatment brought about a slight swelling of the jelly layers. Then the eggs were subjected to acid sea water of pH 5.6–5.8 for 2–3 minutes, this procedure causing a complete removal of the jelly, cf. [6]. The eggs were again washed in sea water and allowed to settle in a test tube in order to separate eggs and water.

In the experiments eggs and sea water were mixed in equal proportions and the suspension was resuspended many times during the course of the

experiment. Every second hour the supernatant sea water was tested for its sperm agglutinating capacity, though no agglutination was detected before 12–16 hours after the beginning of the experiment. (Temperature 20°C.) The secretion of agglutinin increased until 24–30 hours (as measured by the duration of sperm agglutination) when the common cytolysis made observations difficult. The reduced agglutinating capacity of samples containing cytolysed eggs might also depend upon the release of the ant-agglutinating factor, antifertilizin, from the eggs, cf. [8].

During the experiments the eggs were also examined in the phase-microscope with the oil immersion lens. Before the secretion of *Cf* had started the eggs showed no visible changes but when the secretion had started a very striking phenomenon was observed. The cortical granules began to make jerking movements and the dissolution of single cortical granules could be watched under the microscope. In time large areas of the egg surface showed a complete lack of granules and there was a formation of clusters or aggregates of cortical granules in the egg surface. In the surrounding medium, and to lesser extent also in the egg cortex, small granules appearing dark in phase contrast could be seen exhibiting Brownian movements, cf. [5]. These small refringent granules are apparently remainders of the dissolved cortical granules. Finally the eggs appeared to be completely deprived of cortical granules. However, at that time the eggs already showed a marked tendency to cytolyse and began to break up.

As was shown by Lindahl [13] the storage of the eggs in Ca-free sea water prolongs their life-span. The elevation of the fertilization membrane is very high after such treatment. Because the results described above suggested that the production of *Cf* was concerned with the breakdown of the cortical granules it also seemed suitable to follow the production of agglutinin when the eggs were stored in Ca-free sea water.

Parallel series with eggs in normal sea water and in Ca-free sea water were examined for the occurrence of *Cf*. The results showed that the eggs in Ca-free medium started to produce sperm agglutinin much later than did the control in normal sea water. Thus, in one experiment with *Psammechinus miliaris* no agglutinin was detectable in Ca-free sea water when the production of *Cf* was already optimal in the control. The concentration of Ca ion in the *Cf* of the two series was not equal and therefore the Ca-free *Cf* was diluted with normal sea water and the control-*Cf* with Ca-free sea water giving the same concentration of Ca ion in the agglutination experiments. The test experiments were performed according to the method by Vasseur and Hagström [32].

Also in these experiments there was a close correlation between the state of the cortical granules and the agglutinating capacity of the supernatant in contact with the eggs. In Ca-free sea water the cortical granules remained intact for a much longer period of time than did the granules of the corresponding control. This fact indicates that the cortical granule, or at least a certain part of it, represents the source of *Cf*.

However, another possibility is that the ground-substance surrounding the cortical granules is the source of *Cf*. This ground-substance is identical with the luminous layer of the unfertilized egg which layer also is responsible for the yellow dark-field color of the egg [5, 1].

According to electron micrographs the cortical granules consist of spherical units embedded in a matrix [3, 16]. Thus it might be possible that the small refringent granules observed in preparations of *Cf* have some identity with the spherical "units" when the matrix of the cortical granule is the source of *Cf*. The secretion of *Cf* might of course be caused by a submicroscopic change though this change must be simultaneous with the dissolution of the cortical granules. The interpretation presented above, where the cortical granules are suggested to be the source of *Cf*, is also supported by Moser's [17, 18] results, which made it evident that Ca ion is essential for the breakdown of the cortical granules. More evidence about the importance of Ca ion for the release of *Cf* will be presented below.

The influence of Cf on the fertilization rate.—All the preparations of *Cf* were tested in fertilization rate experiments. (47 experiments were carried out.) Normal eggs with jelly as well as jelly-free eggs were used. The jelly-free eggs were obtained according to the method previously described [6]. Many different types of experiments were made and the concentration of *Cf* was varied over a wide range. Thus dilution series were made where the concentration of *Cf* ranged from 0.1 per cent (volume/volume) to 10 per cent. The eggs were pretreated for 10–15 minutes and inseminated in the presence of *Cf* or after several washings in sea water. Furthermore, experiments were performed in which *Cf* and sperm were added at the same time without any pretreatment of the eggs.

The results show that *Cf* in the concentrations used enhances the fertilization rate of both normal eggs and jelly-free eggs if *Cf* was present at insemination. Pretreatment and subsequent fertilization in the presence of *Cf* did not increase the fertilization rate beyond the rate obtained in experiments where the *Cf* was added in immediate connection with insemination. In experiments where the eggs were only pretreated with *Cf* and washed in sea water before insemination, the improvement was not so evident. As a matter of fact, in

some of these experiments the pretreated eggs showed the same fertilization rate as did the control (cf. Fig. 1).

As already mentioned *Cf* was also prepared by ageing the eggs in Ca-free medium. Eggs from the same bulk were likewise aged in sea water and the

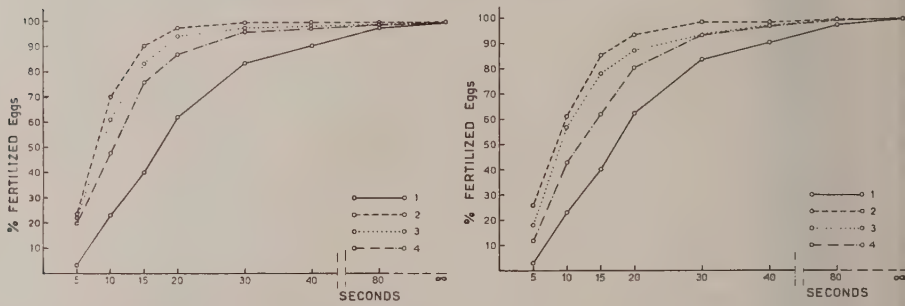

Fig. 1 *a* (left). Eggs from *Paracentrotus lividus*. The cytofertilizin was prepared by heating a dense egg suspension to 75°C for 1 minute (cf. methods).
1. Control. Eggs with jelly layers. *2.* 5 per cent (volume/volume) cytofertilizin present at insemination. No pretreatment of the eggs. *3.* Pretreatment of the egg suspension for 10 minutes with cytofertilizin in a concentration of 5 per cent v/v. Cytofertilizin present at insemination. *4.* Pretreatment of the egg suspension for 10 minutes with cytofertilizin in a concentration of 5 per cent v/v. The egg suspension was washed in sea water 3 times before insemination. Total volume of sea water 900 ml.
The concentration of sperm was 2×10^5 per ml. 5, 10, 15, 20 etc. seconds after insemination sodium-lauryl-sulphate was added to a final concentration of 0.001 per cent.
Fig. 1 *b* (right). Eggs from *Paracentrotus lividus*. The cytofertilizin was prepared by heating a dense egg suspension to 75°C for 1 minute (cf. methods).
1. Control (cf. Fig. 1 *a*). *2.* 5 ml of cytofertilizin heated for 10 minutes at 100°C was added to 95 ml of egg suspension. Insemination in the presence of the heated cytofertilizin. No pretreatment of the egg suspension. *3.* 5 ml of cytofertilizin heated for 10 minutes at 100°C was added to 95 ml of egg suspension.
The eggs were pretreated for 10 minutes and inseminated in the presence of cytofertilizin. *4.* 95 ml of egg suspension was pretreated for 10 minutes with 5 ml cytofertilizin heated for 10 minutes at 100°C. The eggs were washed 3 times in sea water before insemination. Total volume of sea water 900 ml.
The concentration of sperm was 2×10^5 per ml. 5, 10, 15, 20 etc. seconds after insemination sodium-lauryl-sulphate was added to a final concentration of 0.001 per cent.

two preparations of *Cf* were tested in parallel fertilization rate experiments. The results showed (cf. Fig. 2) that the secretion of *Cf* is depressed in the absence of Ca ion.

The effect on Cf of prolonged heating.—The heat stability of *Cf* is obviously very high since the preparation of this factor includes the heating to 75–100°C for 1 minute. However, it seemed also desirable to investigate if a prolonged heating of *Cf* would effect a loss in the promoting action on fertilization. The *Cf* prepared at 75°C (see above) was heated at 75 or 100°C for 10–15 minutes.

The heated preparations were then tested in fertilization experiments and it appeared that the promoting action persisted, though there was possibly a slight decrease in the activity. Neither was the agglutinating capacity of *Cf* destroyed by this heating.

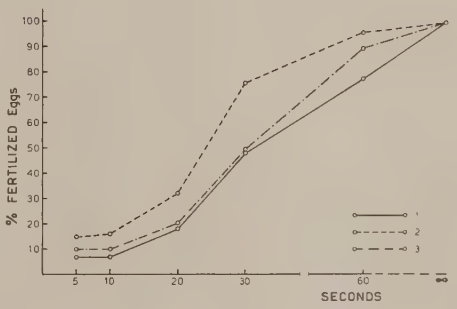

Fig. 2. Eggs from *Psammechinus miliaris*. The two preparations of cytofertilizin were obtained by ageing 5 ml jelly-free eggs in 10 ml sea water and 10 ml Ca-free sea water respectively. The ageing egg suspensions were stored in a refrigerator at + 4°C for 45 hours, whereupon eggs and liquid were separated by filtration. *1*. Control. Eggs with jelly layers. *2*. 7 per cent (v/v) of cytofertilizin prepared by ageing the eggs in sea water was present at insemination. No pretreatment of the eggs. *3*. 7 per cent (v/v) of cytofertilizin prepared by ageing the eggs in Ca-free sea water was present at insemination. No pretreatment of the eggs. The concentration of sperm was 4×10^6 per ml. 5, 10, 20 etc. seconds after insemination sodium-lauryl-sulphate was added to a final concentration of 0.001 per cent.

Preparation of Cf at pH 4.5.—The present writer has also prepared *Cf* at a pH of 4.5 by pouring boiling sea water acidified with HCl over jelly-free eggs from *Paracentrotus*. Motomura [19] failed to demonstrate any agglutinin after such treatment and concluded that *Cf* is less soluble in acid than in normal sea water. In this respect, however, the results with the *Paracentrotus*-eggs are at varians with Motomura's results and the *Cf* prepared at pH 4.5 seems to have the same properties as does the *Cf* prepared in normal sea water.

The effect of Cf on membrane formation and cleavage.—The influence of *Cf* was entirely advantageous according to the results referred to above. However, in experiments with jelly-fertilizin Runnström *et al.* [23, 24] showed that jelly solution impairs membrane formation and therefore the influence of *Cf* was also studied. Normal eggs and jelly-free eggs were used but both kind of eggs reacted in the same way to *Cf*. Different amounts of *Cf* (0.05–0.4 ml) and egg suspension were mixed to give a final volume of 10 ml. These mixtures and a control without *Cf* were inseminated with the same concentration of sperm.

The presence of *Cf* at insemination resulted in a marked improvement in membrane formation. The membranes became more highly elevated as compared with the control. Cleavage was also improved and was more uniform and simultaneous than in the control.

Cf from *Paracentrotus* was also tested for its action on eggs from *Arbacia*. This latter species is very common in the Gulf of Naples and seems to live under optimal conditions. However, the eggs give as a rule no membrane elevation upon insemination though cleavage and ensuing development is quite normal. In *Arbacia* the removal of the jelly often results in a complete membrane formation when the eggs are inseminated [6] and it has also been demonstrated that egg homogenates effect the elevation of a normal membrane, cf. [25].

In the presence of *Cf* from *Paracentrotus* (concentration: 0.5–4 per cent v/v) there was a clear tendency to membrane elevation in normal eggs as well as in jelly-free eggs from *Arbacia*. In this respect *Cf* obviously acts different from jelly-fertilizin [23, 24]. It is also evident that the membrane promoting action is not species-specific. The sperm agglutinating action, on the contrary, seems to be fairly species-specific as no cross agglutination was obtained with *Cf* from *Paracentrotus* and sperm from *Arbacia* and *Psammechinus microtuberculatus*.

DISCUSSION

Lillie, cf. [12], arrived at the conclusion that fertilizin is secreted by the egg. He was also able to demonstrate that fertilizin is heat stable to a certain extent and stands heating to 90°C for five minutes [10]. The influence on fertilizin of heating has later been thoroughly investigated by Vasseur and Wicklund [33], who found that the component of jelly solution which interferes with membrane elevation and effects sperm agglutination is more or less inactivated by heating. On the contrary, the sperm activating principle was not affected by heating. However, the ideas concerning fertilization in sea urchins have changed very much since Lillie made his investigations (for general ref. cf. [31]). Thus it was demonstrated that the jelly layer and fertilizin are synonymous [4, 26, 27, 30, 31] and recently it was shown that the jelly layer *in situ* and jelly solution are inhibitors of fertilization [6]. Motomura's discovery of the *Cf* [19] seemed again to actualize Lillie's theory [12]. According to Motomura [19] the solubility of *Cf* differs from that of jelly-fertilizin but the continuous secretion and the considerable heat resistance was in agreement with Lillie's theory.

The present writer was able to show that *Cf* is also extractable at pH 4.5 and consequently there is no absolute difference in solubility between jelly-fertilizin and *Cf*. This disagreement with Motomura's results may be dependent upon species differences. That species differences might occur is indicated by the fact that Byers [2] failed to extract any *Cf* from the eggs of *Arbacia punctulata*.

One essential point is of course the fact that no *Cf* is obtained from jelly-free eggs before the eggs show microscopical cortical changes. In Lillie's experiments [11] the production of fertilizin was likely to be concerned with a gradual dissolution of the jelly, which was already pointed out by Loeb [14, 15]. The production of *Cf* is evidently preceded by a disintegration of the luminous layer and the cortical granules.

In a recent investigation of the carbohydrates of the sea urchin egg, Immers [9] found that the cortical ground substance and the cortical granules probably contain different carbohydrates. Thus the ground substance is rich in acid polysaccharides, whereas the cortical granules seem to contain polysaccharides which are not of acid character. *Cf* and jelly-fertilizin show entirely different action on the fertilization rate and on membrane elevation; *Cf* always giving an improvement. These differences indicate that *Cf* and the jelly coat have different chemical properties, which in fact favors the assumption of the cortical granules as the source of *Cf*. Moser's observation that calcium is necessary for the breakdown of the cortical granules is also in support of this view.

At present it cannot be decided whether the secretion of *Cf* is essential for fertilization or not. The methods applied to obtain the factor for laboratory experiments are very rough and include a more or less far-reaching destruction of the egg. On the other hand, Motomura's finding of *Cf* in the perivitelline space of the fertilized egg shows that the factor may also be released under physiological conditions.

SUMMARY

Cytofertilizin, a sperm agglutinating factor, was prepared from jelly-free sea urchin eggs.

Cytofertilizin acts improving upon membrane formation and cleavage. The fertilization rate is improved by cytofertilizin.

The release of cytofertilizin is favored by the presence of calcium.

It was observed that the release of cytofertilizin is correlated with morphological changes in the cortex of the egg.

The author wishes to express his gratitude to Professor John Runnström for reading the manuscript and for valuable discussions. Sincere thanks are also due to Dr. G. Gustafson, Kristineberg, and Drs. R. and P. Dohrn, Naples, for supply of material and for working facilities.

The work was supported by grants from "J. A. Ahlstrands stipendiefond" and the Swedish Natural Science Research Council.

REFERENCES

1. Allen, R. D. and Hagström, B. E., *Exptl. Cell Research Suppl.* **3**, 1 (1955).
2. Byers, H. L., *Biol. Bull.* **101**, 218 (1951).
3. Cheney, R. H. and Lansing, A. I., *Exptl. Cell Research* **8**, 173 (1955).
4. Cornman, I., *Biol. Bull.* **80**, 202 (1941).
5. Hagström, B. E., *Exptl. Cell Research* **9**, 407 (1955).
6. —— *Exptl. Cell Research* **10**, 24 (1956).
7. Hagström, B. E. and Hagström, B., *Exptl. Cell Research* **6**, 479 (1954).
8. Hagström, B. and Hagström, B. E., *Arkiv Zool.* **7**, 579 (1955).
9. Immers, J., *Arkiv Zool.* in preparation (1956).
10. Lillie, F. R., *J. Exptl. Zool.* **14**, 515 (1913).
11. —— *J. Exptl. Zool.* **16**, 523 (1914).
12. —— Problems of Fertilization. Chicago University Press, 1919.
13. Lindahl, P. E., *Acta Zool.* **17**, 179 (1936).
14. Loeb, J., *J. Exptl. Zool.* **17**, 123 (1914).
15. —— *Am. Naturalist* **49**, 257 (1915).
16. McCulloch, D., *Exptl. Cell Research* **3**, 605 (1952).
17. Moser, F., *J. Exptl. Zool.* **80**, 423 (1939).
18. —— *J. Exptl. Zool.* **80**, 447 (1939).
19. Motomura, I., *Sci. Repts. Tohôku Univ. Fourth Ser.* **18**, 554 (1950).
20. —— *Sci. Repts. Tohôku Univ. Fourth Ser.* **20**, 93 (1953).
21. —— *Exptl. Cell Research* **5**, 187 (1953).
22. Runnström, J., *Advances in Enzymol.* **9**, 241 (1949).
23. —— *Exptl. Cell Research* **1**, 304 (1950).
24. Runnström, J. and Wicklund, E., *Arkiv Zool.* **1**, 179 (1950).
25. Runnström, J., Wicklund, E., and Löw, H., *Exptl. Cell Research* **6**, 459 (1954).
26. Tyler, A., *Biol. Bull.* **81**, 190 (1941).
27. —— *Physiol. Revs.* **28**, 180 (1948).
28. Tyler, A., and Fox, S. W., *Science* **90**, 516 (1939).
29. —— *Biol. Bull.* **79**, 153 (1940).
30. Vasseur, E., *Acta Chem. Scand.* **2**, 900 (1948).
31. —— The Chemistry and Physiology of the Jelly Coat of the Sea-urchin Egg. Stockholm 1952.
32. Vasseur, E. and Hagström, B., *Arkiv Zool.* **37 A**, No. 17 (1946).
33. Vasseur, E. and Wicklund, E., *Arkiv Zool.* **4**, 363 (1953).

AN INTEGRATOR FOR MEASURING THE "DRY MASS" OF CELLS AND ISOLATED COMPONENTS

H. G. DAVIES and E. M. DEELEY

Medical Research Council Biophysics Research Unit and Wheatstone Physics Laboratory, King's College, London, England

Received January 25, 1956

A method has recently been developed [3, 4, 1] for measuring the total mass of substances other than water (i.e. the so-called dry mass) in living or fixed cells. The method has been found to have many uses [5]. For example, serial measurements of the "dry mass" of a living cell may be used as a measure of its growth. It has been shown that the *dry mass per unit area* is proportional to the difference between the refractive indices of the cell and water multiplied by the cell thickness, that is, the optical path difference of the cell in water. The proportionality factor has been termed $1/\chi$ and the method relies on the fact that the value of χ is approximately constant for all the different chemical substances occurring in cells. The measurements of optical path difference can be made with an interferometer microscope (e.g. [7]). In order to measure the *total dry mass* of substance per cell it has been necessary to measure the average optical path difference, obtained by a series of measurements, and then multiply by the projected area of the cell. (See [2] for an alternative scanning method.) This integration may be inaccurate, especially if the area is ill-defined or the cell of irregular shape, and it is laborious. Under certain conditions, which will be defined, the method described in this paper enables the total dry mass of certain cell types to be measured with a speed and accuracy which was not previously possible. No measurement of cell area is required and the method is applicable to cells of irregular shape.

METHOD

The method for determining total dry mass is based on the fact that over a restricted range (< 0.2 wavelengths) the relationship between optical path difference (or phase difference) and light intensity in the image plane in the interferometer microscope (Fig. 1) is approximately linear. The dry mass can be calculated from measurements of light energy (i.e. intensity times area)

made in the image plane of the microscope. The following analysis shows how this calculation is made.

The interferometer microscope is adjusted for the even-field condition, that is, a constant path difference between the interfering beams at any point in the field. Rotation of the micrometer phase screw in the Dyson microscope varies the path difference between the two beams and causes the light intensity, I, in the image plane to vary according to the well-known expression

$$I = r_2^1 + r_2^2 + 2 r_1 r_2 \cos \theta \tag{1}$$

where r_1 and r_2 are the amplitudes of the two interfering beams and θ (in radians) is the phase difference between them. The phase difference θ is $2\pi\phi/\lambda$ where ϕ is the optical path difference (in cm), and λ is the wavelength of the light (in cm) *in vacuo*.

Consider an idealised object, a thin flat plate of area a (cm²) with its plane at right-angles to the optic axis; let the image fall within an aperture of area A (cm²). Let θ_0 be the phase difference due to the object and I_1 and I_2 be the light intensities at the image plane in the background field and object respectively. The light energies through the aperture with and without the object present are $I_2 a x^2 + I_1(A - a x^2)$ and $I_1 A$ respectively, where x is the magnification. Hence the change in energy (E_1) when the object is moved outside the aperture, is given by

$$E_1 = (I_1 - I_2) x^2 a \tag{2}$$

$$= 2 r_1 r_2 x^2 a \,(\cos \theta_1 - \cos (\theta_1 + \theta_0)) \tag{3}$$

where θ_1 is the phase difference between the two interfering beams in the clear field. When θ_1 and $(\theta_1 + \theta_0)$ are chosen to lie on the straight part of the curve (Fig. 1), the following approximation holds

$$E_1 = 2 r_1 r_2 x^2 a \theta_0 \tag{4}$$

$$= 2 r_1 r_2 x^2 a \frac{2\pi\phi_0}{\lambda} \tag{5}$$

where ϕ_0 is the optical path difference corresponding to the phase difference θ_0.

The value of $r_1 r_2$ is obtained from measurements of the change in light energy (E_2) through the aperture of area A, with the object absent, the phase difference being adjusted for maximum ($\theta = 0°$) and then for minimum ($\theta = 180°$) light intensity. Hence from equation (1)

$$E_2 = 4 r_1 r_2 A. \tag{6}$$

Eliminating $r_1 r_2$ from equations (5) and (6)

$$\phi_0 a = \frac{A}{x^2}\frac{E_1}{E_2}\frac{\lambda}{\pi}\,\text{cm}^3. \tag{7}$$

Hence the product of optical path difference and area can be determined by measuring the energy differences E_1 and E_2, the magnification x and the aperture area A having been determined.

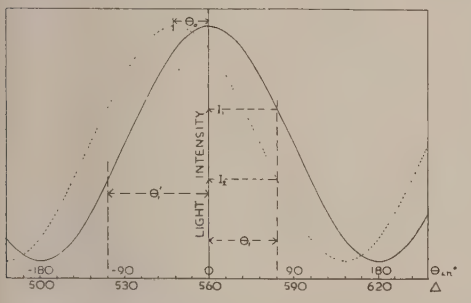

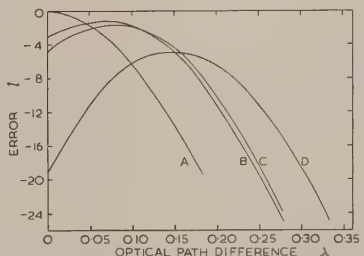

Fig. 1 (*left*). The light intensity in the Dyson interferometer microscope as a function of micrometer screw reading Δ (typical readings only), and values of the phase difference θ (in degrees) between the two interfering beams in background field (full line) and in object of path difference θ_0 (broken line) where $\theta_0 = 36°$, i.e. 0.2 π radians. The central maximum corresponds to the zero order, i.e. $\theta = 0$. When the phase screw is adjusted to $\Delta = 584$, the path difference between the two interfering beams in the clear field is $\theta_1 = 72°$ and the light intensities are I_1 and I_2 in background and object respectively, i.e. the object looks darker than the background. An alternative setting which would give the same value for mass is $\theta_1' = -108°$, when the object looks lighter than the background.

Fig. 2 (*right*). The percentage error in measuring the mass of plate-like objects as a function of their optical path difference for various values of θ_1, the path difference between the two clear-field interfering beams; $\theta_1 = 90°$ (A); $\theta_1 = 72°$ (B); $\theta_1 = 70°$ (C); $\theta_1 = 54°$ (D).

It has been shown previously [2, 3] that the dry mass m is given by

$$m = \frac{\phi_w a}{\chi}\,\text{g}. \tag{8}$$

where ϕ_w is the optical path difference in water.

Hence from (7) and (8)

$$m = \frac{\lambda}{\chi}\frac{E_1}{E_2}\frac{A}{\pi x^2}\,\text{g}. \tag{9}$$

It is will be obvious from the analysis that the substance comprising the plate could have been split up (in a plane at right-angles to the optic axis) into smaller parts of varying optical thickness, without affecting the value of E_1,

provided that the optical thickness does not exceed a value for which the approximation in equation (4) holds. Hence, according to the above analysis, the method can be used to weigh inhomogeneous objects without any "distributional" error. Out-of-focus effects are considered below.

Errors due to non-linearity. –In the above analysis it has been assumed that there is a strictly linear part to the light intensity curve (Fig. 1). This is approximately true. The error in measuring the mass of a plate-like object due to departure from linearity is, from equations (3) and (4), given by

$$\% \text{ Error} = 100 \frac{\theta_0 - (\cos \theta_1 - \cos (\theta_1 + \theta_0))}{\theta_0}. \quad (10)$$

This error has been plotted (Fig. 2) as a function of the path difference due to the object for various values of θ_1. The curves show that the measured value of mass will always be too low and that θ_1 must be chosen carefully so as to reduce this error to a minimum. For example, with the micrometer phase screw adjusted for $\theta_1 = 70°$ the measured values over a range of path difference 0.00–0.17 wavelengths are on average about per 4 cent low, and they vary in a non-random way with change in path difference by about ± 2 per cent. When the path difference exceeds 0.17 wavelength the errors increase.

It is clear from an examination of equation (10) that the errors arising from non-linearity are a function of the path difference in the object. Hence this equation only indicates the errors in measuring objects which are uniform plates. When the object is, for example, a homogeneous sphere in which the optical thickness varies from a maximum at the centre to zero at the edge, the errors will be somewhat different. It has been shown (Appendix 1) that the error in measuring a sphere as a function of θ_0, the phase difference at the centre, is

$$\% \text{ Error} = 100 \left[1 - \frac{3}{\theta_0}\left(\frac{\cos \theta_1}{2} - \frac{1}{\theta_0} \sin (\theta_1 + \theta_0) + \frac{2}{\theta_0^2} \sin \left(\theta_1 + \frac{\theta_0}{2}\right) \sin \frac{\theta_0}{2}\right)\right]. \quad (12)$$

The errors for two values of θ_1 are shown in Fig. 3.

To summarise, total dry mass can be calculated from measurements of light energy made in the evenly illuminated image plane of the interferometer microscope. The mass of all phase-retarding structures lying within the aperture is measured, irrespective of the amount of unoccupied area. The method can therefore be used to measure the dry mass of whole cells or parts of cells which have been isolated, e.g. for biochemical analysis. This method is not so readily applicable to parts of intact cells, such as irregularly

shaped nuclei, the image of which cannot be localised by means of a circular aperture.

In practice the optical path difference and shape of the object should first be ascertained roughly. Many objects approximate in shape to a sphere or a flat plate. This approximate data can then be used in conjunction with equations (10) and (11) and Figs. 2 and 3 to choose the best value for θ_1 and to predict approximately the errors to be expected.

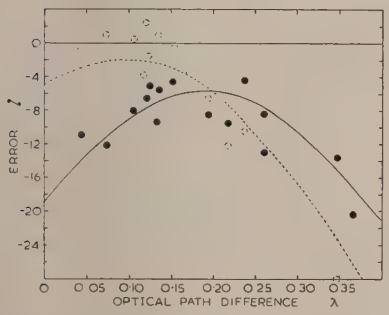

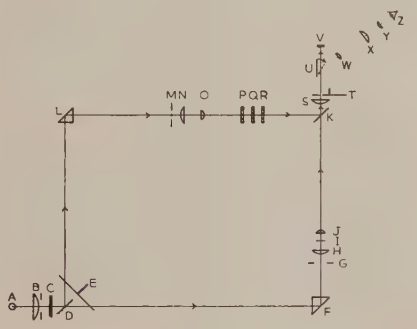

Fig. 3 (*left*). The percentage error in measuring the mass of homogeneous spheres as a function of their central optical path difference. $\theta_1 = 54°$ theoretical (full curve) and experimental (full circles); $\theta_1 = 72°$ theoretical (broken curve), experimental (broken circles).

Fig. 4 (*right*). Schematic diagram of optics of integrator. A, 250-watt compact-source mercury-arc; B, Köhler lens and iris diaphragm; C, Wratten filters 77A, 58; D, semi-aluminised beam splitter; E, beam chopper; F, L, prisms; G, aperture stop; H, condenser of interferometer microsope; I, specimen; J, objective of interferometer microscope; K, beam combiner; M, aperture stop; H, condenser; O, objective; P, Q, R, polaroids; S, lens; T, rotatable disc containing a set of apertures; U, moveable mirror; V, photomultiplier cathode; W, X, Y, lens forming an eyepiece.

APPARATUS

The apparatus for measuring dry mass incorporates a Dyson interferometer microscope (manufactured by Messrs. Cooke, Troughton and Simms Limited). It was designed for making accurate measurements of small changes in light energy. The optical components are shown schematically in Fig. 4. An image of the mercury arc at A is formed on apertures M and G by the Köhler lens at B. These apertures are of the same diameter and M contains a central stop of effective size equal to that of the obstruction in the objective of the interferometer microscope. This arrangement minimises fluctuations in the output of the photomultiplier due either to change in the overall light intensity of the arc, or to change in the position of the arc caused by flickering.

The focal lengths of the condenser N and objective O are about twice the focal lengths of the condenser H and objective J of the interferometer microscope. Each condenser-objective system forms an image of the field stop B on to the disc T; these images, one of which contains an image of the object at I, are the same size. They are observed through the eyepiece XY and can be made to coincide by centering the objective O. With the eyepiece XY replaced by a telescope, the two images of the back focal planes of objectives

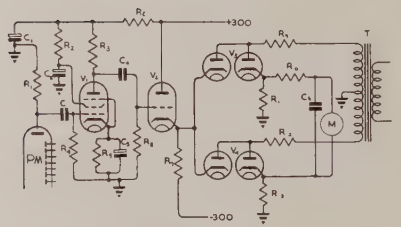

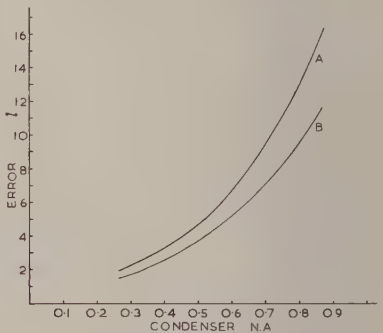

Fig. 5 (*left*). Electric circuit. PM photomultiplier (6685 E.M.I.); R_1, 2.2 M; R_2, 270 K; R_3, 100 K; R_4, 2 M; R_5, 3 K; R_6, 27 K; R_7, 33 K; R_8, 2.2 M; R_9, 270 K; R_{10}, 100 K; R_{11}, 10 K; R_{12}, 270 K; R_{13}, 10 K; C_1, 32 μF; C_2, 8 μF; C_3, 0.01 μF; C_4, 0.1 μF; C_5, 50 μF; C_6, 8 μF; V_1, Pentode EF 37 A; V_2, Triode 2 × 65N7; V_3V_4, double diodes EB32; M, meter ± 25 μA (100 K impedance); T, transformer input 230 v, 50 cycles A.C., output + 350, 0, v.—350

Fig. 6 (*right*). The percentage error in measuring the optical path difference of a flat plate as a function of the numerical aperture (N.A) of the condenser in the Cooke-Dyson interference microscope. The curves start at 0.265, the N.A. of the central obstruction in the objective; the angle subtended by this obstruction is 19°40′. A, object immersed in a medium of refractive index 1.33; B: object immersed in a medium of refractive index 1.52; in both cases the refractive index of the microscope immersion medium is 1.52.

O and J, formed by the lens S, are also brought into coincidence by adjusting K. As a result, when the mirror U is moved to the recording position the object and comparison beams are imaged on to the same part of the photocathode. This eliminates possible errors due to varying sensitivity and fatigue over the photocathode.

P, Q and R are three polaroids, P and R being fixed and oriented with their axes at 90°. The polaroid Q can be rotated and its angular position read off on a scale. This arrangement permits the light energy in the comparison beam to be altered in a known way. The plane of polarization of the light passing through the polaroid R is fixed and independent of the angular setting of the polaroid Q. Hence errors due to change in reflectivity (from

surface K) with plane of polarisation are avoided. If I is the light intensity incident on the first polaroid, and β the angle between the polaroids P, Q, then the light transmitted through the polaroid R is $I \cos^2\beta \sin^2\beta$ which is equal to $\frac{1}{8} I (1 - \cos 4\beta)$. It is convenient to construct a table relating this expression with β, the angular scale setting.

The function of the electrical circuit (Fig. 5) is to produce a meter reading which indicates the magnitude and sign of the difference in light energy between the specimen and comparison beams. In practice this meter reading is reduced to zero by means of the adjustable polaroid, so that changes in the angular position of the polaroid are a measure of the changes in light energy in the specimen beam. With the beam chopper E operating at 50 c.p.s. light from the specimen and comparison beams fall alternately on the photocathode. In general, the light energies in these beams are unequal so that a 50 c.p.s. alternating component of voltage appears at the anode of the photomultiplier. This A.C. voltage is amplified by the valve V_1 and applied via the cathode follower V_2 to a phase sensitive rectifier (valves V_3, V_4). The centre-zero meter M indicates the D.C. voltage output from this rectifier.

EXPERIMENTAL TESTS AND DISCUSSION

Tests on model objects.—The instrument was tested by measuring spheres obtained by dispersing a mixture of paraffin and cetane in a glycerol–water mixture. The refractive index was adjusted to a convenient value by varying the proportions. The difference between the refractive indices of the paraffin-cetane spheres and the medium was determined from a series of measurements of optical path difference and diameter (d). If this difference in refractive index is $\Delta\mu$, then the value of the integral of optical path difference over the projected area of the sphere can be calculated from the expression $\frac{1}{6} \pi d^3 \Delta\mu$. This has been calculated on the assumption that light rays pass parallel through the sphere. Values of this integral were compared with experimental determinations on a series of spheres; two values of θ_1 were used. The errors calculated from these values are superimposed on the theoretical curves in Fig. 3. It is concluded that the experimentally determined values of the product of optical path difference and area are lower than the calculated true values by an amount in satisfactory agreement with that predicted by theory. Probably the largest source of error in this experimental check is the measurement of the diameter of the spheres.

Reproducibility.—In order to test the reproducibility of the instrument a series of measurements of the product of optical path difference and area

was made on one sphere (Table I). The probable error of a single observation is about ± 1 per cent. The equivalent mass of the sphere obtained by using equation (8) is about 10×10^{-12} g. A clear distinction must be drawn between the above instrumental error and the overall error in determining dry mass. The latter error will be greater than ± 1 per cent and will depend on the error due to non-linearity, and on the variations in the value of χ for the different chemical substances found in cells [5].

Change of focus and contrast.—The effect of change in focus on the measurement of mass was tested by experiment. Model spheres of optical path dif-

TABLE I

Repeated integrator reading on model sphere.

Reading No.	Optical path difference × area (cm^3)
1	1.90×10^{-12}
2	1.92
3	1.92
4	1.98
5	1.90
6	1.93
7	1.96
8	1.93
9	1.91
10	1.94
11	1.85
12	1.90
Average	1.92

ference 0.1 to 0.3 wavelengths were measured on the integrator first in and then out of focus. The out of focus image of the sphere could only just be detected in the microscope. In order to collect out-of-focus light energy an aperture two to three times larger in diameter than the sphere was used. Due to large changes in focus small variations, about ± 3 per cent, in integrator reading could be detected.

Under the usual working conditions the interferometer plates in the Dyson microscope are carefully adjusted to give maximum contrast. Imperfections in the adjustment, while reducing contrast, do not introduce any systematic error into the measurements of mass. Thus, in one experiment in which the

contrast, defined as the ratio of maximum to minimum light intensity, was reduced from 13 to 3, negligible change in the ratio E_1/E_2 could be detected.

Glare.—The effect of glare is to reduce the contrast in the interference microscope; if glare is constant in amount no error is introduced [5]. However, when the intensity of glare light alters with the phase angle between the two interfering beams an error may be introduced in measurements under even-field conditions. The effect may be examined by measuring the change in light intensity inside an opaque object (e.g. carbon black) viewed in interference contrast; in the absence of glare there is no change in light intensity. The change in light intensity inside the opaque body, between light and dark field conditions, can be used to correct the experimentally determined value of E_2 (cf. equation (6)). It was found experimentally that with small fields (diameter $< 50\ \mu$) errors due to glare are less than one per cent in our microscope.

Light scatter.—When the object scatters or diffracts light energy outside the collecting aperture of the objective, the amplitude of the light beam through the object is reduced. As a result (see equation (1)) there is a change of contrast in the image of the object [5]. Objects which scatter light in this way can be detected by upsetting the adjustments on the interferometer microscope so that the object is viewed in ordinary light contrast. There will then be a change in light energy (ΔE) measured on the calibrated polaroid, when the object is removed from the field. If E_s (analogous to E_1 in equation (2)) is the change in light energy with interference contrast when the object is removed from the field then the measured ratio $\Delta_s E/E$ can be used, as follows, to predict the magnitude of the error in measuring mass due to the light scatter. Using previous nomenclature, if I_1 is the background intensity, I_2 the intensity in an object free from scatter, and I_s the intensity in a light scattering object of the same optical thickness, then

$$I_1 = r_1^2 + r_2^2 + 2r_1r_2 \cos \theta_1$$

$$I_2 = r_1^2 + r_2^2 + 2r_1r_2 \cos (\theta_1 + \theta_0)$$

$$I_s = r_s^2 + r_2^2 + 2r_sr_2 \cos (\theta_1 + \theta_0)$$

where $r_1 \rightarrow r_s$ on account of light scattering; i.e. $\Delta E = (r_1^2 - r_s^2)x^2 a$, where a is the area of the object and x the magnification of the microscope.

If, as in Fig. 1, the object in interference contrast is darker than the background, then if, in addition, light is scattered outside the collecting aperture the object will look darker still. Hence the measured mass will be greater

than true mass. Expressing this error as a fraction of the measured mass the percentage error is

$$\% \text{ Error} = 100 \frac{(I_2 - I_s)\, a x^2}{(I_1 - I_s)\, a x^2}$$

$$= 100 \frac{[(r_1^2 - r_s^2) + 2 r_2 (r_1 - r_s) \cos (\theta_1 + \theta)]\, a x^2}{E_s}$$

$$= 100 \frac{\Delta E}{E_s} (1 + RK \cos (\theta_1 + \theta_0)) \qquad (13)$$

where $K = 2/(1 + r_s/r_1)$ and $R = r_2/r_1$.

In the interferometer microscope $R \sim 1$ and so is K; for objects which scatter light to give an equivalent optical extinction as high as 0.1, $K = 1.05$. Hence to a good approximation the error is given by

$$\% \text{ Error} = 100 \frac{\Delta E}{E_s} (1 + \cos (\theta_1 + \theta_0)). \qquad (14)$$

The term $\cos (\theta_1 + \theta_0)$ will be known approximately and will in general be small.

There is another way of determining whether the object scatters light energy outside the objective aperture. E_s is measured with the object darker and then lighter than the background, corresponding to settings θ_1 and θ_1' respectively in Fig. 1. If the object scatters light, the two values obtained for E_s will be different; the first will be higher and the second lower than the true value. It can be shown that the difference between the two values is $2\Delta E$, and hence that the true value is very nearly equal to the average of the two readings. In our experience, errors due to light scattering are in general small and usually negligible.

Errors due to finite condenser aperture.—When the object is a flat plate oriented at right-angles to the optic axis the optical paths for rays which do not pass through it normally increase inversely as the cosine of the angle of obliquity. As a result, measurements of optical path difference made with a finite condenser aperture will be too high. In addition it might be expected that the contrast in the object will decrease somewhat since the path differences of the interfering rays arriving at a point in the image are varying, by an amount depending on the aperture. It has been found that errors from this second cause are small compared with those due to the first, which are shown in Fig. 6. (See Appendix II.)

These points are illustrated in the vector diagram, Fig. 7. The vector OC

represents the amplitude and phase of the comparison beam, and may be considered as being made up of a series of short vectors, each short vector representing the amplitude in an annular illuminating cone defined by angles θ and $\theta + d\theta$ to the optic axis. When the variation in optical path in the specimen is ignored the amplitude in the specimen beam is OS where ideally $OS = OC$. The phase angle is $\theta_1 + \theta_0$ where θ_1 is the phase difference due to the micrometer screw setting and θ_0 is the phase difference due to the specimen for rays parallel to the optic axis.

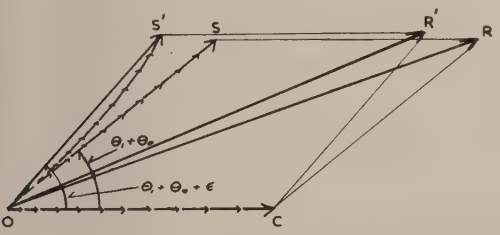

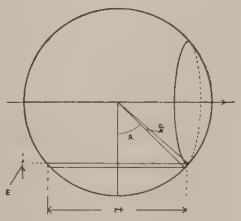

Fig. 7 (*left*). Vector diagram showing how measurements on flat plates are affected by the finite numerical aperture of the condenser (see text).
Fig. 8 (*right*). The sphere is divided up into thin walled cylinders, depth t and wall thickness w, for the purposes of mathematical integration.

When the variation in path in the object is taken into account the arc OS' is constructed from a series of short vectors, the final vector making an angle $\theta_1 + \theta_1/\cos\tau$ (Fig. 9) with the vector OC. Hence the resultant amplitude R' ($R' < R$) is obtained by adding the vectors along the arc OS' (equivalent to the vector OS') with the vector OC. It will be noticed that the length of the arc OS' is equal to OS and hence the resultant vector OS' is less than the vectors OS and also OC.

In summary, as a result of the increase of path difference with angle in the specimen the phase of the resultant vector OS' relative to OC is increased from $\theta_1 + \theta_0$ to $\theta_1 + \theta_0 + \varepsilon$. In addition the vector OS' is less than the vector OC. Hence the interference in the image plane occurs between two beams of slightly different amplitudes. As a result the beams, when out of phase by 180°, do not quite cancel each other out; i.e. the specimen does not completely "black out".

Choice of band-order and condenser aperture.—A consideration of the manner in which the Dyson interferometer microscope operates to give even-field interference contrast indicates that for any one condenser aperture the contrast will decrease slowly with increasing order of interference. Also,

increasing the condenser aperture increases the rate at which the contrast decreases and also increases the distance between successive light intensity minima as measured on the micrometer phase screw. These effects are small in the first few orders. However, it is desirable and convenient to work with a fixed condenser aperture and at the zero order. The position of zero order is chosen by examining the interference pattern formed in white light. The choice of condenser aperture is governed by the errors described in Section 6 and by considerations of contrast. Thus in the Dyson interferometer microscope as the condenser aperture is increased above about 0.6 the contrast will slowly decrease as a result of glare due, for example, to multiple reflections in the interferometer plates. In most of our experiments we use a condenser aperture of about 0.5 at which value the contrast, expressed as the ratio of maximum to minimum light intensity, ranges from about 10–20, partly depending on the nature and number of the objects in the comparison beam.

Objects of large optical path difference.—The method we have described is applicable to objects whose optical path difference does not exceed a certain value, the magnitude of which depends on the permissible error. It is sometimes possible to reduce optical thickness to a value for which errors are small by squashing the object.

An alternative method of reducing optical path difference to the required values is to immerse the object in a medium of refractive index greater than that of water. When ϕ_m is the optical path difference in the medium of refractive index μ_m, it has been shown [5] that the dry mass m is

$$m = \frac{\phi_m a}{\chi} + (\mu_m - \mu_w)\frac{v}{\chi}\,\mathrm{g}. \tag{15}$$

where v is the cell volume. However, the cell volume is often difficult to determine. The dry mass can also be deduced from measurements of optical path difference in two media of different refractive indices. It can be shown that if ϕ_1 and ϕ_2 are these optical path differences in media of refractive indices μ_1 and μ_2 respectively then the dry mass m is given by

$$m = \frac{\phi_1 a}{\chi}\frac{\mu_2 - \mu_w}{(\mu_2 - \mu_1)} - \frac{\phi_2 a}{\chi}\frac{\mu_1 - \mu_w}{\mu_2 - \mu_1}\,\mathrm{g}. \tag{16}$$

Hence two measurements of optical path difference times area will be required. The values of μ_1 and μ_2 are chosen so that the resulting optical path differences lie on the linear part of the light intensity curve.

There is a variation of this latter method which can be conveniently used to measure the mass of individual cells in a population in which the refractive index of the cell substance remains constant from cell to cell. This refractive index is measured by one of the usual methods, for example by extrapolation from measurements of optical path difference in two media of known refractive index [5]. If μ_c is the refractive index of the cell and the optical path difference is ϕ_m in a medium of refractive index μ_m then the dry mass is given by

$$m = \frac{a}{\chi}\frac{\phi_m}{\mu_c - \mu_m}\frac{\mu_c - \mu_w}{\mu_c - \mu_m}\,\text{g}. \tag{17}$$

APPENDIX I: ERRORS IN THE MEASUREMENT OF HOMOGENEOUS SPHERICAL OBJECTS

We will suppose that the sphere is divided up into concentric thin-walled cylinders (Fig. 8) of diameter $d\cos\alpha$ where d is the diameter of the sphere. The depth (t) of the cylinder is $d\sin\alpha$ and the wall-thickness w is $d/2\sin\alpha\, d\alpha$. The cross-sectional area of this cylinder is therefore $\pi d\cos\alpha w$ and the phase retardation of a beam of light parallel to the axis is $t/d\theta_0$, i.e. $\theta_0\sin\alpha$ where θ_0 is the angular retardation along the diameter of the sphere. Hence the change in light energy dE (cf. equation (3)), due to the presence of the cylinder is

$$dE_1 = 2r_1 r_2 x^2 \pi \frac{d^2}{2} d\alpha \sin\alpha\cos\alpha(\cos\theta_1 - \cos(\theta_1 + \theta_0\sin\alpha)). \tag{18}$$

Integrating over the whole sphere the total energy change E_1 is given by

$$\begin{aligned} E_1 &= \pi d^2 r_1 r_2 x^2 \int_0^{\pi/2} \sin\alpha\cos\alpha\,[\cos\theta_1 - \cos(\theta_1 + \theta_0\sin\alpha)]\,d\alpha \\ &= \pi d^2 r_1 r_2 x^2 \left[\int_0^{\pi/2} \cos\theta_1,\ \sin\alpha\, d\sin\alpha - \int_0^{\pi/2} \cos\,(\theta_1 + \theta_0\sin\alpha)\sin\alpha\, d\sin\alpha\right] \\ &= \pi d^2 r_1 r_2 x^2 \left[\frac{1}{2}\cos\theta_1 - \frac{1}{\theta_0}\sin(\theta_1 + \theta_0) - \frac{1}{\theta_0^2}\cos(\theta_1 + \theta_0) + \frac{1}{\theta_0^2}\cos\theta_1\right]. \end{aligned} \tag{19}$$

Now on the assumption that the approximation in equation (4) holds (i.e. the characteristic is linear), the above equation reduces to

$$E_{\text{lin}} = \frac{1}{3}\pi d^2 r_1 r_2 x^2 \theta_0. \tag{20}$$

Hence the percentage error in measuring the mass of spheres is given by

$$\% \text{ Error} = 100 \frac{E_{\text{lin}} - E_1}{E_{\text{lin}}}$$

$$= 100 \left[1 - \frac{3}{\theta_0} \left(\frac{\cos \theta_1}{2} - \frac{1}{\theta_0} \sin (\theta_1 + \theta_0) + \frac{2}{\theta_0^2} \sin (\theta_1 + \frac{\theta_0}{2}) \sin \frac{\theta_0}{2} \right) \right]. \quad (21)$$

APPENDIX II: ERRORS DUE TO A FINITE CONDENSER APERTURE

We will consider rays which, within the specimen, are inclined between the angles τ and $\tau + d\tau$ to the optic axis (Fig. 9). Then, in accordance with

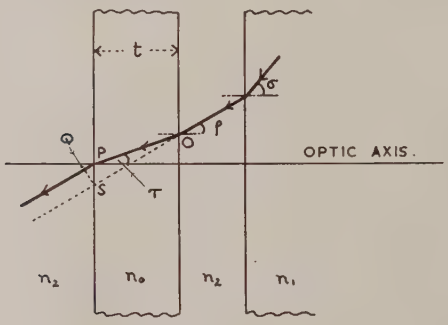

Fig. 9. Increase in optical path with illuminating angle in flat plate oriented at 90° to optic axis (see text).

well-known optical theory [8, p. 410], the amount of light energy (dE) falling in the absence of the lower beam splitting plate on an area A of the specimen is given by

$$dE = B 2\pi \sin \tau \cos \tau \, n_0^2 A \, d\tau \quad (22)$$

where B is the specific intensity of the source and n_0 is the refractive index of the object.

By Snell's law and its differential

$$n_0 \sin \tau = n_1 \sin \sigma \quad (23)$$

and

$$n_0 \cos \tau \, d\tau = n_1 \cos \sigma \, d\sigma. \quad (24)$$

Substituting equations (23) and (24) in (22) we obtain:

$$dE = B 2 \pi \sin \sigma \cos \sigma n_1^2 A \, d\sigma. \quad (25)$$

This is a more convenient expression since it gives dE in terms of the numerical aperture of the condenser $n_1 \sin \sigma$.

The optical path difference between specimen ray and comparison ray caused by the presence of the object of thickness t is from Fig. 8

$$(n_0 OP + n_2 PQ) - n_2 OS \tag{26}$$

where $n_0 OP + n_2 PQ$ is given by

$$\frac{n_0 t}{\cos \tau} + n_2 \sin \varrho \, (\tan \varrho - \tan \tau) \, t. \tag{27}$$

The latter expression is cumbersome but can be replaced by the simpler expression $n_0 OS$ from which it differs by only a few per cent for numerical apertures up to 0.8 and a ratio of n_0/n_2 up to 1.2, a ratio not exceeded in practice. Hence, the angular phase difference θ due to the object for rays at an angle τ in it is $2\pi(n_0 - n_2)t/\lambda \cos \varrho$ and this is equal to $\theta_0/\cos \varrho$ where θ_0 is the angular phase difference due to the object for rays parallel to the optic axis.

Let x_1 be the fraction of the light energy leaving the condenser between angles σ and $\sigma + d\sigma$ which passes through the specimen, and x_2 the fraction in the comparison beam. Then in the interference image of area kA the amplitudes of the two interfering beams will be $\sqrt{dE x_1/kA}$ and $\sqrt{dE x_2/kA}$. In the ideal system $x_1 = x_2 = \frac{1}{2}$; that is, the amplitudes of the interfering rays are equal. Hence according to equation (1) the light intensity dI in the image plane is given by

$$dI = \frac{dE}{A}\frac{x_1}{k} + \frac{dE}{A}\frac{x_2}{k} + \frac{2\,dE}{Ak}\sqrt{x_1 x_2}\cos\left((\theta_1 + \frac{\theta_0}{\cos \varrho}\right) \tag{30}$$

where θ_1 is the phase difference between the two beams, in the absence of the object, due to the wedge setting.

Hence the total light intensity I is given by

$$I = \frac{B\,2\,n_1^2}{k}\left[(x_1 + x_2)\int_{\sigma_1}^{\sigma_2} \sin \sigma \cos \sigma \, d\sigma + 2\sqrt{x_1 x_2}\int_{\sigma_1}^{\sigma_2} \sin \sigma \cos \sigma \cos (\theta_1 + \frac{\theta_0}{\cos \varrho}) \, d\sigma\right] \tag{31}$$

$$= k_1 \int_{\sigma_1}^{\sigma_2} \sin \sigma \cos \sigma \, d\sigma + k_2 \cos (\theta_1 + \theta_0) \int_{\sigma_1}^{\sigma_2} \sin \sigma \cos \sigma \cos \theta_0 \, (\sec \varrho - 1) \, d\sigma$$

$$- k_2 \sin (\theta_1 + \theta_0) \int_{\sigma_1}^{\sigma_2} \sin \sigma \cos \sigma \sin \theta_0 \, (\sec \varrho - 1) \, d\sigma \tag{32}$$

where k_1 and k_2 are constants. The terms $n_1 \sin \sigma_2$ and $n_1 \sin \sigma_1$ are the numerical apertures of the condenser and central obstruction respectively.

The value of ϱ is determined from Snell's law by the expression

$$n_1 \sin \sigma = n_2 \sin \varrho. \tag{33}$$

Equation (32) can be written in the form

$$I = k_3 + k_4 \cos(\theta_1 + \theta_0) - k_5 \sin(\theta_1 + \theta_0) = k_3 + \sqrt{k_4^2 + k_5^2} \cos(\theta_1 + \theta_0 + \varepsilon) \tag{35}$$

where k_3, k_4 and k_5 are constants, the value of which can be calculated.

The value of ε is given by

$$\tan \varepsilon = \frac{k_5}{k_4} = \frac{\int_{\sigma_1}^{\sigma_2} \sin \sigma \cos \sigma \sin \theta_0 (\sec \varrho - 1)\, d\sigma}{\int_{\sigma_1}^{\sigma_2} \sin \sigma \cos \sigma \cos \theta_0 (\sec \varrho - 1)\, d\sigma}. \tag{36}$$

If the variation of path difference with angle in the specimen is ignored then the resultant intensity I' in the image is given by

$$I' = k_3 + 2\sqrt{x_1 x_2} \cos(\theta_1 + \theta_0) \int_{\sigma_1}^{\sigma_2} \sin \sigma \cos \sigma \, d\sigma = k_3 + k_6 \cos(\theta_1 + \theta_0). \tag{37}$$

Thus the effect of the oblique rays is to increase the measured optical retardation by an amount ε. In the special case when $n_1 = n_2$ the coefficients k_4 and k_5 can be found analytically for θ_0 approaching zero, whereas graphical methods are necessary when $n_1 \neq n_2$. Fig. 6 illustrates ε as a percentage of θ_0 plotted as a function of condenser numerical aperture. Both curves are almost independent of the value of θ_0 up to path differences of 2 wavelengths.

It may be shown that the error due to the change in contrast in the object is given by

$$\% \text{ Error} = \frac{k_6 - \sqrt{k_4^2 + k_5^2}}{k_6}. \tag{38}$$

Calculation shows that the change in contrast is negligibly small.

SUMMARY

In general the total "dry mass" of a cell may be determined by measuring first the average optical path difference of the cell in water and then multiplying this value by the cell projected area. It is shown that this product

can be measured directly provided that the maximum optical path difference of the cell in water is less than about 0.2 wavelengths. The method may be extended to cells with higher optical path difference by immersing them in media, of refractive index greater than water. No measurement of cell area is required and the method is applicable to cells of irregular shape. The method is not readily applicable to measuring the dry mass of the components of intact cells but may be used to measure the dry mass of isolated cell components, e.g. nuclei, nucleoli, chromosomes etc.

The apparatus described for making the measurements employs a Cooke-Dyson interference microscope, but can be constructed with any two-beam interference microscope. A feature of the apparatus is that it measures small changes in light energy with high accuracy. Hence it has possible applications to the measurement of faintly stained objects, e.g. single Feulgen stained chromosomes produced by the cell crushing method [5].

The apparatus can also be used to make "point" measurements of optical path differences, sensitive to about $^1/_{1000}$ wavelenghts.

The method of measuring dry mass has been tested experimentally on model spheres. The results obtained were in good agreement with those predicted by theory.

Possible errors due to light scattering by the object, out of focus errors, and the variation in optical path in plate-like objects with illuminating aperture have been examined.

We wish to thank Professor J. T. Randall, F.R.S., for his encouragement and for providing us with the facilities for our work. We would also like to thank Dr. M. Mitchison for discussion and for calling our attention to a somewhat similar method [9] of measuring mass specifically applicable to the interference microscope manufactured by C. Baker. We also wish to point out that Dr. L. Ornstein has independently conceived the notion of making measurements of dry mass by using the linear part of the light intensity curve [10]. One of us (E. M. D.) acknowledges a Fellowship from the Nuffield Foundation.

REFERENCES

1. Barer, R., *Nature* **169**, 366 (1952).
2. Caspersson, T., Carlson, L., and Svensson, G., *Exptl. Cell Research* **7**, 601 (1954).
3. Davies, H. G. and Wilkins, M. H. G., Report to the Cytochemistry Commission of the Society for Cell Biology: Physical Aspects of Cytochemical Methods, 1951.
4. Davies, H. G. and Wilkins, M. H. F., *Nature* **169**, 541 (1952).
5. Davies, H. G., Wilkins, M. H. F., and Boddy, R. C. H. B., *Exptl. Cell Research* **6**, 550 (1954).
6. Davies, H. G., Wilkins, M. H. F., Chayen, J., and La Cour, L. F., *Quart. J. Microscop. Sci.* **95**, 271 (1954).
7. Dyson, J., *Proc. Roy. Soc. A* **204**, 170 (1950).
8. Hardy, A. C. and Perrin, F. H., The Principles of Optics. McGraw-Hill Book Comp. New York, 1932.
9. Mitchison, J. M., Passano, L. M., and Smith, F. H., *Quart. J. Microscop. Sci.* (in press).
10. Ornstein, L., Personal communication.

Experimental Cell Research, **11**, *186–196 (1956)*

STUDIES ON ISOLATED CELL COMPONENTS

IX. THE SOLUBLE PHASE[1]

N. G. ANDERSON

Biology Division, Oak Ridge National Laboratory, Oak Ridge, Tennessee

Received January 25, 1956

It is evident that the physical properties and reactions of the cytoplasm are a reflection of the interactions of the many molecular species and particulates of which it is composed. While emphasis has long been laid on the lability of the cytoplasm and its rapid reaction to injury, it is difficult to conclude that the substances or structures that give rise to these properties are necessarily so labile that it is impossible to isolate them. It appears justified, therefore, to explore brei fractions for both the molecules or structures and the reactions which give rise to such fundamental properties as the sol-gel reaction and cytolytic reaction to injury. In previous studies by Hultin and Gross [14, 15, 8, 9, 10] the possibility that whole brei may react in a manner parallel to that of whole cells has been examined. The addition of calcium was shown to stimulate markedly the formation of acid and to cause clumping of subcellular particulates in sea urchin egg breis. These effects have been explained on the basis of Heilbrunn's theory of the central mediating role of calcium in stimulation and cytoplasmic "gelation" [9, 10, 11].

In the present series of studies, an attempt is made to explore the soluble phase of the perfused rat liver to see: (*a*) whether it is capable of exhibiting reactions analogous to those of the cytoplasm of intact cells; (*b*) whether the components of a sol-gel system can be isolated from it; and (*c*) to ascertain whether or not any organization of the constituent macromolecules survives the isolation procedure. Although a number of studies have been carried out on the soluble phase,[2] previously reviewed by Barry [4] and Sorof *et al.* [26], the results obtained in these studies differ in many respects from those previously reported. The differences are thought to be caused, at least in part, by the rapid method of preparation.

In this paper, the preparation of the soluble phase is described, together with data on its stability and composition.

[1] Work performed under Contract No. W-7405-eng-26 for the Atomic Energy Commission.

[2] This term emphasizes the concept that many molecular species may exist in several phases in the cell, i.e., they may be dissolved or in a soluble state, absorbed on particulates, or bound as parts of cell structures.

MATERIALS AND METHODS

Sprague Dawley rat livers were perfused *in situ* with complete Locke's solution by the rapid perfusion method previously described [2]. Weighing and homogenization were done in cold 0.25*M* sucrose. Except as otherwise noted, the final volume of the brei in milliliters was equal to three times the liver weight in grams. The brei was immediately centrifuged in an International Equipment Co. high speed head No. 295 at 3500 rpm (13,330 × *g* at the center of the tube, $R_{min} = 2.5$ cm, $R_{max} = 6.7$ cm) for 20 minutes. The average time between stunning the rat and the beginning of centrifugation in 44 preparations was 10.1 minutes. The temperature of the brei was 7°C immediately after preparation but had dropped to 2.5° during the first centrifugation, which was carried out at − 5 to − 8°. When two livers were perfused, the first brei was centrifuged as soon as prepared. When the second brei was ready (approximately 10 minutes later), the centrifuge was stopped and the tubes containing the second brei added, after which it was run for the full 20 minutes. The centrifuge head was allowed to decelerate free at the end of the run. The lipid film at the top was carefully removed with a suction pipette and the supernatant fluid transferred to tubes for the Spinco No. 40 rotor (prechilled to − 5°) and spun at 40,000 rpm for one hour (105,000 × *g* at the center of the tubes, $R_{min} = 3.8$ cm, $R_{max} = 8.1$ cm). The lipid layer was again removed and the clear yellow supernatant fluid (final temperature 10°C), referred to as the soluble phase (SP), recovered.

Nitrogen analyses were done by the method of Ma and Zuazaga [18].

RESULTS

If the preparation described is contaminated with microsomes or other particulate material, then the composition of the SP should vary with centrifugation time. However, if centrifugation is carried out until a range of centrifugation times is reached where very little change in composition occurs, then the preparation may be assumed to be homogeneous and contain only soluble molecules or isopyknic particles.

The results of a study of supernatant fluid nitrogen content versus centrifugation time are shown in Fig. 1. The entire supernatant fluid was removed in each instance after pipetting off the fatty layer. Although the density of the solution near the bottom is greater than that near the top, owing to sedimentation of protein during the longer runs, the amount of nitrogen in the whole SP varies little over a wide range of centrifugation times. It is evident that the treatment chosen is not critical, and lies in a broad plateau where little change in nitrogen content occurs when the treatment is varied.

To ascertain whether particles might be present that were not sedimented because they had the same density as the SP, a preparation was diluted with equal volumes of *M*/15 sodium phosphate buffer, pH 7.8, and centrifuged

for one hour at 40,000 rpm in the Spinco No. 40 rotor. A very tiny pellet believed to be sedimented protein was observed in both the experimental and undiluted control. There do not appear to be particles of microsomal dimensions isopyknic with the SP as prepared here.

Analysis of the nitrogen content of 14 different breis gave an average nitrogen content of 9.51 mg of N/ml (maximum 10.75, minimum 7.70). Analysis

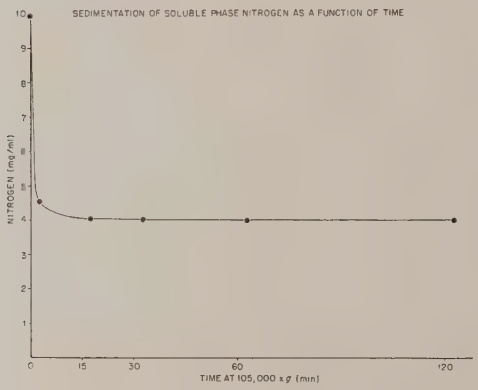

Fig. 1. Concentration of nitrogen in supernatant solutions removed after centrifugation equivalent to 105,000 × g for the times indicated. Centrifugation done during acceleration and deceleration was disregarded.

of 8 SP preparations gave an average of 4.12 mg of N/ml (maximum 4.49, minimum 3.75). An average of 43 per cent of the total brei nitrogen was therefore recovered in the soluble phase. Dialysis of 3 preparations against 0.02M sodium phosphate (pH 7.8) showed that 87.5, 87.6, and 87.9 per cent of the SP nitrogen was nondialyzable.

The absorption spectra of the SP before and after dialysis are shown in Fig. 2. The undialyzed sample, diluted 1:80 with phosphate buffer, shows a curve in the ultraviolet that is typical of a protein solution containing a small amount of either nucleic acid or nucleotides. The ratio of absorption at 280 mμ to that at 260 mμ was 0.89. After dialysis for 22 hours against M/15 sodium phosphate at 5°C, pH 7.8, the ratio was increased to 1.28, closer to the value of 1.75 characteristic of many proteins [27]. The maximum difference between the two absorption spectra was observed at 260 mμ. The volume of the dialyzed sample was adjusted in such a manner that it was comparable to the undialyzed sample. The absorption spectrum from

Fig. 2. Absorption spectrum of undialyzed (○) and dialyzed (●) soluble phase preparations. Solutions diluted 1:80 with M/15 phosphate buffer pH 7.8 for measurements in the deep ultraviolet (top). Near ultraviolet through infrared spectrum done on samples diluted 1:1 with same buffer (bottom). Dialysis was against buffer used for dilution.

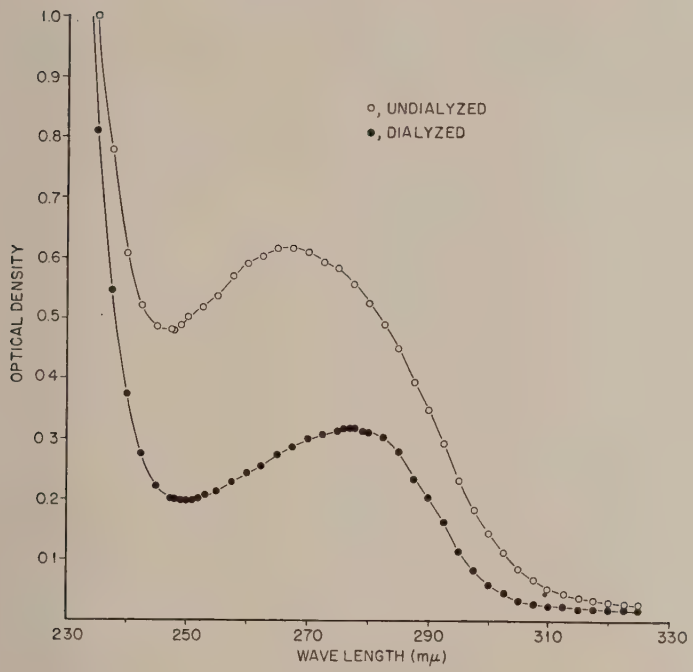
1.0
0.9
0.8
0.7
0.6
0.5
0.4
0.3
0.2
0.1
OPTICAL DENSITY
o, UNDIALYZED
•, DIALYZED
230
250
270
290
310
330
WAVE LENGTH (mμ)

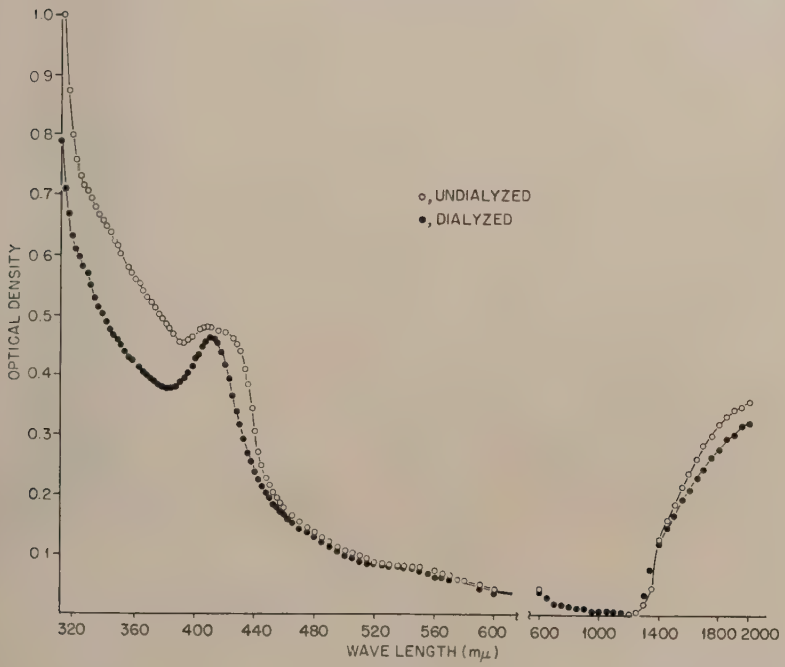
1.0
0.9
0.8
0.7
0.6
0.5
0.4
0.3
0.2
0.1
OPTICAL DENSITY
o, UNDIALYZED
•, DIALYZED
320
360
400
440
480
520
560
600
600
1000
1400
1800
2000
WAVE LENGTH (mμ)

310–2000 mμ was done on an undialyzed preparation diluted 1:1 with pH 7.8 phosphate buffer. The peak at 407 mμ is characteristic of metallo enzymes such as catalase. After dialysis, this peak was sharpened considerably, suggesting that several dialyzable compounds with peaks in this region exist. No evidence of hemoglobin was found. The rise in absorption from 1300–2000 occurs in both dialyzed and undialyzed samples.

The results of these experiments suggest that only a very small amount of 260 absorbing material exists in the SP which is nondialyzable. Since the very real possibility exists that the results may be caused by depolymerization of ribonucleic acid during prolonged dialysis, the experiment was repeated using electrodialysis in a modified electroconvection apparatus for 42 minutes. The untreated SP was diluted 1:50 with phosphate buffer and the electrodialyzed sample, which increased in volume during treatment, was diluted to give a dilution comparable with that of the original material. The 280:260 ratio for the SP was 0.81; after electrodialysis it rose to 1.22. The greater part of the 260 absorbing material is therefore in a readily dialyzable form.

The pH stability of the SP was studied by mixing equal volumes of SP and sodium phosphate buffers in the cold, allowing them to stand 30 minutes (in the cold) and then centrifuging them for 60 minutes at 2400 rpm (1460 × g at bottom of tube). The pH of the supernatant solution and the nitrogen content of the supernatant and pellet were then determined. The results, expressed as percentage of the original total nitrogen remaining in the supernatant solution with buffers prepared as indicated, are shown in Fig. 3. The preparation was completely soluble under these conditions from pH 1.3–3.5, and from 6.3–11 (the highest pH examined). No precipitation occurs at low pH with phosphate even if the SP is mixed with equal volumes of concentrated phosphoric acid. If, instead of mixing with buffer, dilute phosphoric acid is added slowly, a precipitate is formed which redissolves on the addition of more acid. When a series of very dilute hydrochloric acid solutions were used in place of phosphate buffers, a curve similar to that of Fig. 3 was obtained with the exception that in the more acid ranges (pH 1) a voluminous precipitate occurred. The addition of NaCl to clear phosphoric acid solutions of soluble proteins also produced precipitation. Sulfuric and acetic acids produced effects resembling those of phosphoric acid. In very acid solutions the chloride ion appears to have a specific precipitating effect.

Further experiments showed that the protein precipitated at pH 4.8 in phosphate could be redissolved at pH 6.9 or higher if handled quickly and in the cold. If kept at the lower pH for any length of time, denaturation occurred. Purification of this fraction will be described in a subsequent paper.

When the pH of the SP was changed by dialysis against $M/15$ phosphate buffers of various pH's; somewhat different results were obtained. No precipitation was seen at pH 1–2. However, precipitation occurred in varying amounts from pH 3–8 with a maximum in the 3–6 range, suggesting that some proteins may be solubilized by dialyzable substances.

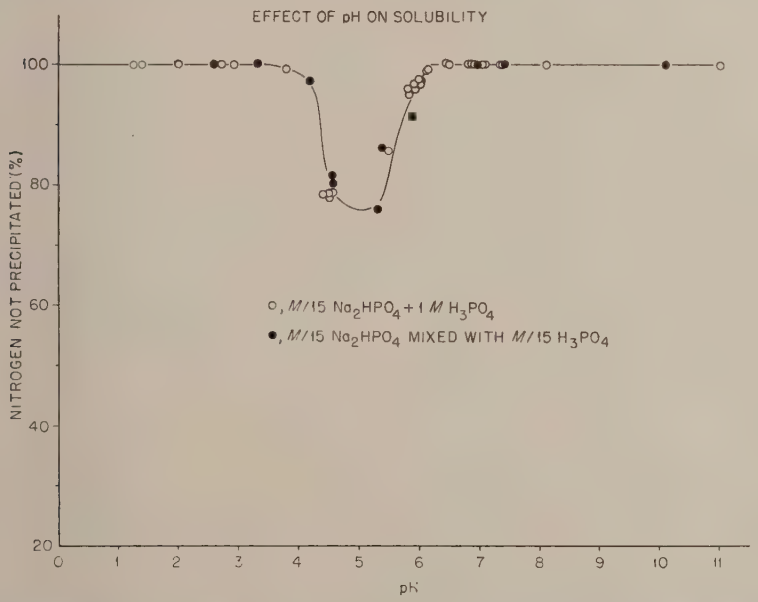

Fig. 3. Effect of pH on solubility of soluble phase proteins. Soluble phase mixed with equal volumes of phosphate buffers, allowed to stand for 30 minutes in the cold, and then centrifuged. Results expressed as percentage of nitrogen remaining in solution. Buffers prepared by mixing varying proportions of $M/15$ Na_2HPO_4 and $1M$ H_3PO_4 (○); buffers prepared from $M/15$ Na_2HPO_4 and $M/15$ H_3PO_4 (●). Extreme pH values were studied using either phosphoric acid or tribasic sodium phosphate.

The solubility of SP constituents as a function of NaCl concentration was studied by dialyzing fresh preparations against various concentrations of NaCl in the cold. As much as 42 per cent of the undialyzable nitrogen is precipitated in distilled water, whereas 6.2 per cent was precipitated in $0.1M$ NaCl and only 0.56 per cent in $1M$ NaCl.

The problem of the nature and amount of 260 mμ absorbing material in the SP was investigated further, since there is little agreement in previous work as to the amount of nucleic acid in this fraction. If the 260 mμ absorbing

material consists of a spectrum of compounds ranging from simple nucleotides to long RNA chains, the results of attempts to separate various fractions would be expected to show considerable variations. The acid soluble 258 mμ absorbing material was, therefore, studied first and was found to be highly reproducible in parallel extractions of any one brei or SP preparation. In

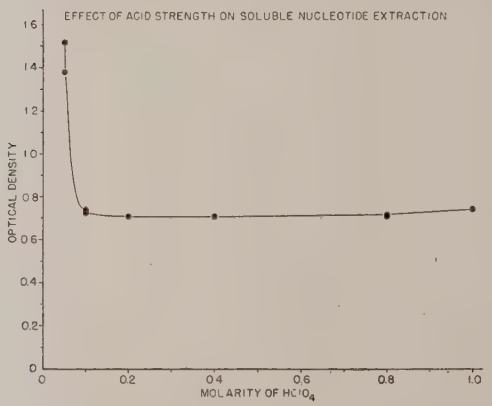

Fig. 4. Effect of acid strength on acid-soluble nucleotide extraction. Brei samples (3-ml) containing 50 mg of liver per milliliter extracted twice with 6-ml volumes of $HClO_4$ of molarities indicated. Extracts diluted to 25 ml and read against acid blank in 1 cm cells at 258 mμ.

one experiment, for example, 16 3-ml brei samples (each containing 50 mg of the same liver per milliliter) were extracted with 0.2M $HClO_4$ [20]. The extracts were diluted to 25 ml with 0.2N $HClO_4$ and the density at 258 mμ determined in 1 cm light path cells. The average for the 16 determinations was 0.753, S.D. $\pm$ 0.011. The effects of variation in strength of acid used for extraction was examined by extracting 3 ml brei samples with cold $HClO_4$ solutions whose final concentrations varied from 0.05–1.0N (Fig. 4). Identical results are obtained between 0.2–0.4M with a very slight rise at 0.8–1.0M; 0.05M was insufficient to precipitate the protein and RNA present. Although the actual amount of acid used will depend on the amount of protein and other buffering substances present, it does not appear that the strength of the acid used is critical for the extraction of acid soluble nucleotides.

In three successive experiments with three different livers the $E_{258}^{1\text{ cm}}$ of preparations containing the extract from 1 ml of homogenate (0.33 g liver), prepared as described and diluted to 50 ml, were 0.840, 0.785, and 0.874, whereas the SP from the same livers, similarly extracted and diluted, yielded solutions whose densities were 0.540, 0.555, and 0.594. The per cent of the total acid soluble material of the brei, which was recovered in the SP was 64.3, 68.0, and 67.0 per cent (average 66.4). It appears that a considerable

fraction of the acid soluble 258 mμ absorbing material is bound to particulate material. Further experiments showed that the amount recovered in the SP varied considerably with the dilution of the brei, suggesting that part of it was adsorbed.

RNA of the SP was determined by prolonged hydrolysis, in 1*N* $HClO_4$ in the cold, of samples previously extracted with dilute acid to remove acid soluble nucleotides [20]. The amounts of RNA found in four successive preparations were 237, 247, 224, and 241 μg (average 237) of RNA/ml of soluble phase. This amounts to approximately 10 per cent of the RNA of the whole liver.

As an alternate method, the RNA was extracted by heating samples of the SP made 1*M* with respect to NaCl in a boiling water bath for 10 minutes [6]. The extraction was repeated once. After centrifugation, two volumes of alcohol was added to the clear supernatant fluid. A fine precipitate formed, which was centrifuged down, after standing 24 hours in the cold. The precipitate was extracted for 24 hours with 1*N* $HClO_4$. The absorption spectra of the alcohol solution and the acid extract showed that nearly all of the RNA was sufficiently highly polymerized to be insoluble in 70 per cent alcohol.

No deoxyribonucleic acid could be detected in the SP by the Dische reaction [22].

DISCUSSION

The data presented suggest that a reproducible fraction, the soluble phase (SP), can easily be obtained from rapidly perfused rat liver by high speed centrifugation. No evidence of insoluble particulate matter was found in it.

Study of the SP preparation described here is considered of interest for the following reasons. In studies aimed at elucidating the "intracellular distribution" of enzymes, substances, or activities, the SP is generally composed of the supernatant fluid left after sedimentation of the microsomes plus the washings from particulate fractions. These washings may be expected to include a maximum of loosely adsorbed materials. By preparing the SP in the highest practical concentration with the greatest possible speed, and by excluding washings from sedimented material, a better approximation of the intracellular SP is obtained. A comparison of the constituents of the SP prepared by the two different methods should yield a better indication of which substances are loosely bound to particulate matter. For work at high concentrations it is also unnecessary to add salts since the components are subjected to the same ions in a lower concentration as in the cell (except for the perfusion solution included). Furthermore, as shown by Sorof and

Cohen [24], the protein concentration is in the proper range for electrophoretic study.

Only very gentle "homogenization" is used and every effort is made to handle the material as gently as possible in the hope that a minimum number of mitochondria and nuclei will be macerated. Autolytic effects, which occur rapidly in the liver, are minimized by sedimenting all the nuclei and the greater part of the mitochondria within 13–14 minutes after death of the animal. These two fractions contain 77 per cent of the catheptic activity of the liver [19].

In the present study an average of 43 per cent of the total nitrogen of the brei was recovered in the soluble phase. This finding is in the general range reported by previous workers who found 31 per cent [13]; 41.3 per cent [23]; 42 per cent [1]; 38.6 per cent [19]; and 55 per cent [25] for rat liver. Barnum and Huseby [3] found 29.2 per cent for mouse liver.

The pH stability studies are of interest from several points of view. A number of studies on the viscosity of the cytoplasm have shown that a decrease in pH results in an increase in cytoplasmic viscosity. In these studies, a fraction of the SP has been found to be insoluble over the range of pH 3.5–6.3 with a maximum precipitation around pH 5. This fraction may well be the basis for the changes observed in intact cells. During cytolysis after injury, the cytoplasmic pH may drop to this range with accompanying coagulation. The precipitation observed *in vitro* resembles the intracellular change in that it is at first reversible in the cold, but becomes irreversible with time. The finding of Barth [5] that cells immersed in acid solutions below pH 5 coagulated more rapidly when the acids were dissolved in NaCl than in sea water may be related to the precipitating effects of the chloride ion in acid solutions found here.

From the point of view of the isolation of cell components, it is evident that the pH range 3.5–6.3 should be avoided since the particulate fractions will be grossly contaminated with precipitated protein. This was found to be the case by Dounce [7] who has frequently pointed out that nuclei may be isolated above and below this general range but not within it. In addition to the SP protein precipitated, microsomes are agglutinated at pH 5 and have been prepared in this manner by Hers *et al.* [12]. The method does not appear suitable for the removal of microsomes from the SP however, since soluble proteins are also precipitated.

The results of the dialysis experiments suggest that some of the cytoplasmic proteins are solubilized by dialyzable substances. This phenomenon will be discussed in detail in a subsequent paper on cytoplasmic complex formation.

Only a small fraction (approximately 10 per cent) of the liver RNA has been found in the soluble phase. Previous reports [3, 13, 17, 21] indicate that between 19–33 per cent of the liver RNA was in the soluble fraction. The discrepancy may possibly be due to loosely adsorbed RNA removed from particulate material during washing, where washings have been included in the SP, or to incomplete sedimentation of microsomes. The SP prepared as described here would be expected to contain a minimum of material desorbed from particles because (*a*) the dilution of the original cellular SP has been kept to a minimum, (*b*) the particulate fractions have been sedimented as rapidly as possible, and (*c*) the sedimented material has not been reextracted.

SUMMARY

The soluble phase (SP) of rat liver has been prepared by a method in which the liver is rapidly perfused and centrifuged so that the nuclei and nearly all of the mitochondria are sedimented within 13–14 minutes after the death of the animal. An average of 43 per cent of the total nitrogen of the brei is recovered in the SP together with approximately 10 per cent of the RNA. An average of only 66 per cent of the acid soluble nucleotides of the liver were recovered in the soluble phase.

In phosphate buffers the SP was stable between pH 1.26 and 3.5, and between 6.3 and 11. Between 3.5 and 6.3 marked precipitation occurred with a maximum of 24 per cent of the SP nitrogen precipitated near pH 5. An average of 12.3 per cent of the SP nitrogen was dialyzeable. The relation of the pH stability of the SP to viscosity changes in cells in slightly acid media is discussed.

REFERENCES

1. Albert, S. and Johnson, R. M., *Cancer Research* **14**, 271 (1954).
2. Anderson, N. G., *Exptl. Cell Research* **8**, 91 (1955).
3. Barnum, C. P. and Huseby, R. A., *Arch. Biochem.* **19**, 17 (1948).
4. Barry, G. T., *Cancer Research* **10**, 694 (1950).
5. Barth, L. G., *Protoplasma* **7**, 505 (1929).
6. Brues, A. M., Tracy, M. M., and Cohen, W. E., *J. Biol. Chem.* **155**, 619 (1944).
7. Dounce, A. L., *Ann. N.Y. Acad. Sci.* **50**, 982 (1950).
8. Gross, P. R., *Biol. Bull.* **103**, 293 (1952).
9. —— *Biol. Bull.* **107**, 298 (1954).
10. —— *Biol. Bull.* **107**, 364 (1954).
11. Heilbrunn, L. V., An Outline of General Physiology. 3rd ed., Saunders, Philadelphia, 1952.
12. Hers, H. G., Berthet, J., Berthet, L., and De Duve, C., *Bull. soc. chim. biol.* **33**, 21 (1951).
13. Hogeboom, G. H., Schneider, W. C., and Palade, G. E., *J. Biol. Chem.* **172**, 619 (1948).
14. Hultin, T., *Exptl. Cell Research* **1**, 159 (1950).
15. —— *Exptl. Cell Research* **1**, 272 (1950).

16. Huseby, R. A. and Barnum, C. P., *Arch. Biochem.* **26**, 187 (1950).
17. Lowe, C. U. and Lehninger, A. L., *J. Biochem. Biophys. Cytol.* **1**, 89 (1955).
18. Ma, T. S. and Zuazaga, G., *Ind. Eng. Chem., Anal. Ed.* **14**, 280 (1942).
19. Maver, M. E. and Greco, A. E., *J. Natl. Cancer Inst.* **12**, 37 (1951).
20. Ogur, M. and Rosen, G., *Arch. Biochem. Biophys.* **25**, 262 (1950).
21. Price, J. M., Miller, E. C., Miller, J. A., and Weber, G. M., *Cancer Research* **10**, 18 (1950).
22. Schneider, W. C., *J. Biol. Chem.* **161**, 293 (1945).
23. —— *J. Biol. Chem.* **176**, 259 (1948).
24. Sorof, S. and Cohen, P. P., *J. Biol. Chem.* **190**, 303 (1951).
25. —— *J. Biol. Chem.* **190** 311 (1951).
26. Sorof, S., Golder, R. H., and Ott, M. G., *Cancer Research* **14**, 190 (1954).
27. Warburg, O. and Christian, W., *Biochem. Z.* **310**, 384 (1942).

CELL SITES OF PROTEIN SYNTHESIS IN THE EARLY CHICK EMBRYO, AS INDICATED BY AUTORADIOGRAPHS

J. L. SIRLIN and C. H. WADDINGTON

Institute of Animal Genetics, University of Edinburgh, Scotland

Received January 30, 1956

In the course of study of protein synthesis in the early chick embryo, Feldman and Waddington [11] used autoradiography for assessing the uptake of methionine-S-35 into protein of different embryonic tissues. In the present work it was intended to trace the incorporation of the tracer into the protein of the individual cells.

MATERIAL AND TECHNIQUE

Chick embryos were labelled with DL-methionine-S-35 by essentially the same procedure as described by Feldman and Waddington [11]. Fertile eggs were injected with a total activity of 8 μc each (specific activity of the methionine: 24.7 mc/mM). After allowing the tracer to diffuse in the eggs for 17 hours at room temperature, they were incubated for 29 hours at 37.5°C. After incubation the embryos were carefully rinsed in carrier-methionine saline of the same concentration used for the injections, fixed in Carnoy and classified according to the stages proposed by Hamburger and Hamilton [19]. Though only typical embryos were selected for study, the whole batch showed no obvious effect of radiation damage after incubation with the tracer.

Labelled embryos were transversely sectioned at 2 or 3 μ and 5 μ for autoradiography. Unlabelled embryos were sectioned at 2 or 3 μ for control autoradiographs (ARGs), and at 8 μ for cytological study. Sections were coated with Kodak autoradiographic film, and exposed in the refrigerator for 2 to 6 days. The film was developed with Kodak D 19 b for 2 to 4 minutes at 17.5°C.

Most of the ARGs were stained with methyl green-pyronin [4], others with Giemsa [18]. Of several stains tested these proved the most efficient for elucidating cytological detail under the ARGs. Because of the greater specificity of methyl green-pyronin, only the observations made with it will be reported here. Following the recommendations of Brachet, methyl green Anachemia (or Grübler) and pyronin Geigy were used. Some ARGs were left unstained for cytological study under phase contrast. Other sections for cytological study, prepared at a time when the foreign dyes were not yet available to us, were stained with methyl green-pyronin BDH. All staining was carried out at pH 4.8.

It is worth considering here the dimensions of the cell structures in a chick embryo that an ARG is expected to resolve. In the embryonic stages under investigation (stages 6–8) the average diameters are: cell, 7–10 μ, nucleus, 5–6 μ, nucleolus 2–3 μ,

cytoplasm 2–3 μ. Some of these dimensions are near the resolving limit of an ARG and therefore the conditions for maximum resolution have to be fulfilled. Sulphur-35 is suitable because of its soft radiation. Thin sections avoid spreading of the ARGs and, being almost a single cell layer, minimise the overlapping of different ARGs (it will be seen that the thinnest sections gave the best resolution). Proper stretching of the film on water ensures its maximum thinness after drying. Careful handling and storage in the cold for exposure keep the background low. A convenient grain density is obtained with short exposure and development times; the latter also controls grain size.

OBSERVATIONS

Methyl green-pyronin stain.—Our material gave the classical picture for this stain, i.e. cytoplasm and nucleolus bound the pyronin, chromatin the methyl green. The chromatin filled the greater part of the nucleus and patches of it were often condensed on the nucleolus, giving the impression of a shell; careful examination could not exclude the possibility that some of it may be contained inside the nucleolus.

Autoradiographs.—The individual cell ARGs of all tissues in embryos in stages 6, 7 and 8 were studied. In all tissues the ARGs showed an essentially similar localization of the tracer inside the cell (Figs. 1–5).

The *cytoplasm* was always active. Sometimes there were indications of tracer concentrated on the cell wall. Frequently the cytoplasm close to the nuclear membrane was quite active.

The *nucleolus* showed a great activity, though sometimes an inactive nucleolus was observed in a cell with active cytoplasm. The ARGs corresponded with either (*a*) the contour of the nucleolus, or (*b*) the whole nucleolus or (*c*) the contour and part of the body of the nucleolus. Clear ARGs of the nucleolus have been marked in the figures with an arrow; typical instances of the three types have been labelled with a circle (*a*), a solid circle (*b*) and a half-solid circle (*c*). A considerable activity was present in the *chromatin associated with the nucleolus.* On occasion the contour ARGs definitely corresponded with the shell of chromatin around the nucleolus. As can be seen in the figures, a "lump" of high activity was frequently attached to the nucleolus; we presumed that this activity corresponded with chromatin near the nucleolus.

The ARGs were interpreted as indicating that tracer was definitely present in the periphery (*a*) and probably sometimes in the entire nucleolus (*b*). The alternative view that the activity was only peripheral to the nucleolus, i.e. in the chromatin, could not be excluded. For example, ARGs of type *b* could be produced either by a nucleolus active throughout its whole mass or

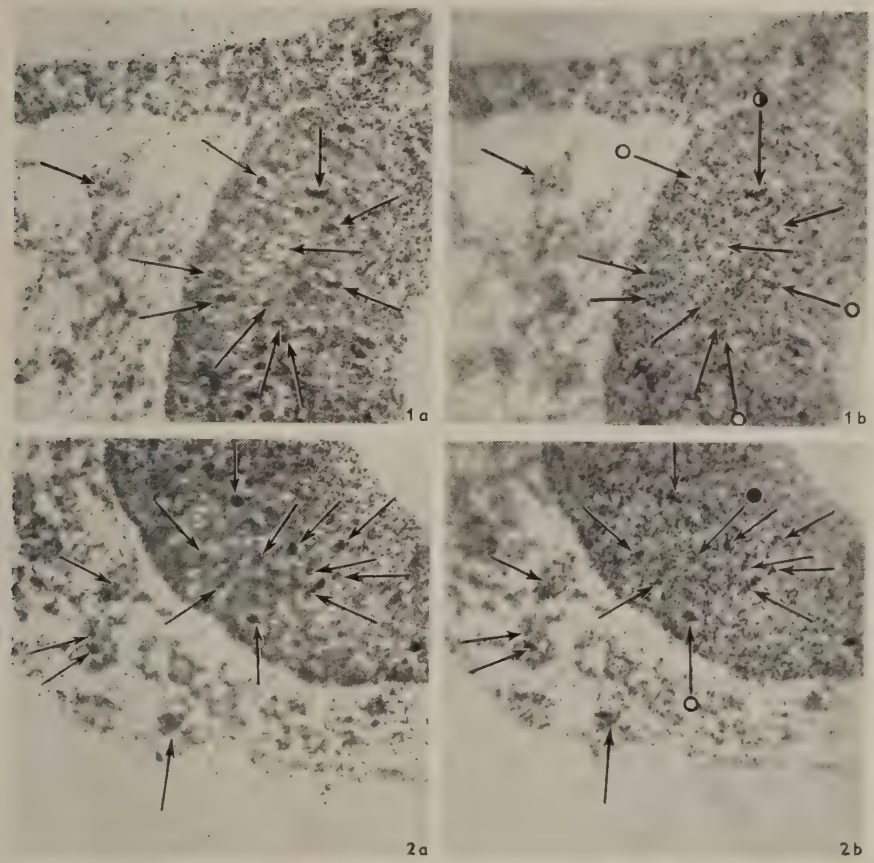

All sections are of embryos in stage 8, 2.5 μ thick and stained with methyl green-pyronin. Photographs were taken under phase contrast. In the centre of Figs. 1 a, 2 a, 3 a, 4 a and 5 a the focus is on the section, in the centre of Figs. 1 b, 2 b, 3 b, 4 b and 5 b the focus is on the corresponding ARGs. In the periphery of the photographs the focus is slightly higher than in the centre owing to optical aberration. Thus, for example, the ARGs of ectoderm and mesoderm are readable in Fig. 1 a, those of the neural fold in Fig. 1 b. For explanation and symbols see text. Photographs in Figs. 1, 2 and 4, × 700; in Figs. 3 and 5, × 1100.

Figs. 1 a and 1 b. Neural fold (right), ectoderm (above) and mesoderm, at a level anterior to the somites.

Figs. 2 a and 2 b. Neural fold (right) and mesoderm. Same section as in Fig. 1.

by a layer of active chromatin included in the sectional plug containing the nucleolus. Sections 5 μ thick offered the same picture as those 2.5 μ thick, but with impaired resolution.

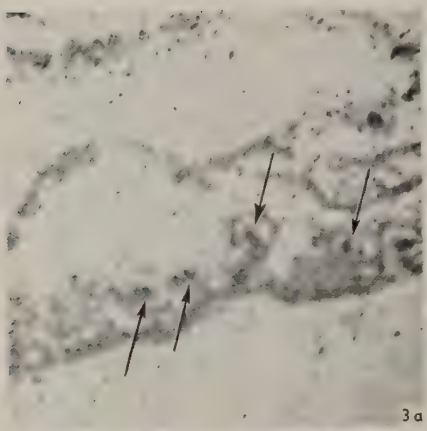
3a

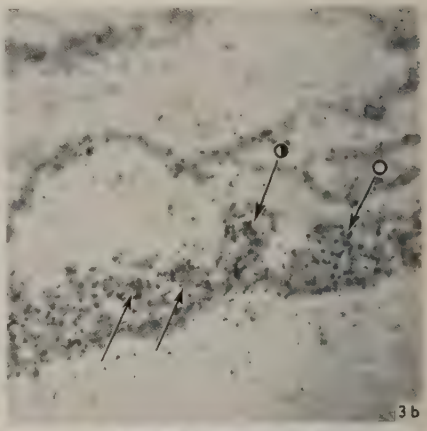
3b

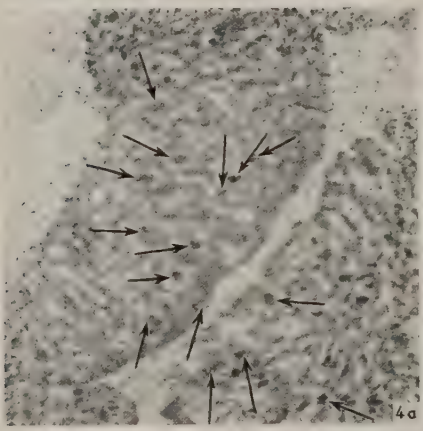
4a

4b

5a

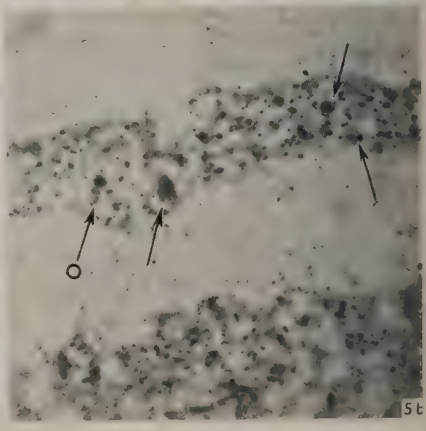
5b

The *nucleus*, apart from the chromatin associated with the nucleolus, showed variable activity, generally less than the cytoplasm and nucleolus. Sets of *chromosomes* showed no, or variable, activity.

It seemed likely that in all tissues the activities of the cell components were positively correlated, in the sense that they tended all to be higher or lower, according to the tissue. We compared in photographs the ARGs of cells in some different tissues. To minimize any effect of the photographic reproduction (because of different exposures, etc.), comparisons were confined to tissues within a single field. The lower activity of mesoderm compared with ectoderm, and of ectoderm compared with neural fold, visible in Fig. 1, is probably determined mainly by the lesser aggregation of cells (mesoderm < ectoderm < neural fold). Probably the activity of the individual cells is approximately similar in the three tissues. Fig. 2 permits the same comparison between mesoderm and neural fold. Conversely, in Fig. 4 it seems likely, though it is not quite obvious, that the lesser activity of the somite as compared with the neural folds is due to a lesser activity of the cells in the somite, the cell density being similar in both tissues. Fig. 3 shows that the lesser activity of the lateral mesoderm compared with the endoderm is accounted for by the lesser activity of the mesodermal cells.

DISCUSSION

The sections from which our autoradiographs were prepared contain all the materials rendered insoluble by Carnoy. This includes most of the cell proteins, though there may be some loss of albumin [24]. It is probable that the sulphur-35 is incorporated in the whole range of proteins present in the cells, and some may also be taken into glutathione attached to protein (for the gradient of SH groups in the chick embryo, see [3, 5 a, 23]). It should be noted that the tracer used contained both D- and L-methionine, and it is uncertain whether the chick embryo utilises the former, although the rat does [cf. 17].

Our observations point to three loci of intense protein metabolism in the cell: the cytoplasm, the nucleolus, and the chromatin associated with the nucleolus. The uptake into proteins of the *cytoplasm* is now accepted as of general occurrence in investigations using biochemical or autoradiography

---

Figs. 3 a and 3 b. Endoderm (below), splanchnopleure (middle) and somatopleure (above). Section at approximately same level as Fig. 1.
Figs. 4 a and 4 b. Neural fold (left) and somite.
Figs. 5 a and 5 b. Ectoderm (above) and lateral mesoderm, at the level of the primitive streak.

techniques [cf. 5; 31]. We found that activity was very evident close to the nuclear membrane, and possibly, too, near the cell wall. These findings agree with the abundance of nucleoprotein complexes near the nuclear membrane, shown spectrophotometrically [6], and with substantially the same results, together with some localization near the cell wall, obtained with the use of dyes [3]. In our experiments, however, we cannot decide at present how significant the incorporation on the cell wall is for cell synthesis; some tracer may be bound to the intercellular matrix.

Apart from the chromatin near the nucleolus, we found a rather moderate activity in the *nucleus*. Though in earlier biochemical research the activity of the nuclear protein appeared similar to that of the cytoplasmic protein (in several tissues of the rat [8, 28]), in later autoradiographical work it appeared higher (in oocytes [12, 14, 15], in other cells [13, 16, 25]). The discrepancies in activity of the protein of liver nuclei found in earlier biochemical and in later autoradiographical work can be explained by losses incurred during isolation of the nuclei in the biochemical work [cf. 9; 16]. In some of the previous autoradiographical work the activity of the nucleolus was not clearly distinguished from that of the chromatin; in none of it, was the activity of the chromatin associated with the nucleolus resolved from that of the remaining chromatin. This imprecision leads to overestimation of the activity in the remaining chromatin at the expense of that in the nucleolus and associated chromatin. However, in a recent study of RNA metabolism in *Drosophila* larval cells, the activity of the nucleolus and its associated chromatin was definitely higher than that of the remaining chromatin [31].

In support of our observations on the high activity of the *nucleolus and associated chromatin*, it has been found that RNA-associated protein in the liver nucleus had a marked incorporation [28]; this was confirmed for the thymus nucleus, where the DNA-associated protein showed still higher incorporation [2]. In the nucleus of *Acetabularia* the greatest amount of RNA-P-32 was incorporated in the nucleolus [29], but the procedure followed could not exclude some chromatin attached to the isolated nucleoli used for activity determinations. Our observations also confirm previous autoradiographical work, some examples of which follow. A constant great activity was found in the nucleolar protein and nucleic acids of various types of cells [12, 13, 14, 15, 16]; as pointed out before, some of the activity may actually have been in the nucleolus-associated chromatin. In mouse oocytes the incorporation of phosphorus-32 into RNA was higher in the nucleolus than in the nucleus, and was sometimes on the "nucleolar membrane" [22]; in the same material, using several tracers, the activity was found to be

higher in the nucleolus and associated chromatin than in the remaining chromatin (R. G. Edwards and J. L. Sirlin, unpublished). After our work had been completed, a careful description of the pattern of incorporation of RNA-P-32 in larval cells of *Drosophila* has appeared: it was found that the incorporation started in the chromatin near the nucleolus and proceeded through the periphery to the whole body of the nucleolus, the incorporation in the cytoplasm increasing gradually at the same time [31]. These observations strongly suggest that our ARGs can be regarded as showing a similar trend of events during protein synthesis. This is made the more likely because of the close relationship existing between RNA and protein synthesis [5]. They also support the view that there is at times a true internal activity of the nucleolus; the high, uniform protein content of the nucleolus [32] is another argument in favour of that view.

In this paper we have included under the name of "nucleolus-associated chromatin" (after Caspersson) both the lumps of chromatin attached to the nucleolus, which show considerable activity, and that in the whole perinucleolar shell. In many kinds of cells similar structures have been recognised with the use of methyl green [21], the Feulgen test and ultra-violet microscopy [cf. 10]; in particular, one description of the shell [7, p. 150] clearly resembles ours. Currently this structure is regarded as rich in DNA or, more precisely, high-polymer nucleic acid [cf. 30]. Its important role in protein metabolism [6] is confirmed by the present study. Whether to consider the shell the outer part of, or external to, the nucleolus becomes rather a semantic issue, since the nucleolus seems to possess no limiting membrane [32]; in any case, according to our observations and those made by others, possibly some of it is within the nucleolus. This shell is also present in cells of the amphibian neurula (J. L. Sirlin, unpublished).

The predominant protein metabolism in the nucleolus, in the associated chromatin and in the cytoplasm, especially around the nuclear membrane, suggests a functional system that comes remarkably close to that proposed by Caspersson [6]. The uniform pattern of intracellular activity in all the tissues of the embryo, together with the correlation in activity shown by the cell components, are in accordance with Caspersson's view of a protein metabolism common to all actively growing cells; in point of fact, his material was also the chick embryo at slightly later stages of development [7]. Unpublished work in the amphibian (J. L. Sirlin) and in the early mouse embryo (R. G. Edwards and J. L. Sirlin) indicates a distribution of intracellular activity essentially similar to that in the chick. In earlier stages (pregastrula) of the amphibian embryo no nucleolus is present, and it is probably

significant that massive incorporation begins only at about the stage at which the nucleoli first appear; it occurs in the nuclei, but its relation to the developing nucleoli needs further investigation [25, 27].

Our comparisons of the total activity of tissues confirm some data of Feldman and Waddington [11]. In Fig. 1 the order of activity of the tissues (neural fold > ectoderm > mesoderm) is the same as they found for the same embryonic stage 8 (their Table 2A). In Fig. 4, the greater activity of the neural fold compared with the somite, coincides with what they described for stages 8 and 8–9 (their Tables 2B and 3B).

The distribution of the protein-bound SH groups in the chick embryo has been described by Buño [5a] using the nitroprusside reaction. At somite stages, he found a medio-lateral gradient, with a peak on the embryonic axis, which corresponds in general with the conditions found by Feldman and Waddington [11] for protein-bound S-35. At the head process stage, he describes a consistent negative reaction in the notochord and adjacent mesoderm, although there was little possibility that the reagent had failed to penetrate to these tissues. Feldman and Waddington showed that the protein-bound S-35 decreases in the notochordal cells after their invagination to about the same level as that in the nearby mesoderm, which is about half that of the overlying neural plate. Since the neural plate shows a clear positive reaction to nitroprusside, it seems difficult to explainthe completely negative reaction of the notochord and adjacent mesoderm solely by a lower sulphur content. It may be case of refractoriness of the reaction, or, perhaps, it might be due to a low content of cysteine. If the latter suggestion is the explanation, the ARGs of these tissues must have mainly detected S-35 from methionine and/or cystine.

A high incorporation in the axial organs occurs both in the chick and in the amphibian embryo (for references to the chick, cf. [11]; for Amphibia, cf. [33] and see also [20]). It seems likely that this is related to cell differentiation. In the amphibian embryo the incorporation of amino acids begins first and proceeds most rapidly in the nuclei of the axial organs [25, 27]. Later in development the uptake was highest in the epidermis [33]. This seemed rather unexpected; but it should be remembered that in Amphibia the epidermis differentiates very early into a regulative and ciliated covering for the embryo.

In view of our results it seems possible that high-resolution autoradiography may permit the identification of grafts consisting of only a few labelled cells, thus widening the scope of the method originally introduced for the chick embryo [1]. For instance, accuracy would be gained by substituting labelled

grafts for the less dependable classical markers, such as vital dyes and carbon particles, in the mapping of morphogenetic movements. This has already been shown in the amphibian embryo [26].

SUMMARY

Labelling of cell proteins in the early chick embryo was studied by means of high-resolution autoradiography. Three loci of intense protein synthesis were apparent in the cell: the nucleolus, the chromatin associated with the nucleolus, and the cytoplasm. The results are discussed in connection with the related literature.

We are pleased to thank Miss M. M. Perry for her very efficient technical assistance. The work was carried out under a grant from the British Empire Cancer Campaign to one of us (J. L. S.); it also received financial help from the Agricultural Research Council.

REFERENCES

1. Abercrombie, M. and Causey, G., *Nature* **166**, 229 (1950).
2. Allfrey, V. G., Mirsky, A. E., and Osawa, S., *Nature* **176**, 1042 (1955).
3. Brachet, J., Embryologie Chimique. Desoer, Liège, 1947.
4. —— *Quart. J. Microscop. Sci.* **94**, 1 (1953).
5. —— The Nucleic Acids **2**, 476, 1955.
5 a. Buño, W., *Anat. Rec.* **111**, 123 (1951).
6. Caspersson, T., Cell Growth and Cell Function. Norton, New York, 1950.
7. Caspersson, T. and Thorell, B., *Chromosoma* **2**, 132 (1941–44).
8. Daly, M. M., Allfrey, V. G., and Mirsky, A. E., *J. Gen. Physiol.* **36**, 173 (1952).
9. Dounce, A. L., *Internatl. Rev. Cytology* **3**, 199 (1954).
10. —— The Nucleic Acids **2**, 93, 1955.
11. Feldman, M. and Waddington, C. H., *J. Embryol. Exptl. Morphol.* **3**, 44 (1955).
12. Ficq, A., *Experientia* **9**, 377 (1953).
13. —— *J. Embryol. Exptl. Morphol.* **2**, 194 (1954).
14. —— *Arch. Biol.* **66**, 509 (1955).
15. —— *Exptl. Cell Research* **9**, 286 (1955).
16. Ficq, A. and Errera, M., *Biochim. et Biophys. Acta* **16**, 45 (1955).
17. Greenstein, J. P., *Advances in Protein Chemistry* **9**, 122 (1954).
18. Gude, W. D., Upton, A. C., and Odell, Jr., T. T., *Stain Technol.* **30**, 161 (1955).
19. Hamburger, V. and Hamilton, H. L., *J. Morphol.* **88**, 59 (1951).
20. Hansborough, L. A. and Denny, D., *Proc. Soc. Exptl. Biol. Med.* **78**, 437 (1951).
21. Kurnick, N. B., *Stain Technol.* **27**, 233 (1952).
22. Odeblad, E. and Magnusson, G., *Acta Endocrinol.* **17**, 290 (1954).
23. Rulon, O., *Protoplasma* **24**, 346 (1935).
24. Sandritter, W. and Hartleib, J., *Experientia* **11**, 313 (1955).
25. Sirlin, J. L., *Experientia* **11**, 112 (1955).
26. —— *Arch. Entwicklungsmech.* **148**, 489 (1956).
27. Sirlin, J. L. and Waddington, C. H., *Nature* **174**, 309 (1954).
28. Smellie, R. M. S., McIndoe, W. M., and Davidson, J. N., *Biochim. et Biophys. Acta* **11**, 559 (1953).
29. Stich, H. and Hämmerling, J., *Z. Naturforsch.* **8 b**, 329 (1953).
30. Swift, H., The Nucleic Acids **2**, 51, 1955.
31. Taylor, J. H., McMaster, R. D., and Caluya, M. F., *Exptl. Cell Research* **9**, 460 (1955).
32. Vincent, W. S., *Internatl. Revue Cytology* **4**, 269 (1955).
33. Waddington, C. H. and Sirlin, J. L., *J. Embryol. Exptl. Morphol.* **2**, 340 (1954).

BRIEF NOTES

CYTOCHEMICAL REACTIONS OF NORMAL AND STARVING *AMOEBA PROTEUS*

II. LOCALIZATION OF MINERALS

IDA M. HELLER[1,2] and M. J. KOPAC

Department of Biology, Graduate School of Arts and Science, New York University, New York, N.Y., U.S.A.

Received May 2, 1956

Several minerals have been studied in normal and starved amoebas by cytochemical means. The results from this work confirm and extend the results obtained in previous work in which the microincinerative method was used for mineral localization [6].

Materials and Methods.—The manner of handling, e.g., culturing, embedding of the normal and starved amoebas, has been described [5]. The fixative used in the following cytochemical procedures, unless otherwise indicated, consisted of 1 part neutral formalin and 9 parts absolute ethanol. Paraffin sections were cut at 4 μ.

Magnesium. Sections and whole mounts of normal amoebas as well as whole mounts of amoebas starved for 1, 9, and 19 days were stained according to the Broda procedure [1].

Calcium.—The Rabl test [12] for soluble calcium was applied to living unstarved amoebas as well as to amoebas starved for 1, 7, 20, and 22 days. The amoebas were fixed in a mixture of equal parts of 4 per cent ammonium oxalate and 25 per cent neutral formalin. A positive test is indicated by the appearance of calcium oxalate crystals in the specimen.

The Manigault modification [9] of the Crétin test [3] for the localization of calcium salts was applied to whole mounts of normal amoebas.

Iron.—Sectioned and whole mount amoebas were tested for inorganic iron by the Turnbull blue method [8], as well as by the Prussian blue method [2]. For these tests, some amoebas were fixed in 10 per cent aqueous formalin, buffered at pH 7, and the others with the alcoholic fixative described above.

For the demonstration of organic iron, sections and whole mounts were first hydrolyzed in 4 per cent sulfuric acid in 95 per cent ethanol for 24 to 36 hours at

[1] Work carried on as a Predoctoral Fellow of the National Cancer Institute, National Institutes of Health, Federal Security Agency.

[2] Present address, Department of Surgery, New York University Post-Graduate Medical School, 550 First Ave., New York 16, N.Y.

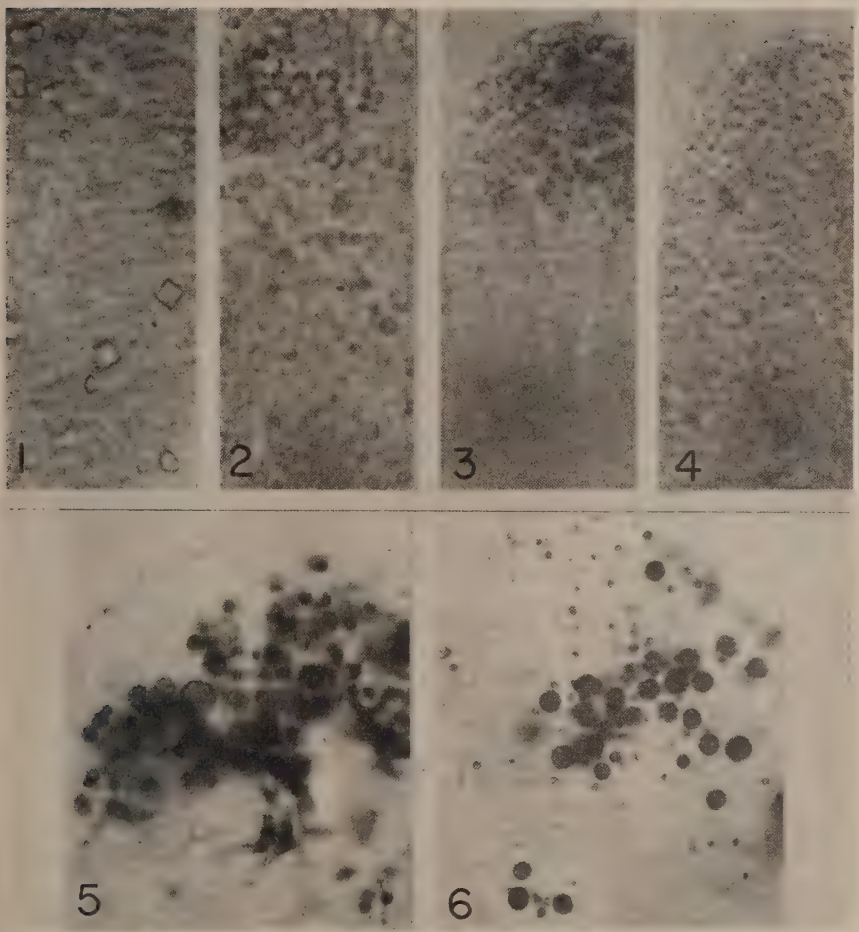

Fig. 1. Portion of the cytoplasm of a whole mount amoeba which had been fixed in Rabl's solution. Note the large calcium oxalate crystals. Approx. × 600.
Fig. 2. Portion of the cytoplasm of a whole mount amoeba which had been centrifuged prior to fixation in 25 per cent neutral formalin. Note the appearance of the many round refractive bodies. Approx. × 600.
Fig. 3. Centrifugal end of a whole mount amoeba which was fixed for 24 hours in Rabl's solution. Note the numerous small crystals of calcium oxalate. Approx. × 600.
Fig. 4. Centrifugal end of the same amoeba as in Fig. 3, a short time after sulfuric acid was applied.
Fig. 5. Whole mount amoeba stratified prior to staining with Quinalizarin, showing a concentration of deeply staining refractive bodies in the centrifugal end. Note particularly the darkly staining core and paler annulus seen in many of the refractive bodies. Wrattan filter no. 58. Approx. × 800.
Fig. 6. Whole mount amoebas treated with Titan yellow. Note the similarity between the appearance of these refractive bodies to those seen in the above figure. Wrattan filter no. 58. Approx. × 800.

35°C and then treated with either the Prussian blue reagent for 5 minutes [8], or with a freshly prepared solution of equal volumes of 1.5 per cent potassium ferrocyanide and 0.5 per cent hydrochloric acid [4].

As a check on the reactivity of the reagents, sections of rat liver and spleen were included in each series.

Zinc.—The Mendel and Bradley method [11] was applied to sections and whole mounts of normal amoebas as well as to whole mounts of amoebas starved for 1, 9, 17, and 19 days. A purple color indicates zinc and possibly copper.

Copper. The Waterhouse method [13] for the detection of copper was tested on both living and whole mount normal amoebas, as well as on whole mounts of amoebas which had been starved for 1, 9, and 20 days.

Results. Spot tests were carried out to determine whether the three dyes of the Broda test, Quinalizarin, Azo blue, and Titan yellow, specifically demonstrate magnesium. It was observed that magnesium chloride formed solid colored precipitates with all three of the alkalinized dyes, while calcium chloride formed flocculent precipitates. The color reactions of calcium and magnesium to Azo blue and Quinalizarin were practically indistinguishable. With alkalinized Titan yellow, the magnesium precipitate was bright red, and that of calcium pink and yellow. When these dyes were tested on filter paper previously impregnated with calcium or magnesium chlorides, again only the Titan yellow adequately distinguished between the two.

The Titan yellow applied to sections and whole mounts produced an orange color in the cytoplasm and a deeper orange color in the nucleus and food vacuoles. The refractive bodies were seen to have a bright red core surrounded by a paler annulus (Fig. 6). Amoebas stained with Quinalizarin or Azo blue display the same pattern of color distribution in the refractive bodies (Fig. 5). Amoebas which had been starved for varying lengths of time prior to testing with the Broda stains showed no appreciable difference relative to each other or to the normal controls.

Precipitated calcium oxalate was observed in amoebas treated with Rabl's mixture (Fig. 1). The major portion of the calcium oxalate appears to be due to the calcium derived from the refractive bodies. On application of the reagent most of the refractive bodies disappear and calcium oxalate crystals appear. In amoebas stratified prior to fixation in Rabl's mixture, the calcium oxalate crystals can be seen in the centrifugal end where the refractive bodies are normally found (cf. Figs. 2 and 3). The crystals were identified as calcium oxalate by their crystalline form and by their solubility. They are soluble in 2 per cent sulfuric acid (Fig. 4) and insoluble in 20 per cent acetic acid. Mast and Doyle [10] reported the refractive bodies to be soluble in 20 per cent acetic acid.

No significant differences in the occurrence or number of calcium oxalate crystals were noted between amoebas starved for 1, 7, 20, and 22 days, nor between them and the unstarved amoebas.

Application of the modified Crétin test to the centrifuged normal whole mounts [5] indicated the centrifugal end to be pinkish-brown in some or bluish or greenish-brown in others. The alkalinity of the reagent caused disruption and possibly a partial dissolution of the refractive bodies. A few intact refractive bodies were seen; of these, several contained a darkly colored pinkish or bluish interior with a paler annulus. With this reagent, a positive reaction for calcium is indicated by a blue

color; and a positive reaction for magnesium by a yellow-rose color. Several other minerals as well, react giving individual color reactions. The observed coloration is not pure and therefore indicates a mixture of several reactive minerals in the fluid interior of the refractive body.

No iron, either free or organically bound was demonstrated in normal amoebas by the procedures applied. Negative results were obtained as well for normal and starved amoebas tested for copper and zinc.

Discussion.—Previous work involving microincineration [6] indicated a high concentration of minerals, possibly calcium and magnesium to be associated with the refractive bodies of *Amoeba proteus*. The cytochemical studies reported here confirm and further define this association. It was demonstrated that the calcium and magnesium are localized primarily in the innermost portion or core of the refractive body. Other minerals in lower concentrations may be present as well. The minerals are in a highly reactive form.

The failure to demonstrate zinc and copper in the amoebas is not a surprising result. The total amount of each in the amoeba is probably low. The tests used are not highly sensitive. These procedures were used in spite of this consideration because of the anticipation that these minerals might be concentrated in or on some inclusion. As indicated, this is not so. The absence of cytochemically detectible iron is in agreement with the negative results for iron in microincinerative studies [6].

Summary.—Cytochemical methods of mineral localization were applied to normal and starved *Amoeba proteus*. Neither iron, zinc, nor copper could be demonstrated by the procedures used. The concentration of these minerals is apparently below the sensitivity limits of the applied tests. Magnesium and calcium, presumably in their ionized form, were found to be concentrated in the fluid core of the refractive bodies.

REFERENCES

1. Broda, B., *Mikrokosmos* **32**, 184 (1939).
2. Bunting, H., *Stain Technol.* **24**, 109 (1949).
3. Crétin, A., *Bull. histol. appl. physiol. et pathol. et techn. microscop.* **1**, 125 (1924).
4. Glick, D., Techniques of Histo- and Cytochemistry. Interscience Publishers, Inc., New York, 1949.
5. Heller, I. M. and Kopac, M. J., *Exptl. Cell Research* **8**, 62 (1955).
6. —— *Exptl. Cell Research* **8**, 563 (1955).
7. Langeron, M., Précis de Microscopie. Masson et C^{ie}, Éditeurs, Paris, 1949.
8. Lison, L., Histochimie Animale. Gauthier-Villars, Éditeur, Paris, 1936.
9. Manigault, P., *Ann. inst. oceanog.* **18**, 385 (1939). (*Vide*, Langeron, 1949.)
10. Mast, S. O. and Doyle, W. L., *Arch. Protistenk.* **86**, 155 (1935).
11. Mendel, L. B. and Bradley, H. C., *Am. J. Physiol.* **14**, 313 (1905).
12. Rabl, C. H. R., *Klin. Wochschr.* **5**, 365 (1926). (*Vide* Lison, 1936.)
13. Waterhouse, D. F., *Council for Scientific and Industrial Research, Commonwealth of Australia, Melbourne Bull.* no. 191, 7 (1945).

ÜBER ENZYMSYSTEME DES AMINOSÄURE-ABBAUS IN GEWEBEKULTUREN

L. STOCKINGER, G. KELLNER, E. BRODA, H. PERSCHKE und O. HOFFMANN-OSTENHOF

Histologisch-Embryologisches Institut und Erstes Chemisches Laboratorium der Universität Wien, Österreich

Eingegangen am 12. Mai 1956

In früheren Veröffentlichungen aus unseren Laboratorien [4, 7, 8] berichteten wir über ein Verfahren zur Untersuchung des oxydativen Stoffwechsels von Gewebekulturen. Dieses beruht im wesentlichen darauf, daß man der Kultur Nährstoffe zusetzt, welche durch C^{14} markiert sind, und die Entstehung radioaktiven Kohlendioxyds mit Hilfe des Gas-Geiger-Zählrohrs [1] verfolgt. Auf diese Weise ließ sich u.a. nachweisen, daß die Gewebekulturen Enzymsysteme besitzen, welche Glucose, Mannose, Fructose und Glycerin zu Kohlendioxyd oxydieren können, während ein entsprechendes Enzymsystem zum oxydativen Abbau von Saccharose nicht vorhanden ist [4]. Wir haben auch gefunden, daß 1-^{14}C-Palmitinsäure $^{14}CO_2$ liefert (unveröffentlicht).

Wir wollen nunmehr über eine Versuchsreihe berichten, welche dazu dienen sollte, die Anwesenheit von spezifischen Enzymsystemen, die den oxydativen Abbau der Aminosäuren Glykokoll, Alanin und Tyrosin katalysieren, in den Gewebekulturen nachzuweisen. Es wurde mit embryonalen Hühnerfibroblasten (Extremitätenmesenchym) gearbeitet; die angewandte Methode wurde in der vorhergehenden Publikation [4] beschrieben. Die verwendeten Aminosäuren waren durchwegs an sämtlichen Kohlenstoffatomen markiert; sie wurden aus Harwell bezogen. In jedem Fall wurde auch die — relativ geringe — Erzeugung von $^{14}CO_2$ durch die Nährlösungen (ohne Gewebe) bestimmt (Blindwerte).

Die Ergebnisse dieser Versuchsserien sind in Tabelle I dargestellt. Wie man daraus ersehen kann, werden alle drei Aminosäuren — allerdings in verschiedenen Ausmaß - zu Kohlendioxyd abgebaut. Diesen Unterschieden wollen wir aber wegen des doch nur semiquantitativen Charakters unserer Methode weniger Bedeutung zumessen; der Zweck unserer Untersuchung war vor allem die Feststellung, ob ein geeignetes Enzymsystem für die Oxydation eines jeden Substrats überhaupt vorhanden ist.

Unsere Daten zeigen also eindeutig, daß die Gewebekulturen Enzymsysteme besitzen, welche den Abbau der genannten Aminosäuren in einer solchen Weise vollziehen, daß Kohlendioxyd entsteht. Über den Weg dieses Abbaus läßt sich aber auf Grund unserer Ergebnisse noch wenig aussagen: es wäre denkbar, daß es sich um eine einfache Decarboxylierung handelt, welche durch Enzyme katalysiert wird, die als Aminosäure-Decarboxylasen klassifiziert werden müßten. Als wahrscheinlicher muß allerdings angenommen werden, daß wir es in den hier besprochenen Fällen mit einem direkten oder indirekten oxydativen Abbau der Aminosäuren zu tun haben. Dies gilt vor allem für das Alanin, von dem man weiß, daß es im Gewebe

TABELLE I

Bildung von radioaktivem Kohlendioxyd aus markierten Aminosäuren in Gewebekulturen.

1	2	3	4	5	6	7
Versuch Nr.	Substrat	Eingesetzte Menge (μg)	Eingesetzte Aktivität (Stöße/Min)	Blindwert (Stöße/Min im CO_2)	Gewebeleistung (Stöße/Min im CO_2)	Mittlerer Umsatz (% der eingesetzten Aktivität im CO_2)
1 A, B, C	Alanin	1,2	$1{,}4 \times 10^5$	985	5280; 5450; 4400	2,9
2 A, B	Glykokoll	2,1	$1{,}54 \times 10^5$	118; 162	814; 645	0,38
3 A, B, C, D	Tyrosin	3,3	3×10^5	53; 74	138; 175; 172; 240	0,04
4 A, B, C	Tyrosin	2,0	$1{,}8 \times 10^5$	0; 0; 11	5; 12; 16	0,004

TABELLE II

Beschleunigung der Bildung von Kohlendioxyd aus Tyrosin durch L-Ascorbinsäure.

1	2	3	4	5
Versuch Nr.	Blindwert (Stöße/Min im CO_2)	Gewebeleistung mit 0,001 m Ascorbinsäure (Stöße/Min im CO_2)	Mittlerer Umsatz (% der eingesetzten Aktivität im CO_2)	Verhältnis des Umsatzes mit und ohne Ascorbinsäure
3 E, F, G	53; 74*	278; 370; 303	0,08	2
4 D, E, F	49; 42; 30**	85; 129; 90	0,04	10

* Ohne Zusatz von Ascorbinsäure.
** Mit Zusatz von 0,001 m Ascorbinsäure.

durch Transaminierung leicht in Brenztraubensäure überführt wird [6], welche dann der Oxydation über den Citronensäure-Zyklus anheimfällt. Weniger eindeutig ist der Fall des Glykokolls, wo einerseits eine direkte Oxydation und andrerseits ein Abbauweg über C_1-Übertragung in Betracht gezogen werden sollte. Zur Klärung dieser Frage sind Versuche über die beim Abbau des Glykokolls entstehenden C^{14}-markierten Zwischenprodukte geplant.

Beim Tyrosin, dessen Abbau allerdings nur sehr langsam erfolgt, glauben wir, daß ein zusätzlicher Befund eindeutig für einen oxydativen Abbau durch das Tyrosinoxydase-System, d.h. über *p*-Oxyphenylbrenztraubensäure und Homogentisinsäure [2], spricht. Wir konnten nämlich bei Zusatz von 0,001 m L-Ascorbinsäure zu einer Anzahl parallel gehaltener Kulturen der Serien 3 und 4 die Kohlendioxyd-Ausbete aus Tyrosin wesentlich erhöhen (Tabelle II). Die L-Ascorbinsäure

spielt bei einem Teilenzym des genannten Systems die Rolle eines Cofaktors [3, 5]. Daß die Steigerung in den beiden Versuchsserien in ungleichem Maß erfolgt, darf insofern nicht Wunder nehmen, als über den ursprünglichen Ascorbinsäuregehalt der Nährlösungen nichts bekannt ist; er mag unterschiedlich gewesen sein.

Die Untersuchungen wurden durch eine Subvention des Jane Coffin Childs Memorial Fund for Medical Research, dem wir unseren Dank aussprechen, wesentlich gefördert.

LITERATUR

1. Broda, E. und Rohringer, G., *Z. Elektrochem.* **58**, 634 (1954).
2. Knox, W. E., *in* W. D. Elroy und B. Glass, Amino Acid Metabolism. S. 836. Baltimore, 1955.
3. Painter, H. A. und Silva, S. S., *Biochem. J.* **46**, 542 (1950).
4. Perschke, H., Broda, E., Hoffmann-Ostenhof, O., Stockinger, L., Enzl, H., und Kellner, G., *Monatsh. Chem.* **87**, 235 (1956).
5. Rienits, K. G., *J. Biol. Chem.* **182**, 11 (1950).
6. Still, J. L., Buell, M. V., und Green, D. E., *Arch. Biochem.* **26**, 413 (1950).
7. Stockinger, L., Enzl, H., Broda, E., Suschny, O., und Sverak, L., *Monatsh. Chem.* **85**, 327 (1954).
8. Sverak, L., Suschny, O., Manner, G., Stark, R., Stockinger, L., und Enzl, H., *Monatsh. Chem.* **86**, 124 (1955).

EFFECT OF X-RAYS ON MITOCHONDRIAL DESOXYRIBONUCLEASE II

S. OKADA and E. KALLEE

Department of Experimental Radiology, University of Rochester School of Medicine and Dentistry, Rochester, N.Y., U.S.A.

Received May 17, 1956

The present investigation dealing with the effect of X-rays on desoxyribonuclease II (DNase II) in isolated mitochondria[1] was initiated in an attempt to elucidate the mechanism underlying the increase in DNase II activity per mg of radiosensitive tissues observed in X-irradiated rats [3, 6].

Mitochondria were isolated from rat liver by the method of Kay *et al.* [4] and suspended in 15 per cent sucrose solution. Determination of DNase II was carried out by a method which combined the essential features of two previously published procedures [1, 5] with slight modifications. The buffer solution used by Kowlessar *et al.* [5] was made up with 15 per cent sucrose instead of distilled water. Since this interferes with the Dische diphenylamine reaction, the products of depolymerization of desoxyribonucleic acid (DNA) by DNase II were estimated by means of their optical absorption at 300 mμ [7]. All enzyme determinations were carried out at

[1] The term "mitochondria", as used in this paper, includes the cytoplasmic granules which have been named "lyosomes" by de Duve *et al.* [2]. The latter group of investigators have claimed that DNase II was contained largely in this lyosome fraction.

levels of mitochondrial concentrations which yielded optical density readings within the range of 0.0–0.9.

Mitochondria were prepared from 2.8–0.9 g of rat liver and suspended in 10 ml of 15 per cent sucrose. Some aliquots of untreated mitochondria were set aside for assay, whereas others were placed in a 25-ml Erlenmayer flask and exposed to varying doses of X-rays at room temperature. The X-rays used in these experiments had the following characteristics: 2530 roentgens per minute, 200 K.V.P. (20 ma., no filtration and target-to-sample distance, 7–8 cm).

After irradiation, one portion of the mitochondrial suspension was subjected to sonic vibrations (9 Kc.) followed by DNase II assay, whereas the other portion was assayed without prior sonic vibration. A third portion of the irradiated mitochondria also untreated by sonic vibration was centrifuged at 10,000 *g* in a Serval SS Centrifuge and the supernatant phase was retained for enzyme assay.

TABLE I

Effect of X-rays on mitochondrial DNase II activity.

Dose of X-rays (r)	Per cent change in DNase activity* Mitochondria	
	After X-ray treatment	After X-ray and sonic** treatment
0	100	100
25,300	107—27	95—5
50,600	108—8	108—15
101,200	124—19	101—12
126,500	136—9	99—18

* Per cent change in DNase activity: $\frac{\text{DNase II activity of irradiated mitochondria}}{\text{DNase II activity of non-irradiated mitochondria}} \times 100.$

** The DNase activity of mitochondria after sonic treatment was approximately five times greater than before treatment. All DNase activities were determined after approximately five hours of aging at room temperature.

It is evident from data presented in Table I that irradiated mitochondria suspended in 15 per cent sucrose have a higher activity of DNase II than do non-irradiated mitochondria. Exposure of mitochondria to sonic vibrations alone increased DNase II activity approximately five-fold as compared with non-treated mitochondria; prior X-irradiation does not produce a further increase in the enzymatic activity of the mitochondria so treated with sonic vibration. The supernatant fluid obtained from the third portion of the irradiated and centrifuged mitochondrial suspension did not show an increase in DNase II activity.

This suggests that the "structural" damage inflicted upon mitochondria by high doses of X-rays did not release the enzyme into the suspending fluid; rather, it allowed more enzyme molecules to have access to the substrate, probably as a result of fragmentation or disruption of the subcellular particulates. The results indicate that the DNase II activity is not readily dissociated from fragments of disintegrated or radiation-damaged mitochondria. Apparent "structural" damage of subcellular

particulates of this type induced by X-rays may be an important factor in "amplifying" the biochemical effects noted in radiation-injured cells at various time intervals subsequent to the primary action of the radiation.

REFERENCES

1. Allfrey, V. and Mirsky, A. E., *J. Gen. Physiol.* **36**, 227 (1952).
2. De Duve, C., Pressman, B. C., Gianetto, R., Wattiaux, R., and Appelmans, F., *Biochem. J.* **60**, 604 (1955).
3. Fellas, V. M., Meschan, I., Day, P. L., and Douglass, C. D., *Proc. Soc. Exptl. Biol. and Med.* **87**, 231 (1954).
4. Kay, E. R. M., Simmons, N. S., and Dounce, A. L., *J. Am. Chem. Soc.* **74**, 1742 (1952).
5. Kowlessar, O. D., Altman, K. I., and Hempelmann, L. H., *Arch. Biochem. and Biophys.* **52**, 362 (1954).
6. Okada, S., Gordon, E., King, R., and Hempelmann, L. H., unpublished data.
7. Schneider, W. C. and Hogeboom, G. H., *J. Biol. Chem.* **198**, 155 (1952).

THE SUBMICROSCOPIC STRUCTURE RESPONSIBLE FOR THE CYTOPLASMIC BASOPHILIA OF THE RAT SPERMATID[1]

Y. CLERMONT

Department of Anatomy, McGill University, Montreal, Canada

Received May 29, 1956

The basophilic material of the cytoplasm, classically referred to as ergastoplasm, is located in cytoplasmic areas where the electron microscope generally shows two types of structures: (1) membrane bound, elongated and often flattened cavities, described under the names: endoplasmic reticulum [15], α-cytomembranes [19] or even ergastoplasm [2, 20] and which will be referred to here as ergastoplasmic vesicles; (2) small, dense granules approximately 150 Å in diameter, which may or may not be associated with the vesicles and have been described under the names: small particulate component [13], Palade's granules [1] and will be referred to here as ergastoplasmic granules.

It was of interest to determine which one of these two components was the support of the ribonucleic acid responsible for cytoplasmic basophilia. Palade [13] who made observations on a variety of cells exhibiting faint to intense basophilia suggested that the small particulate component or ergastoplasmic granules correlated with basophilia better than the ergastoplasmic vesicles and thus were the likely support for the cytoplasmic RNA. Porter [17] also supported this view, while Bernhard *et al.* [1] felt that both the membranes of the vesicles and the granules contained RNA.

Using biochemical techniques, Littlefield *et al.* [11] and Palade and Siekevitz [16] isolated the ergastoplasmic granules from liver homogenate by centrifugation and found them to contain almost all the cytoplasmic RNA, whereas Kuff, Hogeboom

[1] This investigation was supported by the Anna Fuller Fund.

and Dalton [9] using a similar technique claimed that 26 per cent of the RNA was associated with the ergastoplasmic vesicles.

In the present investigation the problem was reexamined in an electron microscope study of the rat spermatid. The cytoplasm of these cells contains intensely basophilic as well as non-basophilic areas and therefore a comparison between the structural components of these two areas may be made within a single cell type.

The *distribution of RNA in the rat spermatids* has been investigated in sections treated with desoxyribonuclease and stained with pyronine or toluidine blue [5, 8]. The material stained under these conditions was considered to be RNA. The young spermatids (steps 1–7 of spermiogenesis in the classification of Leblond and Clermont [10]) display fine RNA-containing granules throughout the cytoplasm, except in the Golgi zone and associated structures (head cap, acrosome) which did not contain any. Later as the spermatids matured (steps 8–18), the RNA granules become increasingly coarse and stain more intensely. At steps 17 and 18, the RNA is gathered into circular or nearly circular globules in the caudal portion of the cytoplasm. Finally, after the spermatids transformed into spermatozoa (step 19) and discarded most of their cytoplasm, the cytoplasmic remnant, called "residual body", contained a few large masses of RNA-containing material with an irregular, ragged outline. Meanwhile, the Golgi zone, which by that time had been separated from the acrosome and head cap, remained free of RNA.

Examination of the spermatids with the electron microscope was used to decide whether or not the RNA rich globules and the RNA free Golgi zone contained ergastoplasmic vesicles and/or granules.

The structure of the cytoplasmic RNA-containing bodies of maturing spermatids as revealed by the electron microscope.—Small pieces of rat testis were fixed for one hour in 1 per cent buffered osmic acid [12] and embedded in *n*-butyl methacrylate. Sections were cut with the Porter–Blum microtome and examined with the RCA-EMU 2E electron microscope. The steps of development of the young spermatids was readily identified by the presence of the growing acrosomic system at the surface of their spherical nuclei. The identification of the older spermatids was made by reference to the younger ones as indicated elsewhere [10].

The cytoplasm in the older spermatids displayed aggregates of fine granular particulates. At steps 17–18, the outline of each aggregate was circular or almost circular, as is the case with the RNA-containing globules seen at that stage with the light microscope. In the residual bodies, similar aggregates were present, but displayed a ragged outline, as in the same structures observed with the light microscope. In both cases the aggregates were composed exclusively of granules with an average diameter of approximately 150 Å, which were thus identified as ergastoplasmic granules. No ergastoplasmic vesicles were present.

Structure of the Golgi zone of spermatids as revealed by the electron microscope.—The Golgi zone of the rat spermatids was found to be devoid of ergastoplasmic granules and to be composed of membranous structures, that is flat and spheroidal vesicles [4, 14], in agreement with observations made in cat spermatids [3] and other cell types [6]. The flat vesicles were parallel to one another and made up of stacks or piles of lamellar appearance (Fig. 2, FV). The resemblance which exists between the vesicular structures of the Golgi zone and those of the ergastoplasm suggested to Palade [14] that the Golgi zones might be merely a local differentiation of the ergasto-

plasmic vesicles. However, the flat vesicles found in the Golgi region are more closely packed than the ergastoplasmic vesicles and, in contrast to the latter, do not display ergastoplasmic granules along their outer surface.

Dalton and Felix [7] on the basis of the finding of Schneider and Kuff [18] who reported that the isolated Golgi zone of epididymal cells shows a threefold concentration of RNA over homogenate, suggested that the membranes of the Golgi vesicles are the likely site in which RNA is concentrated. This conclusion cannot apply to the rat spermatids, since the well limited Golgi zone of these cells showed no histochemically detectable RNA. In fact, the absence of RNA was attributed to the absence of ergastoplasmic granules.

Conclusion. —On examination of the cytoplasm of maturing spermatids of the rat under the electron microscope, the large, basophilic, RNA-containing globules are found to be made up exclusively of small granular particulates, 150 Å in diameter (ergastoplasmic granules). The non-basophilic, RNA-free Golgi zone on the other hand includes stacks of vesicles but no ergastoplasmic granules. It may be concluded that in rat spermatids the ergastoplasmic granules alone are responsible for the cytoplasmic basophilia indicative of the presence of ribonucleic acid.

REFERENCES

1. Bernhard, W., Gautier, A., and Rouiller, C., *Arch. Anat. microscop. Morphol. exptl.* **43**, 236 (1954).
2. Bernhard, W., Haguenau, F., Gautier, A., and Oberling, C., *Z. Zellforsch.* **37**, 281 (1952).
3. Burgos, M. H. and Fawcett, D. W., *J. Biophys. Biochem. Cytol.* **1**, 287 (1955).
4. Clermont, Y. and Haguenau, F., *Compt. Rend. Acad. Sci.* **241**, 708 (1955).
5. Daled, H. J., *Arch. Anat. microscop. Morphol. exptl.* **40**, 183 (1951).
6. Dalton, A. J. and Felix, M. D., *Am. J. Anat.* **94**, 171 (1954).
7. —— A study of the Golgi substance and ergastoplasm in a series of mammalian cell types. *Symposium on Fine Structures of Cells*, Interscience Publishers, Inc., New York, p. 274 (1955).
8. Daoust, R. and Clermont, Y., *Am. J. Anat.* **96**, 255 (1955).
9. Kuff, E. L., Hogeboom, G. H., and Dalton, A. J., *J. Biophys. Biochem. Cytol.* **2**, 33 (1956).
10. Leblond, C. P. and Clermont, Y., *Am. J. Anat.* **90**, 167 (1952).
11. Littlefield, J. W., Keller, E. B., Gross, J., and Zamecnik, P. C., *J. Biol. Chem.* **217**, 111 (1955).
12. Palade, G. E., *J. Exptl. Med.* **95**, 285 (1952).
13. —— *J. Biophys. Biochem. Cytol.* **1**, 59 (1955).
14. —— *ibid.* **1**, 567 (1955).
15. Palade, G. E. and Porter, K. R., *J. Exptl. Med.* **100**, 641 (1954).
16. Palade, G. E. and Siekevitz, P., *J. Biophys. Biochem. Cytol.* **2**, 171 (1956).
17. Porter, K. R., *Federation Proc.* **14**, 673 (1955).
18. Schneider, W. C. and Kuff, E. L., *Am. J. Anat.* **94**, 209 (1954).
19. Sjöstrand, F. S., *in* Pollister, A. W., Electron Microscopy of Cells and Tissues. Vol. III, New York (in press), 1956.
20. Weiss, J. M., *J. Exptl. Med.* **98**, 607 (1953).

Fig. 1. An aggregate of ergastoplasmic granules (EG) can be seen close to the tail (T) of a maturing spermatid. The position and the circular outline of this aggregate permitted its identification as an RNA-containing globule seen with the light microscope. × 28,500.

Fig. 2. Portion of the cytoplasm of a maturing spermatid showing a Golgi zone (GZ) in which only flat and spheroidal vesicles can be seen (V). Outside the Golgi zone small clumps of ergastoplasmic granules (EG) are present. Mitochondria (M) are also seen along the cell membrane (CM). × 20,000.

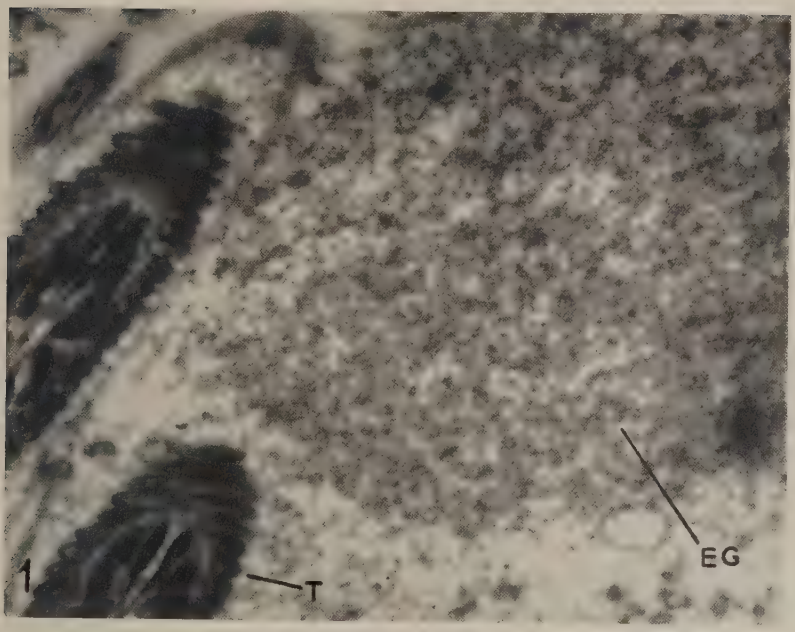
1
T
EG

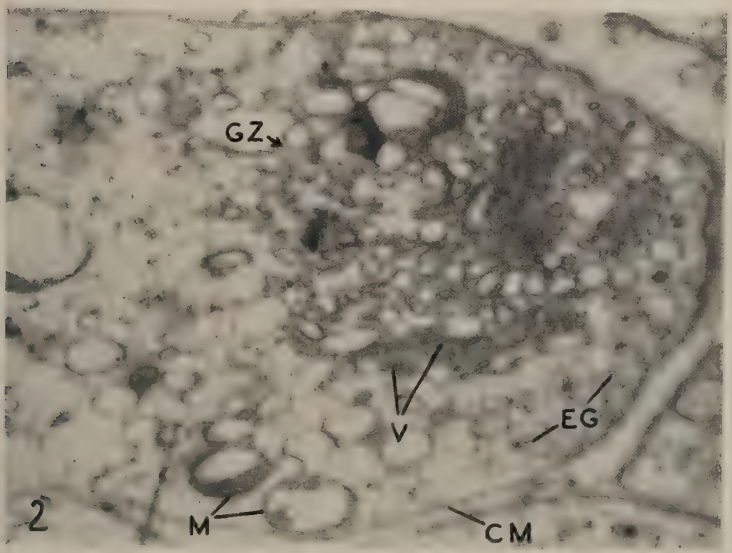
GZ
V
EG
2
M
CM

RADIATION-INDUCED FISSION BLOCK IN SYNCHRONIZED CULTURES OF *TETRAHYMENA PYRIFORMIS* W.[1]

H. S. DUCOFF

Division of Biological and Medical Research, Argonne National Laboratory, Lemont, Ill., U.S.A.

Received May 31, 1956

At doses of ionizing radiation which block division without killing appreciable numbers of cells, the synthesis of most cellular constituents continues unabated [1, 3, 4]. The one constituent whose synthesis is markedly inhibited is deoxyribose nucleic acid (DNA) [2, 4, 6]. These and similar findings have led to the concept that the radiation-induced division block is a result of an inhibition of DNA synthesis. On the other hand, it has been suggested that the inhibition of DNA synthesis is a direct result of the division block, and only a limited amount of new DNA can be synthesized in the absence of cell division.

An approximately fourfold increase in average DNA content has recently been reported in *Tetrahymena pyriformis* subjected to a series of temperature cycles [7], a treatment which permits both cytoplasmic and nuclear enlargement without division, and which results, on return to a constant "normal" temperature, in several successive synchronous divisions [5]. This finding suggests that division block alone does not necessarily result in inhibition of DNA synthesis, at least in this amicronucleate ciliate. It therefore became of interest to determine whether the accumulation of DNA by the organism alters its susceptibility to the division block induced by radiation.

Cultures of *T. pyriformis* W in 2 per cent proteose peptone supplemented with 0.1 per cent liver fraction L (PPL medium) were subjected to temperature cycling between 28° and 34°C for 10 to 16 hours, as described by Scherbaum and Zeuthen [5]. In eight experiments, 50 cc volumes of culture in 125 cc flasks were kept without aeration in a water bath whose temperature was controlled by two thermoregulators, a 600-watt heater, and a solenoid-operated cooling coil; in three experiments, an aerated volume of 600 cc was placed in a cold room, and the thermoregulators and a quartz heater were immersed directly in the culture medium. The best level of synchronization achieved was a fission index of 75 per cent, and 60 per cent was more usual.

Portions of the temperature-cycled cultures and of uncycled, exponentially growing cultures were exposed to 60 kr of X-rays (250 kV, 30 ma, Maxitron unit, hvl 7.0 mm Al). Irradiated and unirradiated portions were gently agitated by a magnetic stirrer during the exposure period, diluted four- to tenfold with fresh PPL medium, and incubated at 25°C. Samples were removed at intervals and fixed with two or three drops of Lugol's iodine for population and fission index determinations. Other portions of the cultures were centrifuged in the cold and resuspended in distilled water; after removal of aliquots for population determinations, trichloroacetic acid was added to give a final concentration of 5 per cent, and the DNA

[1] Work performed under the auspices of the U.S. Atomic Energy Commission.

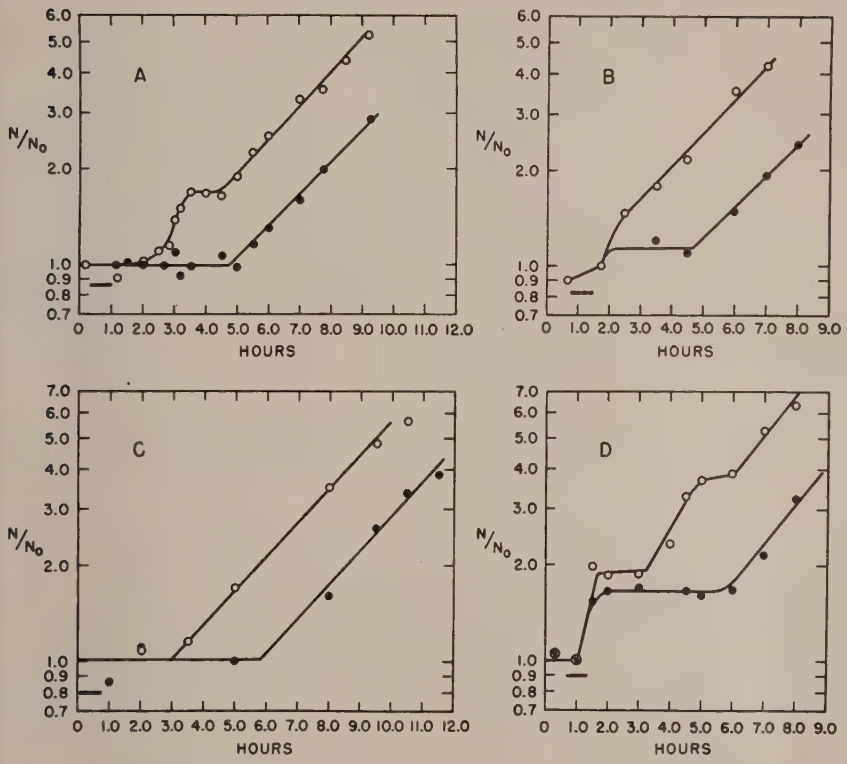

Fig. 1. The response of temperature-cycled and of exponentially growing populations of *Tetrahymena pyriformis* in Liver-Proteose peptone to 60,000 r of X-rays. Open circles—unirradiated groups; solid circles—irradiated groups. N/N_0 indicates animals per cc at given time divided by animals per cc during exposure. Solid bar shows time under X-ray beam; height (ordinate) of bar has no significance.

A, exposed before the first synchronous division; *B*, exposed after cycling, but with poor synchronization; *C*, exposed during exponential growth; *D*, exposed at time of first synchronous division.

was separated by a modified Schmidt–Thannhauser procedure. Relative DNA content was estimated on the basis of the ultraviolet absorption per million animals of a hot perchloric acid extract of the acid-precipitable fraction of the alkaline hydrolysate. In all experiments, even those in which a poor degree of synchronization was achieved, the marked increase in DNA per animal, found by microbiological assay [7], was confirmed.

When temperature-cycled cultures were irradiated before the first synchronous division (Fig. 1, *A*), between the first two synchronous divisions, or shortly after

cycling in cultures where the usual DNA increase had occurred but synchronization was poor (Fig. 1, *B*), radiation-induced division delay was the same—about one generation time or 2 $^{3}/_{4}$ to 3 hours in PPL at 25°C—as that in exponentially growing cultures exposed to the same dose (Fig. 1, *C*). Of particular interest is one experiment (Fig. 1, *D*), in which the first synchronous division began about the middle of the exposure period. Most of the irradiated individuals completed the first division, but the fission process was slowed down; consequently, at the end of the exposure period the irradiated population exhibited a higher fission index (12 per cent) than the unexposed population (< 2 per cent) which had already completed division.

These preliminary results confirm the finding that *Tetrahymena*, during ten or more hours of temperature cycling, are able to continue synthesis of DNA or DNA-like material in the absence of division. They demonstrate further that the fission delay induced by ionizing radiation is the same regardless of the content of DNA-like material. Inhibition of the synthesis of this material is not the mechanism of radiation-induced fission block in *Tetrahymena*.

I am deeply indebted to Dr. Erik Zeuthen for his generosity in making available to me a copy of his manuscript [5] prior to publication.

REFERENCES

1. Brace, K. C., *Proc. Soc. Exptl. Biol. Med.* **74**, 751 (1950).
2. Hevesy, G., *Nature* **163**, 869 (1949).
3. Holmes, B. E. and Mee, L. K., *Brit. J. Radiol.* **25**, 273 (1952).
4. Lajtha, L. G., Oliver, R., and Ellis, F., *Brit. J. Cancer* **8**, 367 (1954).
5. Scherbaum, O. and Zeuthen, E., *Exptl. Cell Research* **6**, 221 (1954).
6. Vermund, H., Barnum, C. P., Huseby, R. A., and Stenström, K. W., *Cancer Research* **13**, 633 (1953).
7. Zeuthen, E. and Scherbaum, O., *in* Recent Developments in Cell Physiology, J. A. Kitching, ed., Proceedings of the Seventh Symposium of the Colston Research Society, London, p. 141, 1954.

THE UPTAKE OF I^{131} BY THE THYROID GLAND OF THE ADULT MOUSE AFTER *IN VITRO* CULTIVATION

ARLENE R. SEAMAN and SHEILA STAHL

Department of Anatomy, State University of New York, College of Medicine at New York City, Brooklyn, U.S.A.

Received June 10, 1956

It is known that embryonic rat thyroid glands can be cultivated *in vitro* for extensive periods [4, 5], although to date adult thyroid glands have not been successfully cultivated. The function of the embryonic thyroid gland, cultivated *in vitro*, was

investigated by means of radioactive iodine by Gaillard [3], and Carpenter, Beattie, Chambers [1].

The present investigation was undertaken to ascertain (1) whether whole thyroid glands of adult mice could be cultivated and satisfactorily maintained *in vitro*, and (2) to determine whether, and to what extent, adult thyroid glands maintained *in vitro* were physiologically active as tested by their capacity to concentrate selectively the radioactive isotope I^{131}.

It was found that cultures of the thyroid gland of adult CFW mice would maintain themselves satisfactorily when cultivated in a modified chamber technique [7, 8, 9], using the alkaline fluid medium of Pikowski [6] in a controlled gaseous atmosphere (5 per cent CO_2, 95 per cent O_2). With this cultivation method the connective tissue elements were suppressed while highly differentiated follicular epithelium could be maintained satisfactorily *in vitro* for a 2–6-day period.

At the end of the cultivation period (2–6 days), the organ explants were washed with physiological saline and placed in another Trowell chamber containing a 10–20 uc I^{131} in 10 ml Tyrode's solution. The organ explants and the uncultivated castrate thyroids remained in this solution for varying periods (2–18 hours), after which they were removed, fixed in Bouin's solution, counted, embedded in paraffin, and sectioned at 5 μ. Radio-autographs were made of these sections according to the stripping film technique of Doniack and Pelc [2].

Preliminary results show that cultivated adult thyroid glands accumulate less radioactive iodine than non-cultivated adult thyroid glands. The accumulation of I^{131} also progressively decreases in the cultivated adult thyroid gland with increased periods of cultivation. Autoradiographic preparations of the cultivated glands after being kept in I^{131} for two hours were found to accumulate appreciable amounts of I^{131}, concentrated mainly in the follicular epithelial cells. After 18 hours, the labelled element is concentrated only in the colloid and in such amounts that the autoradiogram becomes fully blackened. Evidence indicates that I^{131} present in cultivated thyroid tissue is probably bound to a protein molecule. Further metabolic and physiological studies are in progress.

REFERENCES

1. Carpenter, E., Beattie, J., and Chambers, R., *J. Exptl. Zool.* **127**, 249 (1954).
2. Doniack, I. and Pelc, S., *Brit. J. Radiol.* **23**, 184 (1950).
3. Gaillard, P. J., *Internatl. Rev. Cytology* **2**, 331 (1953).
4. Martinovich, R. N., *Meet. Med. Res.* **4**, 2381 (1951).
5. —— *Exptl. Cell Research* **4**, 490 (1953).
6. Pikowski, M. A., *Exptl. Cell Research* **7**, 72 (1954).
7. Trowell, O. A., *Exptl. Cell Research* **3**, 79 (1952).
8. —— *ibid.* **6**, 246 (1954).
9. —— *ibid.* **9**, 277 (1955).

THE INCORPORATION *IN VITRO* OF 1-C^{14}-GLYCINE INTO LIVER PROTEINS VISUALIZED AS A TWO-STEP REACTION

T. HULTIN

The Wenner-Gren Institute for Experimental Biology, University of Stockholm, Sweden

Received June 16, 1956

It has been known for some years that the submicroscopic structures of liver cells are the sites of a particularly rapid incorporation of amino acids into proteins [4, 1]. Under suitable conditions a fairly rapid incorporation of labeled amino acids can be observed even in cell-free liver preparations containing submicroscopic structural fragments ("microsomes") and soluble, non-dialysable factors from the cytoplasmic fluid, in the presence of a supply of continuously regenerated adenosine triphosphate (ATP) [6, 7]. In this incorporation process an essential role has recently been attributed to enzymatic systems in the soluble cell fraction which have the capacity to activate amino acids at the expense of added ATP [2, 3].

In this communication a few experiments will be described pertaining to the incorporation of 1-C^{14}-glycine into the proteins of a cell-free liver preparation containing microsomes and soluble cell constituents. It will be shown that the incorporation process is conditioned by a preceding activation step, at which ATP can be used as a source of energy. An activated intermediate apparently accumulates in the system and is successively introduced into protein molecules by a mechanism which operates efficiently even at very low ATP-levels.

Experimental.—Albino rats (175–190 g) were used. Liver homogenates, largely freed from mitochondria, were prepared essentially according to the procedure of Zamecnik and Keller [7], $MgCl_2$ (0.01 *M*), potassium phosphate (0.02 *M*, pH 7.8), $KHCO_3$ (0.03 *M*), KCl (0.025 *M*), and sucrose (0.35 *M*) being included in the homogenization medium. Of the homogenates 0.7 ml samples were incubated in final volumes of 1 ml with 0.4–0.5 μM (cf. Fig. 1) of 1-C^{14}-glycine (0.69 m*M*/mC) at 37°C and with 5 per cent carbon dioxide in the gas phase. Creatine phosphate (20 μM) and ATP (1 μM) were added as the source of energy.

After the incubation the proteins of the samples were precipitated with trichloroacetic acid (TCA) and purified according to a slightly modified Schneider procedure [5]. The specific activities of the protein samples were recalculated for indefinite sample thickness (1 cm^2 plate area) on the basis of an empirical activity saturation curve.

Effects of postponed isotope additions.—In experiments in which the labeled glycine was added to the homogenate samples at the start of the incubation, the incorporation of the isotope into proteins proceeded approximately as is shown in Fig. 2, curve 2. In an experiment of this type the amount of isotope which has been incorporated into proteins during different time intervals can be calculated by simple subtraction. In this way it should be possible to predict the incorporation values which would be expected if the C^{14}-glycine were added to the samples at successive periods after the start of the incubation, all samples being simultaneously precipi-

tated with TCA at the end of the experiment (Fig. 2, curve 3). However, in all experiments aimed at substantiating these predictions, curves with a fairly deviating course resulted (Fig. 2, curve 4). The C¹⁴-glycine obviously had to be added to the system during the first few minutes of incubation in order to be incorporated to any significant extent into protein molecules, in spite of the fact that the incorporation proceeded at a fairly rapid rate for considerable time in the control samples to which the labeled glycine had been added at the beginning.

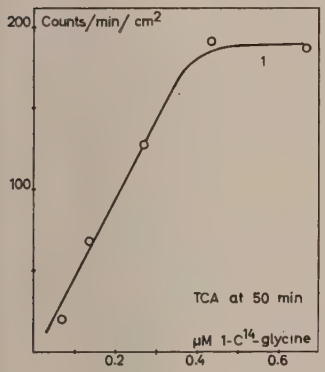

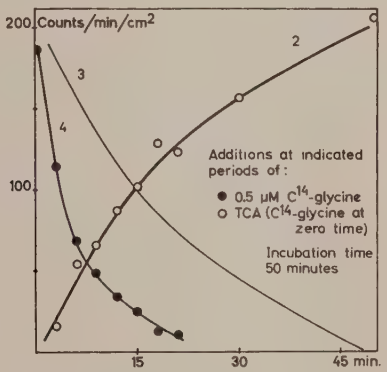

Fig. 1 (*left*). Influence of the concentration of 1-C¹⁴-glycine on the isotope incorporation.
Fig. 2 (*right*). Time course of 1-C¹⁴-glycine incorporation, and deficit in expected incorporation caused by delayed addition of isotope to the system.

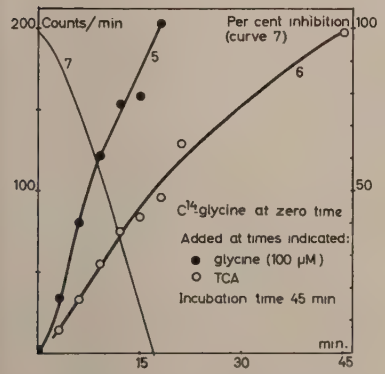

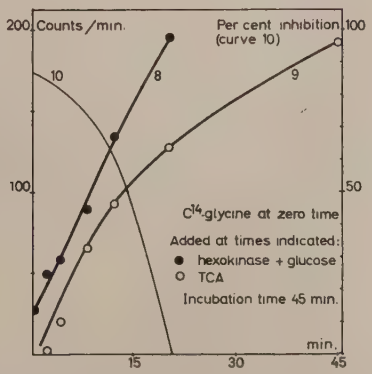

Fig. 3 (*left*). Effects of isotope dilution at different periods of incubation.
Fig. 4 (*right*). Inhibitory effect of hexokinase and glucose (40 μM) added to the incorporation system at different periods.

Effects of isotope dilution.—At different periods after the start of the experiment unlabeled glycine in very great excess (100 μM) was added to the incorporation system for the purpose of isotope dilution (Fig. 3, curve 5). In the very early samples the subsequent isotope incorporation was almost entirely suppressed. However, in the samples to which glycine had been added only a few minutes later the inhibition, exerted on the subsequent isotope incorporation by the isotope dilution, was already considerably less, and after 15–20 minutes no effect could be observed any longer in comparison with the series with non-diluted control-samples (curve 6). The percentage inhibition of the subsequent incorporation, effected by the isotope dilution at different periods after the start of the experiment, is represented by curve 7.

The dilution experiments are considered to show that after the first 15–20 minutes of incubation the isotope incorporation was no longer supplied from the glycine pool, but from an intermediate no longer equilibrating with this pool.

Effects of hexokinase and glucose.—Homogenates not supplied with ATP and creatine phosphate gave very low incorporation values.

Glucose and hexokinase were added at intervals to complete incorporation systems in order to effect a rapid depletion of the energetic system (Fig. 4, curve 8). A pronounced depression of the isotope incorporation in comparison with the controls (curve 9) was observed in those samples to which the hexokinase system had been added during the first minutes of incubation. The inhibition became progressively less in samples which had been incubated with the labeled glycine for a few minutes, and no effect of the ATP-depletion could be observed any longer in samples incubated for 15–20 minutes. The percentage inhibition of the subsequent isotope incorporation at different periods is shown in curve 10.

It is considered on the basis of the hexokinase experiments that phosphate-linked energy is required for the formation of the non-protein intermediate, while the final incorporation of this intermediate into protein proceeds with no, or only very small, further energy investments.

REFERENCES

1. Borsook, H., Deasy, C. L., Haagen-Smit, A. J., Keighley, G., and Lowy, P. H., *J. Biol. Chem.* **187**, 839 (1950).
2. Hoagland, M. B., *Biochim. et Biophys. Acta* **16**, 288 (1955).
3. Hoagland, M. B., Keller, E. B., and Zamecnik, P. C., *J. Biol. Chem.* **218**, 345 (1956).
4. Hultin, T., *Exptl. Cell Research* **1**, 376 (1950).
5. Schneider, W. C., *J. Biol. Chem.* **161**, 293 (1945).
6. Siekevitz, P., *J. Biol. Chem.* **195**, 549 (1952).
7. Zamecnik, P. C. and Keller, E. B., *J. Biol. Chem.* **209**, 337 (1954).

UTILIZATION OF SULFATE ION BY EOSINOPHILE MYELOCYTES IN THE RAT[1]

R. C. GREULICH[2]

Department of Medical Physics, Karolinska Institutet, Stockholm, Sweden

A recent autoradiographic and histochemical study [8] of the metabolism of S^{35}-labeled sulfate ion in bone matrix and cartilage has also revealed an interesting feature in the bone marrow. Examination of marrow in autoradiograms of decalcified sections of rat bone, following a variety of histochemical treatments, indicates that eosinophile myelocytes retain radioactive sulfur within their cytoplasm, apparently in association with the granular component. This observation confirms the findings of Odell *et al.* [14].

Application of histochemical methods in the present work has further shown that the sulfur label in these cells is highly resistant to treatments which remove sulfated polysaccharides from histological material. While the chemical nature of the sulfur-labeled constituent in eosinophile myelocytes has not been determined definitely, the fact that it does not share the histological properties usually ascribed to sulfated polysaccharides suggests that it may be very closely associated with protein.

Experimental.—The observations reported herein were made by examination of preparations of marrow from the long bones of two littermate albino rats of 78 g body weight. These animals were killed by exsanguination 24 hours following a single intraperitoneal injection of 100 μc S^{35} as carrier-free sodium sulfate. Long bones were removed immediately after death, were stripped of most of the adherent soft tissues, and were split longitudinally. The samples were fixed for 48 hours at 25°C in two fixatives, either 3.7 per cent (w/v) aqueous unneutralized (i.e., acidic) formaldehyde, or a formaldehyde solution of similar strength which had been saturated with barium hydroxide, according to the method of Dziewiatkowski [4].[3] The bones were then washed in water, and were decalcified in 28 per cent aqueous tetrasodium ethylene diamine tetra-acetate buffered to pH 7.5. After decalcification, the bones were washed, dehydrated, and embedded in paraffin for sectioning at 7 microns.

The effect of hyaluronidase hydrolysis on bound sulfur was investigated by treating hydrated sections of acidic formalin-fixed bone with a 0.1 per cent aqueous solution of testicular hyaluronidase at 37°C for 3 to 6 hours. This technique was first shown to abolish cartilage metachromasia. Control sections were incubated under the same conditions with beta amylase, which was known to have no effect upon cartilage metachromasia.

[1] This study was supported in part by research grant D-177 from the National Institute of Dental Research, United States Public Health Service.

[2] Bank of America Giannini Foundation Fellow, on leave from the Department of Anatomy, University of California Medical Center, Los Angeles, U.S.A.

[3] It is a pleasure to acknowledge the kind cooperation of Dr. Dziewiatkowski in providing the bone samples for this investigation.

Sections for histological study were stained with hematoxylin-eosin, periodic acid Schiff, safranine O, and toluidine blue. Autoradiographic preparations were also stained by these methods, or were left unstained.

Autoradiography was carried out by means of the "coated" technique [2, 9], using Eastman Kodak NTB3 bulk emulsion.[1] Exposures ranged from three weeks to two months.

Results.—Examination of autoradiograms of stained and unstained bones fixed in unneutralized formalin revealed that the greatest uptake of S^{35} had occurred in the epiphyseal cartilages. Less intense, although well defined reactions were exhibited by bone matrix.

Cellular reactions of marrow elements were still less intense, being present (in order of decreasing intensity) in mast cells, megakaryocytes and eosinophile myelocytes. The accumulation of labeled sulfur in all of these cells appeared to be related to cytoplasmic structure, and was not seen to be associated with nuclei.

While all mast cells contained a sulfur-labeled cytoplasmic component, examination of megakaryocytes and eosinophile myelocytes revealed that they were not uniformly labeled. Differences in morphology between reactive and unreactive megakaryocytes were not apparent upon careful study. On the other hand, eosinophile myelocytes which contained an S^{35} label seemed to be immature. They were characterized by the presence of polymorphic, usually bilobed nuclei, whereas the unlabeled myelocytes possessed ring-shaped nuclei similar to those of mature eosinophile leucocytes. Approximately 70 per cent of the total eosinophile myelocyte population exhibited autoradiographic reactions. The overall percentage occurrence of eosinophiles in these marrow samples (6 to 7 per cent) fell within the range of values reported by others [6, 16].

Exposure of acidic formalin-fixed specimens to testicular hyaluronidase brought about two changes in the distribution of labeled sulfur. Epiphyseal cartilages were cleared of their content of the isotope, except for a very slight residual activity immediately adjacent to the chondrocytes. Secondarily, it caused a generalized, though barely perceptible reduction in the reactions of the other labeled structures. However, this effect was also noted after incubation with beta amylase, and so was considered to be non-specific. Beta amylase had no significant effect upon the sulfur content of epiphyseal cartilage. Neither enzyme produced a significant change in the S^{35}-content of bone matrix, mast cells, megakaryocytes, or eosinophile myelocytes.

Barium hydroxide-saturated formalin caused a very striking reduction in the S^{35}-labeled materials. There was a complete loss of the isotope from cartilage, bone matrix, mast cells, megakaryocytes, and peripheral connective tissue elements. Only the eosinophile myelocytes remained reactive (Fig. 1). Fixation of these cells in alkaline formalin caused their granules to coalesce into an irregular mass. Coupled with this was an increased brilliancy of staining with the periodic acid Schiff technique, an effect which is probably related to the previously reported enhancement of Schiff staining by treatment with alkali [10]. After this fixation, the eosinophile myelocytes were essentially the only marrow component to retain an affinity for

[1] I am greatly indebted to the Eastman Kodak Co., Rochester, New York, U.S.A., for supplying this emulsion.

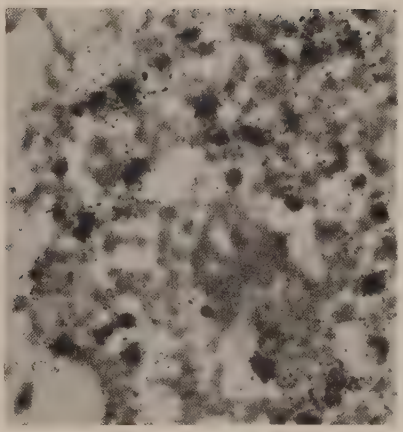

Fig. 1. Autoradiogram of bone marrow from rat 24 hours after administration of S^{35}-sulfate. Sample fixed in barium hydroxide-saturated formalin, decalcified in EDTA, and stained by the periodic acid Schiff technique.

The only element of marrow which contains a sulfur label is the eosinophile myelocyte, many examples of which may be seen in the figure.

the Schiff reagent, and their relationships to the residual autoradiographic reactions were thus easily assessed.

Discussion.—Interest in the relationship of bone marrow to S^{35}-sulfate began with the finding of Singher and Marinelli [15] that this tissue concentrated relatively large proportions of the administered isotope. Dziewiatkowski [5] subsequently investigated the kinetics of sulfate accumulation in marrow and showed that the peak concentration was reached 24 hours after injection. The same investigator later demonstrated the presence of S^{35} in marrow by autoradiography [4]. Other workers have since described the distribution of S^{35}-sulfate in marrow elements of various species under different experimental conditions [1, 11, 14].

While little attention has been given to the chemical significance of marrow-bound sulfur, some pertinent features may be discussed here. Using *undecalcified* bones, Dziewiatkowski found that barium hydroxide–formalin removed cartilage–bound sulfur, presumably by forming a soluble barium salt with chondroitin sulfate. Acidic formalin, however, did not alter cartilage S^{35}, nor did either fixation significantly affect the distribution of sulfur in marrow. However, in view of the present findings, using *decalcified* bone, it appears likely that, except for the sulfur label in eosinophile myelocytes, the residual sulfur demonstrated in the marrow of his barium hydroxide–formalin-fixed specimens was in the form of sulfate ion, or in a form otherwise readily soluble in the decalcifying medium used here.

The mechanism by which barium hydroxide removes not only cartilage sulfur (chondroitin sulfate), but also almost all of the other sulfur-labeled components in marrow is not clearly evident. However, it should be noted that common to many chemical methods for the extraction of mucopolysaccharides is treatment with dilute alkali [12]. The work of Dziewiatkowski and that of Boström and Åqvist [3] has suggested, on the basis of chemical analyses, that nearly all of the incorporation of sulfate-sulfur *in vivo* occurs during the synthesis of sulfated mucopolysaccharides. But the fact that the sulfated component in eosinophile myelocytes is resistant to both alkaline fixation and hyaluronidase (which removes chondroitin sulfate)

strongly suggests that it is in a form other than that of a sulfated polysaccharide. It is tentatively suggested that the sulfur in these cells is very closely related to a protein constituent, and may even have been synthesized into a protein molecule. Strength is lent to this view by the fact that inorganic sulfate as well as organic sulfated compounds of low molecular weight (an example of which, uridine diphosphate galactosamine sulfate, has been shown to become labeled with S^{35}-sulfate [17]) are removed during histological processing. Further investigation of the chemical aspects of this problem are contemplated.

From the physiological point of view, it is interesting that the formation of sulfur-labeled material in eosinophile myelocytes occurs in the cytoplasm of only a part of the total population of these cells. This fact, coupled with the relative immaturity of the reactive cells, suggests that the labeling proceeds during a precise period in the developmental history of the cell, and does not continue after the cell has attained a specific stage of maturity. Similar conclusions have been drawn by others [7, 13], in analogous isotopic studies of bone marrow metabolism.

REFERENCES

1. Bélanger, L. F., *Anat. Rec.* **118**, 755 (1954).
2. Bélanger, L. F. and Leblond, C. P., *Endocrinology* **39**, 8 (1946).
3. Boström, H. and Åqvist, S., *Acta chem. scand.* **6**, 1551 (1953).
4. Dziewiatkowski, D. D., *J. Exptl. Med.* **93**, 451 (1951).
5. —— *J. Biol. Chem.* **178**, 197 (1949).
6. Endicott, K. M. and Ott, M., *Anat. Rec.* **92**, 61 (1945).
7. Gavosto, F., Ficq, A., and Errera, M., *Exptl. Cell Research* **6**, 238 (1954).
8. Greulich, R. C., *J. Bone and Joint Surg.*, in press.
9. Gross, J., Bogoroch, R., Nadler, N. J., and Leblond, C. P., *Am. J. Roentgenol.* **65**, 420 (1951).
10. Hale, A. J., *Quart. J. Microscop. Sci.* **94**, 303 (1953).
11. Lajtha, L. G., Ellis, F., and Oliver, R., *Brit. J. Cancer* **7**, 401 (1953).
12. Meyer, K., *in* Connective Tissue in Health and Disease. Munksgaard, Copenhagen, 1954, p. 55.
13. Morse, W. I., *Am. J. Med. Sci.* **220**, 522 (1950).
14. Odell, T. T., Tausche, F. G., and Gude, W. D., *Am. J. Physiol.* **180**, 491 (1955).
15. Singher, H. O. and Marinelli, L., *Science* **101**, 414 (1945).
16. Stasney, J. and Higgins, G. M., *Anat. Rec.* **63**, 77 (1935).
17. Strominger, J. L., *Biochim. et Biophys. Acta* **17**, 283 (1955).

A PRINCIPLE OF AUTO-REGULATION OF GROWTH

PRODUCTION OF ORGAN SPECIFIC MITOSE-INHIBITORS IN KIDNEY AND LIVER

H. SAETREN

Zoological Laboratory, University of Oslo, Oslo-Blindern, Norway

Received June 30, 1956

The mechanism which controls the rate of growth of a "vegetative" organ as e.g. a kidney represents one of the fundamental problems in developmental physiology. This preliminary communication presents evidence that in rats both the kidney and the liver maintain a certain blood level of a thermolabile non-dialyzable substance which exerts a specific inhibitory action on the growth of its organ of origin.

The experiments outlined below are on the whole based upon the degree of realization of the mitose maximum normally occurring in the remaining half of the left kidney 48 h. after subtotal nephrectomy (Fig. 1). At present there seems to be no reason not to consider the rate of mitosis in the kidney as a direct expression of growth. In the liver a greater part of the growth is realized through endomitoses instead of mitoses. The "48-hour readings" from smears of samples about one mg in size demonstrate a remarkable constancy of the incidence of mitoses throughout the outer cortex: double samples from three different kidneys gave 14 and 16, 130 and 137, and 254 and 267 mitoses per mg.

Any ability of a tissue to inhibit mitoses (the *m*-inhibitory effect) was disclosed by spreading a macerate of the organ in the peritoneal cavity. In all experiments on inhibition, care was taken always to use animals of the same age, sex and origin both as donor and as receiver.

Fig. 2 curve *B* relates the incidence of mitoses 48 h. after the partial nephrectomy with the amount of kidney macerate returned simultaneously with the operation. The sudden onset of inhibition, if the latter amount equals the kidney mass removed, indicates a well-defined critical threshold for the *m*-inhibitory effect. Any inhibitor released from the kidney macerate must pass through the peritoneum and effectuates inhibition due to its higher blood level. By spreading kidney macerate in large subcutaneous pockets a direct transmission of inhibitor to the half kidney was excluded, the inhibitory effect being still the same.

One may assume that after partial nephrectomy alone, cells in the half kidney start dividing because the critical blood level is no longer maintained. Such a mechanism for the regulation of the rate of mitosis (or growth) in kidney tissue may be realized if the *m*-inhibitor is subject to a high rate of inactivation in the organism, and if it is highly specific with respect to the type of cells it prevents from dividing. If the inhibitor is subjected to a continuous inactivation, the suppression of mitoses by the intraperitoneally-applied kidney macerate may be considered the accumulated effect of (1) the remainder of the activity level maintained until operation by the

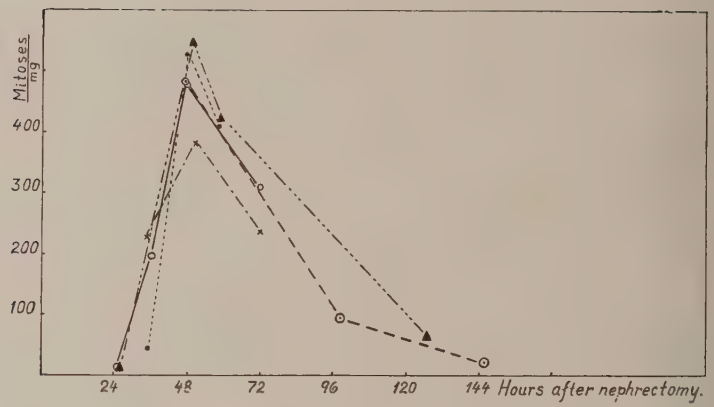

Fig. 1. The maximum of mitosis 48 h. after subtotal nephrectomy. 3 to 5 samples from 5 different rats. The steep ascending towards the 48-hour maximum indicates the abolishing of an inhibitor of mitosis.

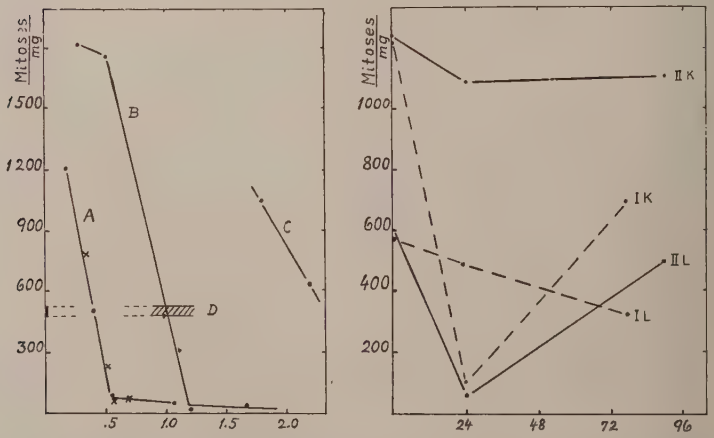

Fig. 2 (*left*). The inhibitory action of relative amounts of kidney macerate returned 18 (*A*), 48 (*B*) and 72 h. before the 48-hour maximum.
Fig. 3 (*right*). The specific and temporary inhibition of mitosis in youngsters by macerates of kidney and liver.

1 ½ kidneys removed, (2) the activity effectuated by the remaining left kidney half, and (3) the residual activity released from the kidney macerate.

The conception that the *m*-inhibitor is inactivated at a high rate is supported by the much smaller amount of macerate needed if it is returned only 18 h. before the 48-hour reading (Fig. 2, curve *A*). Curve *C* demonstrates the opposite effect. The application, 24 h. before the operation, of even twice the amount of kidney mass removed did not result in any *m*-inhibition. With decreasing quantities of returned macerate the curves ascend steeply past the level of unaffected 48-hour readings (Fig. 2, *D*). Any relationship between this stimulation of mitotic rates by sub-inhibitory amounts of macerate and the findings of Friedrich-Freksa and Zaki [2] and Anders [1] awaits adequate eperiments.

The nature of the inactivation of the *m*-inhibitor is under investigation, four main possibilities being considered: (1) The inhibitor is an unstable molecule; (2) it is inactivated by an enzyme; (3) its active part is blocked by combining with another substance participating in the all-over regulation of mitotic rates in the organism (a "growth-hormone"); or, finally (4) it is in some way used up through the very blocking of the growth processes which are registered as mitoses in the present investigation.

Experiments have in a double sense provided unequivocal support to the postulated organ-specificity of the *m*-inhibitor: If ⅔ of the liver were removed simultaneoulsy with 1 ½ kidneys, the rate of mitoses released 48 h. later was for one group of rats between 400 and 500 cell divisons per mg in both organs. Kidney macerate applied intraperitoneally 18 h. before the expected 48-hour peak, reduced the latter to about 60 mitoses per mg in the kidney cortex while it remained at 430 in the liver. A threefold repetition of this experiment gave the same result in principle. In youngsters the *m*-inhibitor of kidney and liver selectively prevents mitoses in the respective growing organs. Fig. 3, I*K* shows how the mitotic rate of the kidney temporarily diminishes while that of the liver (I*L*) remains unaffected by the introduced kidney mass. The curves II*K* and II*L* demonstrate the corresponding specific action on liver by liver macerate. Fig. 3 represents one out of five similar experiments giving the same results, letting the specific and temporary *m*-inhibitory effect of the introduced macerate appear unequivocally.

The specific action of an *m*-inhibitor on the organ in which it is produced excludes the action of such inhibitors amongst the organs. Tests with macerate of liver, spleen, testes and brain tissue confirm this supposition. Provided the animals stayed comparatively healthy with the heavy loads of macerates (3 brains, one liver, 4 spleens or 4 testes) no lowering of the 48-hour peak in cortex of the half kidney was detectable.

Another important feature of the specificity of the *m*-inhibitory effect was demonstrated by introducing liver macerate into the body cavity 30 hours after partial hepatectomy. It was evident that by far the greater part of the few mitoses remaining of the 48-hour peak occurred in the blood vessels etc. and not in the liver epithelium proper.

A few physical properties of the inhibitor have been tracked down, even opening up the possibility of isolating the *m*-inhibitor. Fresh whole kidneys lost only a minor part of their inhibitory activity if kept sterile at + 1°C for ten days. A heating to 60°C for ten minutes abolishes the *m*-inhibitory property of fresh kidney macerate. Freezing and thawing and even drying in vacuum do not inactivate the inhibitor.

The author has not been successful in making the inhibitor pass through a membrane for dialysis.

Investigations into the probable protein nature of the *m*-inhibitor and its state in the cells are in progress. That the *m*-inhibitor of the kidneys is no longer produced in the "defunctioned" organ has been indicated by obstructing one urether for 10 days. The 48-hour peak is unaffected by macerate prepared from such nonfunctioning kidneys.

REFERENCES

1. Anders, G., *J. Expll. Zool.* **130**, 221 (1955).
2. Friedrich-Freksa, H. and Zaki, F. G., *Z. Naturforsch.* **9 b**, 394 (1954).

THE PERMEABILITY OF ERYTHROCYTE GHOSTS

W. D. STEIN[1]

Zoology Department, King's College, London, England

Received July 4, 1956

Teorell [5] was able to prepare erythrocyte ghosts which behaved as almost perfect osmometers and was able to determine the potassium and sodium permeability of these cell derivatives. He further showed, qualitatively, that the ghosts were permeable to glucose but impermeable to sucrose. Such erythrocyte ghosts have recently been used in metabolic studies [2]. The present paper reports some recent quantitative measurements of the permeability of ghosts to non-electrolytes. The results indicate that the non-electrolyte permeability of the ghosts is similar to that of intact red cells and that, in particular, the ghosts retain the system responsible for the facilitated diffusion [1] of glycerol.

Studies were made on ghosts from human erythrocytes. The ghosts were prepared by a method similar to that of Teorell [5], except that haemolysis was carried out in 2½ volumes of distilled water, rather than the five volumes recommended by him. The absence of contaminating intact red cells in the ghost preparation was checked by observation in the light- and interference-microscope, the latter instrument being especially valuable for the rapid identification of intact cells. Permeability measurements were made by the photometric method of Orskov [3]. The saline suspension of

[1] This investigation has been aided with a post-graduate scholarship from the University of the Witwatersrand, South Africa.

ghosts used for permeability measurements had to be some ten times as concentrated as a solution of intact cells, to give a comparable optical density, presumably due to the loss of light-scattering and light-absorbing material during haemolysis. All permeability measurements were made in an isotonic saline medium buffered with barbitone at pH 8, the pH maximum of the system facilitating the diffusion of glycerol.

Table I shows the results obtained, the permeabilities being recorded as $t_{\frac{1}{2}}$ values in seconds, where $t_{\frac{1}{2}}$ is the half-time of decrement of the optical density of the cell suspension, after the permeant has been added [4].

TABLE I

Permeant	Inhibitor	Relative permeability (in seconds, see text)	
		Ghosts	Intact cells
glecerol monoacetate	—	9–10	8–10
α, γ-propylene glycol	—	1–2	1–2
glycerol	—	9–13	5–7
glycerol	$+10^{-4}$ *M* $CuSO_4$	150–300	350–400
1:2:4 butan-triol	—	15–20	10–12
1:2:4 butan-triol	$+10^{-4}$ *M* $CuSO_4$	60	250–300

Further studies on the glycerol facilitating system showed that the Michaelis constant for the affinity of the system with glycerol [4] was similar for ghosts and intact red cells (0.25 *M* and 0.5 *M* respectively); that in the range of copper concentrations between 25 and 75 per cent inhibition of the system, the cells bound similar amounts of copper (1 ion per 30 sq. Å and 1 per 60 sq. Å for ghosts and intact cells); and finally that the strength of binding of copper to the facilitating system (as measured by the reversal of copper inhibition by alternative copper-complexing agents [6]) was similar for the ghosts and for intact cells.

It can thus be concluded that ghosts prepared by gentle hypotonic haemolysis possess a selective permeability barrier and that this barrier is of much the same nature as in the intact cell. Furthermore, the ghosts have the ability to facilitate the diffusion of glycerol and the indications are that the system has much the same affinity for glycerol and for copper as in the intact cell and is present to about the same extent. Thus the glycerol facilitating system is localised in the cell membrane and can function without the intervention of diffusible components from the cell interior.

It would appear, therefore, that even after the structural reorganisation of the cell membrane necessary for the outward passage of haemoglobin molecules during haemolysis, the membrane can be reconstituted so as to present a largely unaltered barrier towards permeating molecules. Future concepts of erythrocyte membrane structure and of the molecular mechanisms of haemolysis must be capable of explaining this phenomenon.

REFERENCES

1. Danielli, J. F., *Symposia Soc. Exptl. Biol.* **8**, 502 (1954).
2. Lionetti, F., Rees, S. B., Healey, W. A., and Walker, B. S., *J. Biol. Chem.* **220**, 467 (1956).
3. Orskove, S. L., *Biochem. Z.* **279**, 241 (1935).
4. Stein, W. D. and Danielli, J. F., *Faraday Soc. Discussions* (in the press).
5. Teorell, T., *J. Gen. Physiol.* **35**, 669 (1952).
6. To be published.

THE INTRACELLULAR DISTRIBUTION OF PYRIDINE NUCLEOTIDES IN RAT LIVER

G. E. GLOCK and P. McLEAN

Courtauld Institute of Biochemistry, Middlesex Hospital, London, England

Received July 17, 1956

The intracellular distribution of pyridine nucleotides in rat liver has already been determined [1, 3, 4] but only total pyridine nucleotide (PN) was estimated and this by somewhat nonspecific methods [2, 5]. For these reasons we have reinvestigated this problem using recently devised sensitive methods for the separate determination of oxidised and reduced diphosphopyridine nucleotide (DPN) and triphosphopyridine nucleotide (TPN). These methods [6] involve coupling the enzymically reduced pyridine nucleotides with cytochrome *c* by means of their respective cytochrome *c* reductases and following the rate of reduction of cytochrome *c* spectrophotometrically.

In preliminary experiments, one part of rat liver was homogenised in nine parts of 0.25 *M* sucrose containing 0.1 *M* nicotinamide, pH 7.4, filtered through flannelette and the cellular constituents separated according to Schneider [8]. Oxidised and reduced pyridine nucleotides were determined, respectively, in neutralised acid and alkaline extracts of the separated cellular fractions, using portions for extraction corresponding to 200 mg of the original liver. The average results of five experiments for the DPN^+, DPNH, TPN^+ and TPNH contents of whole liver homogenate, unwashed nuclei, mitochondria and microsomes and of the soluble fraction are given in Table I. Of the total PN content of the homogenate, 65 per cent was recovered in the soluble fraction, 20 per cent in the mitochondria, 7 per cent in the nuclei and only 3 per cent in the microsomes.

In order to reduce mitochondrial contamination of the nuclear fraction, further experiments included the layering procedure of Hogeboom and Schneider [7]. In these experiments, filtered rat liver homogenate in 0.25 *M* sucrose containing 0.1 *M* nicotinamide, pH 7.4, was layered over an equal volume of 0.34 *M* sucrose containing

TABLE I

Intracellular distribution of pyridine nucleotides in rat liver.

	DPN^+ μg	DPNH μg	DPN^+ + DPNH μg	DPN^+ + DPNH %	TPN^+ μg	TPNH μg	TPN^+ + TPNH $g\mu$	TPN^+ + TPNH %
Whole homogenate	425±41	116±8	541±40	100	25±14	231±23	256±13	100
Nuclei	22±4	13±2	35±12	6	5±3	17±5	22±6	9
Mitochondria	47±2	21±5	68±4	13	3±2	90±9	93±11	36
Microsomes	16±4	<3	16±4	3	4±2	<3	4±2	2
Soluble fraction	359±41	50±18	409±36	75	26±10	88±12	114±14	45
Total recovery	444	84	528	97	38	195	233	92

(All values expressed as means ± S.E.M. Pyridine nucleotide results expressed as μg in the tissue fraction isolated from 1 g liver.)

TABLE II

Pyridine nucleotide content of rat liver mitochondria and nuclei separated by the layering technique.

	Unwashed fraction	Fraction washed once	Fraction washed twice
		MITOCHONDRIA	
Number of assays	6	4	4
Pyridine nucleotide content (μg)			
DPN^+	45±3	38±5	41±3
DPNH	26±2	24±7	13±4
DPN^+ + DPNH	71±3	62±7	54±1
TPN^+	8±3	7±2	16±4
TPNH	68±6	63±4	40±6
TPN^+ + TPNH	76±3	70±6	56±3
Nitrogen content (mg)	9.16±0.32	9.10±0.39	8.40±0.25
		NUCLEI	
DPN^+	12±2	10±3	8±3
DPNH	5±2	2±0.6	<2
DPN^+ + DPNH	17±1	12±3	8±3
TPN^+ + TPNH	5±2	3±1	<2

(All values expressed as means ± S.E.M. Pyridine nucleotide results expressed as μg in the mitochondria or nuclei isolated from 1 g liver. Nitrogen results expressed as mg N in the mitochondria isolated from 1 g liver.)

nicotinamide and differential centrifugation then carried out as previously [8]. Mitochondrial and nuclear fractions were washed by resuspension in isotonic sucrose containing nicotinamide followed by centrifugation. Average results for the DPN^+, DPNH, TPN^+ and TPNH contents of unwashed and washed mitochondrial and nuclear fractions are given in Table II. As judged by RNA determinations, microsomal contamination of the mitochondria was only slight. In contrast to nuclei, washed mitochondria still retain a large proportion of the PN present in the unwashed fraction. The reduction in both total DPN and total TPN contents of mitochondria after two washings is due mainly to a loss of reduced nucleotide, thus resulting in an increase in the DPN^+/DPNH and TPN^+/TPNH quotients. It is of interest that the total TPN (chiefly TPNH) content of rat liver mitochondria is of the same order as the total DPN (chiefly DPN^+) content. The total PN content (DPN^+ + DPNH + TPN^+ + TPNH) of unwashed mitochondria amounts to approximately 18 per cent of that of the whole homogenate and is markedly different from the results of previous workers [1, 3, 4].

The marked reduction in both total DPN and TPN contents of the unwashed nuclear fraction, separated by the layering procedure, indicates that the relatively high values shown in Table I are due chiefly to mitochondrial contamination. Further marked losses after two washings are presumably due to loss by diffusion since both pyrophosphatase and nucleosidase activities of isolated nuclei were found to be negligible at 0°.

This work is being extended to tumours and to the livers of rats under different hormonal treatments.

REFERENCES

1. Carruthers, C. and Suntzeff, V., *Cancer Research* **14**, 29 (1954).
2. —— *Arch. Biochem. Biophys.* **45**, 140 (1953).
3. Carruthers, C., Suntzeff, V., and Harris, P. N., *Cancer Research* **14**, 845 (1954).
4. Dianzani, M. U., *Biochim. et Biophys. Acta* **17**, 391 (1955).
5. Feigelson, P., Williams, J. N., and Elvehjem, C. A., *J. Biol. Chem.* **185**, 741 (1950).
6. Glock, G. E. and McLean, P., *Biochem. J.* **61**, 381 (1955).
7. Hogeboom, G. H. and Schneider, W. C., The Nucleic Acids. Vol. II, p. 212. Academic Press Inc., New York, 1955.
8. Schneider, W. C., *J. Biol. Chem.* **176**, 259 (1948).

ELECTRON MICROSCOPY OF CELL NUCLEI ISOLATED IN AQUEOUS MEDIA[1]

P. F. DAVISON and E. H. MERCER

Chester Beatty Research Institute, London, England

Received July 25, 1956

In the course of our comparative studies of the histones extracted from isolated cell nuclei by dilute mineral acids [1], a variable proportion of non-basic proteins has been detected by electrophoresis and chromatography. To determine whether these proteins were a result of cytoplasmic contamination, a number of preparations of isolated nuclei were examined by electron microscopy.

None of the methods normally used for the relatively large-scale preparations used in biochemical analysis was found to give nuclei free of material adhering to the outside of the nuclear membrane.

Acid media. With very dilute citric acid [2, 3] and acetic acid [4], nuclei were isolated from calf and mouse liver, thymus and spleen, from the mouse Ehrlich ascites tumour, and from rat liver.

Most of these nuclei when stained, counterstained and examined in the *light* microscope, appeared very clean (Fig. 1). However, the same preparations fixed in buffered osmium tetroxide, embedded in methacrylate, sectioned and examined in the electron microscope, appeared far less satisfactory (Fig. 2).

The material on the outside of the nuclear membrane was particularly prominent in tumour preparations. This contamination was least in nuclei prepared by Stedman's method, but these were very empty in appearance, with sparse regions of coagulated material; in many places the nuclear membrane was ruptured.

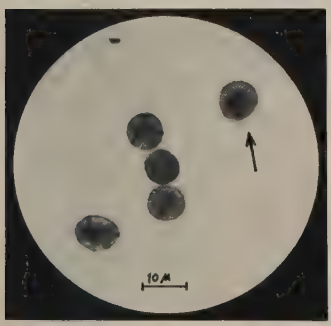

Fig. 1. Light micrograph of mouse liver nuclei isolated in pH 4 citric acid. Stained Ehrlich Haematoxylin. In one nucleus an adhesion can be detected (arrow).

[1] This investigation has been supported by grants to the Chester Beatty Research Institute (Institute of Cancer Research: Royal Cancer Hospital) from the British Empire Cancer Campaign, Jane Coffin Childs Memorial Fund for Medical Research, the Anna Fuller Fund, and the National Cancer Institute of the National Institute of Health, U.S. Public Health Service.

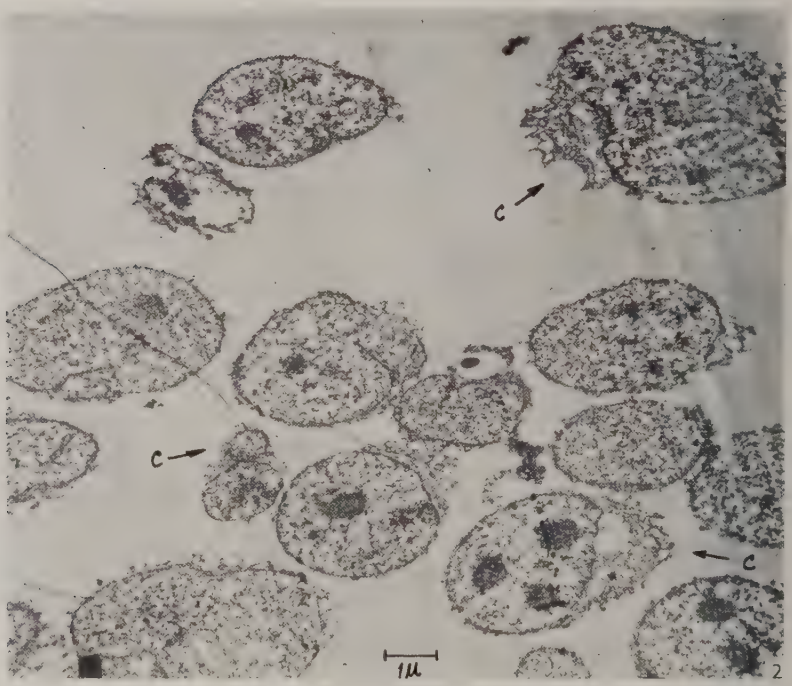

Fig. 2. Electron micrograph of a similar preparation to that shown in Fig. 1. Note contaminant at *C*.

Sucrose nuclei.—Calf spleen and mouse ascites nuclei were prepared in calcium chloride–0.25 *M* sucrose [5]. They were more difficult to isolate by this method, but there was a greater and more even density of intranuclear material, in agreement with the findings of Kay *et al* [6]. The membrane remained encrusted.

Nuclei isolated by Dr. J. Stanier in a sucrose-glycerol gradient [7] differed greatly from those described above and deserve special comment. They showed only a trace of a nuclear membrane, and contained evenly dispersed fibrils about 100 Å in diameter which may be threads of nucleoprotein (Fig. 3). Such preparations might be useful for detecting any enzymes bound to the membrane, but they cannot be made in very large quantities.

These experiments have demonstrated that the light microscope cannot adequately control the preparation of clean cell nuclei. The same situation arises in the preparation of mitochondria and microsomes [8]. By testing for enzymes restricted, *in vivo*, to the cytoplasm or the nucleus, enzyme contamination or loss may be assayed [9], but for macromolecules having no enzyme properties it is necessary to determine electron microscopically the purity of the sample.

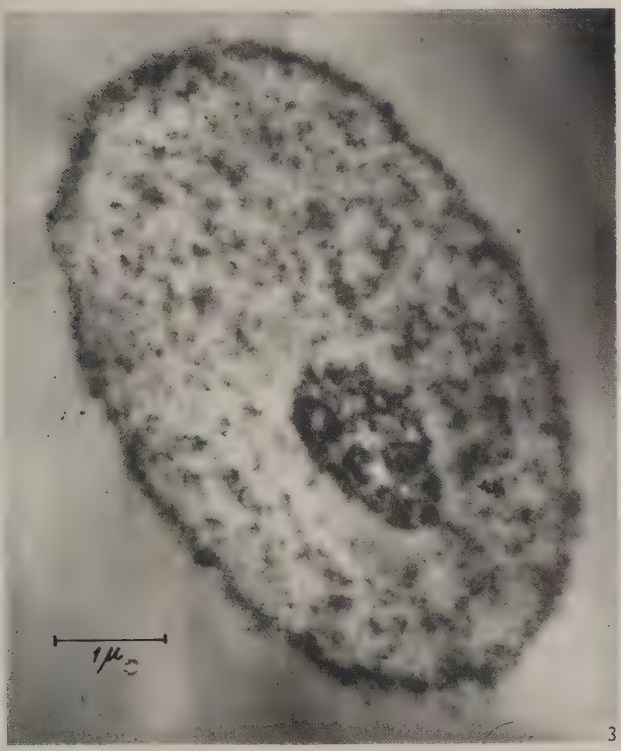

Fig. 3. Electron micrograph of rat liver nuclei isolated in glycerol-sucrose. Note absence of nuclear envelope and presence of fine threads (ca. 100 Å diameter)—nucleoprotein (?).

REFERENCES

1. Birbeck, M. S. C. and Reid, E., *Biochim. et Biophys. Acta* **20**, 419 (1956).
2. Davison, P. F., In preparation.
3. Dounce, A. L., *J. Biol. Chem.* **151**, 235 (1943).
4. Hogeboom, G. N., Schneider, W. C., and Striebich, M. J., *J. Biol. Chem.* **196**, 111 (1952).
5. Kay, E. R. M., Smellie, R. M. S., Humphrey, G. F., and Davidson, J. N., *Biochem. J.* **62**, 160 (1956).
6. Mirsky, A. E. and Pollister, A. W., *J. Gen. Physiol.* **30**, 117 (1946).
7. Philpot, J. St. L. and Stanier, J. E., *Biochem. J.* **63**, 214 (1956).
8. Stedman, E. and Stedman, E., *Biochem. J.* **47**, 508 (1950).
9. Stern, H. and Mirsky, A. E., *J. Gen. Physiol.* **37**, 177 (1953).

ELECTRON MICROSCOPY OF THE DEVELOPING SPERM-HEAD IN THE SPARROW TESTIS

G. YASUZUMI

Electron Microscope Research Laboratory, Department of Anatomy, Nara Medical College, Kashiwara, Japan

Received March 6, 1956

A CONSIDERABLE literature relating to the electron microscopy of sperm has appeared in recent years. It has been largely concerned with the examination of smear preparations [1 3, 6, 10 15, 18] and of fragmentation [5]. The sectioning technique has been used in a few cases only [4, 7, 17 20], the results concerning the head structure having been moderately successful. In this report, the characteristics of developing sperm-head as seen in thin sections will be dealt with briefly.

Small blocks of an adult sparrow (*Passer montanus saturatus* Sejneger) testis were fixed in 1 per cent osmium tetroxide solution, buffered to pH 7.4 with Michaelis acetate-veronal [9], dehydrated and embedded in a mixture of 80 per cent butyl methacrylate and 20 per cent methyl methacrylate [8]. Sections 20 to 50 mμ in thickness were cut on a Shimadzu thin sectioning microtome and examined in a Hidachi electron microscope model HU-10, without removing the plastic.

When the spermatid nucleus has been projected outside the cell body, the nucleus (primitive sperm-head) is of a conical shape with a well-defined head cap. The size of the primitive sperm-head in this stage is 1.9–2.05 μ in length and 0.85 1.15 μ at the base (Fig. 1). The fibrillar structure in the head can be seen along its longitudinal axis: the fibrils are clearly packed in the center of the head as well as at the peripheral portion. The oblique section of the nucleus is occupied by the fibrils 20 45 mμ in diameter, which are immersed in a matrix, the whole being enclosed by a thin head cap. The matrix possesses no structure within the limiting resolution of the present investigation. The cross-sections of fibrils appeared as bodies of an irregular round shape (Fig. 2). The fibrils are less clearly defined in the longitudinal section than the cross or oblique section: this seems to be due to a twisted array of fibrils along the longitudinal axis of the head.

In a sufficiently thin oblique section of primitive sperm-head, the longitudinal and cross-sections of fibrils are clearly visualized, suggesting a finer filamentous structure in each fibril (Fig. 3). At a higher magnification of a part of Fig. 3, the basic

---

Fig. 1. A vertical section through the primitive sperm-head portion in the sparrow testis, showing a more or less regular array of fibrillar derivatives of the chromosomes. The conical-shaped primitive sperm-head is enclosed by a thin head cap composed of apparently three layers at the point indicated by the arrow. At the bottom of the figure, the spermatid body (*SB*) is visible, comprising the material of a low density. The acrosome (*AC*) is scarcely discernible on the left upper corner. Magnification × 40,000.

Fig. 2. An oblique section through the primitive sperm-head portion in the sparrow testis, showing cross and oblique sections of fibrils more prominently than in the previous figure. The head cap with a fibrillar structure can be clearly identified at the point marked by the arrow. Magnification × 45,000.

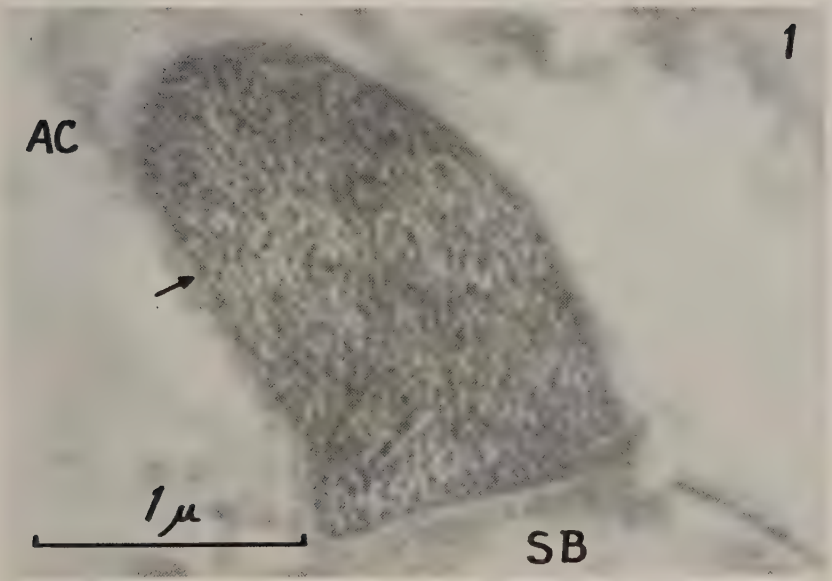
1
AC
1 μ
SB

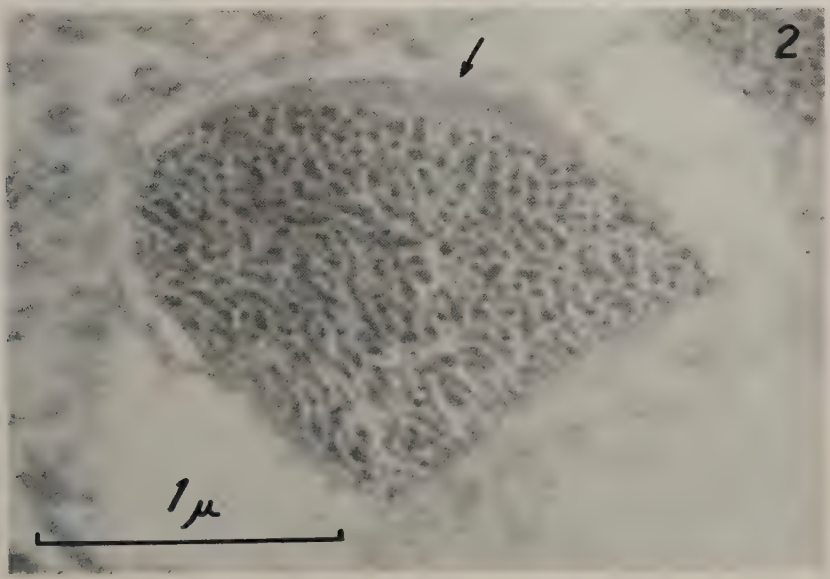
2
1 μ

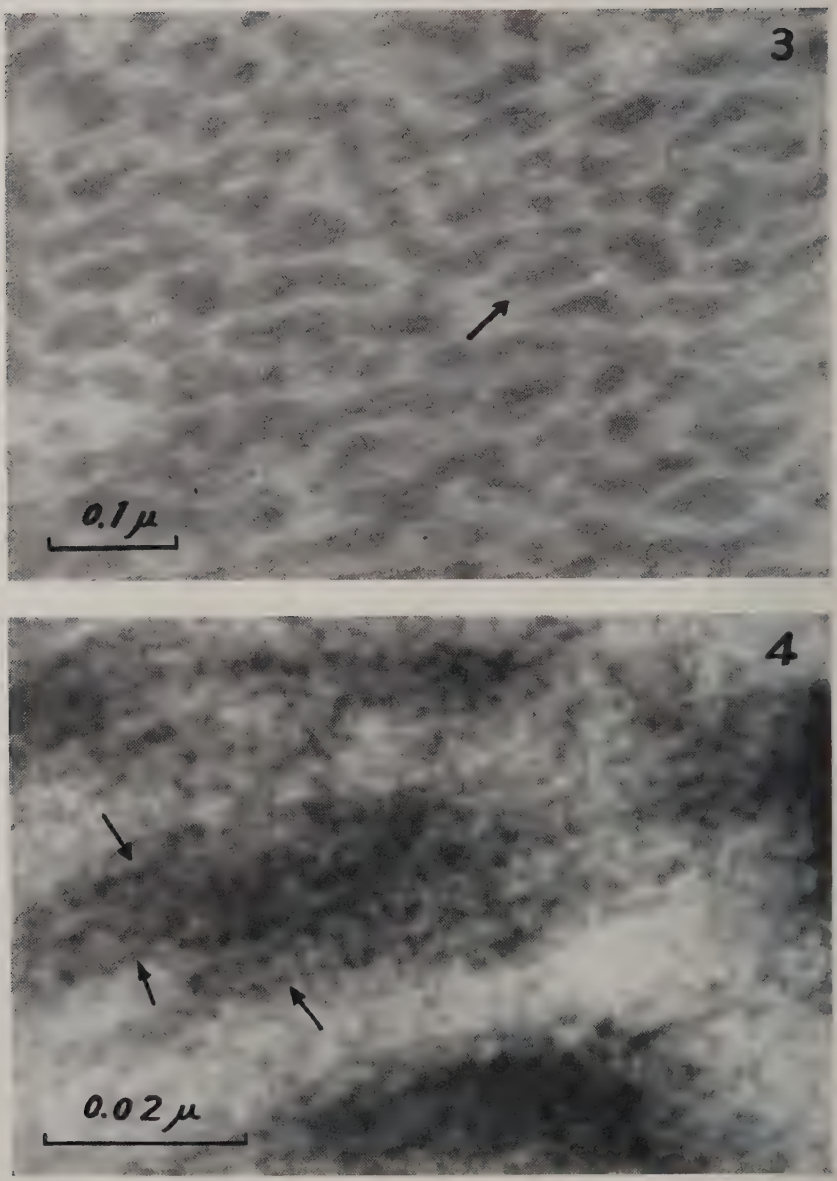
3
0.1μ
4
0.02μ

structure of fibrils can be seen in longitudinal and cross sections (Fig. 4). It is suggested that in the fibril the nucleoprotein is in the form of filaments oriented parallel to the fibril axis, existing in a helical configuration. In a previous study [16] it has been reported that the metabolic chromosome in triton erythrocyte nucleus is composed of at least 32 constituent chromofilaments 100 Å in diameter. Furthermore, it would seem that the present study has covered even the molecular aspect, referring to the fact that the chromosome or its derivative is composed of infinite nucleoprotein filaments. This novel feature of the chromosome or its derivative structure seems to be in harmony with the helical structure of sodium desoxypentose nucleate proposed by Watson and Crick [21].

REFERENCES

1. Baylor, M. R. B., Nalbandov, A., and Clark, G. L., *Proc. Soc. Exptl. Biol. Med.* **54**, 229 (1943).
2. Bretschneider, L. H., *Koninkl. Nederland. Akad. Wetenschap.* **52**, 301 (1949).
3. —— *Koninkl. Nederland. Akad. Wetenschap.* **53**, 531 (1950).
4. Burgos, M. H. and Fawcett, D. W., *Biophys. and Biochem. Cytol.* **1**, 287 (1955).
5. Fischer, H., Hug, O., and Lippert, W., *Chromosoma* **5**, 69 (1952).
6. Fujimoto, T. and Takaoka, K., *Electronmicroscopy* **3**, 10 (1954).
7. Kakinuma, T., Abe, H., and Nomura, Y., *Okajimas Folia Anat. Japonica* **27**, 97 (1955).
8. Newman, S. B., Borysko, E., and Swerdlow, M., *J. Research Natl. Bureau Stand.* **43**, 183 (1949).
9. Palade, G. E., *J. Exptl. Med.* **95**, 285 (1952).
10. Randall, J. T. and Friedlaender, M. H. G., *Exptl. Cell Research* **1**, 1 (1950).
11. Rötheli, A., Roth, H., and Medem, F., *Exptl. Cell Research* **1**, 115 (1950).
12. Seymour, F. L. and Benmosche, M., *J. Am. Med. Assoc.* **116**, 2489 (1941).
13. Takashima, T., *Electronmicroscopy* **2**, 32 (1952).
14. Yamanaka, T., *J. Osaka Med. Univ.* **6**, 307 (1954).
15. Yasuzumi, G., *Electronmicroscopy* **1**, 25 (1950).
16. —— *Biochim. et Biophys. Acta* **16**, 322 (1955).
17. —— *J. Biophys. and Biochem. Cytol.* **2** (1956).
18. Yasuzumi, G., Fujimura, W., Tanaka, A., Ishida, H., and Masuda, T., *Okajimas Folia Anat. Japonica* (in press).
19. Yasuzumi, G. and Minamino, T., International Congress of Electron Microscopy, London, 1954 (in press).
20. Watson, M. V., *Biochim. et Biophys. Acta* **8**, 369 (1952).
21. Watson, J. D. and Crick, F. H. C., *Nature* **171**, 737 (1953).

Fig. 3. An oblique section through the primitive sperm-head, showing clearly cross and oblique sections of fibrils. In the fibril marked by the arrow, helical filaments are scarcely visible. Magnification × 193,000.

Fig. 4. Micrograph represents at a higher magnification a portion indicated by the arrow in Fig. 3. This picture reveals an intimate arrangement of helical filaments in the fibrils at the points marked by the arrows. Magnification × 1,467,000.

THE CULTURE OF ORGANS FROM THE EMBRYONIC CHICK ON CELLULOSE-ACETATE FABRIC

B. M. SHAFFER

Strangeways Research Laboratory, Cambridge and Microbiological Research Establishment, Porton, Wilts, England

Received July 25, 1956

Though tissue fragments have survived in liquid in a flask [5], most organs do not thrive *in vitro* when completely submerged and have to be maintained at or near an air interface. This is achieved very simply in Fell's watch-glass method [3] by growing the organ on the surface of a mixture of fowl plasma and chick-embryo extract clotted in a watch-glass, which is placed in the middle of a ring of wet cotton wool in a Petri dish. This method gives excellent results with some tissues [2], but others that rapidly digest the clot soon find conditions in the resultant pool of liquid to be unfavourable, and those that spread freely and invade the clot are damaged or severely disturbed in transfer and lose much of their substance. Martinovich [4] has given such organs further support by laying them across thin glass rods resting on the clot and has discouraged cellular migration by pushing the explants along the rods at frequent intervals.

A liquid medium, however, enables a highly secretory gland to dispose of its products more freely; it may also facilitate studies on nutrition, metabolism, and the effects of biologically active substances. Trowell maintained rat lymph glands at a liquid gas interface by growing them originally [6] on cotton wool soaked in nutrient and later [7] on lens paper supported on a table of tantalum gauze standing in the nutrient. Chen [1], working with organs from foetal rats, has dispensed with the tantalum by using a brand of lens paper that floats indefinitely. For histological examination, the organs have to be dissected off the paper during processing, after which any remaining cellulose fibres, which would otherwise cause razor marks in the sections, have to be sought with a microscope and plucked out. Many mammalian organs remain compact even after prolonged cultivation, and can easily be removed from the lens paper, but others tend to flatten and spread, so that a large proportion of the explant has to be sacrificed on dissection; the removal of fibres embedded in the tissue is extremely tedious and damaging. Most chick organs sink into and infiltrate the paper to such an extent that it becomes impossible to recover them. To surmount this difficulty, successful attempts have been made to replace the pure cellulose of the lens paper by a cellulose ester that would dissolve in a convenient reagent; the acetate has been chosen because it is readily soluble in acetone and easily obtainable as a fabric. Some fabrics are toxic and others of so-called acetate are insoluble or have an insoluble component; several weaves have been tried and that found most suited to the majority of organs is a net in which the holes are 0.5–1 mm square; such a net is sold, undyed, as curtain material.[1]

[1] That used in this study was *Voile*, Silene V. V. & Co.; obtained through Robert Sayle & Co., Cambridge (John Lewis's Cat. No. M. 5325).

If a liquid medium is to be used, the procedure is as follows. The fabric is cut into pieces of convenient size, which are piled up and washed for some hours in three changes of glass-distilled water, two of absolute alcohol, and two of ether. They are then given a silicone covering to make them repel water: they are immersed in a solution of a methyl-chlorosilane in carbon tetrachloride,[1] drained, allowed to dry, and left overnight in a damp atmosphere. The hydrochloric acid produced by hydrolysis

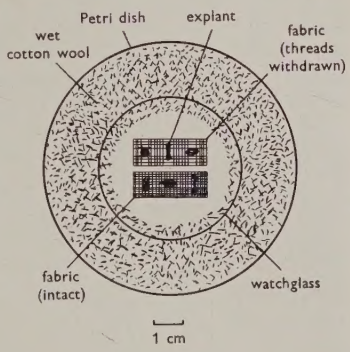

Text-fig. 1. The culture vessel, showing diagramatically a variety of explants supported in different ways.

is removed by washing with glass-distilled water. The net is given a final rinse with absolute alcohol, dried, cut into rectangles 1.5–2 cm × 0,5–1 cm, and sterilized by dry heat at 130°C.

A drop of Tyrode or embryo extract is placed on the bottom of a Petri-dish or in a cavity slide, and a piece of fabric laid on top of it; there should be no more liquid than is needed to fill the interstices. According to the mesh of the net, the size of the explant and the type of support it needs, one or more threads may be pulled out with forceps in order to produce a larger gap across which the explant can be stretched. Small organs or pieces of organ, 2–3 mm in diameter, are washed in Tyrode and arranged on the fabric; if necessary, they are oriented under the dissecting microscope. The fabric is then freed from surplus liquid with a fine pipette, or by resting it momentarily on dry glass, and gently lowered on to the surface of about 0.5 ml of the nutrient, either natural or synthetic, in a watch-glass (Text-fig. 1). Every other day the fabric is lifted and washed by floating it on Tyrode; it is transferred to fresh nutrient after the free liquid has been removed. Though the siliconed fabric can be made to float after it has been submerged in water, it will not do so if it is wetted with a protein solution; if this happens accidentally during culture, provided that it has not become overloaded with a solid mat of cells nor been submerged long enough to be completely covered with denatured protein, it can often be refloated after being thoroughly washed and then freed from surplus liquid. If this treatment fails, the net may be supported at the surface of the nutrient on glass beads of a suitable size.

The natural medium used first, consisted of equal parts of cock serum and extract made from 12-day chick embryos by mincing and grinding them, incubating them for 30 minutes with an equal volume of Tyrode and then centrifuging. As Fell achieved

[1] *Repelcote*, Hopkin and Williams, Ltd., Chadwell Heath, Essex.

better results in "horseshoe" hanging-drop cultures by substituting for this mixture the exudate obtained from incubating a cut-up plasma–embryo-extract clot, a similar medium has been developed for use in watch-glasses. First one part of plasma diluted with one or two parts of Tyrode and then one part of concentrated embryo extract are drawn into a wide syringe (without a needle) and rapidly mixed by swirling; as it clots the mixture is forced out through the nozzle into a bolt-head flask and then sucked up and forced out again a number of times. The product may with advantage be incubated for 1–2 hours to allow subsidence of the froth and further enzymic action on the remnant of the clot. The issuing liquid, obtained in high yield, has been found to be a much more satisfactory medium for organ cultures than a mixture of serum and embyro extract.

Even when organs are to be grown on a plasma–embryo-extract clot, it may be advantageous to explant them on a layer of fabric, for this reduces the loss of tissue and the disturbance at each subculturing. Treatment with silicone is not needed; the net is just washed in ether, glass-distilled water, and alcohol. To discourage migration into the clot, it is advisable to use the intact fabric and not to withdraw any threads from it. The embryo extract in the clotted medium should be at most half the strength of that used in the liquid medium, otherwise the fibrin will be digested too rapidly and the explants inundated. The fabric is wetted with embryo extract, the explants arranged on it, the surplus fluid removed, and the fabric then laid on the clot. Every two days it is lifted, washed in Tyrode, moistened with embryo extract, and placed on fresh nutrient; only a few cells are left behind, and their number can be still further reduced by moving the fabric over the surface of the clot from time to time, though this is rarely necessary.

The explants are prepared for histological examination as follows. The area of rayon bearing the organ is cut out with scissors and laid flat on the bottom of a clean dry specimen tube. Fixative is then poured on and the tube is immediately shaken vigorously. For general purposes, good results are obtained with 3 per cent acetic Zenker for 30 minutes followed by 2 hours in Zenker without acetic acid, but Susa, formol-saline and methyl alcohol have also been used successfully. The tissue is dehydrated in the usual way and is then treated with acetone to dissolve the fabric (3 changes, 30 minutes in each, or until the washings do not produce milkiness on mixing with water), transferred to the clearing agent (cedar wood oil, 3 changes), and embedded in paraffin wax. If the organs are grown on a natural nutrient, the fabric becomes coated with a layer of denatured protein, which increases in thickness as cultivation is prolonged. Moreover fibroblasts and to some extent epithelial cells

---

Fig. 1. Ovary from a 12-day embryo, after 10 days' cultivation. A horizontal section near the base of the explant, showing how the tissue has infiltrated the fabric. The empty spaces were occupied by rayon fibres. × 32.

Fig. 2. The same ovarian explant as that shown in Fig. 1 cut at a higher level. Parts of two cortical sex cords: their oocytes are at various stages of meiotic prophase. × 770.

Fig. 3. Spinal ganglion from an 11-day embryo, after 12 days' cultivation. × 380.

Fig. 4. Metanephros from a 12-day embryo, after 10 days' cultivation. Glomeruli and tubules. × 58.

Fig. 5. Part of the same section as that shown in Fig. 4. × 440.

All the organs shown were grown on clot exudate and stained with Azan. c.c., cortical sex cords; r.g., rayon ghost.

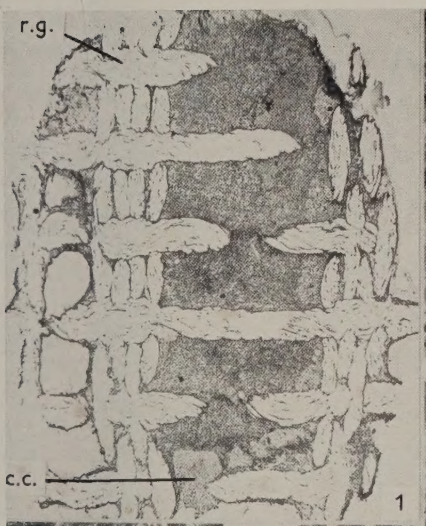
r.g.
c.c.
1

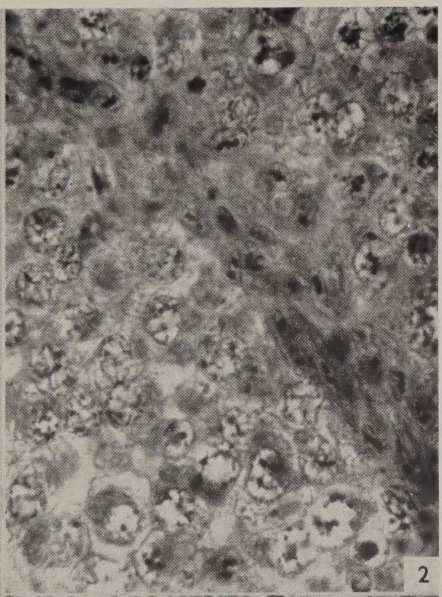
2

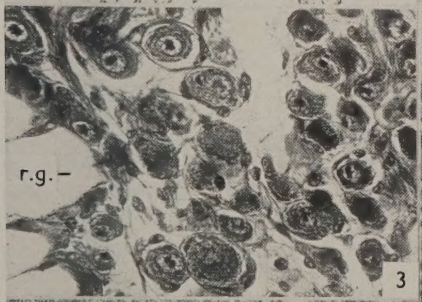
r.g.
3

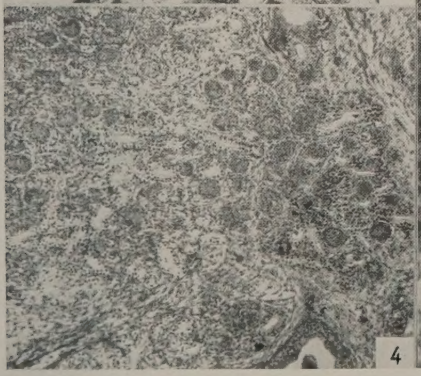
4

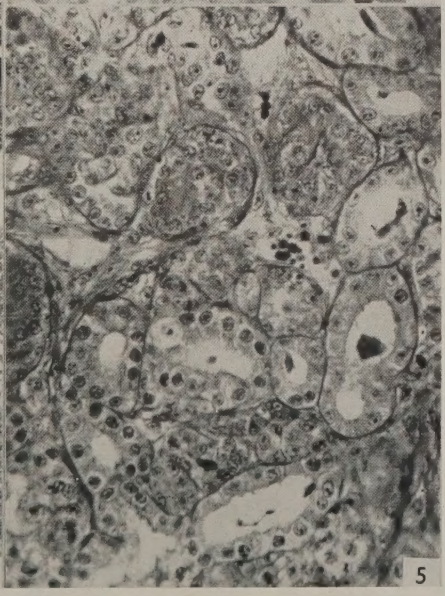
5

spread along the synthetic fibres outside the explants and invest them with sheaths; consequently a "ghost" remains after the fibres have been dissolved, which may be mistaken for the fabric itself. The weave is reproduced also within the parts of the explants that have infiltrated the fabric (Fig. 1).

Very prolonged treatment with fixative may make the fibres insoluble in acetone: this happens to an appreciable extent with aqueous picric acid after several days and with some other fixatives after a month. Lengthy exposure to chemicals for special purposes should be avoided until the acetate has been shown to be unaffected.

A variety of organs from 6- to 13-day chick embryos have been cultivated successfully for 2 to 3 weeks: they continue their development and then retain their normal differentiation and activity. The bronchi of the lungs branch, and within them débris may be seen spinning round under the action of the cilia. Heart goes on beating; long bones increase in length, deposit cartilage matrix, and ossify. Voluntary muscle fibres become striated; the secondary sexual cords of the ovary continue to grow and develop (Figs. 1 and 2), and the neurones of spinal ganglia form Nissl-substance (Fig. 3). Metanephros is well differentiated (Figs. 4 and 5). Even with a liquid medium, the loss of a few of the outer cells of an explant is unavoidable, for they round up and fall to the bottom of the watch-glass. Not all of them are moribund, and if a coverslip is laid beneath the fabric, cells may settle on the glass, singly and in small groups, and produce a flourishing culture.

The cellulose-acetate method is particularly well adapted to cultivation of organs, such as the skin, which, though initially flat, soon round up into a ball completely covered by epithelium, if placed directly on a clot; this makes nutrition difficult or, in the case of skin, which keratinises, impossible. If, however, the flat piece anchors itself to fabric, curling up is prevented. Thus if a length of intestine from a 12-day embryo is slit down one side, opened out and laid on fabric with the mucosa upwards, it shows gentle peristalsis in culture, and the longitudinal ridges initially present break up into villi. Unkeratinised skin from the shank of a 13-day embryo, grown flat with the epidermis upwards, produces normal keratin scales and has remained healthy for 18 days in culture, the longest period attempted.

Acetate-rayon net is now being used by several workers in the Strangeways Research Laboratory, including Dr. Fell, who finds that with it she can obtain much larger and healthier cultures of skin.

REFERENCES

1. Chen, J. M., *Exptl. Cell Research* **7**, 518 (1954).
2. Fell, H. B., *Science Progress* **41**, 212 (1953).
3. Fell, H. B. and Robison, R., *Biochem. J.* **23**, 767 (1929).
4. Martinovich, P. N., *Exptl. Cell Research* **4**, 490 (1953).
5. Parker, R. C., *J. Exptl. Med.* **64**, 121 (1936).
6. Trowell, O. A., *Exptl. Cell Research* **3**, 79 (1952).
7. —— *Exptl. Cell Research* **6**, 246 (1954).